UNIVERSITY OF OTTAWA
Department of Chemical and Biological Engineering

DEVELOPMENT OF A DYNAMIC CELL PATTERNING STRATEGY ON A HYALURONIC ACID HYDROGEL

By
Catherine Anne Goubko

A thesis submitted to the Faculty of Graduate and Postdoctoral Studies in fulfillment of the requirements for the

Doctoral Degree
Chemical Engineering

STATEMENT OF CONTRIBUTIONS AND COLLABORATORS

I hereby declare that I am the sole author of this thesis.

My thesis advisor, Dr. X. Cao provided guidance and editing throughout the work.

During the writing of "Chapter 3: Patterning multiple cell types in co-cultures: A Review", Susan Badel assisted in locating and summarizing some literature. I am the sole author of the written work, and independently reviewed all of the articles discussed.

For "Chapter 4: Photolabile molecules as light-activated switches to control biomolecular and biomaterial properties," Nan Cheng provided suggestions and wrote the majority of section "4.3.1 Patterning Biomolecules and Cells on Solid Surfaces" which I edited. I wrote all of the remaining portions of the book chapter. So, I wrote all of Chapter 4 with the exception of section "4.3.1 Patterning Biomolecules and Cells on Solid Surfaces."

Chapters 5-8 involve the use of caged amino acids and peptide synthesis. All such syntheses were conducted at Dr. Ajoy Basak's laboratory at the Ottawa Hospital Research Institute (OHRI) which specializes in peptide chemistry and synthetic chemistry. I had the opportunity to train under Dr. Basak and his post-doctoral fellow, Dr. Swapan Majumdar who both contributed to this project in the planning and discussing of synthesis routes and subsequent purification steps. Dr. Majumdar synthesized the initial amino acids and peptides (i.e. caged Gly, caged Asp, RGDS and R[-]GDS) while I assisted him, and he trained me. I synthesized subsequent batches of caged amino acids and peptides by both solid phase and liquid phase synthesis myself.

In "Chapter 5: "Hydrogel cell patterning incorporating photocaged RGDS peptides, Dr. Majumdar analyzed the NMR results while providing me training in this analysis. The Materials and Methods Sections 5.2.3 and 5.2.5 were written by Dr. Basak and Dr.

Majumdar. Molecular modeling using Hyperchem software was conducted by Dr. Basak and he wrote section 3.3.1. All of the remaining sections and work were conducted by me. Dr. Basak additionally provided scientific guidance and editing for this paper.

In "Chapter 6: Comparative analysis and modeling of photocaged Arg-Gly-Asp Ser-(RGDS) peptides for cell patterning," access to software and scientific guidance related to the modeling work was provided by Dr. Harold Jarrell and Nam Khieu working in the research group of Dr. Brisson at the National Research Council (NRC). Dr. Basak kindly provided scientific guidance related to the peptide research and editing of the paper.

In "Chapter 7: Novel cell patterning platform employing photocaged RGDS peptides on a hydrogel," and "Chapter 8: Dynamic Cell Patterning of Photoresponsive Hyaluronic Acid Hydrogels" HUVEC and media were kindly provided by Drew Kuraitis and Dr. Suuronen at the Ottawa Health Research Institute.

With the exception of the assistance and/or advice received, as discussed above for Chapters 5-8, I conducted all of the work and writing shown. Similarly, unless otherwise specified within Chapters 9-10, I conducted all of the work and writing shown.

ABSTRACT

Cell behavior is influenced to a large extent by the surrounding microenvironment. Therefore, in the body, the cellular microenvironment is highly controlled with cells growing within well-defined tissue architectures. However, traditional culture techniques allow only for the random placement of cells onto culture dishes and biomaterials. Cell micropatterning strategies aim to control the spatial localization of cells on their underlying material and in relation to other cells. Developing such strategies provides us with tools necessary to eventually fabricate the highly-controlled microenvironments found in multicellular organisms. Employing natural extracellular matrix (ECM) materials in patterning techniques can increase biocompatibility. In the future, with such technologies, we can hope to conduct novel studies in cell biology or optimize cell behavior and function towards the development of new cell-based devices and tissue engineering constructs.

Herein, a novel cell patterning platform was developed on a hydrogel base of crosslinked hyaluronic acid (HA). Hydrogels are often employed in tissue engineering due to their ability to mimic the physicochemical properties of natural tissues. HA is a polymer present in all connective tissues. Cell-adhesive regions on the hydrogel were created using the RGDS peptide sequence, found within the cell-adhesive ECM protein, fibronectin. The peptide was bound to a 2-nitrobenzyl "caging group" via a photolabile bond to render the peptide light-responsive. Finally, this "caged" peptide was covalently bound to the hydrogel to form a novel HA hydrogel with a cell non-adhesive surface which could be activated with near-UV light to become adhesive. In this way, we successfully formed chemically patterned cell-adhesive regions on a HA hydrogel using light as a stimulus to form controlled cell patterns.

While the majority of cell patterning strategies to date are limited to patterning one cell population and cannot be changed with time, our strategy was novel in using small, adhesive, caged peptides combined with multiple, aligned light exposure steps to allow for dynamic chemical cell patterning on a hydrogel. Multiple cell populations, even held apart

from one another, were successfully patterned on the same hydrogel. Furthermore, cell patterns were deliberately modified with time to direct cell growth and/or migration on the hydrogel base.

RÉSUMÉ

Le comportement des cellules est influencé en grande partie par la nature du microenvironnement. En conséquent, dans le corps humain, le microenvironnement cellulaire est hautement contrôlé, et les cellules grossissent dans des tissus ayant des architectures bien définies. Cependant, les techniques traditionnelles de culture permettent seulement le placement aléatoire de cellules sur des boîtes de culture ou des biomatériaux artificiels. Les stratégies de microstructure cellulaire visent à contrôler la localisation spatiale des cellules non seulement sur le matériau sous-jacent mais également par rapport aux autres cellules. Le développement de telles stratégies nous aide à découvrir les outils nécessaires à la fabrication de microenvironnements hautement contrôlés qui se retrouvent à l'intérieur des organismes multicellulaires. L'emploi de substances de matrice extracellulaire naturelle dans ces techniques de structuration peut accroître la biocompatibilité. Dans le futur, ce genre de technologie pourrait nous permettre de mener des études novatrices en biologie cellulaire ou d'optimiser le comportement des cellules, ce qui pourrait nous guider vers le développement de nouveaux dispositifs à bases de cellules et de construction à base d'ingénierie tissulaire.

Dans ce travail, une nouvelle plateforme de structure cellulaire a été développée sur une base d'hydrogel d'acide hyaluronique (HA) réticulé. Les hydrogels sont souvent employés dans l'ingénierie tissulaire en raison de leur capacité à imiter les propriétés physicochimique des tissus naturels. Le HA est un polymère présent dans tous les tissus conjonctifs. Des régions de l'hydrogel attribuées à l'adhésion des cellules ont été créées en utilisant la séquence peptidique RGDS, que l'on retrouve à l'intérieur de la protéine MEC de l'adhésion des cellules, soit la fibronectine. Le peptide a été lié à un groupe protecteur 2-nitrobenzylique, ou un « groupe en cage », par un lien photolabile pour le faire réagir à la lumière. Enfin, ce peptide « en cage » a été lié par covalence à l'hydrogel afin de créer un nouveau hydrogel HA ayant une surface non-adhésive aux cellules pouvant être activé à l'aide de lumière ultraviolet proche pour la rendre adhésive. Avec cette méthode, nous

avons réussi à créer des régions chimiques adhésives aux cellules sur un hydrogel HA en utilisant la lumière à titre de stimulant pour créer des structures cellulaires contrôlées.

La majorité des stratégies de structure cellulaire jusqu'à présent sont limitées à la structuration d'une seule population de cellules et ne peuvent être modifiées avec le temps. À cet effet, notre stratégie ce distingue en utilisant des peptides en cage, petites et adhésives, combinés avec une multitude d'étapes d'exposition à la lumière alignée, ce qui permet la création de structures cellulaires chimique plus dynamiques sur un hydrogel. Nous avons réussi à développer des structures contenant une multitude de populations de cellules sur le même hydrogel, même lorsqu`on les écarte l`une de l`autre. De plus, les structures cellulaires ont été volontairement modifiées avec le temps afin de diriger la croissance et/ou la migration des cellules sur la base de l'hydrogel.

ACKNOWLEDGEMENTS

I'd like to first thank my family for their amazing support and encouragement through the years. Special thanks to my father, Richard, brother, Paul, and my husband, Joël. Thanks to Mom, Suzanne Goubko, who was forever proud of me – rest in peace. May the new research avenues of today bring about changes to save and improve future lives.

I'd like to thank my thesis group. My thesis advisor was Dr. Xudong Cao who introduced me to this project and provided me with the opportunity to work in a field of great interest to me. Thank you also to all the group members throughout the years including Nan Cheng, Benu Sethi, Yiping Tian, Sagedeh Sadat Shahabi, and all the others for both their technical and emotional support, and for just making the lab a more enjoyable place to work.

Thank you to Dr. Ajoy Basak at the OHRI for your invaluable input, and for always being available to share your knowledge and expertise with such patience. Thanks to Dr. Swapan Majumdar for the organic chemistry training and to Andrew Chen for all the technical advice and training, and to all the friendly staff and students at the OHRI for making me feel so welcome in your labs.

Thank you to the research group of Dr. Brisson at the NRC including Dr. Harold Jarrell and Nam Khieu for access to your facilities, and for your guidance and discussions. Thanks to Dr. Hanan's group including Brett and Katherine for collaborating in preliminary 2-photon laser work, and to Dr. Tsai's group including Matt and Usha for discussions and training involving neural stem/progenitor cells. Thanks to Dr. Suuronen's group, especially Drew Kuraitis, for sharing equipment and cells.

Thanks to the faculty, staff, and fellow students in the Department of Chemical and Biological Engineering for sharing your knowledge, your supplies and equipment, and for being so willing to take time out of your day to address issues ranging from the professional to the personal. Thanks to Louis Tremblay, Gérard Nina, and Franco Ziroldo for their technical support. I also greatly appreciate the financial support received from NSERC, OGS, and IODE Canada, which allowed me to take the time to pursue this degree. Thank you again to all the friends I've met along the way – it's been quite a journey.

TABLE OF CONTENTS

LIST OF FIGURES

LIST OF TABLES

NOMENCLATURE AND ABBREVIATIONS

μCP	microcontact printing
μFn	microfluidic network
ADH	adipic acid dihydrazide
ADP	adenosine diphosphate
AEIDGIEL	peptide with amino acid sequence Ala-Glu-Ile-Asp-Gly-Ile-Glu-Leu
Arg	arginine amino acid
Asn	asparagine amino acid
Asp	aspartic acid amino acid
ATP	adenosine triphosphate
BAEC	bovine aortic endothelial cells
BMA	n-butylmethacrylate
BS^3	bissulfosuccinimidyl suberate
BSA	bovine serum albumin protein
cAMP	cyclic adenosine monophosphate
CD44	cell surface glycoprotein
CNB	α-carboxy-2-nitrobenzyl
CNS	central nervous system
D	aspartic acid amino acid
DCM	dichloromethane
DG	dentate gyrus
DGEA	peptide with amino acid sequence Asp-Gly-Glu-Ala
DIC	diisopropylcarbodiimide
DIPEA	N,N-diisopropylethylamine
DMAP	4-dimethylaminopyridine
DMEM	Dulbecco's Modified Eagle's Medium
DMF	dimethylformamide
DMNPE	4,5-dimethoxy-2-nitrophenethyl
DMSO	dimethyl sulfoxide
DNA	deoxyribonucleic acid
EC	endothelial cells
ECM	extracellular matrix
EDC	1-ethyl-3-(3-dimethylaminopropyl)carbodiimide
ELISA	enzyme-linked immunosorbent assay
FBS	fetal bovine serum
FITC-BSA	fluorescein isothiocyanate dye bound to bovine serum albumin protein
Fn	fibronectin
G	glycine amino acid
GAG	glycosaminoglycan
GFOGER	peptide with amino acid sequence Gly-Phe-Pyl-Gly-Glu-Arg
GlcNAc	N-acetyl-D-glucosamine

GlcUA	D-glucuronic acid
Glu	glutamic acid amino acid
Gln	glutamine
Gly	glycine amino acid
GM	Goeppert-Mayer units, 1 GM = 10^{-50} cm^4 s $photon^{-1}$
HA	hyaluronic acid
HATU	2-(1H-7-Azabenzotriazol-1-yl)-1,1,3,3-tetramethyl uranium hexafluorophosphate methanaminium
HC	hepatocytes
HELA	cervical cancer cells originally from the woman **He**nrietta **La**cks
HPLC	high performance/pressure liquid chromatography
HUVECs	human umbilical vein endothelial cells
IKVAV	peptide with amino acid sequence Ile-Lys-Val-Ala-Val
IR	infrared
LDV	peptide with amino acid sequence Leu-Asp-Val
LGDW	laser-guided direct writing
LPPS	liquid (or solution) phase peptide synthesis
Lys	lysine amino acid
MALDI-tof	matrix-assisted laser desorption/ionization-time of flight
MES	2-(*N*-morpholino) ethanesulfonic acid
mRNA	messenger RNA
MS	mass spectrometry
MTT	3-(4,5-Dimethylthiazol-2-yl)-2,5-diphenyltetrazolium bromide
NB or 2-NB	2-nitrobenzyl / o-nitrobenzyl
NHS	N-hydroxysuccinimide
NMR	nuclear magnetic resonance
NPE	o-nitrophenethyl
NRK	normal rat kidney epithelial cells
NSC	neural stem cell
NSPCs	neural stem/progenitor cells
NVOC	6-nitroveratryloxycarbonyl
OEG	oligo(ethylene glycol)
Pbf	2,2,4,6,7-pentamethyldihydrobenzofuran-5-ylsulfonyl
PBS	phosphate buffered saline solution
PDMS	poly(dimethylsiloxane)
PEG	polyethylene glycol
PEGDA	polyethylene glycol-diacrylate
PEI	poly(ethylenimine)
Phe	phenylalanine amino acid
PHSRN	Pro-His-Ser-Arg-Asn
PIPAAm	poly(*N*-isopropylacrylamide)
PLGA	poly(lactic-*co*-glycolic) acid
PLL	poly(L-lysine)
PMMA	poly methyl methacrylate
R	arginine amino acid
RGDS	peptide with amino acid sequence Arg-Gly-Asp-Ser

R[-]GDS	RGDS peptide with NB caging group bound to the peptide
RHAMM	receptor for hyaluronic acid mediated motility
RNA	ribonucleic acid
RP-HPLC	reversed-phase HPLC
RT	room temperature
S	serine amino acid
SAM	self-assembled monolayer
SCI	spinal cord injury
SELDI-TOF	surface-enhanced laser desorption/ionization-time of flight
Ser	serine amino acid
SGZ	subgranular zone
siRNA	small interfering RNAs
SPPS	solid phase peptide synthesis
SVZ	sub-ventricular zone
TCP	tissue culture plate
TFA	trifluoroacetic acid
TIPS	triisopropylsilane
TLC	thin layer chromatography
TMB	3,3′,5,5′-tetramethylbenzidine
tRNA	transfer RNA
TTSWSQ	peptide with amino acid sequence Thr-Thr-Ser-Trp-Ser-Gln
Tyr	tyrosine amino acid
UV	ultraviolet
Val	valine amino acid
YIGSR	peptide with amino acid sequence Tyr-Ile-Gly-Ser-Arg

CHAPTER 1:
INTRODUCTION

1.1 Subject and Hypothesis

The subject of this work is the patterning of cells on a material of biological origin. Traditionally, cells seeded on biomaterials are not organized in pre-determined geometries - or patterns - to better control or fit their function. Instead, cells are seeded randomly on their supporting material. The ultimate goal of this study was to create a novel cellular micropatterning platform to enable control over the spatial localization of multiple cell types and of cells over time. The design was to consist of a hydrogel which could be stimulated with light to create areas on the material where cells could adhere. It was hypothesized that such a cell-patterned material could be created using a hyaluronic acid (HA) hydrogel base incorporating photocaged cell adhesive peptides. The goal was to develop the material and ultimately test its ability to control cell adhesion with animal cells.

The nature of the microenvironment surrounding cells has a substantial impact on cell behavior.[1-3] In the body, the local cell microenvironment consists of the scaffold on which cells grow, known as the extracellular matrix (ECM), as well as neighboring cells which can consist of multiple cell types. Generally, cells must adhere to the ECM to survive. Cells can connect to the ECM through adhesion molecules located on their surfaces (such as integrin receptors). In turn, stimulation of these adhesion molecules by the ECM can result in a cascade of signaling events being sent through the cell which ultimately influences cellular behavior such as growth, migration, and even survival.[4] Neighboring cells can also influence each other by both sending out and receiving soluble signals as a form of communication. Moreover, cells can form direct physical contacts to other cells of either the same cell type (homotypic) or of a different cell type (heterotypic). Direct cell-cell contacts are formed through specialized adhesion proteins (such as cadherins) that can interact with the cellular cytoskeleton, which determines a cell's structure, and with cell signaling pathways that can influence numerous aspects of a cell's function.[5] Considering the complex inter-play between all of these elements in a cell's environment, it is no surprise that in the body complex tissue architectures exist with carefully crafted microenvironments containing different cell types, in fixed geometries, which serve to guide cell behavior.[6] It is therefore necessary for biological material research to find ways to re-create and manipulate such cell geometries and eventually full tissue architectures.

Techniques are needed to gain *in vitro* design control over the cell microenvironment to allow for the creation of improved cell-based devices and to assist us in advancing our current knowledge of cell biology. In contrast to random cell seeding, cell patterning systems can allow for control over the spatial localization of cells, or cellular geometry. Patterning assists in controlling the degree of contact that cells make with an underlying material substrate and with neighboring cells of either the same or different cell type (homotypic or heterotypic).[7,8] Cell pattern parameters can therefore be manipulated to optimize or explore cell functions while the high degree of control attained with cell patterning can allow for improved experimental reproducibility and lowered variability in cell-based devices.

As such, the potential applications for cell patterning systems are numerous and are beginning to be realized. For example, in the field of biological research, cell patterning can be used to control cell shape[9] and it has shown that cell shape can influence whether cells grow or die.[7] It has been demonstrated that the geometric features of cell patterns can be adjusted to control the direction of cell movements.[10] A review by Kolind et al. highlights works in which stem cell fate has been controlled via cell patterning *in vitro*.[11] Furthermore, techniques are being developed to create patterned neural networks,[12-14] including some networks patterned atop electrode arrays which allowed for electrophysiological measurements to be taken[15] in order to reach a greater understanding of the nervous system's organization and function in information processing. Therefore, by using cell patterning to create a more highly controlled microenvironment compared to traditional random cell cultures, novel studies can be conducted into cell biology.

Increased control over the cell microenvironment can also allow for optimization of cell function towards the production of a certain cell product or towards maintenance of *in vivo* viability and function for employment in biosensors. Biosensors are being developed out of spatially organized cells to detect toxins and bacteria, and to study cell responses to potential toxins.[16-18] In addition, Zheng et al. recently published a review discussing various cell-patterned arrays designed as testing devices to examine cell-drug interactions.[19]

Furthermore, a number of examples of cell patterning applications can be found in the tissue engineering field. Epithelial cells were patterned and organized atop human lens capsules with the ultimate goal of developing a retinal implant.[20] Bone cells including endothelial cells, osteocytes, and osteoblasts were patterned towards the development of a spatially organized structure mimicking bone tissue.[21] Recently, cells were patterned to create a mimetic liver lobule, a centimeter scale division of liver tissue.[22] Numerous other examples can be found in the literature and the future will undoubtedly bring more fascinating and far-reaching applications as patterning techniques are further developed, improved, and applied.

The ability to create cell patterns on a hydrogel material has the potential to enhance patterning applications such as those described above – in cell biology research, biosensors, and tissue engineering – by allowing for a highly controlled microenvironment through cell patterning on a material that can also mimic the properties of natural tissues. Hydrogels are materials made up of networks of insoluble hydrophilic polymer that possess a high water content. They have tissue-like mechanical properties and can be made to mimic the ECM of body tissues. As such, hydrogels are often implemented in tissue engineering designs[23] and used in the fields of cell biology research and *in vitro* diagnostics.[24] The hydrogel used throughout this work is based on a natural, biocompatible material, HA. Recently, the biomaterial field has been moving increasingly away from the design of materials intended to be inert to the biological environment towards natural and mimetic devices which demonstrate some physiological function.[25] Natural materials also tend to be biodegradable with mechanical properties closer to native tissue. Furthermore, creating a suitable environment for nerve regeneration is of particular interest to our research group and it is the opinion of some, such as Khaing et al. "that natural materials can ultimately better replicate components within the natural nerve tissue for overall improved therapeutic strategies".[26] Gaining control over the spatial localization of cells on or within a hydrogel derived from natural materials through cell patterning can further enhance the hydrogel's ability to mimic natural tissues, since cells are highly spatially organized in body tissues, and this organization is necessary for their function.[6] By creating materials that better mimic the natural cell environment, it is hoped that cell behavior can be made to ultimately better

mimic *in vivo* behavior and therefore improve the function of cell-based materials. It is envisioned that the cell patterning platform based on a HA hydrogel developed for this thesis work will ultimately have the potential to be employed in fundamental biological research – to study various behaviors of cells under a controlled, increasingly natural, microenvironment – and tissue engineering applications.

To date, many of the cell patterning strategies found in the literature are based on photolithography which is employed in manufacturing patterned microchips and involves harsh solvents which can harm cells, proteins, and other biological materials. The use of various solvents and other cytotoxic chemicals in many patterning strategies limit them to the creation of a single pattern that cannot be changed with time. So, while numerous examples of patterns made up of single cell populations were found in the literature during this work,[27,28]only a limited number of techniques were found for patterning multiple cell populations and creating patterns that can be manipulated with time.[29] Such techniques involving natural and biocompatible materials, such as hydrogels, were found to be especially elusive. However, they are especially needed; one of the factors hindering our ability to rationally design natural tissue structures – like a suitable environment for nerve regeneration – is our limited understanding of how important biological cues play out both spatially and temporally during tissue generation or regeneration. New methods for elucidating such biological processes can potentially be realized by designing cell-patterned materials with spatial control over multiple cell types and the ability to be altered with time via an external cue.[30] By creating such a platform using biocompatible materials, there is the hope that it can be used for *in vitro* investigations and optimization, but also have the ability to be later translated into an *in vivo* device for treatment.

1.2 Relation of Study to Thesis Group Research in SCI

Our research group is particularly interested in tissue engineering applications for the treatment of spinal cord injuries (SCIs). In the future, it is desired to adapt and apply the hydrogel cell patterning technique developed in this thesis work to the design of a biomaterial scaffold for the treatment of SCI. Other group members have been engaged in

various aspects of the design of such an implantable device. As such, a brief background of SCI and biomaterials follows.

SCI is a costly disease both in terms of patient quality of life and economic costs. Even if an individual with SCI is able to survive the initial injury, the result is often a high level of disability causing drastic lifestyle changes.[31] In addition to loss of sensory and motor function to limbs and torso, a number of other health conditions can result from SCI including pain, inability to regulate bowel and bladder, muscle spasms, fatigue, and osteoporosis. As individuals with SCI age they can be at higher risk for cardiovascular disease, diabetes, respiratory complications, or infections.[22] In addition to the suffering of individual SCI patients, there are the economic ramifications of the disease to consider. A recent study published in 2013 found that, in Canada, an average of 1,389 people survive SCI each year which results in an annual economic burden of 2.67 billion dollars. It was further estimated that the average lifetime economic burden associated with SCI per individual in Canada ranged from 1.5 million dollars for those suffering from incomplete paraplegia (partial loss of function in lower limbs) to 3.0 million dollars for those with complete tetraplegia (loss of control of all limbs and torso).[32]

At the cellular level, SCIs cause significant changes to the cellular environment within the spinal cord at the site of injury. SCIs immediately damage the neural tissue by breaking open blood vessels, killing neural cells, and damaging the axons of nerve cells. Note that axons are projections originating from the nerve cell body and they carry motor and sensory signals through the spinal cord.[33] Upon injury, these axons can be severed, which cuts off communications between nerve cells, and ultimately results in disability. After SCI, the local environment surrounding the damaged area is inhibitory towards regeneration both physically and chemically. A scar is formed involving local glial cells, which are neural cells that normally support neurons. Along with a build-up of ECM molecules, this leads to the formation of a physical barrier that prevents axons from reconnecting with existing neural architecture across the injury site. In addition, the injury results in the release of a number of biochemical signals and cues that produce inflammation, fluid build-up, the destruction of local blood vessels, the loss of myelin (which normally acts

as neural insulation to allow for signal transduction), among other negative effects. These not only prevent regeneration, but even promote further cell death and a loss of neural connections near the injury site.[34] Ultimately, in most incidences of SCI in humans, a significant amount of tissue is lost and a cavity forms at the injury site.[35] In this inhibitory environment, axons from the central nervous system (CNS) do not regenerate. Conversely, in an a different environment permissive to regeneration, such as nerve grafts with Schwann cells, it has been shown that these same axons can regenerate.[36,37] Outside of the brain and spinal cord which make up the CNS, axons of the peripheral nervous system can grow and regenerate post-injury.[26]

In the treatment of SCI, biomaterial scaffolds implanted or injected at the site of injury have the potential to promote tissue regeneration in several different manners. First of all, the material can serve to bridge tissue gaps or cavities to direct re-growth while providing structural support. The material itself can also be used to provide a local, permissive environment that promotes tissue regeneration. The physical and chemical nature of the material itself, like substrate stiffness,[38] surface roughness,[39] hydrophobicity,[40] or electric charge[41] among others, can significantly impact cell behavior. Furthermore, the material can deliver cells (e.g. neural stem cells) to the injury site in order to replace lost cells and/or deliver signals to promote the survival of existing cells and promote the re-sprouting of axons. The material can aid in keeping cells localized at the site of injury as well as increasing cell survival.[42] For example, stem cells implanted into the body, and specifically the spinal cord, have shown increased survival when delivered within biomaterials as opposed to simply injected in solution.[43] The material can also be used as a sustained delivery device of proteins known to promote regeneration at the injury site. The challenge is to design a material which creates an environment where neural cells can adhere and survive, and ultimately allow axons to elongate and essentially migrate across areas of damaged tissue in a directed manner to appropriately re-connect with the body's existing, intact neural architecture to restore function.[34,42]

Proposed general designs for the group SCI treatment device can be seen in Figure 1(A) and 1(B). These figures represent conduits to be implanted at the site of injury. In Figure 1 (A) and (B), the devices contain a cylindrical, rigid, porous, polymeric outer layer (made up of poly(lactic-*co*-glycolic) acid (PLGA)) with mechanical properties similar to the spine to protect the site of injury.[44] Pores within this structure are essential to allow for the exchange of nutrients and waste for cells within the implant. Furthermore, pores can potentially be loaded with proteins such as those cellular signals known to aid in regeneration, for gradual delivery to the injury site over time.[45] The material is designed to be degradable so that it can slowly be replaced by healed native tissue with no need for additional surgeries for device removal. The devices in Figure 1 also contain an inner hydrogel layer. Hydrogels have shown great promise in peripheral nerve regeneration; a hydrogel nerve guidance channel made of a naturally-derived material, agarose, containing concentration-gradients of laminin-1 and nerve growth factor was shown to promote peripheral nerve regeneration over a long - 20 mm - nerve gap with axonal regeneration comparable to nerve autografts, the current clinical gold standard.[46] In addition, cells can be seeded on or encapsulated within hydrogels for delivery and localization at the injury site.

Smaller, aligned channels within the implant are advantageous as they can direct cellular or axonal growth through the biomaterial conduit across the injury site to reconnect with existing neural architecture. Several such designs in the literature have been shown to promote regeneration.[47-49] It is our hope to create such channels through patterned chemical adhesive regions in an otherwise non-adhesive hydrogel. In Figure 1(A), the inner side of the rigid conduit is coated with a hydrogel layer which consists of cell-adhesive lanes (shown in green) to guide cells through the device and cell non-adhesive areas (shown in red). In Figure 1(B), hydrogel fills the inner volume of the conduit, and 3D cell-adhesive lanes (shown in green) run through the otherwise non-adhesive (shown in red) hydrogel. There are advantages to both designs. Figure 1(A) – the coated device – allows for increased mass transport of nutrients and waste to promote cell survival within the device. This may be especially important considering the instability of blood vessels in injured areas. Furthermore, the hydrogel can be made denser since cells do not have to navigate through it, which allows for much increased pattern resolution.

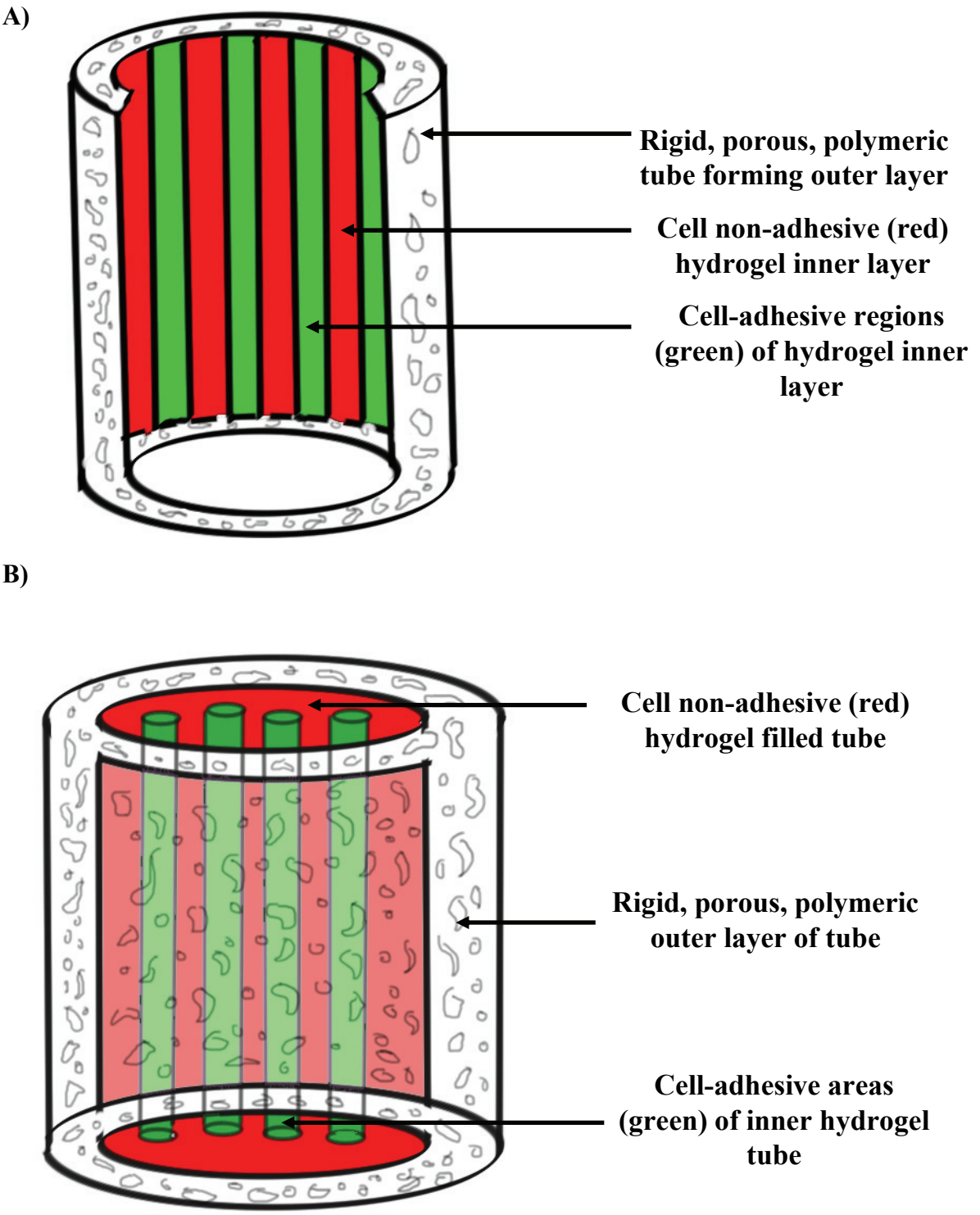

Figure 1.1: General design of proposed conduit device for SCI treatment having either **(A)** the inner side of the conduit coated with a hydrogel layer or **(B)** a 3-D hydrogel occupying the whole inner volume of the conduit. In both cases, the hydrogel is patterned with the bulk material being cell non-adhesive (red) and containing cell-adhesive lanes (green).

In addition, there is an increased number and availability of analytical tools to study 2D cell culture systems such as this prior to implantation, which may allow for improved optimization *in vitro* prior to *in vivo* work. Figure 1(B) – hydrogel filling the volume of the device – provides a 3D scaffold for cells which is the natural *in vivo* environment and so better mimics native tissues. Such a design will allow for increased loading of therapeutic cells which can be seeded in the volume of the hydrogel along with therapeutic proteins.

1.3 Description of the Cell Patterning Strategy and Novelty

The following outlines our specific cell patterning strategy. It consisted of a hydrogel base made of cross-linked HA. HA is naturally non-adhesive, which is beneficial for cell patterning as it can help to prevent cells from binding off-pattern. HA also appears promising for use in tissue engineering for CNS applications. Fetal brains have high concentrations of HA, neural progenitor cells express HA, and HA is thought to be a critical component of the adult neural stem cell niche (which is the microenvironment where these adult neural stem cells are found in the body).[26] HA hydrogels implanted into injured brain tissue, without any cells, were shown to decrease glial scar formation and promote blood vessel formation.[50] The crosslinker employed was adipic acid dihydrazide (ADH), a readily-available commercial crosslinker, which allows for crosslinking under mild, aqueous conditions to form a clear HA hydrogel. The hydrogel was rendered cell-adhesive by covalently binding the peptide sequence RGDS, found in the protein fibronectin in the body, to the HA polymer. The RGDS peptide has the ability to bind to cells via surface receptors, termed integrins. Approximately half of the members of the integrin family have been found to bind to the ECM in a manner dependent on the Arg-Gly-Asp sequence.[51] In order to render the RGDS peptides non-adhesive and light-responsive, they were bound to a 2-nitrobenzyl (2-NB) group. This group is photolabile such that it can be removed upon exposure to near-UV light (at approximately 365 nm) leaving behind intact, adhesive RGDS. All the components of the system including the gel, crosslinker, peptide, and caging group were joined via covalent bonds to ensure stability.

Together, the components described above can be made to form cell patterns as follows. The hydrogel made up of HA bound to 2-NB-photocaged RGDS is designed to be cell non-adhesive. Wherever near-UV light strikes this gel, a photoreaction should occur resulting in the release of the 2-NB caging group to create a cell adhesive region of exposed RGDS peptides on the gel. Therefore, cells should stick to areas that have been exposed to near-UV light and be unable to adhere to any other regions due to the presence of the 2-NB caging group blocking access to the RGDS peptides combined with the cell non-adhesive properties of HA. By using light to create cell adhesive regions, multiple cell populations could theoretically be pattered via multiple light exposure steps followed by cell seeding on the same material. Similarly, it was hypothesized that cell patterns could be dynamically changed with time by exposing select non-adhesive regions of the pattern with focused near-UV light to render them adhesive to the initially seeded cells.

When this thesis began, photocaging of an RGD peptide had not been carried out previously in the literature. During this thesis, two communication papers were released whereby different RGD peptides (i.e. cyclo(-Arg-Gly-Asp-D-Phe-Val-) and YAVTGRGDSPASS) were caged to control cell adhesion.[52,53] We released the first full-length paper detailing the use of photocaged RGD peptides for cell patterning, and this work was novel in that the patterning took place on a hydrogel material, and fibroblast cells were shown to remain on-pattern longer (i.e. 2.5 days vs. 6 hours).[52,54] In our second research paper, we compared properties of RGD peptides caged in the different locations explored in the literature thus far for the first time, and introduced the idea of using docking software as a method to assess various caging locations within in a peptide.[55] In the future, this may be a useful tool to employ prior to more expensive peptide synthesis. In our third full-length paper, we were the first to show that photocaged RGDS peptides could be used to create dynamic cell patterns over several weeks to control cell adhesion and growth/migration with time as well as to pattern multiple cell populations on a hydrogel material.[56]

The number of strategies to generate cell patterns on hydrogels was limited when this study began, and even in their 2011 review paper, Turunen et al. concluded that “Hydrogel applications are widely studied in vitro and in vivo, but gel patterning is a relatively new

approach to this area of research."[57] With limited studies examining the patterning of hydrogels themselves, through an extensive literature review we found much fewer studies attempting to culture multiple cell populations on the same gel.[29,58] Only a restricted number of patterning strategies currently exist that are dynamic, whereby changes in the adhesive pattern can be made with time. Several studies have produced hydrogels that can be physically degraded with light to achieve spatio/temporal control over gel mechanical properties in the presence of cells which can influence cell spreading, morphology, and migration.[59-63] Several strategies have been developed that allow for spatio/temporal control over the presentation of biochemical cues using light – which influences cell adhesive patterns - on or within a hydrogel platform.[64-66] While the referenced studies demonstrated cell guidance along the biochemical cues, changes to the generated chemical patterns were not induced after initial seeding of the cells. Lee et al. were able to seed a fibrin gel containing a cluster of fibroblasts within their polyethylene glycol (PEG)-based gel and then guide cell spreading and migration with light.[67] These works relied on multi-step chemistries for pattern generation that needed to be performed after light exposure which could impact already-seeded cells. While these studies could introduce multiple biochemical cues, ours relies on only one cue, RGDS. However, one of the benefits of our patterning strategy is that the cell-adhesive peptide regions required for cell pattern generation are formed directly after light exposure and require no further chemical steps which could impact initial cell patterns and cell viability. DeForest and Anseth created peptide patterns within hydrogels whereby the peptides could be removed upon UV light exposure in the presence of patterned cells.[68] Such dynamic patterning allows for the removal of adhesive regions with time, while our strategy allows for the addition of such regions in the presence of cells with time.

Overall, the cell patterning strategy presented in this thesis is novel in that the technique allows for a method to chemically pattern cells on a hydrogel material, using photocaged small adhesive peptides, such that multiple cell populations can be patterned on this same hydrogel and cell patterns can be spatio/temporally controlled so that additional adhesive regions can be created at desired times on the cell-seeded material to control cell growth and/or migration.

1.4 Organization of Thesis

This section has provided an introduction to the subject of cell patterning and discussed the objectives, applications, and novelty of the project in addition to providing an overview of the major work in this thesis. In the next section, a literature review will be provided which will include further details of the components of, and methodologies involved in, our cell patterning strategy. Further detailed information on subjects central to this work, such as patterning multiple cell populations on the same material and detailed information on photolabile molecules and their applications, are included in the papers titled "Patterning Multiple Cell Types in Co-Cultures: A Review" published in *Materials Science and Engineering C* [29] and a published book chapter titled "Photolabile Molecules as Light-Activated Switches to Control Biomolecular and Biomaterial Properties" published by Nova Publishers in the book "Photochemistry: UV/VIS Spectroscopy, Photochemical Reactions and Photosynthesis",[69] respectively. This will be followed by the results we have achieved in developing our patterning strategy including three full length research papers and a conference paper for the AIChE Conference in Nashville, TN, USA (2009). Please note that each of these are independent scientific contributions and as such there is some degree of material repetition in terms of background information and some experimental details. The works included are titled "Hydrogel Cell Patterning Incorporating Photocaged RGDS Peptides" published in *Biomedical Microdevice*s,[54] "Novel Cell Patterning Platform Employing Photocaged RGDS Peptides on a Hydrogel" published in the AIChE Annual Meeting, Conference Proceedings,[70] "Comparative Analysis of Photocaged RGDS Peptides for Cell Patterning" published in the *Journal of Biomedical Materials Research - Part A*,[55] and an article accepted and in press with the *Journal of Biomedical Materials Research - Part A* titled "Dynamic Cell Patterning of Photoresponsive Hyaluronic Acid Hydrogels"[56]. A discussion section will further summarize and comment on these contributions. This will be followed by conclusions and a section detailing preliminary studies and future work which will describe of a number of preliminary studies conducted which demonstrate promising opportunities for further research.

1.5 References

1. Liu WF, Chen CS. Engineering biomaterials to control cell function. *Materials Today.* 2005;8(12):28-35.

2. Rosso F, Giordano A, Barbarisi M, Barbarisi A. From Cell-ECM interactions to tissue engineering. *Journal of Cellular Physiology.* 2004;199(2):174-180.

3. Sands RW, Mooney DJ. Polymers to direct cell fate by controlling the microenvironment. *Current Opinion in Biotechnology.* 2007;18(5):448-453.

4. Luo B-H, Carman CV, Springer TA. Structural Basis of Integrin Regulation and Signaling. *Annual Review of Immunology.* 2007;25(1):619-647.

5. Yamada S, Nelson WJ. Synapses: Sites of Cell Recognition, Adhesion, and Functional Specification. *Annual Review of Biochemistry.* 2007;76(1):267-294.

6. Rivron NC, Rouwkema J, Truckenmüller R, Karperien M, De Boer J, Van Blitterswijk CA. Tissue assembly and organization: Developmental mechanisms in microfabricated tissues. *Biomaterials.* 2009;30(28):4851-4858.

7. Chen CS, Mrksich M, Huang S, Whitesides GM, Ingber DE. Geometric Control of Cell Life and Death. *Science.* May 30, 1997 1997;276(5317):1425-1428.

8. Nelson CM, Chen CS. Cell-cell signaling by direct contact increases cell proliferation via a PI3K-dependent signal. *FEBS Letters.* 2002;514(2-3):238-242.

9. Vignaud T, Galland R, Tseng Q, Blanchoin L, Colombelli J, Thery M. Reprogramming cell shape with laser nano-patterning. *Journal of Cell Science.* 2012;125:2134–2140.

10. Kushiro K, Chang S, Asthagiri AR. Reprogramming Directional Cell Motility by Tuning Micropattern Features and Cellular Signals. *Adv. Mater.* 2010;22:4516-4519.

11. Kolind K, Leong KW, Besenbacher F, Foss M. Guidance of stem cell fate on 2D patterned surfaces. *Biomaterials.* 2012;33:6626-6633.

12. Morin F, Nishimura N, Griscom L, et al. Constraining the connectivity of neuronal networks cultured on microelectrode arrays with microfluidic techniques: A step towards neuron-based functional chips. *Biosensors and Bioelectronics.* 2006;21(7):1093-1100.

13. Vogt AK, Brewer GJ, Decker T, et al. Independence of synaptic specificity from neuritic guidance. *Neuroscience.* 2005;134(3):783-790.

14. Vogt AK, Wrobel G, Meyer W, Knoll W, Offenhausser A. Synaptic plasticity in micropatterned neuronal networks. *Biomaterials.* 2005;26(15):2549-2557.

15. Suzuki M, Ikeda K, Yamaguchi M, et al. Neuronal cell patterning on a multi-electrode array for a network analysis platform. *Biomaterials.* 2013;34:5210-5217.

16. Yoo SK, Lee JH, Yun S-S, Gu MB, Lee JH. Fabrication of a bio-MEMS based cell-chip for toxicity monitoring. *Biosensors and Bioelectronics.* 2007;22(8):1586-1592.

17. Itle LJ, Pishko MV. Multiphenotypic Whole-Cell Sensor for Viability Screening. *Analytical Chemistry* 2005;77(24):7887-7893.

18. Veiseh M, Veiseh O, Martin MC, Bertozzi C, Zhang M. Single-cell-based sensors and synchrotron FTIR spectroscopy: A hybrid system towards bacterial detection. *Biosensors and Bioelectronics.* 2007;23(2):253-260.

19. Zheng XT, Yu L, Li P, et al. On-chip investigation of cell–drug interactions. *Advanced Drug Delivery Reviews.* 2013;In Press.

20. Lee CJ, Blumenkranz MS, Fishman HA, Bent SF. Controlling Cell Adhesion on Human Tissue by Soft Lithography. *Langmuir.* 2004;20(10):4155-4161.

21. Sala A, Hanseler P, Ranga A, et al. Engineering 3D cell instructive microenvironments by rational assembly of artificial extracellular matrices and cell patterning. *Integrative Biology.* 2011;3:1102-1111.

22. Jensen MP, Truitt AR, Schomer KG, Yorkston KM, Baylor C, Molton IR. Frequency and age effects of secondary health conditions in individuals with spinal cord injury: a scoping review. *Spinal Cord.* 2013;In press.

23. Nisbet DR, Crompton KE, Horne MK, Finkelstein DI, Forsythe JS. Neural tissue engineering of the CNS using hydrogels - A review. *Journal of Biomedical Materials Research Part B: Applied Biomaterials.* 2009;88B(1):304.

24. Seliktar D. Designing Cell-Compatible Hydrogels for Biomedical Applications. *Science.* June 1, 2012 2012;336(6085):1124-1128.

25. Bellis SL. Advantages of RGD peptides for directing cell association with biomaterials. *Biomaterials.* 2011;32(18):4205-4210.

26. Khaing ZZ, Schmidt CE. Advances in natural biomaterials for nerve tissue repair. *Neuroscience Letters.* 2012;519(2):103-114.

27. Falconnet D, Csucs G, Michelle Grandin H, Textor M. Surface engineering approaches to micropattern surfaces for cell-based assays. *Biomaterials.* 2006;27(16):3044-3063.

28. Yao X, Peng R, Ding J. Cell–Material Interactions Revealed Via Material Techniques of Surface Patterning. *Advanced Materials.* 2013;25(37):5257-5286.

29. Goubko CA, Cao X. Patterning multiple cell types in co-cultures: A review. *Materials Science and Engineering: C.* 2009;29(6):1855-1868.

30. Sala A, Hänseler P, Ranga A, et al. Engineering 3D cell instructive microenvironments by rational assembly of artificial extracellular matrices and cell patterning. *Integr. Biol.* 2011;3(11):1102-1111.

31. Yuri Kawanishi C, Greguol M. Physical Activity, Quality Of Life, and Functional Autonomy of Adults With Spinal Cord Injuries. *Adapted Physical Activity Quarterly.* 2013;30:317-337.

32. Krueger H, Noonan VK, renaman LM, Joshi TP, Rivers CS. The economic burden of traumatic spinal cord injury in Canada. *Chronic Diseases and Injuries in Canada.* 2013;33(3):113-122.

33. McCreedy DA, Sakiyama-Elbert SE. Combination therapies in the CNS: Engineering the environment. *Neuroscience Letters.* 2012;519(2):115-121.

34. Pêgo AP, Kubinova S, Cizkova D, et al. Regenerative medicine for the treatment of spinal cord injury: more than just promises? *Journal of Cellular and Molecular Medicine.* 2012;16(11):2564-2582.

35. Joosten EAJ. Biodegradable biomatrices and bridging the injured spinal cord: The corticospinal tract as a proof of principle. *Cell and Tissue Research.* 2012;349(1):375-395.

36. Richardson PM, McGuinness UM, Aguayo AJ. Axons from CNS neurones regenerate into PNS grafts. *Nature.* 1980;284(5753):264-265.

37. David S, Aguayo AJ. Axonal elongation into peripheral nervous system 'bridges' after central nervous system injury in adult rats. *Science.* 1981;214 (4523):931-933.

38. Pelham RJ, Wang Y-l. Cell locomotion and focal adhesions are regulated by substrate flexibility. *Proceedings of the National Academy of Sciences.* 1997;94(25):13661-13665.

39. Martin JY, Schwartz Z, Hummert TW, et al. Effect of titanium surface roughness on proliferation, differentiation, and protein synthesis of human osteoblast-like cells (MG63). *Journal of Biomedical Materials Research.* 1995;29(3):389-401.

40. Allen LT, Fox EJP, Blute I, et al. Interaction of soft condensed materials with living cells: Phenotype/transcriptome correlations for the hydrophobic effect. *Proceedings of the National Academy of Sciences.* 2003;100(11):6331-6336.

41. Ito Y. Surface micropatterning to regulate cell functions. *Biomaterials.* 1999;20(23-24):2333-2342.

42. Kim H, Cooke MJ, Shoichet MS. Creating permissive microenvironments for stem cell transplantation into the central nervous system. *Trends in Biotechnology.* 2012;30(1):55-63.

43. Cooke MJ, Vulic K, Shoichet MS. Design of biomaterials to enhance stem cell survival when transplanted into the damaged central nervous system. *Soft Matter.* 2010;6(20):4988-4998.

44. Dalton PD, Flynn L, Shoichet MS. Manufacture of poly(2-hydroxyethyl methacrylate-co-methyl methacrylate) hydrogel tubes for use as nerve guidance channels. *Biomaterials.* 2002;23(18):3843-3851.

45. Piotrowicz A, Shoichet MS. Nerve guidance channels as drug delivery vehicles. *Biomaterials.* 2006;27(9):2018-2027.

46. Dodla MC, Bellamkonda RV. Differences between the effect of anisotropic and isotropic laminin and nerve growth factor presenting scaffolds on nerve regeneration across long peripheral nerve gaps. *Biomaterials.* 2008;29(1):33-46.

47. Wong DY, Leveque J-C, Brumblay H, Krebsbach PH, Hollister SJ, LaMarca F. Macro-architectures in spinal cord scaffold implants influence regeneration. *Journal of Neurotrauma* 2008;25(8):1027-1037.

48. Stokols S, Sakamoto J, Breckon C, Holt T, Weiss J, Tuszynski MH. Templated agarose scaffolds support linear axonal regeneration. *Tissue Engineering* 2006;12(10):2777-2787

49. Moore MJ, Friedman JA, Lewellyn EB, et al. Multiple-channel scaffolds to promote spinal cord axon regeneration. *Biomaterials.* 2006;27(3):419-429.

50. Hou S, Xu Q, Tian W, et al. The repair of brain lesion by implantation of hyaluronic acid hydrogels modified with laminin. *Journal of Neuroscience Methods.* 2005;148(1):60-70.

51. Hersel U, Dahmen C, Kessler H. RGD modified polymers: biomaterials for stimulated cell adhesion and beyond. *Biomaterials.* 2003;24(24):4385-4415.

52. Petersen S, Alonso JM, Specht A, Duodu P, Goeldner M, del Campo A. Phototriggering of Cell Adhesion by Caged Cyclic RGD Peptides. *Angewandte Chemie International Edition.* 2008;47(17):3192-3195.

53. Ohmuro-Matsuyama Y, Tatsu Y. Photocontrolled Cell Adhesion on a Surface Functionalized with a Caged Arginine-Glycine-Aspartate Peptide. *Angewandte Chemie International Edition.* 2008;47(39):7527-7529.

54. Goubko C, Majumdar S, Basak A, Cao X. Hydrogel cell patterning incorporating photocaged RGDS peptides. *Biomedical Microdevices.* 2010;12(3):555-568.

55. Goubko CA, Basak A, Majumdar S, Jarrell H, Huan Khieu N, Cao X. Comparative analysis of photocaged RGDS peptides for cell patterning. *Journal of Biomedical Materials Research - Part A* 2013;101 A (3):787-796.
56. Goubko CA, Basak A, Majumdar S, Cao X. Dynamic cell patterning of photoresponsive hyaluronic acid hydrogels. *Journal of Biomedical Materials Research Part A.* 2013:In press.
57. Turunen S, Haaparanta A-M, Äänismaa R, Kellomäki M. Chemical and topographical patterning of hydrogels for neural cell guidance in vitro. *Journal of Tissue Engineering and Regenerative Medicine.* 2011;7(4):253-270.
58. Liu V, Bhatia S. Three-Dimensional Photopatterning of Hydrogels Containing Living Cells. *Biomedical Microdevices.* 2002;4(4):257-266.
59. Kloxin AM, Kasko AM, Salinas CN, Anseth KS. Photodegradable Hydrogels for Dynamic Tuning of Physical and Chemical Properties. *Science.* April 3, 2009 2009;324(5923):59-63.
60. Frey MT, Wang Y-l. A photo-modulatable material for probing cellular responses to substrate rigidity. *Soft Matter.* 2009;5(9):1918-1924.
61. Kloxin AM, Tibbitt MW, Anseth KS. Synthesis of photodegradable hydrogels as dynamically tunable cell culture platforms. *Nature Protocols.* 2010;5(12):1867-1887
62. Hahn MS, Miller JS, West JL. Three-Dimensional Biochemical and Biomechanical Patterning of Hydrogels for Guiding Cell Behavior. *Adv. Mater.* 2006;18:2679-2684.
63. Hoffmann JC, West JL. Three-dimensional photolithographic patterning of multiple bioactive ligands in poly(ethylene glycol) hydrogels. *Soft Matter* 2010;6(20):5056-5063
64. Luo Y, Shoichet MS. A photolabile hydrogel for guided three dimensional cell growth and migration. *Nature Materials.* 2004;3:249-253.
65. Wosnick JH, Shoichet MS. Three-dimensional Chemical Patterning of Transparent Hydrogels. *Chemistry of Materials.* 2013/11/10 2007;20(1):55-60.
66. Wylie RG, Ahsan S, Aizawa Y, Maxwell KL, Morshead CM, Shoichet MS. Spatially controlled simultaneous patterning of multiple growth factors in three-dimensional hydrogels. *Nature Materials.* 2011;10(10):799-806.
67. Lee S-H, Moon JJ, West JL. Three-dimensional micropatterning of bioactive hydrogels via two-photon laser scanning photolithography for guided 3D cell migration. *Biomaterials.* 2008;29(20):2962-2968.
68. DeForest CA, Anseth KS. Photoreversible Patterning of Biomolecules within Click-Based Hydrogels. *Angewandte Chemie International Edition.* 2012;51(8):1816-1819.
69. Goubko CA, Cheng N, Cao X. Photolabile Molecules as Light-Activated Switches to Control Biomolecular and Biomaterial Properties. In: Maes KJ, Willems JM, eds. *Photochemistry: UV/VIS Spectroscopy, Photochemical Reactions and Photosynthesis*: Nova Publishers; 2011:175-202.
70. Goubko CA, Majumdar S, Basak A, Cao X. Novel cell patterning platform employing photocaged RGDS peptides on a hydrogel. In: AIChE, ed. *AIChE Annual Meeting*. Nashville, TN: AIChE; 2009.

CHAPTER 2:
LITERATURE REVIEW

The following chapter contains a literature review intended to provide the interested reader with detailed information on the various components of the cell patterning strategy developed for this thesis research. These components include hyaluronic acid - from which the hydrogel base is constructed for the cell patterning platform - and cell adhesive peptides and proteins - which make up the cell adhesive regions of the cell patterning platform. This review also examines several experimental techniques central to the creation of our cell patterning strategy including "photo-control" - whereby a molecule's activity can be controlled with light, which was critical to the creation of cell patterns on the HA hydrogel base - and protein-ligand docking - a modeling technique employed in this work. Lastly, a review will be presented of cell patterning techniques focused on the patterning of hydrogels in the literature to date. The following two chapters represent published literature reviews on the topics of photolabile molecules as light-activated switches - which provides more details on "photo-control" not covered in this chapter - and more detailed information on cell patterning not covered in this chapter with a focus on the patterning of multiple cell types.

2.1 Hyaluronic Acid (Hyaluronan)

Hyaluronic acid, also known as hyaluronan, is classified as a glycosaminoglycan (GAG) - an unbranched polymer, or polysaccharide, with repeating disaccharide units that generally include an amino sugar and an uronic acid. In HA, the disaccharide unit consists of N-acetyl-D-glucosamine (GlcNAc) and D-glucuronic acid (GlcUA) (Fig 1).[1] It's molecular weight ranges from 100 to 10^4 kDa with an extended length between 2-25 μm.[2,3]

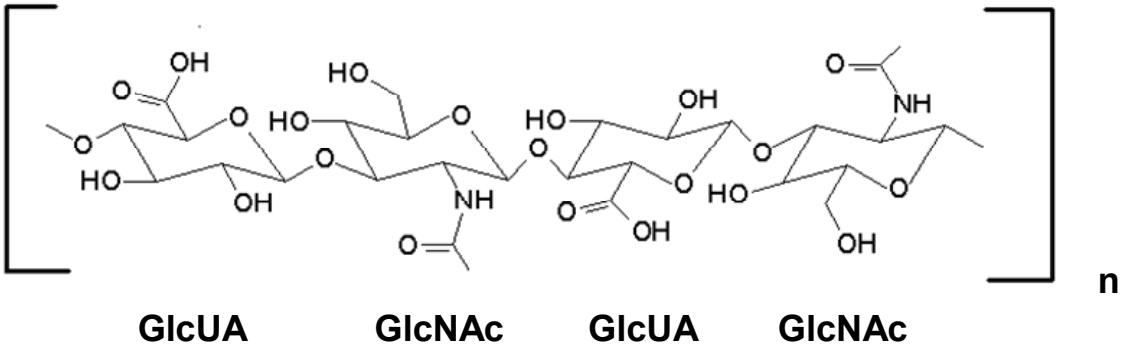

Figure 2.1: The structure of a HA chain composed of repeating disaccharide units consisting of GlcUA and GlcNAc.

GAGs, like HA, make up one of the main classes of extracellular matrix (ECM) molecules found in the body. The ECM material in the body not only surrounds and supports cells in its role as a physical scaffold, but also regulates cell behavior. HA can thus be found in almost all body fluids and tissues; however, it is found in significant concentrations in the synovial fluid of the joints, the vitreous humor of the eye, the skin, and the CNS.[4,5] The molecular weight of HA found in the spinal cord and brain in the non-injured state is approximately 1 million Da similar to the molecular weight of HA used in the production of HA hydrogels in this thesis.[6] GAGs are considered to be the most anionic molecules made by animal cells.[1] As a result, the HA molecule is extremely hydrophilic causing it to form a highly extended conformation in aqueous solution and to occupy a large volume in relation to its mass. Its negative charge attracts cations creating a high osmotic pressure in the polymer matrix. Large volumes of water thus move into the polymer matrix and create a swelling pressure. This allows HA and other GAGs in the body to resist compressive forces.[1]

HA therefore acts as an important structural element in the body. In tissues and joints, it can bear compressive loads. It further acts as a lubricant in the joints.[2] There is evidence that HA is necessary for the creation of cell-free spaces and for tissue volume changes.[7] For example, in embryonic development HA is synthesized by cells. Even a small quantity can draw in large amounts of water to create a significant volume of cell-free space in the form of a porous scaffold through which cells can migrate to form new organs, such as the heart and cornea.[1] HA also appears to regulate the diffusion of molecules through the ECM by acting essentially as a selectively permeable membrane. Hence, one of the roles of HA is thought to be the regulation of mass transport of molecules to and from cells in the tissue. The mass transport properties of the HA-containing ECM can be altered, and thus regulated by the body, since the permeability of HA is affected by calcium ion presence, pH, HA concentration, and the molecular weight of the polymer.[8]

In addition to being an important structural element, HA has also been found to possess significant biological properties. In the body, HA polysaccharides have been found to bind to a number of plasma membrane receptors on the surface of cells. Two of the major receptors include a class of carbohydrate-binding molecules, CD44, and the receptor for HA mediated motility, RHAMM.[8] Note that such receptors are found on the cell types used in

this research including fibroblasts,[9,10] HUVEC,[11] and neural stem cells[12]. All HA binding receptors contain two positively charged amino acids, Arg and Lys, which allow them to bind to the negatively charged carboxyl groups on HA. By binding to cell receptors, HA can directly influence cell behavior. For example, HA is known to be involved in the regulation of angiogenesis (growth of new blood vessels), cell proliferation,[5] wound healing,[13] embryonic development, tissue organization, and may also be involved in the regulation of cell motility and adhesion.[2] HA strongly participates in a scarless wound healing process in the body which further supports its use as a material for tissue engineering applications.[14] HA's high water absorption capacity promotes the delivery of nutrients to wounded tissue and degraded HA in the wound promotes cell proliferation, migration and angiogenesis.[14]

In the body, HA is most often found associated with other ECM molecules, and possesses the ability to bind cells.[7] Although cells can specifically interact with HA through surface receptors like CD44 and RHAMM, HA is recognized as generally cell non-adhesive in its native (i.e. pure) state.[15,16] This is thought to be due to the high degree of hydration of pure HA which makes protein binding, and thus cell binding, energetically unfavorable.[17] Pure HA is considered to be one of the most hydrophilic molecules in nature. Its anti-adhesive properties have been made use of in a number of medical applications. Due to its ability to prevent bacterial adhesion to surfaces, an esterified form of HA has been used in dental implants, intraocular lenses, and catheters to prevent against infection.[18]

One of the benefits of using HA is that it can be degraded enzymatically in the body. However, for the long term stability of HA-based biomaterials, it is necessary to crosslink chains of HA together to delay degradation. In this way, HA hydrogels can be formed. Crosslinked HA has been shown to resist enzymatic degradation for up to 28 months in aqueous solution at 37ºC.[19] HA functional groups which can be targeted for crosslinking include carboxyl and hydroxyl groups. Alternatively, the HA polymer chains can be chemically modified and such added functionality can be used in the crosslinking reaction.[4] Some of the many crosslinkers employed include carbodiimides, divinyl sulfone, poly (ethylene glycol) diglycidyl ether, disulfide-based linkages, and hydrazides.[2] Prestwich's group has extensively studied the modification of HA with hydrazides including the molecule adipic acid dihydrazide (ADH).[20,21] Such hydrazides contain -NH_2 groups having

low conjugate acid pKa values (i.e. 2.0-3.0) compared to primary amines with typical values over 9.0 in water.[21] Therefore, at acidic or neutral conditions, the hydrazides are more nucleophilic which can allow for reactions to occur at fairly mild conditions to prevent degradation of sensitive proteins, peptides, or the HA polymer itself. As such, hydrazides can be used to modify the HA polymer in an aqueous environment under mild conditions and allow for further modification of the polymer via the linking of bioactive proteins or peptides, or crosslinking, or both.[22] HA modified to contain hydrazide groups and subsequently gelled was still found to be degradable via hyaluronidase enzymes which is beneficial for tissue engineering applications.[23] Furthermore, ADH is readily available commercially and is currently used as an industrial crosslinker and epoxy resin hardener among other applications.[24]

HA itself has a history of commercial use in various medicinal and cosmetic applications. It first came to market as Hyalgan in the 1960's for the topical treatment of burns and ulcers. "Healon" from Pfizer was later introduced in 1979 as a surgical aid for cataract extraction and corneal transplants among others. Beginning in the 1980's, HA began to be used for viscosupplementation of arthritic joints, and the polymer is currently used as a tissue filler in cosmetic and reconstructive surgery among other applications.[25] Today, HA is becoming an increasingly popular material for tissue engineering designs, owing to its non-immunogenic properties, biocompatibility, biodegradability, bioactivity, and its widespread availability.[14] Benzyl derivatives of HA are commercially available as Hyalograft C and HYAFF 11, and are used as scaffolds for cartilage tissue engineering.[2] Since it is found with the exact same structure in all chordates and certain bacteria, HA purified from one species can be used in another without eliciting an immunogenic response. Therefore, pharmaceutical grade HA can now be produced through streptococcal (bacterial) fermentation, making it widely available.[8,26]

In addition to the commercially available HA materials, innovative new formulations are being created in a variety of laboratories. For example, HA particles in the form of micro- or nano-gels have been created for drug delivery.[27] Such particles can be loaded with therapeutic molecules such as DNA or RNA and can be taken up by cells with receptors for

HA.[28,29] In addition, photo-crosslinkable HA hydrogels have been developed with the goal of forming a polymeric material that can cure *in vivo*, and was initially created for cartilage synthesis,[30,31] but has rapidly found a number of other biomedical applications. These gels contain methacrylate groups that allow for hydrogel formation via a radical polymerization reaction employing a photoinitiator. More recently, HA scaffolds have been created via an electrospinning process and one such scaffold has incorporated mechanical and adhesive gradients to encourage cell infiltration for tissue engineering applications.[32]

With the combination of availability and extensive research into novel HA-based materials, it is no surprise that HA is being used in a number of new applications including some for nerve tissue repair. HA has been found to play a strong role in the developing nervous system and it has been proposed to play roles in spinal cord cell migration and growth.[33] HA has thus been proposed for use as an implantable scaffold for injury repair, and as an implantable material for the delivery of therapeutic cells and drugs.[34] As a scaffold, high molecular weight (1.6×10^6 Da), crosslinked HA hydrogels implanted after spinal cord injury have been found to reduce scar formation and total inflammatory response.[35] Furthermore, scaffolds employing HA have supported the proliferation and differentiation of neural progenitor cells.[36] Pan et al. demonstrated the ability of a 3D HA scaffold to support neural precursor cell viability and differentiation into neurons.[37] Furthermore, Wang et al. developed an implantable delivery device based on a HA hydrogel which was loaded with microspheres containing both brain-derived neurotrophic factor (BDNF) and vascular endothelial growth factor (VEGF) for release and with neural stem cells to replicate the neural stem cell (NSC) niche for neural tissue repair.[38]

In summary, the choice to use HA as the base material in our patterning strategy was owing to its commercial availability (including pharmaceutical grade product for potential future *in vivo* applications), and the fact that it is naturally non-adhesive in its pure state which makes it ideal to prevent cells from binding off-pattern. Furthermore, its ability to promote cell proliferation and migration could be beneficial for the culture of cells on our gel-based pattern.[2,5,14] Its presence in the nervous system and NSC niche, along with its documented use in tissue engineering devices will help us to later implement our patterning

technology towards the development of a device for use in the treatment of spinal cord injury, our group's long-term, overarching goal.

2.2 Cell Adhesive Peptides and Proteins

Cell adhesive peptides and proteins are often incorporated into biomaterials to enhance cell binding. In the body, there exist various ECM molecules which act specifically to bind cells to an underlying material. Cells recognize and bind to these ECM molecules via cellular surface receptors. Some of these cell-adhesive molecules include fibronectin, laminin, vitronectin, and fibrinogen.

Traditionally, biomaterials have relied on the non-specific adsorption of large proteins to their surfaces to mediate cellular adhesion. However, increased control and efficacy of cell adhesion can be achieved through the direct and deliberate binding of ECM molecules onto material surfaces prior to exposure to cells. Significant advances in the field of biomaterials were made when researchers realized that there exist small amino acid sequences within the larger cell adhesive protein molecules that can be used independently to stimulate cell adhesion and other cellular responses.

There are a number of advantages to employing these smaller peptides in biomaterials. Large proteins can become denatured, or unfolded, upon binding to a surface resulting in cell surface receptors no longer recognizing them. Even the orientation of the protein must be such that the active site for binding is available to cells and not hidden or bound to the material. Conversely, small peptide sequences can be bound to surfaces in such a way that nearly all are active and available to bind with cell surface receptors.[39] Proteins can also be degraded by proteolytic enzymes which are excreted from cells. Small peptides, on the other hand, are more stable and better able to withstand sterilization and storage conditions. Furthermore, proteins must generally be purified from other organisms while peptides can be chemically synthesized.[40] Chemical synthesis usually results in a product that is more pure, that is better chemically defined, and that comes with a decreased cost.[41] Furthermore, because peptides can be chemically synthesized, there are greater opportunities to introduce non-native chemical functions into the amino acid sequence.[41] Also, small

peptides can be packed together at higher densities on surfaces which is ideal in the creation of cell patterns where resolution will depend on the density of peptide binding sites. For all of these reasons, it was decided to implement small, adhesive peptides in our pattern design to serve as the cell-adhesive regions.

There exist a number of small, cell adhesive peptide sequences, but the major sequences used in the literature include RGD, YIGSR, and IKVAV. The sequences YIGSR and IKVAV are derived from the protein laminin. YIGSR binds to the 67 kDa laminin receptor on cell surfaces and has been used in the literature to bind nerve cells.[42,43] IKVAV binds to a 110 kDa laminin binding protein on cell surfaces and has been found not only to mediate neuronal attachment and growth, but also to promote the sprouting of neurites, the projections extending from neurons.[44] Another peptide, DGEA is derived from collagen I.[45] RGD, conversely, was originally derived from the adhesive protein, fibronectin. Since its original discovery, RGD sequences have been identified in a variety of other ECM molecules and proteins mediating cell adhesion including vitronectin, fibrinogen, von Willebrand factor, collagen, laminin, osteopontin, tenascin, and bone sialoprotein.[40] It is recognized by a number of cell surface receptors belonging to the integrin family. While the RGD sequence binds to a number of different integrin receptors, there exist other short peptide sequences which bind only to specific integrins like LDV to α_4 integrins, GFOGER which is recognized by $\alpha_2\beta_1$ integrin receptors which bind to the protein collagen, TTSWSQ which binds to $\alpha_6\beta_1$, and AEIDGIEL to $\alpha_9\beta_1$.[46,47] Furthermore, the sequence PHSRN acts with RGD in synergy to activate $\alpha_5\beta_1$.[45]

In this thesis, the adhesive peptide RGDS was incorporated onto a HA hydrogel. Compared to the other small adhesive peptides discussed, the RGD sequence is considered the most effective for stimulation of cell adhesion on synthetic surfaces due to its widespread distribution throughout multicellular organisms and its ability to mediate the attachment of multiple cell types.[40] The sequence RGDS was selected since Ser (S) is the next amino acid adjacent to the RGD sequence in the protein fibronectin. It has been found in cell attachment assays that soluble RGD alone is unable to inhibit binding to fibronectin to a large extent, while soluble RGDS can effectively inhibit cell binding by saturating cell-surface receptor

sites.[48] This indicates that RGDS may be more effective than RGD alone at promoting cell adhesion.

As previously discussed, RGD sequences bind to integrin receptors on the surfaces of cells. This family of receptors consists of two different subunits, including 18 α units and 8 β units in vertebrates, which combine to form 24 different integrins with varying degrees of specificity for particular ligands.[40] Cells express a wide range of integrins and have been known to adapt to surfaces by upregulating the production of relevant integrins.[40,49] As discussed, the RGD sequence is known to engage a number of different integrins; approximately one third of integrins bind the RGD peptide sequence.[41] Integrins are known to provide a physical link between the ECM in the cell's microenvironment and the cell's cytoskeleton. Integrins can thus allow for the sensing of mechanical forces resulting in the stimulation of various cell signaling pathways to produce a variety of cellular responses and changes in cell physiology.[46] The crystal structure of one particular integrin, $\alpha_v\beta_3$, has been solved in complex with a cyclic RGD ligand.[50] The $\alpha_v\beta_3$ integrin is particularly relevant as it has low specificity, and can thus be found associated with a large number of cell types. It binds to a number of different biomolecules including fibronectin, vitronectin and fibrinogen. The RGDS sequence has the ability to bind to $\alpha_v\beta_3$, among others.[51] This integrin can be found on various cells of the nervous system, which are of particular interest in this study; interactions between $\alpha_v\beta_3$ and the RGD motif have been found to promote neurite outgrowth.[49]

When binding RGD to a material surface, spacers are often employed. It is necessary to make the motif flexible enough so that it can orient itself correctly to interact with integrin receptors. A string of glycine molecules attached to the N-terminus of the RGD sequence is often employed as a spacer. In a study by Beer et al., it was found that increasing the number of glycine molecules increased RGD-integrin interactions with a plateau around 9-11 glycine molecules. It was concluded that longer spacers were detrimental.[52] Another study by Nishi et al. showed the optimal number of glycine spacer molecules for use with the RGDS sequence was 12 for human umbilical vein endothelial cells (HUVECs).[53] Therefore it is beneficial to include spacers between RGD peptides and the surface to which they are bound to enhance cell binding. On the other hand, it is possible that binding a caged peptide

directly to a surface without spacers may limit its ability to undergo conformational changes. This could potentially prevent the caged peptide from interacting with integrin receptors on cell surfaces as desired. Thus, it was decided not to employ spacers in our cell patterning design.

A brief discussion surrounding the process of how cells bind to an underlying cell-adherent substrate follows. When adherent cells come in contact with an underlying substrate several events can occur: the initial cell attachment to the material, the spreading of the cell, the organization of the cell's actin cytoskeleton, and the formation of focal adhesions. During initial cell attachment, the cell physically contacts a protein or peptide sequence, such as RGDS, on the underlying substrate and binds, consequently gaining the ability to withstand low shear forces. Next, the cell begins to flatten with its membrane spreading over the underlying surface. The cell may take on a characteristic shape, depending on its specific cell type. Actin within the cell can become organized into microfilament bundles, which forms an actin cytoskeleton (support structure) within the cell. These are sometimes referred to as stress fibers. Focal adhesions can form where the cell's membrane contacts the underlying substrate. These focal adhesions serve to link underlying ECM molecules directly to the actin cytoskeleton. Focal adhesions are dynamic in that they can mature to grow in size and change protein composition; this maturation may be influenced by assembling stress fibers.[54,55] Integrins appear to play a strong role in focal adhesion formation.[56] Massia and Hubbell classified the morphology of adherent fibroblast cells - which will be utilized extensively in this study as model cells - binding to an underlying substrate containing RGD peptides. They were able to achieve maximal cell spreading on a 2-D surface at bound RGD concentrations of 1 fmol/cm^2, but were unable to note the formation of focal adhesions and stress fibers until concentrations of 10 fmol/cm^2 were reached.[57]

The discovery of RGD has had a huge impact on the field of biomaterials, and has been incorporated into a number of biomaterial designs.[58] The addition of RGD to both synthetic and natural hydrogels has been found to increase neuronal adhesion to these materials.[59] There are a number of studies employing HA bound to RGD peptides. Lei et al. created an HA gel which supported the culture of mesenchymal stem cells; the binding of

RGD to the gel caused cells to spread and migrate.[60] Ananthanarayanan and Kumar developed RGD-functionalized HA hydrogels for use as a future brain-mimetic model to study brain tumor progression, and found that brain tumor cells (specifically glioma tumor spheroids) were able to adhere and invade RGD-HA hydrogels possessing a stiffness in the same range as brain tissues.[61] Cui et al. implanted HA crosslinked with ADH to form hydrogels, and further bound RGDS. They implanted the final material into the brains of rats for repair after injury, and found it to be biocompatible and to provide a scaffold for cell infiltration with neural cells which formed extensions within the material.[62] Due to the widespread use of the RGD sequence in biomaterials to adhere neural cells in addition to a wide range of other cell types including fibroblasts, our model animal cells, along with the other advantages outlined here, it was decided to employ this peptide sequence as the cell-adherent domain in the patterning strategy outlined in this thesis.

2.3 Photo-control

The ability to control a molecule's activity with light can be attained through "photocaging." "Photocaging" is the process of binding a chemical protecting group to a molecule via a photolabile bond in order to render it inactive. The molecule can then be re-activated upon exposure to light of a certain wavelength which catalyzes the removal of the protecting group to regenerate the original molecule. Photocaging can therefore create a biomolecule light-switch,[63] and as such this process has resulted in novel in-depth studies into the biological sciences.[64,65] In this work, the 2-nitrobenzyl (2-NB) protecting group and photocage was bound to the RGDS peptide molecule to prevent its recognition by cell integrin receptors. Near-UV light was used to remove the 2-NB function and regenerate active RGDS capable of binding cells.

In a recent review, 2-NB was described as one of the most useful candidates for implementation as a photoactive group in biomedical hydrogels due to its demonstrated biocompatibility prior to and post irradiation.[66] The 2-NB moiety has a proven safety record in the literature.[67] For a full review of photocaging including the use of 2-NB molecules for photo-control and associated applications in the biomaterial field, please refer to Chapter 4.

Prior to beginning this thesis work, some previous studies had sought photo-control over RGD peptide sequences as well, but instead of using photocaging techniques, they employed the light-responsive molecule azobenzene, which can be induced to isomerize upon exposure to UV light. These studies are described as follows. Shütt et al. (2003), formed a cyclic RGD peptide incorporating azobenzene which was induced to isomerize from trans to cis upon exposure to near-UV light. This resulted in changing the conformation of the RGD-containing peptide ring; the $\alpha_V\beta_3$ integrin was found to bind preferentially to the trans isomer.[68] In another study, RGD peptide was bound to a poly methyl methacrylate (PMMA) surface via a linker containing azobenzene. Upon light irradiation, induced isomerization of the azobenzene resulted in the linker pulling the RGD peptides closer to the PMMA surface which decreased the ability of cells to adhere to the material.[69] In these studies, cell binding to the RGD peptide was altered upon near-UV light exposure.

2.4 Protein-ligand Docking

Protein-ligand docking is a computational method that predicts the conformation of the intermolecular complex formed by a ligand of interest binding to a protein target. Generally, the docking program seeks to predict the location of ligand atoms in 3D, so as to predict ligand conformation and orientation, in relation to the 3D protein structure provided to the program. These programs can also rank the strength of the interaction between different ligands and the target protein. Docking therefore has applications in the fields of biochemistry and medicine, where ligands are often new designer drugs and the protein is a target for therapy. The development of docking methods began in the 1980s and today it is a tool used in a number of drug discovery programs.[70]

In this thesis, it was desired to employ protein-ligand docking to evaluate the relative binding affinities of RGD ligands caged at various functions within the R-G-D sequence to predict the location within the molecule where caging might best inhibit binding to cell integrin receptors. This molecular modeling technique has been used in the past to investigate a photoactive RGD ligand interacting with integrin receptors; it was employed to compare the binding modes and energies of a cyclo RGD molecule containing an

azobenzene molecule, in both cis and trans conformations, since isomerization was shown to have an impact on integrin binding.[71]

A variety of protein-ligand docking programs exist including DOCK,[72] GOLD,[73] FlexX,[74] and AutoDock [75] among others. However, AutoDock has been utilized extensively in the prediction of protein-ligand interactions,[76-79] received the highest number of literature citations for protein-ligand docking owing its popularity to free academic licensing (at http://AutoDock.scripps.edu), and has a reputation for good accuracy and flexibility.[70] It has been shown in the literature to successfully reproduce experimentally determined binding interactions.[80,81] Therefore AutoDock was chosen for use in this study's caged RGD-integrin interaction modeling.

Another reason to support the choice of AutoDock for our simulations is that it has been used previously to investigate protein-ligand interactions where a divalent metal cation is found within the protein binding pocket, and plays an important role in ligand binding, as is the case for RGD-integrin binding.[82] Chen et. al evaluated three different docking programs including AutoDock, LigandFit/Cerius2, and FlexX on their ability to correctly predict ligand positioning in comparison to experimental results when charged metal ions where present in protein binding sites. They found AutoDock to be the most reliable.[83] Furthermore, AutoDock 4 has been used previously for investigations into RGD ligand binding with the $\alpha_V\beta_3$ integrin receptor. Zanardi et al. used AutoDock 4 to study the binding modes of various RGD-cyclopeptides containing different functionalized proline residues to $\alpha_V\beta_3$.[84] In addition, Marinelli et al. used AutoDock to study the interactions and bound conformations between a variety of RGD-containing ligands and the $\alpha_V\beta_3$ integrin receptor in order to attempt to elucidate reasons behind the known biological activity of these ligands.[85]

As input, the AutoDock software requires the 3D structure of both protein and ligand. The publicly available Protein Data Bank (www.rcsb.org/pdb) contains the crystallographic or NMR structures of thousands of proteins and ligands, including the $\alpha_V\beta_3$ integrin in complex with a cyclic RGD ligand. The AutoDock software ultimately predicts a free energy

of binding between a ligand and receptor to describe the strength of binding. These values cannot be taken as absolute, but provide relative values with which to compare the binding of various similar ligands to one protein. In the case of this work, different caged ligands can be compared amongst one another, and against the original non-caged RGD sequence. To arrive at such data, a docking process is conducted, which consists of a search algorithm to find low energy binding conformations, and a scoring function to evaluate them.[70]

A Lamarckian genetic algorithm was used as the search function. In this algorithm, an initial random population of ligands is generated, all having different conformations (based on bond rotations), orientations, and translations in relation to the protein.[86] The ligands with the best binding affinity move on to the "next generation." Other ligands undergo "gene mutation" and "gene crossover" at a different rate to generate ligands in new positions and with new conformations whose binding affinities are subsequently evaluated. The algorithm runs until a certain number of ligand "generations" has passed or a number of energy evaluation calculations has been conducted.[86]

The scoring function is the calculated binding affinity of all the different ligands with different positional and conformation characteristics in each generation. To evaluate this affinity, AutoDock 4 uses a semi empirical approach. It applies molecular mechanics in the evaluation of enthalpic contributions to protein-ligand binding which include such considerations as dispersion/repulsion, hydrogen bonding, and electrostatics. However, it also employs empirical weighting constants based on a large set of experimentally known binding constants.[75] In order to increase the speed of binding energy calculations, prior to the docking simulation, "binding affinity potentials" are calculated for each ligand atom type. To do so, a 3D grid is built around the protein of interest, or approximate protein binding site. Then a probe atom is placed at each grid point and a "binding affinity grid" is calculated for atom type found in the ligand.[86] Afterwards, the search algorithm is conducted and the predicted binding conformations and associated binding affinities are generated.

2.5 Cell Patterning Techniques

A full review of cell patterning techniques, including co-culture cell patterning and dynamic patterning methods, can be found in Chapter 3. A review of some cell patterning applications can be found in Chapter 4. The following review focuses on articles related to hydrogel cell patterning, which has not been extensively covered in the above-mentioned chapters.

The creation of a cell pattern on or within a hydrogel can be generally accomplished in one of two ways: via physical patterning of the gel, chemically patterning biomolecules or cell-adhesive regions, or by a combination of both approaches. Furthermore, the approach to pattern creation can vary; bulk gels can be created and subsequently patterned, or alternatively, a "bottom-up" method can be taken.

Physical patterning of hydrogels involves the creation of structures with physical barriers throughout the gel, which hold the cells in place. For example, Bryant et al. used a photolithography process to create vertical channels in a poly(2-hydroxyethyl) methacrylate hydrogel with bound collagen. Light was passed through a photomask to the liquid polymer solution, resulting in different polymerization kinetics based on the pattern of the photomask. This allowed specific areas to polymerize and gel in a pattern, while the remainder of the material was washed away. Cells were seeded within the gel channels.[87] Another example of physical patterning is micromoulding. This process involves the placement of a physical mould in a liquid material so that it gels around the mould to create channels or shapes of different geometries within the final formed gel. For example, Tang et al. used poly(dimethylsiloxane) (PDMS) moulds to create a patterned collagen gel containing an initial fibroblast cell population, and then filled the "holes" of the first pattern with a second gel containing a second population to create a physically patterned co-culture.[88]

Chemical patterning involves the creation of 2D or 3D patterns of biomolecules or cell-adhesive materials which bind cells in order to create cell patterns in a bulk material. One method to achieve this is through microfluidics. Vermesh et al. used microfluidics to

patterning single stranded DNA oligomers on a glass surface. Multiple cell types were patterned at the single cell level by binding the matching DNA strand to cell surface receptors. Cells were then transferred from the glass to a hydrogel which was formed on, and removed from, the glass surface.[89]

Creative chemical hydrogel patterning strategies have also been developed using a variety of external stimuli to ultimately form the cell patterns. For instance, Albrecht et al. patterned cells using an electric field; cells were embedded in micro-scale alginate hydrogels and placed in an agarose polymer precursor solution. The microgels were induced to form patterns in the bulk non-adhesive agarose as a result of dielectrophoretic forces in the non-uniform electric field applied to the precursor solution followed by gelation.[90] In another example using temperature changes as the stimulus, Tekin et al. used a thermo-responsive hydrogel to create patterned co-cultures (including 3T3 fibroblasts with HUVECs and HepG2 cells with HUVECs) in limited geometries.[91]

Light is ideal for use as a stimulus for the generation of cell-adhesive regions due to its ease of use, its ability to be controlled both spatially and temporally, the ready availability of light sources, and light's known safety to biological materials where the risk of harm tends only to be significant in the deep-UV region and beyond.[59,84] As a result, a number of recent studies have employed hydrogel patterning strategies using light to form the patterns. For instance, Deforest and Anseth developed a hydrogel containing alkene groups to which thiol-containing biomolecules could be selectively added via a radical-mediated reaction initiated and controlled by visible light exposure. They further created dynamic cell patterns by linking RGDS to the gel via a caging group. In this way, the adhesive RGDS regions could be released with light exposure, thereby removing selective cells from the pattern after initial cell culture.[92] Seidlits et al. patterned methacrylated HA hydrogels by direct photo-patterning of proteins via a multiphoton light-initiated reaction in 3D with which they were able to guide neural cells.[16]

The chemical patterning of hydrogels has also been combined with physical patterning. Gu and Tang combined photocaging and enzymatic degradation to develop a

technique coined "enzyme assisted photolithography" to produce cell patterns and a cell sorting technique on hydrogels made up of crosslinked PEG. They created a peptide crosslinker cleavable by the enzyme caspase 3, but photocaged to prevent enzyme recognition. Upon selective near-UV light exposure, the caging group was released, resulting in a patterned enzyme-degradation of the gel and the presentation of free amines in the degraded, physically patterned regions. The free amines were then used to further chemically pattern the hydrogel with cell adhesive groups.[93]

A large number of hydrogel patterning techniques have used PEG hydrogels as the pattern base due to biocompatibility and the fact that these gels are naturally cell non-adhesive. PEG-diacrylate (PEGDA) polymers can form hydrogels in the presence of a photoinitiator and upon UV light exposure. Here again, light is used as the pattern stimulus. In one example, Liu and Bhatia formed patterned hydrogel micro-structures with embedded cells using a photolithography-inspired process in which UV light was shone through a photomask to crosslink the PEGDA polymer, while uncrosslinked polymer in non-patterned regions was washed away. Additional patterned hydrogel layers could be formed atop the initial pattern.[94] Hahn et al. further showed that unreacted acrylate groups in the PEGDA polymers could be used bind biomolecules upon further exposure to UV light through another photomask to form a chemical pattern on the hydrogels.[95] Moon et al. used such a method to form RGDS patterned PEGDA hydrogels to investigate angiogenesis. They cultured endothelial cells on lined patterns of RGDS peptides of various sizes and found that cells formed cord-like structures only on lines that were no wider than 50 μm, demonstrating that micropatterning can be used to optimize blood vessel formation towards vascularized tissue engineering devices.[96]

Many of the methods previously discussed involved patterning bulk gels. However, "bottom-up" design approaches are increasingly being more popular in the literature. In "modular" or "bottom up" approaches a smaller patterned gel structure is created and different structures can be added together to eventually create a more complex artificial scaffold. In one example, Du et al. created patterned micro-scale donut-shaped PEGDA hydrogels which were then assembled together to create a tubular structure with a patterned

co-culture to mimic vasculature channels.[97] Sala et al. used a "layer-by-layer" technique and formed patterned PEG hydrogels by casting the gel in a mold, and using robotic printing to create cell patterns on the hydrogel layer, followed by a repetition of this process to add additional hydrogel layers to the first which could further be printed. Through this process, they produced a device mimicking vascularized bone tissue.[98] Stereolithography is another method using a layer-by-layer technique combined with photolithography. This technique does not require the use of a photomask, and instead uses a computer aided design to essentially print structures in three dimensions. Zorlutuna et al. created a patterned co-culture, including primary hippocampus neurons and skeletal muscle myoblast cells, in a hydrogel consisting of oxidized methacrylic alginate incorporating RGD peptides crosslinked with poly(ethylene glycol) methyl ether methacrylate using stereolithography; they successfully printed such materials pre-seeded with the cell types in various spatial organizations, and were able to demonstrate enhanced functionality of the hippocampal neurons (as demonstrated by choline acetyltransferase activity, an enzyme involved in neurotransmitter formation) when patterned in co-culture with the skeletal muscle myoblast cells.[99]

In general, techniques to form cell patterns on and within hydrogels have been developed relatively recently. The articles cited herein were all published within the last decade, and mostly in the latter half. As this thesis progressed, an increasing number of articles were published in this emerging field. Furthermore, various stimuli have been used to form cell patterns, but what is coming to the forefront of research is cell patterning with light, and this technique was chosen for the patterning strategy in this thesis.

2.6 References

1. Alberts B, Johnson A, Lewis B, Raff M, Roberts K, Walter P. *Molecular Biology of the Cell*. 4th ed. New York, New York: Garland Science; 2002.

2. Allison DD, Grande-Allen KJ. Review. Hyaluronan: A Powerful Tissue Engineering Tool. *Journal of Histochemistry and Cytochemistry.* 2006;12(8):2131-2140.

3. Burdick JA, Prestwich GD. Hyaluronic Acid Hydrogels for Biomedical Applications. *Adv. Mater.* 2011;23:H41-H56.

4. Collins M, Birkinshaw C. Comparison of the effectiveness of four different crosslinking agents with hyaluronic acid hydrogel films for tissue-culture applications. *Journal of Applied Polymer Science.* 2007;104(5):3183-3191.

5. Slevin M, Krupinski J, Gaffney J, et al. Hyaluronan-mediated angiogenesis in vascular disease: Uncovering RHAMM and CD44 receptor signaling pathways. *Matrix Biology.* 2007;26(1):58-68.

6. Struve J, Maher PC, Li Y-q, et al. Disruption of the hyaluronan-based extracellular matrix in spinal cord promotes astrocyte proliferation. *Glia.* 2005;52(1):16-24.

7. Lee JY, Spicer AP. Hyaluronan: a multifunctional, megaDalton, stealth molecule. *Current Opinion in Cell Biology.* 2000;12(5):581-586.

8. Guelcher SA, Hollinger JO. *An introduction to biomaterials*. Boca Raton, FL: CRC/Taylor & Francis; 2006.

9. Henke C, Bitterman P, Roongta U, Ingbar D, Polunovsky V. Induction of fibroblast apoptosis by anti-CD44 antibody: Implications for the treatment of fibroproliferative lung disease. *American Journal of Pathology* 1996;149(5):1639-1650

10. Hamilton SR, Fard SF, Paiwand FF, et al. The Hyaluronan Receptors CD44 and Rhamm (CD168) Form Complexes with ERK1,2 That Sustain High Basal Motility in Breast Cancer Cells. *Journal of Biological Chemistry.* 2007;282(22):16667-16680.

11. Savani RC, Cao G, Pooler PM, Zaman A, Zhou Z, DeLisser HM. Differential Involvement of the Hyaluronan (HA) Receptors CD44 and Receptor for HA-mediated Motility in Endothelial Cell Function and Angiogenesis. *Journal of Biological Chemistry* 2001;276 (39):36770-36778.

12. Preston M, Sherman LS. Neural Stem Cell Niches: Critical Roles for the Hyaluronan-Based Extracellular Matrix in Neural Stem Cell Proliferation and Differentiation. *Front Biosci (Schol Ed).* . 2012;3:1165–1179.

13. Oksala O, Salo T, Tammi R, et al. Expression of proteoglycans and hyaluronan during wound healing. *Journal of Histochemistry and Cytochemistry.* 1995;43(2):125-135.

14. Xu X, Jha AK, Harrington DA, Farach-Carson MC, Jia X. Hyaluronic acid-based hydrogels: from a natural polysaccharide to complex networks. *Soft Matter.* 2012;8(12):3280-3294.

15. Lapčík J, L., Lapčík L, De Smedt S, Demeester J, Chabreček P. Hyaluronan: Preparation, Structure, Properties, and Applications *Chemical Reviews.* 1998;98(8):2663-2684.

16. Seidlits SK, Schmidt CE, Shear JB. High-Resolution Patterning of Hydrogels in Three Dimensions using Direct-Write Photofabrication for Cell Guidance. *Adv. Funct. Mater.* 2009;19(22):3543-3551.

17. Morra M, Cassineli C. Non-fouling properties of polysaccharide-coated surfaces. *Journal of Biomaterials Science, Polymer Edition.* 1999;10(10):1107-1124.

18. Necas J, L. Bartosikova L, Brauner P, Kolar J. Hyaluronic acid (hyaluronan): a review. *Veterinarni Medicina.* 2008;53(8):397–411.

19. Morra M. Engineering of Biomaterials Surfaces by Hyaluronan. *Biomacromolecules.* 2005;6(3):1205-1223.

20. Pouyani T, Harbison GS, Prestwich GD. Novel Hydrogels of Hyaluronic Acid: Synthesis, Surface Morphology, and Solid-State NMR. *Journal of the American Chemical Society.* 1994;116(17):7515-7522.

21. Pouyani T, Prestwich GD. Functionalized Derivatives of Hyaluronic Acid Oligosaccharides: Drug Carriers and Novel Biomaterials. *Bioconjugate Chemistry.* 1994;5(4):339-347.

22. Prestwich GD, Marecak DM, Marecek JF, vercruysse KP, Ziebell MR. Controlled chemical modification of hyaluronic acid: synthesis, applications, and biodegradation of hydrazide derivatives. *Journal of Controlled Release.* 1998;53:93-103.

23. Vercruysse KP, Marecak DM, Marecek JF, Prestwich GD. Synthesis and in Vitro Degradation of New Polyvalent Hydrazide Cross-Linked Hydrogels of Hyaluronic Acid. *Bioconjugate Chemistry.* 1997;8(5):686-694.

24. Dihydrazides. *Adhesives & Sealants Industry Magazine* October 2005; http://www.adhesivesmag.com/articles/dihydrazides. Accessed October, 2012.

25. Chong BF, Blank LM, McLaughlin R, Nielsen LK. Microbial hyaluronic acid production. *Appl. Microbiol. Biotechnol.* 2005;66(4):341-351.

26. Liu L, Liu Y, Li J, Du G, Chen J. Microbial production of hyaluronic acid: current state, challenges, and perspectives. *Microbial Cell Factories.* 2011;10:art. no. 99.

27. Pitarresi G, Craparo EF, Palumbo FS, Carlisi B, Giammona G. Composite Nanoparticles Based on Hyaluronic Acid Chemically Cross-Linked with α,β-Polyaspartylhydrazide. *Biomacromolecules.* 2007;8(6):1890-1898.

28. Yun YH, Goetz DJ, Yellen P, Chen W. Hyaluronan microspheres for sustained gene delivery and site-specific targeting. *Biomaterials.* 2004;25(1):147-157.

29. Lee H, Mok H, Lee S, Oh Y-K, Park TG. Target-specific intracellular delivery of siRNA using degradable hyaluronic acid nanogels. *Journal of Controlled Release.* 2007;119(2):245-252.

30. Nettles DL, Vail TP, Morgan MT, Grinstaff MW, Setton LA. Photocrosslinkable hyaluronan as a scaffold for articular cartilage repair. *Annals of Biomedical Engineering.* 2004;32(3):391-397.

31. Burdick JA, Chung C, Jia X, Randolph MA, Langer R. Controlled Degradation and Mechanical Behavior of Photopolymerized Hyaluronic Acid Networks. *Biomacromolecules.* 2004;6(1):386-391.

32. Sundararaghavan HG, Burdick JA. Gradients with Depth in Electrospun Fibrous Scaffolds for Directed Cell Behavior. *Biomacromolecules.* 2011;12(6):2344-2350.

33. Mészár Z, Felszeghy S, Veress G, Matesz K, Székely G, Módis L. Hyaluronan accumulates around differentiating neurons in spinal cord of chicken embryos. *Brain Research Bulletin.* 2008;75(2-4):414-418.

34. Khaing ZZ, Schmidt CE. Advances in natural biomaterials for nerve tissue repair. *Neuroscience Letters.* 2012;519(2):103-114.

35. Khaing ZZ, Milman BD, Vanscoy JE, Seidlits SK, Grill RJ, Schmidt CE. High molecular weight hyaluronic acid limits astrocyte activation and scar formation after spinal cord injury *Journal of Neural Engineering.* 2011;8(4):1-12.

36. Jose A, Krishnan LK. Effect of matrix composition on differentiation of nestin-positive neural progenitors from circulation into neurons. *Journal of Neural Engineering.* 2010;7(3):1-10.

37. Pan L, Ren Y, Cui F, Xu Q. Viability and differentiation of neural precursors on hyaluronic acid hydrogel scaffold. *Journal of Neuroscience Research.* 2009;87(14):3207-3220.

38. Wang Y, Wei Y, Zu Z, et al. Combination of Hyaluronic Acid Hydrogel Scaffold and PLGA Microspheres for Supporting Survival of Neural Stem Cells. *Pharmaceutical Research.* 2011;28(6):1406-1414.

39. Hubbell JA. Bioactive biomaterials. *Current Opinion in Biotechnology.* 1999;10(2):123-129.

40. Hersel U, Dahmen C, Kessler H. RGD modified polymers: biomaterials for stimulated cell adhesion and beyond. *Biomaterials.* 2003;24(24):4385-4415.

41. Collier JH, Segura T. Evolving the use of peptides as components of biomaterials. *Biomaterials.* 2011;32(18):4198-4204.

42. Gunn JW, Turner SD, Mann BK. Adhesive and mechanical properties of hydrogels influence neurite extension. *Journal of Biomedical Materials Research - Part A.* 2005;72A(1):91-97.

43. Ardini E, Sporchia B, Pollegioni L, et al. Identification of a Novel Function for 67-kDa Laminin Receptor: Increase in Laminin Degradation Rate and Release of Motility Fragments. *Cancer Research.* 2002;62(5):1321-1325.

44. Nomizu M, Weeks BS, Weston CA, Kim WH, Kleinman HK, Yamada Y. Structure-activity study of a laminin [alpha]1 chain active peptide segment Ile-Lys-Val-Ala-Val (IKVAV). *FEBS Letters.* 1995;365(2-3):227-231.

45. Bellis SL. Advantages of RGD peptides for directing cell association with biomaterials. *Biomaterials.* 2011;32(18):4205-4210.

46. Barczyk M, Carracedo S, Gullberg D. Integrins. *Cell and Tissue Research.* 2010;339(1):269-280

47. Barker TH. The role of ECM proteins and protein fragments in guiding cell behavior in regenerative medicine. *Biomaterials.* 2011;32(18):4211-4214.

48. Pierschbacher MD, Ruoslahti E. Influence of stereochemistry of the sequence Arg-Gly-Asp-Xaa on binding specificity in cell adhesion. *Journal of Biological Chemistry.* 1987;262(36):17294-17298.

49. Yip PM, Zhao X, Montgomery AMP, Siu C-H. The Arg-Gly-Asp Motif in the Cell Adhesion Molecule L1 Promotes Neurite Outgrowth via Interaction with the alpha v beta 3 Integrin. *Molecular Biology of the Cell.* 1998;9(2):277-290.

50. Xiong J-P, Stehle T, Zhang R, et al. Crystal Structure of the Extracellular Segment of Integrin αVβ3 in Complex with an Arg-Gly-Asp Ligand. *Science.* 2002;296(5565):151-155.

51. Okochi M, Nomura S, Kaga C, Honda H. Peptide array-based screening of human mesenchymal stem cell-adhesive peptides derived from fibronectin type III domain. *Biochemical and Biophysical Research Communications.* 2008;371(1):85-89.

52. Beer JH, Springer KT, Coller BS. Immobilized Arg-Gly-Asp (RGD) peptides of varying lengths as structural probes of the platelet glycoprotein IIb/IIIa receptor. *Blood.* 1992;79(1):117-128.

53. Nishi M, Kobayashi J, Pechmann S, et al. The use of biotin-avidin binding to facilitate biomodification of thermoresponsive culture surfaces. *Biomaterials.* 2007;28(36):5471-5476.

54. Short B. Stress fibers guide focal adhesions to maturity. *The Journal of Cell Biology.* 2012;196(3):301.

55. Oakes PW, Beckham Y, Stricker J, Gardel ML. Tension is required but not sufficient for focal adhesion maturation without a stress fiber template. *Journal of Cell Biology.* 2012; 196(3):363-374.

56. LeBaron RG, Athanasiou KA. Extracellular Matrix Cell Adhesion Peptides: Functional Applications in Orthopedic Materials. *Tissue Engineering.* 2000;6(2):85-103.

57. Massia SP, Hubbell JA. An RGD spacing of 440 nm is sufficient for integrin alpha V beta 3- mediated fibroblast spreading and 140 nm for focal contact and stress fiber formation. *The Journal of Cell Biology.* 1991;114(5):1089-1100.

58. Williams DF. The role of short synthetic adhesion peptides in regenerative medicine; The debate. *Biomaterials.* 2011;32(18):4195-4197.

59. Li X, Katsanevakis E, Liu X, Zhang N, Wen X. Engineering neural stem cell fates with hydrogel design for central nervous system regeneration. *Progress in Polymer Science.* 2012;37(8):1105-1129.

60. Lei Y, Gojgini S, Lam J, Segura T. The spreading, migration and proliferation of mouse mesenchymal stem cells cultured inside hyaluronic acid hydrogels. *Biomaterials.* 2011;32(1):39-47.

61. Ananthanarayanan B, Kim Y, Kumar S. Elucidating the mechanobiology of malignant brain tumors using a brain matrix-mimetic hyaluronic acid hydrogel platform. *Biomaterials.* 2012;32(31):7913-7923.

62. Cui F, Tian W, Hou S, Xu Q, Lee IS. Hyaluronic acid hydrogel immobilized with RGD peptides for brain tissue engineering. *Journal of Materials Science: Materials in Medicine.* 2006;17(12):1393-1401.

63. Young DD, Deiters A. Photochemical control of biological processes *Organic and Biomolecular Chemistry.* 2007;5(7):999-1005.

64. Lawrence DS. The preparation and in vivo applications of caged peptides and proteins. *Curr. Opin. Chem. Biol.* . 2005;9(6):570-575.

65. Yu H, Li J, Wu D, Qiu Z, Zhang Y. Chemistry and biological applications of photo-labile organic molecules *Chem. Soc. Rev.* 2010;39(2):464-473

66. Tomatsu I, Peng K, Kros A. Photoresponsive hydrogels for biomedical applications. *Adv. Drug Delivery Rev.* 2011;63:1257–1266.

67. Peng K, Tomatsu I, van den Broek B, et al. Dextran based photodegradable hydrogels formed via a Michael addition. *Soft Matter.* 2011;7(10):4881-4887.

68. Schutt M, Krupka SS, Milbradt AG, et al. Photocontrol of Cell Adhesion Processes: Model Studies with Cyclic Azobenzene-RGD Peptides. *Chemistry & Biology.* 2003;10(6):487-490.

69. Auernheimer Jr, Dahmen C, Hersel U, Bausch A, Kessler H. Photoswitched Cell Adhesion on Surfaces with RGD Peptides. *Journal of the American Chemical Society.* 2005;127(46):16107-16110.

70. Sousa SF, Fernandes PA, Ramos MJ. Protein–ligand docking: Current status and future challenges. *Proteins: Structure, Function, and Bioinformatics.* 2006;65(1):15-26.

71. Milbradt AG, Löweneck M, Krupka SS, et al. Photomodulation of conformational states. IV. Integrin-binding RGD-peptides with (4-aminomethyl)phenylazobenzoic acid as backbone constituent. *Biopolymers.* 2005;77(5):304-313.

72. Ewing TJA, Makino S, Skillman AG, Kuntz ID. DOCK 4.0: Search strategies for automated molecular docking of flexible molecule databases. *Journal of Computer-Aided Molecular Design.* 2001;15(5):411-428.

73. Jones G, Willett P, Glen RC, Leach AR, Taylor R. Development and validation of a genetic algorithm for flexible docking. *Journal of Molecular Biology.* 1997;267(3):727-748.

74. Schellhammer I, Rarey M. FlexX-Scan: Fast, structure-based virtual screening. *Proteins: Structure, Function, and Bioinformatics.* 2004;57(3):504-517.

75. Huey R, Morris GM, Olson AJ, Goodsell DS. A semiempirical free energy force field with charge-based desolvation. *Journal of Computational Chemistry.* 2007;28(6):1145-1152.

76. Vaque M, Arola A, Aliagas C, Pujadas G. BDT: an easy-to-use front-end application for automation of massive docking tasks and complex docking strategies with AutoDock. *Bioinformatics.* 2006;22(14):1803-1804.

77. Macchiarulo A, Nobeli I, Thornton JM. Ligand selectivity and competition between enzymes in silico. *Nat Biotech.* 2004;22(8):1039-1045.

78. Österberg F, Morris GM, Sanner MF, Olson AJ, Goodsell DS. Automated docking to multiple target structures: Incorporation of protein mobility and structural water heterogeneity in AutoDock. *Proteins: Structure, Function, and Bioinformatics.* 2002;46(1):34-40.

79. Park H, Bahn YJ, Jung S-K, et al. Discovery of Novel Cdc25 Phosphatase Inhibitors with Micromolar Activity Based on the Structure-Based Virtual Screening. *Journal of Medicinal Chemistry.* 2008;51(18):5533-5541.

80. Goodsell DS, Morris GM, Olson AJ. Automated docking of flexible ligands: Applications of autodock. *Journal of Molecular Recognition.* 1996;9(1):1-5.

81. Evans DA, Neidle S. Virtual Screening of DNA Minor Groove Binders. *Journal of Medicinal Chemistry.* 2006;49(14):4232-4238.

82. Cheng F, Oldfield E. Inhibition of Isoprene Biosynthesis Pathway Enzymes by Phosphonates, Bisphosphonates, and Diphosphates. *Journal of Medicinal Chemistry.* 2004;47(21):5149-5158.

83. Chen D, Menche G, Power TD, Sower L, Peterson JW, Schein CH. Accounting for ligand-bound metal ions in docking small molecules on adenylyl cyclase toxins. *Proteins: Structure, Function, and Bioinformatics.* 2007;67(3):593-605.

84. Zanardi F, Burreddu P, Rassu G, et al. Discovery of subnanomolar arginine-glycine-aspartate-based αVβ3/αVβ5 integrin binders embedding 4-aminoproline residues. *Journal of Medicinal Chemistry.* 2008;51(9):2870-2870.

85. Marinelli L, Lavecchia A, Gottschalk KE, Novellino E, Kessler H. Docking Studies on αVβ3 Integrin Ligands: Pharmacophore Refinement and Implications for Drug Design. *J. Med. Chem.* 2003;46(21):4393-4404.
86. Morris GM, Goodsell DS, Huey R, et al. *Autodock User's Guide: Automated Docking of Lexible Ligands to Receptors*. La Jolla, CA: The Scripps Research Institute; 2001.
87. Bryant SJ, Cuy JL, Hauch KD, Ratner BD. Photo-patterning of porous hydrogels for tissue engineering. *Biomaterials.* 2007;28(19):2978-2986.
88. Tang MD, Golden AP, Tien J. Molding of Three-Dimensional Microstructures of Gels. *J. Am. Chem. Soc.* 2003;125(43):12988-12989.
89. Vermesh U, Vermesh O, Wang J, et al. High-Density, Multiplexed Patterning of Cells at Single-Cell Resolution for Tissue Engineering and Other Applications. *Angew. Chem., Int. Ed.* 2011;50(32):7378-7380.
90. Albrecht DR, Underhill GH, Mendelson A, Bhatia SN. Multiphase electropatterning of cells and biomaterials. *Lab Chip.* 2007;7(6):702-709.
91. Tekin H, Tsinman T, Sanchez JG, et al. Responsive Micromolds for Sequential Patterning of Hydrogel Microstructures. *J. Am. Chem. Soc.* 2011;133(33):12944-12947.
92. DeForest CA, Anseth KS. Photoreversible Patterning of Biomolecules within Click-Based Hydrogels. *Angew. Chem., Int. Ed.* 2012;51(8):1816-1819.
93. Gu Z, Tang Y. Enzyme-assisted photolithography for spatial functionalization of hydrogels. *Lab Chip.* 2010;10(15):1946-1951
94. Liu VA, Bhatia SN. Three-dimensional photopatterning of hydrogels containing living cells. *Biomed. Microdevices.* 2002;4(4):257-266.
95. Hahn MS, Taite LJ, Moon JJ, Rowland MC, Ruffino KA, West JL. Photolithographic patterning of polyethylene glycol hydrogels. *Biomaterials.* 2006;27(12):2519-2524.
96. Moon JJ, Hahn MS, Kim I, Nsiah BA, West JL. Micropatterning of poly(ethylene glycol) diacrylate hydrogels with biomolecules to regulate and guide endothelial morphogenesis. *Tissue Engineering - Part A.* 2009;15(3):579-585
97. Du Y, Ghodousi M, Qi H, Haas N, Xiao W, Khademhosseini A. Sequential assembly of cell-laden hydrogel constructs to engineer vascular-like microchannels. *Biotechnology and Bioengineering.* 2011;108(7):1693-1703.
98. Sala A, Hänseler P, Ranga A, et al. Engineering 3D cell instructive microenvironments by rational assembly of artificial extracellular matrices and cell patterning. *Integr. Biol.* 2011;3(11):1102-1111.
99. Zorlutuna P, Jeong JH, Kong H, Bashir R. Stereolithography-Based Hydrogel Microenvironments to Examine Cellular Interactions. *Adv. Funct. Mater.* 2011;21(19):3642-3651.

CHAPTER 3:
PATTERNING MULTIPLE CELL TYPES IN CO-CULTURES: A REVIEW

Catherine A. Goubko and Xudong Cao

Reprinted with kind permission from Elsevier
Materials Science and Engineering: C
29, 1855 (2009)

The following chapter represents a published literature review providing detailed information on cell patterning not covered in the previous chapter with a focus on the patterning of multiple cell types. This chapter is intended to provide the interested reader with detailed information on the historical and currently employed methodologies to generate cell patterns in the literature so as to give context to the patterning methodology developed in this thesis. This work will also provide a picture of the state of research near the time this thesis began in relation to the patterning of multiple cell populations or types to form co-culture patterns, which was a goal to achieve with the hydrogel patterning platform developed in this thesis research.

3.1 Introduction

With scientific progress in materials, microelectronics, and biological sciences, we are in the position to design a variety of substrates with pre-determined cell patterns which allow us to control the local cellular environment at the micron-level. Studies focusing on the design of this local microenvironment are critical since it heavily influences cell behavior. In the body, this microenvironment consists of the extracellular matrix (ECM) – to which cells adhere – as well as numerous neighboring cells. These cells send out soluble signals to one another as a form of cellular communication. Neighboring cells can also form physical attachments to each other through adhesion proteins that interact with the cellular cytoskeleton, stimulate different signaling pathways, and thus influence numerous aspects of cell function. Cells also interact with the ECM, which serves to stimulate cell surface receptors, resulting in a cascade of signaling events which can eventually lead to cell proliferation, differentiation, and migration. The structure of the ECM can further impact the mobilization of soluble factors. It is the co-ordination of all of these influences in the microenvironment including soluble signaling, physical cell-cell interactions, and matrix interactions that act as positive or negative effectors which regulate cellular events.[1-5]

Due to this strong cell dependence on their local environment, it becomes extremely important to develop technologies that can design and manipulate the cellular microenvironment. The patterning of cells on a surface allows us to control the degree of cell

contact with supporting materials as well the degree of contact with neighbouring cells, including direct physical contact with both homotypic and heterotypic cell types. This enables us to conduct highly controlled *in vitro* experiments to gain insight into basic cell biology and will allow us a much greater flexibility in the control of cell behavior towards the development of new biotechnologies.

While patterning of single cell types has been extensively reported and reviewed in the literature, relatively few studies were found tackling the additional challenge of patterning multiple cell types on the same substrate. This review will first briefly explore various methods used to design a patterned cellular environment. This will set the stage for techniques to pattern multiple cell types. Focus will be given to the methods used to create controlled co-culture systems and their applications found to date.

3.2 Overview of Patterning Techniques

The concept of single cell-type patterning has been around for decades. Over this period of time several major techniques have evolved. These techniques mark the first steps forward in designing more controlled local cellular environments. Some of the key developments will be briefly reviewed in a historical chronology.

3.2.1 In the Beginning

Cell patterning first originated with Carter in the 1960s. These early works involved metal evaporation and subsequent deposition onto a cell non-adherent surface through a stencil-like mask. The deposited metal created patterned islands that supported the growth of different cell types including mouse fibroblasts and human amnion cells. This technique brought about a way to create more controlled experiments; the pattern allowed one to track individual cells and to monitor their responses for several days *in vitro* over the course of a biological study.[6-8]

Studies employing metal deposition patterning were continued by several other groups.[9-12] Through the 1970s and 1980s new patterning methods were developed with a trend towards using naturally occurring materials found in the cellular environment. Ivanova

and Margolis patterned glass with a layer of nonadhesive phospholipids that could be subsequently scraped off in selected regions to allow cell adhesion.[13] Furshpan et al. applied droplets of collagen to a substrate in a pattern to create adhesive islands for the adhesion of cardiac myocytes and sympathetic neurons in a micro-culture to study chemical signaling between the cell types.[14] Hammarback et al. used UV light to pattern laminin through a mask, and were able to guide neurite outgrowth from primary neuronal cells along paths of unirradiated laminin.[15,16]

3.2.2 Photolithography

A major breakthrough in cell micropatterning came in the late 1980s, when Kleinfeld and colleagues borrowed the photolithography process from the microelectronics industry. Photolithography involves the use of materials termed photoresists that have the characteristic of being altered upon irradiation to become either soluble or insoluble in particular solvents. In this process, substrates are coated with photoresist which is subsequently exposed to irradiation through a stencil-like photomask. Solvent is then used to wash away portions of the photoresist, in what is termed "development", creating a pattern on the substrate as dictated by the original pattern on the photomask.[17] Kleinfeld et al. combined the photolithography process with silane chemistry to pattern cells by the method shown in Figure 3.1.[18]

Since the 1980s, numerous cell patterning studies have employed photolithography.[19-21] This method is well-studied and highly reproducible due to its established application in microelectronics manufacturing. Currently, photolithography can achieve submicron features, even down to tens of nanometers, and patterned molecules can be covalently bound to a substrate for pattern longevity.[22] However, photolithography requires expensive equipment and clean rooms for manufacturing, which are often not available to an average biology laboratory. Furthermore, the use of harsh solvents in the development process can hinder the use of biomolecules which are often easily denatured.

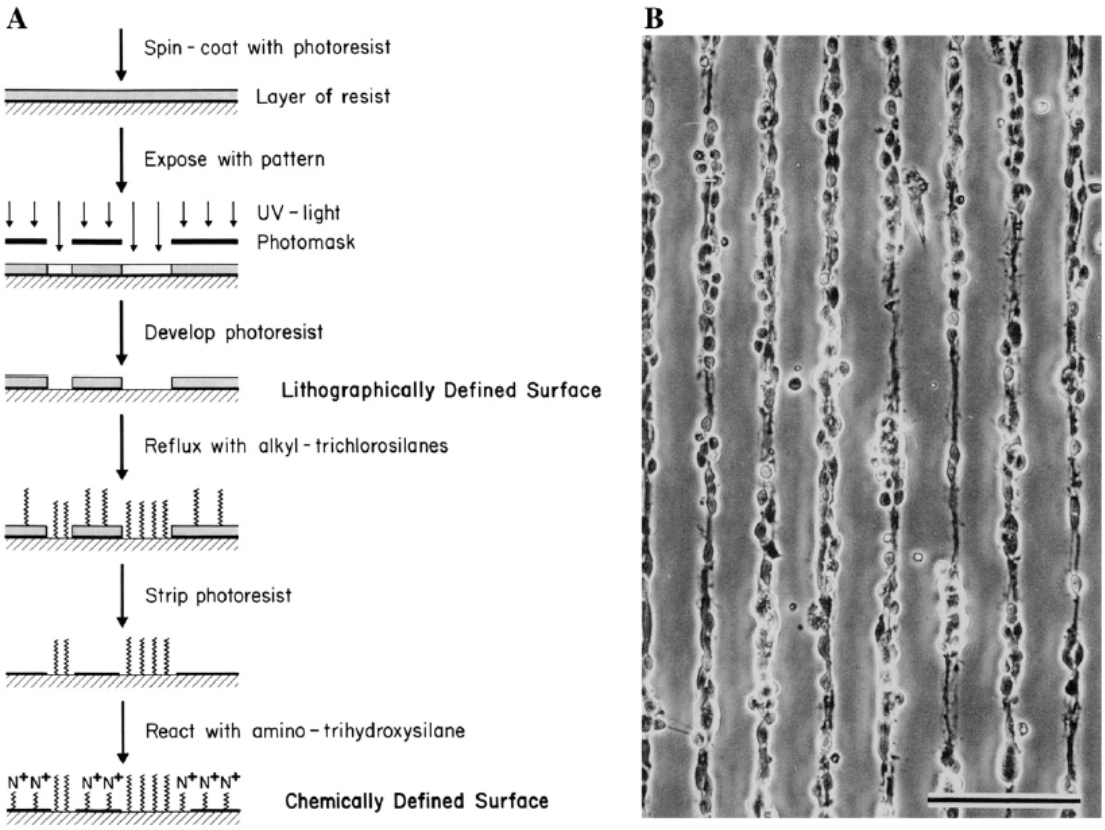

Figure 3.1: (A) Schematic of photolithographic patterning method. The final pattern consists of alkyl-trichlorosilanes (cell non-adhesive) and amino-trihydroxysilanes (cell adhesive) chemically bound to the substrate **(B)** Resulting patterned neurons, scale bar = 100 μm.[18] Reproduced from Kleinfeld, D, et al., Controlled Outgrowth of Dissociated Neurons on Patterned Substrates. *The Journal of Neuroscience* 1988; 8(11): 4098-4120 by permission of The Society for Neuroscience.

3.2.3 Soft Lithography Techniques

To address some of the drawbacks associated with photolithography, Whitesides and colleagues developed a technique called soft lithography. This method utilizes photolithographic techniques to design a patterned, soft, elastic material in the form of a stamp, mould, or mask, which is in turn used to pattern a substrate. Generally, this elastic material is poly(dimethylsiloxane) (PDMS).[23,24] The use of PDMS masters to essentially stamp a pattern onto an underlying substrate through surface adsorption or the formation of self-assembled monolayers (SAMs) is termed microcontact printing (μCP). This technique has been utilized and further developed by a number of groups. Figure 3.2 shows a method developed by Chen et al. to directly stamp protein molecules onto a surface.[25-28]

Based on the soft lithography principle, flexible masks, membranes, or stencils have also been designed such that biomolecules and cells can be patterned directly onto a surface through holes in the pattern.[29,30] In one popular method, microfluidics, a flexible mould or stamp is sealed against a surface to form microchannels. Subsequently, fluid containing active substances can be drawn by capillary forces into the channels in the mould. Pattern formation can then occur in a number of different manners. It can involve 2-D manipulation of surface properties, such as deposition of bioactive molecules onto the substrate through either adsorption or SAM formation, as shown in Figure 3.3.[31,32] In addition, microfluidics can be used to create a 3-D topography by carrying an etching solution through the microchannels to create grooves in the substrate which can be used to guide cell placement.[33] The inverse of this process can also be performed, whereby unpolymerized gel solutions are drawn into the channels within which they polymerize and solidify, producing a pattern in 3-D.[3,34] Drawbacks to microfluidic patterning include limited pattern complexity and generally only continuous pattern features can be achieved. Both are due to the need to have large enough micro-channels for adequate flow and minimal spacing between channels to prevent collapse of the stamp structure.

With the soft lithography techniques, photolithography equipment is still needed to generate the patterned elastomeric master. Fortunately, once generated, the elastic master can be re-used thus making these techniques often cheaper and more accessible than pure photolithography methods to biologists. Using PDMS stamps, features as small as 500 nm can be routinely prepared.[35] However, pattern longevity can be a concern due to the increased reliance on adsorption of this method. Unlike photolithography, soft lithography techniques do not require a planar surface for patterning, due to the highly elastic nature of the PDMS master. 3-D patterns using a variety of materials can easily be generated allowing for the manipulation of topographical as well as chemical cues to influence cell behavior.[23]

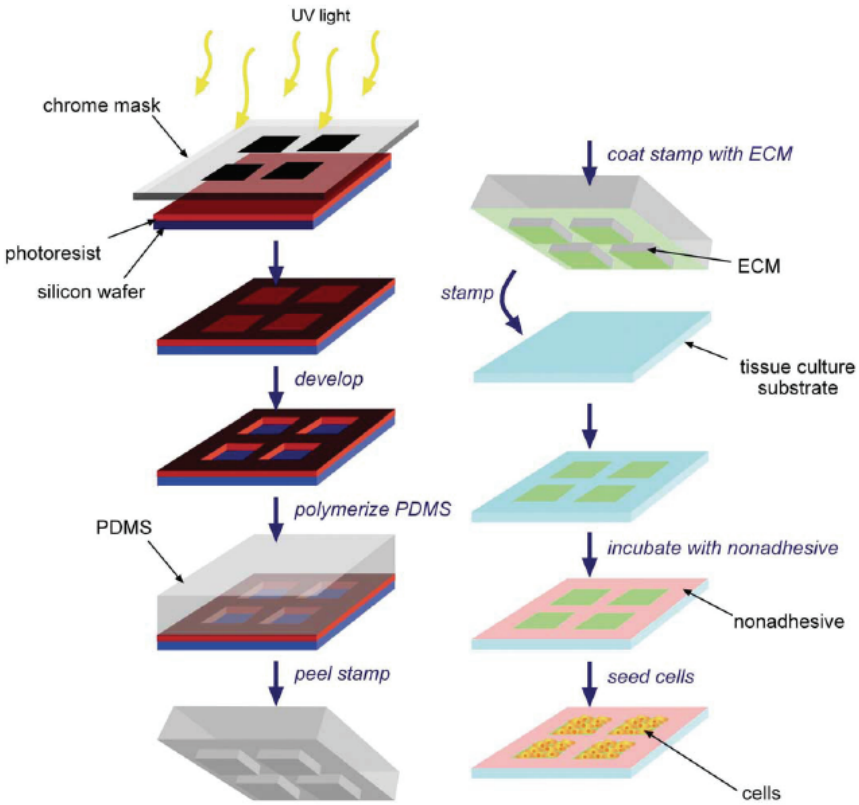

Figure 3.2: Schematic of the μCP process for direct stamping of matrix proteins onto a surface.[27] Reprinted from *Materials Today*, 8(12), Liu, WF and Chen, CS, Engineering Biomaterials to Control Cell Function, pages no. 28-35, Copyright (2005), with permission from Elsevier.

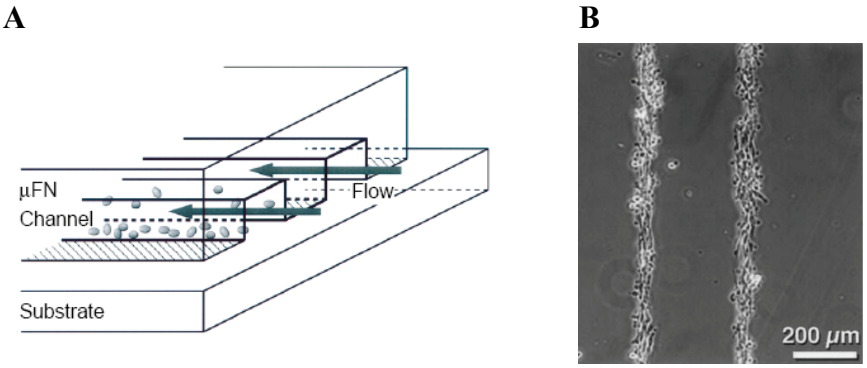

Figure 3.3: **(A)** Schematic of patterning using a microfluidic network (μFN) by Delamarche and Bernard.[31] From Delamarche, E, et al., Patterned delivery of immunoglobulins to surfaces using microfluidic networks. Science 1997; 276(5313): 779-781. Reprinted with permission of AAAS. **(B)** Bovine aortic endothelial cells patterned on lanes containing the cell-adhesive peptide sequence RGD by Patel et al. using microfluidics.[32] Reproduced from Patel, N, et al., Spatially controlled cell engineering on biodegradable polymer surfaces. The *FASEB* Journal 1998; 12(14): 1447-1454 by permission of The Federation of American Societies for Experimental Biology.

3.2.4 Printing Techniques

Another technique that has arisen is the adaptation of ink-jet printers for cellular patterning. In the printing process, droplets of liquid tens of microns in diameter are deposited onto a substrate in a computer-programmed pattern. The liquid can contain a cell-adhesive material, such as fibronectin, which dries onto the printed substrate.[36,37] Interestingly, droplets containing cell suspensions have been reported to be directly printed onto a surface.[38] Recently, researches have designed complex three-dimensional constructs which can be printed in a layer-by-layer fashion.[39,40] While lithography can produce a higher pattern resolution, use of the printing method can be advantageous as one is able to change master design patterns with ease. As a result, high throughput patterning can be achieved by simply "printing" out cell patterns. In addition, equipment needed for this technique can be made by modifying commercial ink-jet printers, dramatically lowering equipment costs.

This section has provided a brief overview of basic cell patterning techniques. For more detailed information, interested readers are referred to more comprehensive reviews on the subject.[41-45] The following section will focus on techniques to pattern different cell types in the same culture (i.e. co-culture) and their potential applications in areas such as cell biology and regenerative medicine.

3.3. Co-culture

One of the greatest challenges in creating a controlled local cellular environment *in vitro* is the development of a micropatterned co-culture system. In order to truly simulate the local cellular environments that comprise multicellular organisms *in vivo*, *in vitro* designs must control both heterotypic and homotypic cell-cell interactions. In the body, various cell types are optimally positioned relative to one another to act in concert in order to perform certain functions within a complex tissue of which they are but a small part. Here, heterotypic interactions provide cells with cues necessary for normal development, differentiation, organization, and homeostasis.[46-48] In order to create designs with controlled cellular microenvironments that mimic the *in vivo* environment, it becomes necessary to develop designs that incorporate spatial patterning of multiple cell types. These designs can

allow for the study of heterotypic cell-cell interactions – through either receptor activated signaling or direct cell-cell contact – necessary for cell survival and maintenance of *in vivo* functions. The knowledge gained from such studies can then be applied towards the creation of new and innovative cell-based devices. However, the design of such a pattern does pose a fascinating challenge. This is because after patterning an initial cell type on a substrate, a second cell pattern must be created without exposing the already patterned cell types to harsh chemical or physical conditions which are often employed in patterning single cell types. Furthermore, pattern alignment must be considered; the second cell pattern must be precisely deposited relative to the first in order to control interactions between the two cell types. The following text will attempt to highlight various co-culture techniques developed to date to address these design issues while demonstrating along the way the growing array of applications that they have found.

3.3.1 Switchable Surfaces

The first design tackles the co-culture patterning challenge through the creation of "switchable surfaces." Such surfaces contain patterned cell-adhesive regions surrounded by regions that are non-adhesive to cells. These non-adhesive regions are designed in such a way that they can be subsequently switched to become cell-adhesive to a secondary cell type under mild conditions, allowing for patterning in co-culture. The second pattern is typically aligned to the first in that the second cell type merely fills the space surrounding the initially seeded cells.

3.3.1.1 Initial Designs with Protein Patterning and Serum Manipulation

The first to develop a micropatterning technique to control the degree of heterotypic cell contact in co-culture was Bhatia et al. in 1997.[49] Photolithography was utilized to generate a pattern of cell adhesive proteins, specifically collagen, on a glass substrate. Prior to cell seeding, the remaining glass surface was exposed to bovine serum albumin (BSA) to create a cell repellant background against the cell adhesive collagen islands. Hepatocytes were first seeded onto the surface in a serum-free medium, and remained attached only to the collagen-patterned regions after rinsing. The second cell type, fibroblasts, was seeded onto the substrate in serum containing media which facilitated cell adhesion to the previously

repellent BSA background. This process is depicted in Figure 3.4, along with an image of the resulting hepatocyte – fibroblast co-culture. In explaining why BSA could be used as a cell repellent to pattern cells only under serum-free conditions, a subsequent study by Nelson et al. found that factors in serum activated cell-secreted proteases, which in turn degraded the BSA, and thus eliminated the cell repellent surface created by the BSA.[50]

Using this patterned co-culture technique, Bhatia et al. investigated the maintenance of hepatocyte liver-specific cell functions *in vitro* by examining the impact of fibroblast co-culture on hepatocytes.[51] This cellular system is frequently the focus of micropatterned co-cultures since cultivation of hepatocytes alone *in vitro* very often leads to loss in liver-specific cell functions. This can greatly hinder the use of these cells that are vitally important in studies of liver diseases, the design of bioartificial livers, and in biosensors for drug toxicity screenings. To this end, co-cultures with sinusoidal cells (mainly endothelial and Kupffer cells) and fibroblasts have been demonstrated to help maintain viability and liver-specific functions of the hepatocytes in culture.[52,53] Bhatia et al. designed three different co-culture systems for study, whereby hepatocyte homotypic and heterotypic interactions were held constant while fibroblast homotypic interactions were varied. With this highly controlled co-culture system, it was demonstrated that increased homotypic fibroblast interactions enhanced the maintenance of liver-specific functions.

Other studies have implemented this co-culture technique.[30,54-56] Beyond studies of basic biology, this technique has found applications in the area of cell-based devices. Such patterned co-cultures were implemented in the development of hepatocyte arrays as screening devices for liver toxicity. It was hypothesized that hepatocytes co-cultured with fibroblasts could maintain liver-specific functions and be made to mimic an *in vivo* liver response to drug candidates in toxicity tests. To demonstrate, Kane et al. patterned a co-culture in an 8x8 array of 3.25mm wells connected to microfluidic perfusion networks delivering fresh media and oxygen. Hepatocytes in this study were shown to produce albumin and urea, two typical liver function markers, reaching steady production by day 20 of the study and continuing until day 32 when the study was terminated.[52]

A

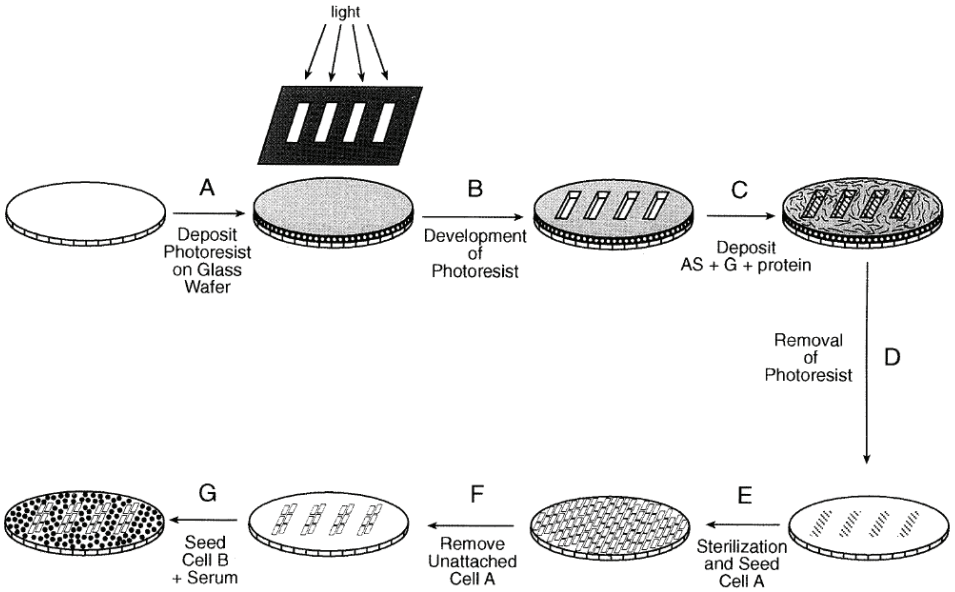

B

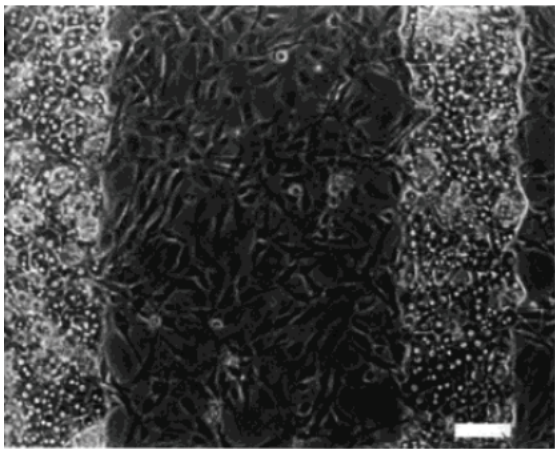

Figure 3.4: (A) Schematic of the process developed by Bhatia et al. (1997) to create micropatterned co-cultures. Photolithography was used to create a pattern in photoresist on a glass wafer. Aminosilanes (AS) were subsequently bound to the patterned surface. Glutaraldehyde (G) was then used to link cell-adhesive protein to the AS. Removal of the photoresist revealed a pattern of cell-adhesive protein. BSA was bound to the glass background. A first cell-type was seeded in serum-free media. After rinsing, cells remained attached only to the patterned proteins. A second cell type was then seeded in the presence of serum facilitating adhesion to the non-patterned regions.
(B) Hepatocytes adhering to 200 μm patterned collagen protein lanes surrounded by fibroblasts.[49] Controlling cell interactions by micropatterning in co-cultures: Hepatocytes and NIH 3T3 fibroblasts, Vol. 34, No. 2, 1997, page no. 189-199. Copyright © (1997, John Wiley & Sons, Inc.) Reprinted with permission of John Wiley & Sons, Inc.

Towards a similar aim, Khetani and Bhatia also developed a cellular array based on multi-well plates. Studies of the device found that liver-specific functions could be optimized by controlling the size and spacing of the collagen islands supporting hepatocytes in the plates. As a result, the liver-specific functions were reported to be maintained for several weeks. Significantly, it was found that there was a several-fold increase in the liver-specific functions for patterned co-cultures as compared to equivalent random co-cultures. This clearly demonstrates how well-controlled local cellular environments, including cell-cell interactions, can lend greatly to the ability to achieve *in vivo* functions *in vitro*. The study was further able to quantify model hepatotoxins using the co-culture system.[57]

These designs have been shown to be effective and have found notable applications. Treatment with repellent BSA and serum manipulations are relatively mild operations that allow for the survival of an already seeded cell type while a previously repellent background is made adhesive. However, these design strategies may present complications. For example, it may be difficult to pattern certain cell types in serum-free media if the cell type traditionally requires serum for survival. Furthermore, given the fact that serum varies in composition from batch to batch and that the serum is critical in switching the cell adhesiveness of the substrate for patterning, the co-culture technique based on this method could produce results that vary from experiment to experiment.

3.3.1.2 Thermally Responsive Polymers

Another major strategy based on switchable surfaces to form patterned co-cultures was originally developed by Yamato et al. who employed thermally responsive polymers.[58,59] One such thermally responsive polymer, poly(*N*-isopropylacrylamide) (PIPAAm), is cell non-adhesive below 32^{o}C but cell adhesive above this temperature. At lower temperatures the material is fully hydrated making it highly hydrophilic and repellent to cells. Above 32^{o}C, the polymer network collapses making the polymer dehydrated and relatively hydrophobic, thereby becoming adhesive to cells.[60] Copolymers of the material can be meticulously designed to vary the transition temperature at which the material becomes adhesive. As a result of this unique thermal responsiveness, PIPAAm can be first used at low temperatures as a cell-repellent background on an otherwise adhesive surface to

pattern one cell type. It can subsequently be switched to become cell-adherent for the patterning of a second cell type by merely increasing the culture temperature above the transition temperature. Based on this principle, Yamato et al. have created a patterned co-culture for use in tissue engineering applications. As shown in Figure 3.5, an entire pattern made out of PIPAAm and its copolymer was prepared to seed cell types at different temperatures in the creation of a patterned co-culture. At lower temperatures, the entire material surface became cell-repellent. Therefore, by dropping the culture temperature of a confluent patterned co-culture, cells could be neatly removed from the PIPAAm-based temperature responsive surface in the form of a cell sheet. Using this method, functional cell sheets containing patterned co-cultures have been harvested and implanted into host tissues.[61,62] Temperature fluctuations within the range of 20˚C to 37˚C are relatively mild for the initially seeded cell type and allow for the switching of a surface from repellent to adhesive or vice versa to create a patterned co-culture.

This approach was used to create bioengineered tissues in which extremely high cell densities are desired, such as in the heart. For instance, Matsuda et al. engineered cardiomyocyte and endothelial co-patterned cell sheets and wrapped them around blood vessels in adult rats. It was shown that the cardiomyocytes were able to pulsate in a synchronized and spontaneous fashion for four weeks. Meanwhile, the endothelial cells in the sheets were found to form blood vessels *in vivo* to support cardiomyocyte survival. Such a technology shows great promise for the development of a cardiac assist device and could be employed towards the regeneration of a wide variety of other tissue types.[61]

Interestingly, Cheng et al. also took advantage of PIPAAm in a novel manner. Photolithography was used to create a microheater array underneath a PIPAAm surface. Individually controlled heaters beneath the polymer were turned on to increase the local temperature in some areas of the material to switch small areas of the surface from cell non-adhesive to adhesive. By turning on selected heaters and seeding one cell type, and then activating more heaters followed by the seeding of a second cell type, a controlled pattern of co-cultured cells was created as seen in Figure 3.6.[63]

A

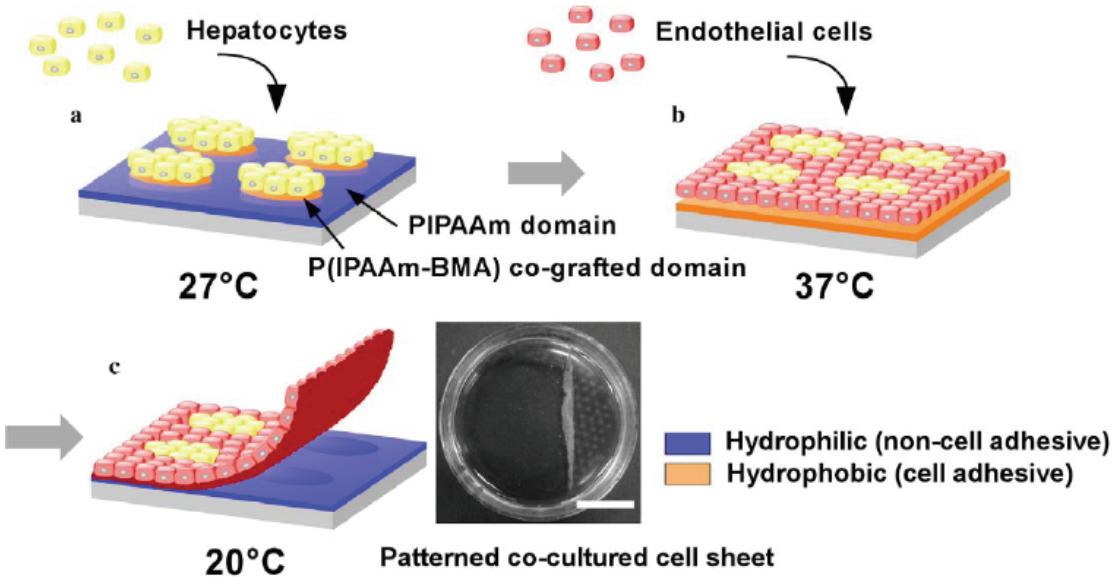

B

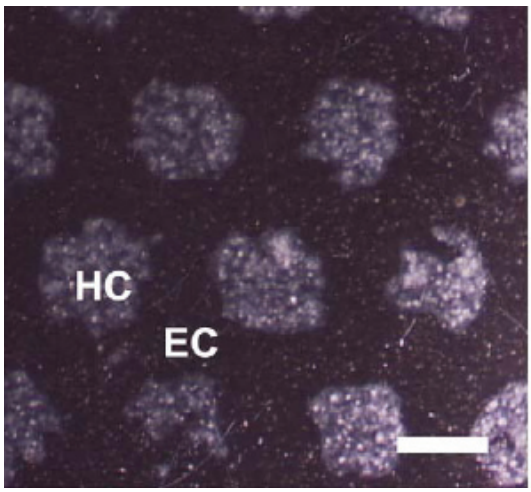

Figure 3.5: (A) Schematic of co-culture sheet design. (a) First, patterned regions on a PIPAAm background containing a copolymer of n-butylmethacrylate (BMA) and PIPAAm are generated, which are cell adhesive at 27°C. (b) The temperature of the material is then raised to 37°C, at which the PIPAAm is also adhesive, and now a second cell type can be seeded. (c) Dropping the temperature to 20°C makes the entire surface nonadhesive, and thus allows for the removal of the entire confluent cell sheet.
(B) A co-culture pattern consisting of hepatocytes (HC) and endothelial cells (EC), scale bar = 500 μm.[62] Reprinted from *Biochemical and Biophysical Research Communications*, 348(3), Tsuda, Y, Kikuchi, A, Yamato, M, Chen, G, Okano, T, Heterotypic cell interactions on a dually patterned surface, pages no. 937-944, Copyright (2006), with permission from Elsevier.

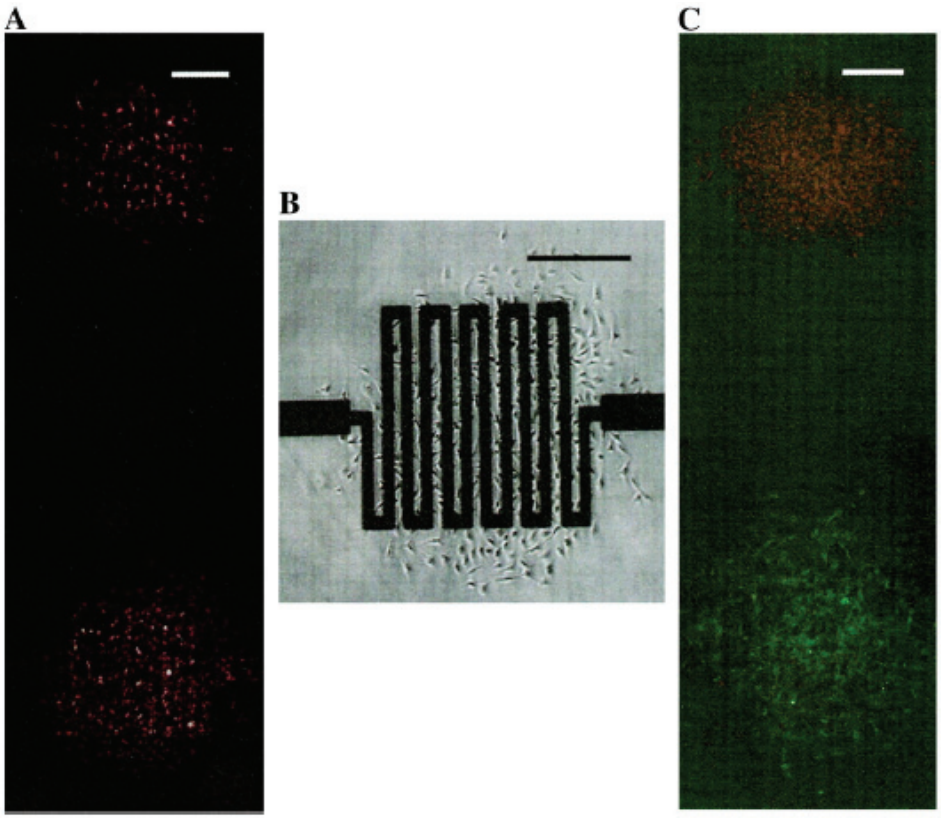

Figure 3.6: (A) Fluorescence micrograph of patterned bovine aortic endothelial cells (BAECs) adhering onto two heated areas of the polymer surface.**(B)** Phase contrast micrograph of BAECs adhering to the region around the top heater from image (A).
(C) Fluorescence micrograph of patterned BAECs and bovine smooth muscle cells adhering to two separate heated regions of the polymer surface, scale bars= 500 μm.[63] *Journal of Biomedical Materials Research Part A*, Vol. 70A, No. 2, 2004, pages no. 159-168. Copyright © 2004, John Wiley & Sons, Inc. Reprinted with permission of John Wiley & Sons, Inc.

This technique allows for the switching of a repellent surface to a cell-adhesive one without exposing the already patterned cells to any temperature fluctuations, as compared to the cell sheet. Furthermore, subsequent cell patterns can be easily aligned to the first; patterns are merely determined by which heaters are turned on during cell seeding. In this way, this method allowed for precise spatial localization of two cell types, and has the potential to pattern even more cell types. However, the minimum size of the adhesive islands could be limited by both the minimum size of the heaters and heat transfer laterally away from the edges of the heater. Furthermore, culture conditions will not be uniform across the polymer substrate since temperature gradients exist around the heaters.

3.3.1.3 Layer-by-Layer Technique and Electrostatic Forces

Another set of "switchable surface" patterning techniques makes use of electrostatic interactions. A charged, cell nonadhesive background is implemented such that it can be switched to cell adhesive by layering a complimentarily charged cell-permissive material onto the surface bound by electrostatic interactions. Yang et al. used soft lithography to generate a pattern of anionic cell-resistant polyelectrolytes, namely oligo(ethylene glycol) methacrylate and methacrylic acid copolymers onto various cell-adhesive substrates. After the initial seeding of neuronal cells onto the areas where the cell-adhesive substrate was exposed, the cell repellant anionic area was rendered adhesive to glial cells through the adsorption of a cationic adhesive material, such as poly(L-lysine) (PLL), chitosan, or poly(ethylenimine) (PEI).[64]

Electrostatics based methods are especially suited for the implementation of materials naturally occurring in the body. For example, glycosaminoglycans such as hyaluronic acid (HA) are natural components of the extracellular matrix and are highly charged. In one study, Fukuda et al. utilized a layer-by-layer deposition approach using extracellular matrix materials, such as HA, collagen, and fibronectin, in the formation a micropatterned co-culture. Pattern generation involved a PDMS mould and capillary force lithography as detailed in Figure 3.7.[65,66] The use of such materials has the potential to more closely mimic the true natural local cellular environment, especially when they are combined with a patterned co-culture.

This layer-by-layer co-culture patterning technique has found applications in the study of cell-cell interactions. Kidambi et al. applied a polyelectrolyte based co-culture pattern to study a primary culture of neuronal cells and astrocytes. In this study, the response of the co-culture to high levels of saturated free fatty acids, which have previously been shown to be involved in the pathogenesis of Alzheimer's, was studied. It was found that the neuronal cells in patterned co-cultures responded quicker to increased free fatty acid levels by elevating cellular levels of reactive oxygen species as compared to separated monocultures and random co-cultures. The patterned co-culture system was an ideal

platform for such a study since astrocytes and neurons are shown to be closely associated *in vivo* where cell-cell communications impact their mutual metabolism and development.

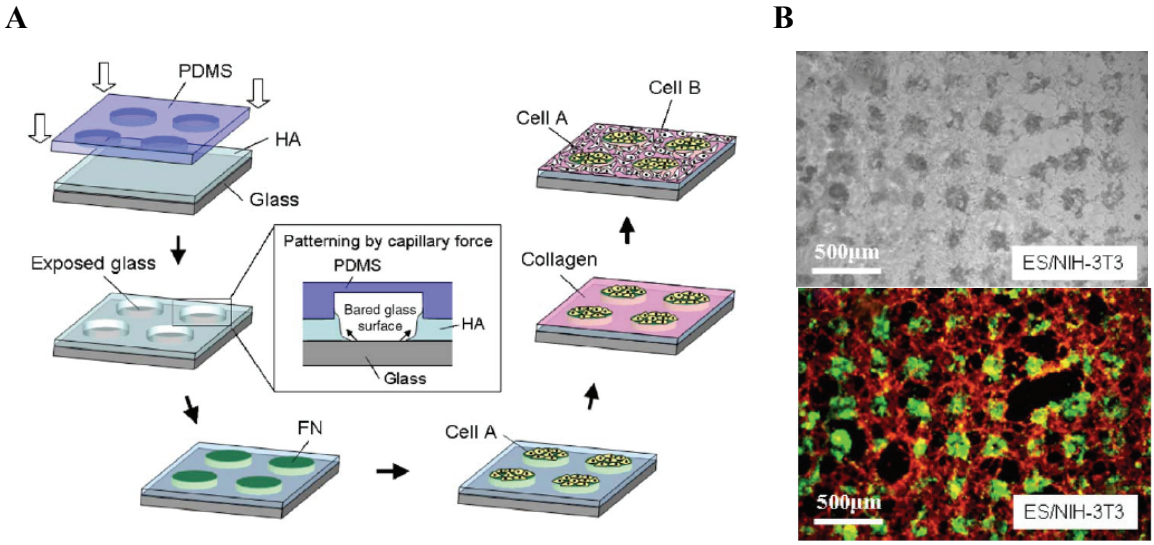

Figure 3.7: (A) A layer of HA was spin coated onto a glass slide, and immediately a PDMS mould was placed atop the surface. The highly hydrophilic HA receded from the void space under the hydrophobic PDMS, leaving patterned bare regions of glass (process of capillary force lithography). These bare regions were then coated with FN. Since HA repels cells, cell type A was seeded and adhered to the FN regions. Then collagen was bound to the HA through electrostatic forces, and cell type B was then seeded onto the surface, adhering to the cell-adhesive collagen layer.
(B) Patterned co-culture of murine embryonic stem cells (green) and fibroblasts (red) as seen using light microscopy and fluorescence.[66] Reprinted from *Biomaterials*, 27(8), Fukuda, J, Khademhosseini, A, Yeh, J, Eng, G, Cheng, J, Farokhzad, OC, and Langer, R, Micropatterned cell co-cultures using layer-by-layer deposition of extracellular matrix components, pages no. 1479-1486, Copyright (2006), with permission from Elsevier.

It is therefore advantageous to study their behavior together as a unit. Furthermore, neural networks in the brain are not random as in a traditional culture but found in highly organized patterns.[67] This example demonstrates the power of patterned co-culture studies to elucidate knowledge of basic biology and specifically further our understanding of neurodegenerative diseases. Further applications in new biotechnologies appear to be on the horizon for this co-culture patterning method as well, since this layer-by-layer technique has the capability to pattern a co-culture within silicon tubing. The ability to pattern within a tubular structure presents unique opportunities as it enables highly controlled studies to test cellular responses to mechanical stresses in a co-culture setting, such as exposure to shear flows inside a tube.

Tubular structures are also commonly found in reactors; patterned tubes could foreseeably be employed in bioreactors with cell functions optimized through co-culture patterning.[68]

In this layer-by-layer design strategy, the cells initially seeded on the pattern are exposed to a soluble cell-adhesive electrolyte that binds to an oppositely charged non-adhesive complimentary electrolyte on the surface. Care must be taken to ensure that solutions of the soluble cell-adhesive electrolyte are not toxic to the first cell type deposited. Once again, the second pattern generally aligns to the first by occupying the space surrounding the initially seeded cells.

3.3.1.4 Miscellaneous

Another unique patterning methodology, also based on a switchable surface, took advantage of the properties of chitosan gel to create a pattern. Fukuda et al. created microwells in a cell-repellent chitosan surface making regions of low shear stress to facilitate cell immobilization. Hepatocytes became trapped in these wells upon seeding and formed 3-D spheroid aggregates while cells outside of these wells were washed away. The photocrosslinkable chitosan changed spontaneously over time after initial cell culture, switching from non-adhesive to cell-adhesive to allow for the deposition of a second cell type on the areas surrounding the microwells. Despite the potential ease of implementation, widespread application of this method may be questionable as the exact reason behind the change in chitosan cell adhesive properties is yet unknown, although it was speculated that this change in chitosan adhesiveness could be due to protein adsorption over time.[69]

All of the methods described so far, either based on serum manipulation, thermo-responsive polymers, electrostatics, or others, are able to solve the design issue of patterning multiple cell types by creating "switchable surfaces" whereby a previously cell nonadhesive background on a material can be made adhesive to a secondary cell type through mild manipulations. These methods rely heavily on surface chemistry. Generally, the first cell type is seeded in a pre-designed pattern, whereas the second cell type seeded merely fills in the background space. While this allows for easy alignment of the two patterns, it can be concluded that spatial control over the seeding of the second cell type is lacking.

Nevertheless, these patterns show great creativity in design and have found numerous applications, such as controlled biological studies investigating cell behavior, development of cellular arrays for screening new drugs, and tissue engineering.

3.3.2 Manipulating Soft Lithography for Co-culture Patterning

Another set of strategies involve the manipulation of soft lithography techniques and PDMS stamps. These stamps have been utilized in a number of unique and creative ways by a variety of groups to facilitate the patterning of multiple cell types without having to create switchable surfaces.

3.3.2.1 Microfluidics

The majority of these strategies are based on microfluidics. Co-culture patterns can be realized through the design of increasingly complex PDMS stamps from those used to develop single-cell patterns. For example, Chiu et al. studied the idea of developing a 3-D microfluidics system in a PDMS stamp for the patterning of multiple cell types. The stamp contained two completely separate channel systems that formed when the stamp was pressed into an underlying substrate. One cell type could flow through one channel and be deposited onto the underlying substrate along that channel, while a second and separate channel could contain a second cell type that could then be deposited onto another area of the substrate. Thus, separate channels allowed for the flow and deposition of different cell types. Figure 3.8(A) shows one such channel system formed by a 3-D pattern in PDMS with channels for one cell type in red and a separate channel system for a second cell type in green. Figure 3.8(B) shows the resulting cell pattern.[70]

In another study, Khademhosseini et al. utilized a similar technique, employing multiple independent microfluidic channels to pattern multiple cell types but with an added feature – patterned microwells in the fluid paths to trap cells in areas of low shear force. Instead of lined patterns of cells, patterns containing small islands of cells of a particular type embedded in microwells were achieved.[71] This group was later able to apply patterned microwells in a PDMS substrate to culture human embryonic stem cells in a patterned co-culture with murine embryonic fibroblasts (the stem cells to remain undifferentiated). The

microwells served to control the size and shape of the stem cell clusters, thus providing a method to produce these valued cells in a controlled manner so that they can be harvested and used in stem cell research.[72]

A **B**

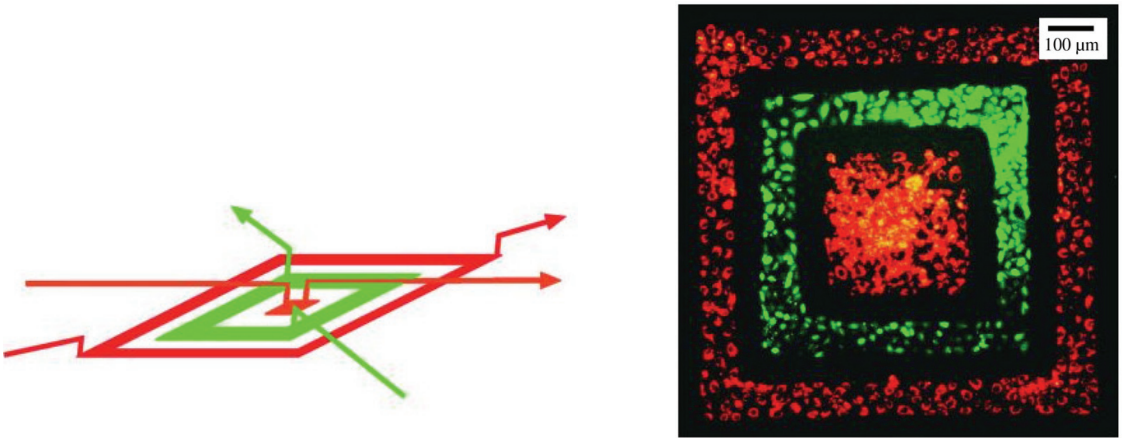

Figure 3.8: (A) 3-D channel micropattern in a PDMS stamp. **(B)** Fluorescence picture of bovine adrenal capillary endothelial cells (red) and human bladder cancer cells (green) patterned using the 3-D stamp.[70] Reproduced from Chiu DT, et al., Patterned deposition of cells and proteins onto surfaces by using three-dimensional microfluidic systems. *Proceedings of the National Academy of Sciences of the United States of America* 2000; 97(6): 2408-2413. Copyright (2000) National Academy of Sciences, U.S.A.

With these co-culture design strategies employing microfluidics, two different cell types can essentially be patterned onto a surface at the same time. This forgoes the need to expose one cell type to changing conditions to allow for the patterning of a second cell type. Pattern alignment is achieved through the design of separate channels in the complex PDMS stamp for the flow of different cell types.

Other patterning strategies have manipulated microfluidics to realize a 3-D co-culture pattern. These strategies have avoided the use of complex PDMS stamps, but focus more on unique strategies for depositing materials in the stamp channels. Tan and Desai developed a strategy which involved flowing ECM solution containing cells through microchannels created by a PDMS stamp against a surface at low temperatures. Heating the ECM material to 37°C facilitated its polymerization. Subsequent contraction of the matrix then occurred as a function of cell concentration, matrix composition, and time. This contraction resulted in

freed space within the PDMS channels through which another solution composed of different matrix components and cells could be passed. Different cell types were therefore patterned by merely depositing one on top of the other. This strategy was used to create three layers of different matrix components and cell types that modeled the structure and composition of a blood vessel wall. A schematic of the process can be seen in Figure 3.9.[73]

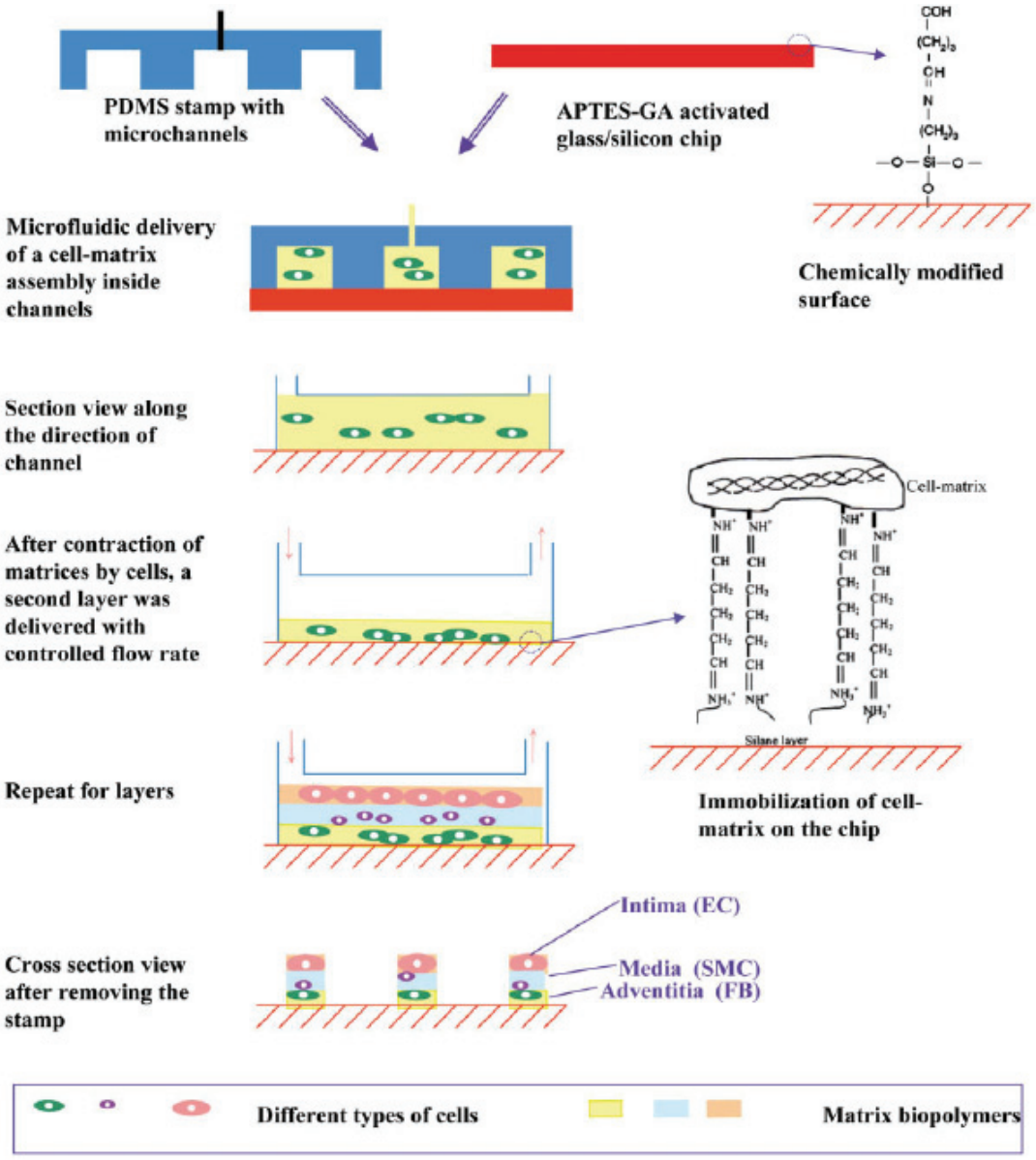

Figure 3.9: Schematic for the creation of a patterned 3-D cell co-culture using microfluidics.[73] *Journal of Biomedical Materials Research Part A*, Vol. 72A, No. 2, 2005, pages no. 146-160. Copyright © (2005, John Wiley & Sons, Inc.) Reprinted with permission of John Wiley & Sons, Inc.

With this technology, however, the stamp had to remain on top of the pattern to prevent extensive migration of cells out of the matrices. This would have prevented optimal imaging of the cells and could ultimately result in diffusional limitations of nutrients to the culture.

Bruzewicz et al. also designed a 3-D co-culture pattern in microfluidic chambers.[74] Modules were created consisting of cells encased in 3-D collagen gels. The modules, with a size in the range of hundreds of microns, some containing fibroblasts and others HepG2 cells, were then injected into microfluidic channels on a chip. The order of the modules containing specific cell types in the channels could be controlled when the width of the microfluidic channels was decreased and began to approach the width of the modules themselves. In this way, multiple cell types in 3-D gels could be ordered, and thus patterned, within the channels. This device was transparent allowing for optical imaging while the microfluidics system provided the opportunity to adjust a variety of inputs to the system and monitor cell outputs. These designs aimed at 3-D co-culture patterns are of especial interest in biological studies since it is known that cells often behave differently in a 3-D environment which more closely mimics *in vivo* conditions than 2-D surfaces.

3.3.2.2 Microcontact Printing

The previous techniques have all dealt with microfluidics. In contrast, Tien et al. developed a complex 3-D PDMS stamp for microcontact printing a patterned co-culture. In order to pattern two different cells using this method, one would normally have to stamp the substrate twice to generate two distinct patterns. However, the second pattern would need to be aligned precisely with the first, and the mechanics of such an alignment at the micron scale can be challenging. This was overcome by the design of a multi-level elastomeric stamp and multi-level membranes, such as those shown in Figure 3.10.[75] Recently, in a much simpler design strategy, Leclerc et al. utilized PDMS stamps to form a patterned co-culture, but by applying the stamp to a pre-cultured surface thereby crushing the cells underneath the pattern. These cells can then be washed away by flowing fluids through the microchannels created by the stamp and a second cell type can be cultured in the resulting voids.[76]

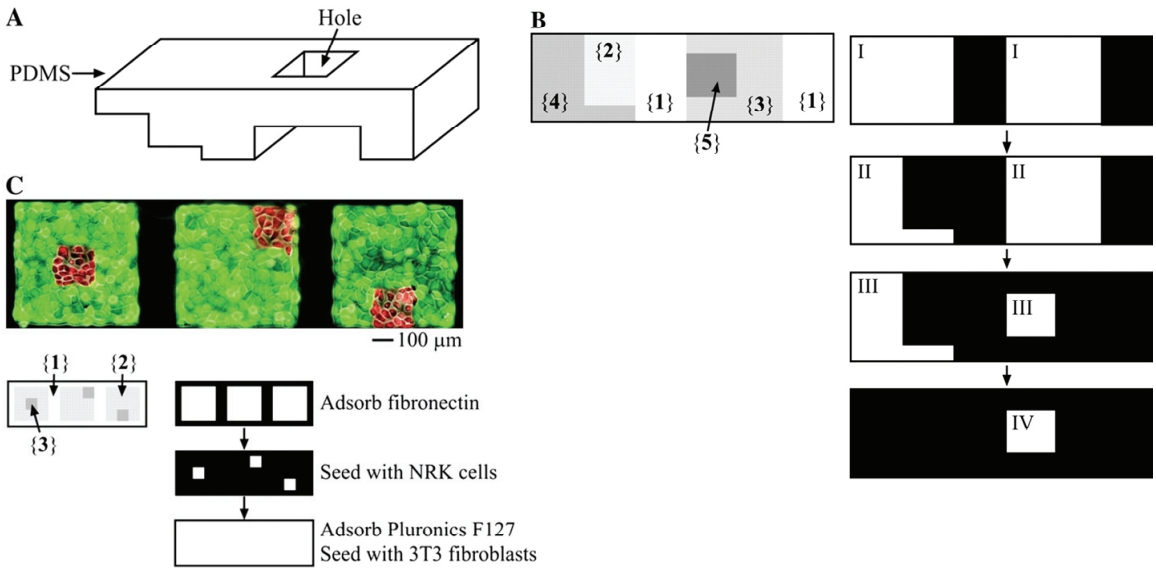

Figure 3.10: (A) Schematic diagram of a five-level PDMS stamp. **(B)** Top view of the patterns that can be created by the stamp as it is pressed increasingly harder onto the substrate. Dark regions indicate areas blocked by the stamp as one or more levels of it are pressed into the substrate. **(C)** Pattern for co-culture of NRK cells and NIH/3T3 fibroblasts created with a 3-layer membrane. While areas 2 and 3 were exposed, they were coated with human fibronectin to create a cell-permissive region, and then area 2 was covered while area 3 alone was seeded with NRK cells (red), and then the membrane was removed, and the whole area was exposed to Pluronics F127, which adsorbed to the only uncoated region, 1. Subsequently, fibroblasts (green) were seeded onto the structure, and they adhered to the uncovered fibronectin region, 2, generating the co-culture pattern seen in the top figure.[75] Reproduced from Tien, J, et al., Fabrication of aligned microstructures with a single elastomeric stamp. *Proceedings of the National Academy of Sciences of the United States of America* 2002; 99(4): 1758-1762. Copyright (2002) National Academy of Sciences, U.S.A.

The techniques discussed here manage to pattern multiple cell types while negating the need to expose an initially patterned cell type to changing culture conditions for switching of a surface from adhesive to non-adhesive and the seeding of a second cell type. Patterning of multiple cell types is achieved through the design of a complex PDMS stamp with multiple channels or layers, or more complex cell seeding techniques within the stamp as in the case of the 3-D structures. For the most part, control over the alignment of the two patterns is accomplished by creating the patterns in a single PDMS stamp. In comparison with switchable surfaces, these techniques can offer improved spatial control over the patterning of multiple cell types since a second cell type can have its own pattern and not merely fill voids left by the originally patterned cells. However, the challenge with these soft

lithography approaches is the complexity of the patterning approach. Many require the construction of very elaborate PDMS stamps. The distance between channels, number of levels, and feature sizes on the stamp can be limited by the structural stability of the stamp itself which in turn imposes limitations on the cell patterns that can be formed from it. Other strategies require complex manipulations in microfluidic channels which would necessitate extensive training and expertise. These limitations may be the reason why these techniques have not yet found many applications. In addition, they may not be readily accessible by an average cell biologist wishing to create patterned co-cultures for study.

3.3.3 Direct Co-culture Patterning Methods

The previously described techniques mostly relied on making modifications to an underlying surface to facilitate the co-culture pattern. The following techniques involve the direct spatial patterning of multiple cells onto a substrate without reliance on surface modifications.

In one such design, Nahmias et al. employed the technique of cell spraying in the creation of a patterned co-culture. Aerosols of cell suspensions were created and a commercial airbrush was used to pattern hepatocytes and fibroblasts onto collagen gels through a mask. It was shown that this technique could be employed to create a 3-D pattern by layering more gel atop the original pattern, and then patterning these layers by cell spraying as well.[77]

Laser-guided direct writing (LGDW) is another such direct method.[78,79] LGDW is based on the principle that laser beams can be used to entrap individual cells and deliver them onto a substrate in a predetermined pattern. When cells move into the path of the laser beam by random movement, the laser draws the cells into a hollow optical fiber and to a secondary laser beam that drives the cells downward onto the substrate.[80,81] This technique has been applied to co-pattern viable neural and glial cells along with polymer microspheres to release growth factors. This strategy has shown great promise in tissue engineering applications because it allows for an investigation into the impact of degradable polymers and controlled release systems on cell-cell interactions in a controlled manner.[82,83] In one

study, human umbilical vein endothelial cells were patterned on Matrigel using LGDW to form vascular structures which were then co-cultured with hepatocytes. Through this process, Nahmias et al. were able to observe an aggregated tubular structure *in vitro* resembling a hepatic sinusoid, a small blood vessel.[81,84] The ability to reproduce complex tissue architectures with patterned co-cultures *in vitro* is an important step towards the *in vitro* reconstruction of complex tissues, such as the liver. The formation of blood vessels among multiple patterned cell types is of critical importance since blood vessels within engineered tissue constructs help to overcome nutrient diffusional limitations upon implantation and thus enhance survival of the implanted constructs.

Such strategies negate the need to modify the underlying substrate for depositions of different cell types so there is no concern with damaging already patterned cell types. Multiple cell types can be patterned directly onto a surface. However, alignment of one cell pattern relative to another must be carefully considered and could be an especial challenge with these techniques. Furthermore, patterned cells are still free to migrate since there is no underlying cell-adhesive boundary layer or PDMS structure holding them in a specific location. This can be beneficial, however, in allowing cells more opportunity to self-assemble to form tissue engineering constructs, or in observing the migration behavior of cells in response to stimuli.

3.3.4 Dynamic Co-culture Systems

Another subset of co-culture systems designed to date are dynamic systems. Previous strategies involving switchable surfaces and soft lithography methods mostly aimed to create a static pattern with longevity. Direct patterning did not always strive for this goal, but the dynamic nature of these surfaces could not be readily controlled. In contrast, patterns created by dynamic systems can be deliberately changed with time in a controlled manner, adding an additional dimension to the patterned co-culture design.

One such system was designed by Hui and Bhatia who employed existing microelectromechanical system fabrication methods to develop a silicon substrate for cell culture with moveable interlocking parts. Two different cell types were separately cultured

on each interlocking part. The two pieces were then locked together to bring the cells into direct contact, held slightly apart to allow the exchange of soluble factors, or moved apart completely, as shown in Figure 3.11.

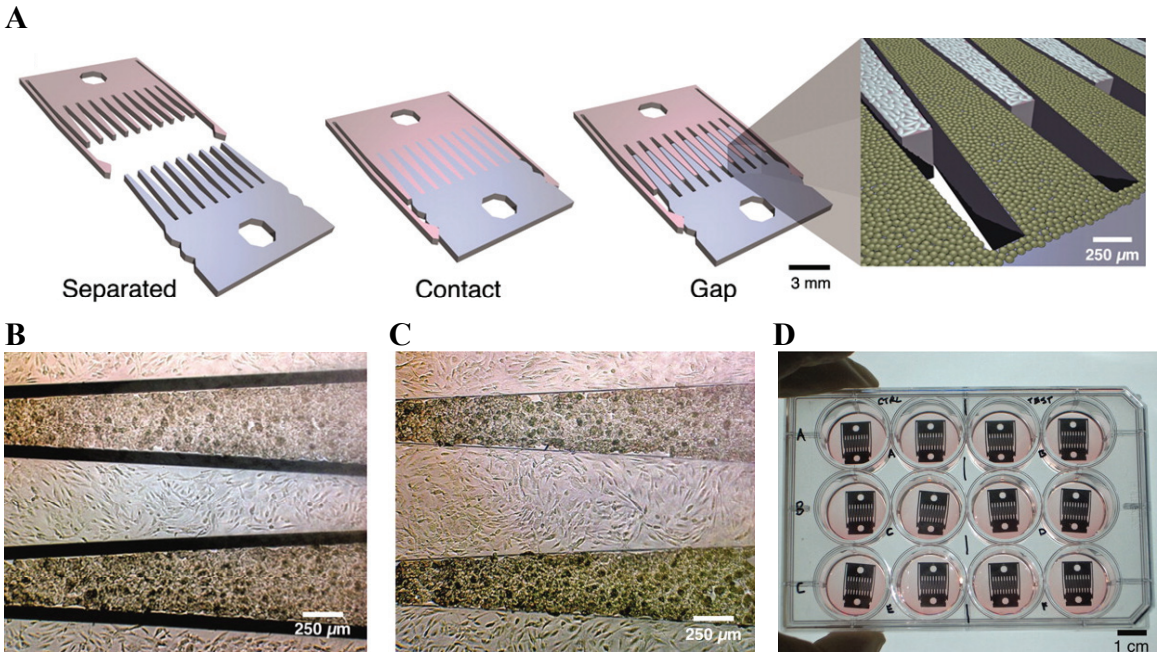

Figure 3.11: (A) Schematic of micromachine with interlocking parts.**(B and C)** Primary hepatocytes and Swiss 3T3 fibroblasts cultured on opposing interlocking comb fingers.**(D)** Devices in 12-well plates.[85] Reproduced from Hui EE and Bhatia SN, Micromechanical control of cell-cell interactions. *Proceedings of the National Academy of Sciences of the United States of America* 2007; 104(14): 5722-5726. Copyright (2007) National Academy of Sciences, U.S.A.

This experimental design was applied towards an investigation into how fibroblast contact influences liver-specific function in hepatocytes, and the group found that maintenance of such function required direct physical contact for a period of time in the range of hours, but only required soluble signaling effective within a 400 μm range afterwards.[85,86]

The ability to independently and dynamically study the effects of soluble signals versus cell-cell physical contacts could easily find this dynamic system a number of biological applications. One compelling potential application is the opportunity to study stem cell fate. It has been shown that contact with other cells influences stem cell fate *in vivo*

and *in vitro*. For example, neural progenitor cells found in the subventricular zone in the brain maintain contacts with neighboring ependymal cells, and when hematopoietic stem cells in the bone marrow break contact with osteoblasts they are found to differentiate. Further examples are provided in the review by Metallo et al.[87] This design could potentially be used to investigate the effects of cell-cell contacts versus soluble signaling on the behavior and differentiation of stem cells. Such controlled experiments which can better separate variables under investigation will enhance our understanding and thus ability to utilize these prized cells for therapeutic purposes.

A couple of other studies have combined soft lithography and switchable surface approaches to produce dynamic co-culture systems. One such system was created using soft lithography to pattern a substrate by seeding cells through a nonadhesive stencil and then modifying the stencil itself to make it adhesive. Cells could then be cultured on the stencil while in contact with the substrate, and the stencil could later be removed, allowing a third cell type to be patterned on the bare areas of the substrate left by the stencil. The design of such a dynamic system allows one to study the effect of time-limited heterotypic interactions which occur naturally when cells interact with neighboring cells for a period of time and then change microenvironments. Such processes occur in immune response and in disease states such as disrupted nerve-nerve and nerve-muscle interactions after spinal cord injuries.[88]

Yet another dynamic system was designed based on the ability to electrochemically activate a surface. Electrical activation has been used in the past to convert a substrate surface from cell repellent to adhesive.[89] Li et al. patterned multiple cell types using microfluidics whereby the space between patterns could be converted from repulsive to adhesive through electrochemical activation. This allows one to convert the spaces separating patterns of different cell types to adhesive at one point in a study allowing for cell migration studies and further insight into cell-to-cell interactions.[90]

The various co-culture patterning methods described in this section present the unique opportunity to not only study homotypic and heterotypic cell-cell interactions in a

controlled environment but also to monitor dynamic cellular responses to specific and controlled changes in co-culture.

3.4 Conclusions

This review has examined a number of techniques that have been developed since the 1960s with the goal of improving control over the cell microenvironment *in vitro* through the spatial localization of cells on a designed substrate, including photolithography, soft lithography methods, and printing techniques. The ability to spatially pattern two or more types of cells brings us closer to designing a cellular microenvironment mimicking that naturally found in multi-cellular organisms. In the past ten years, many creative methods have been crafted to allow such designs, and their applications have just begun to be realized. Designs tackling the problem of seeding additionally patterned cell types onto a surface in a manner such that patterns are aligned and seeded cells are not harmed have made use of switchable surfaces, soft lithography, and direct patterning methods. Even dynamic co-culture patterns that change with time have been created. Much time has been spent on development. Now is the time for the engineers of these designs to pass on their expertise to life scientists for implementation in a wide range of cell studies to realize the full potential of these techniques. It is foreseeable that these technologies could lay the groundwork in tissue engineering. When certain cell types are cultured together they exhibit increased *in vivo* like functions.[91-93] These co-culture patterns also allow us to explore these relationships and improve upon current tissue engineering strategies. Some intricate cell patterned materials could provide the base scaffolding to encourage self-assembly of multiple cell types into functioning tissue. Of particular interest is the recent development in stem-cell based technologies. Co-culture of stem cells with other cell types in patterned environments should lend to a greater understanding of the cues that direct their development.[94,95] Patterned co-culture technologies could also be seized to increase animal cell bioreactor production or create multiple cell type arrays for screening studies. In an era where we have the ability to prepare micron and even sub-micron features with a variety of materials,[96,97] developing the ability to spatially localize multiple cell types is one of the tools that are absolutely necessary to develop any microenvironment of our choosing for applications yet beyond our imagination.

3.5 Acknowledgements

The authors would like to acknowledge financial support from a Discovery Grant by the Natural Sciences and Engineering Research Council of Canada (NSERC). Catherine A. Goubko is supported by a graduate scholarship by NSERC. We would also like to thank Suzan Badel for her help with the manuscript.

3.6 References

1. Rosso F, Giordano A, Barbarisi M, Barbarisi A. From Cell-ECM interactions to tissue engineering. *Journal of Cellular Physiology.* 2004;199(2):174-180.
2. Kasemo B. Biological surface science. *Surface Science.* 2002;500(1-3):656-677.
3. Nelson CM, Chen CS. Cell-cell signaling by direct contact increases cell proliferation via a PI3K-dependent signal. *FEBS Letters.* 2002;514(2-3):238-242.
4. Yamada S, Nelson WJ. Synapses: Sites of Cell Recognition, Adhesion, and Functional Specification. *Annual Review of Biochemistry.* 2007;76(1):267-294.
5. Luo B-H, Carman CV, Springer TA. Structural Basis of Integrin Regulation and Signaling. *Annual Review of Immunology.* 2007;25(1):619-647.
6. Carter SB. Principles of Cell Motility: The Direction of Cell Movement and Cancer Invasion. *Nature.* 1965;208(5016):1183-1187.
7. Carter SB. Haptotactic islands : A method of confining single cells to study individual cell reactions and clone formation. *Experimental Cell Research.* 1967;48(1):189-193.
8. Carter SB. Haptotaxis and the Mechanism of Cell Motility. *Nature.* 1967;213(5073):256-260.
9. Harris A. Behavior of cultured cells on substrata of variable adhesiveness. *Experimental Cell Research.* 1973;77(1-2):285-297.
10. Letourneau PC. Cell-to-substratum adhesion and guidance of axonal elongation. *Developmental Biology.* 1975;44(1):92-101.
11. Cooper A, Munden HR, Brown GL. The growth of mouse neuroblastoma cells in controlled orientations on thin films of silicon monoxide. *Experimental Cell Research.* 1976;103(2):435-439.
12. Albrecht-Buehler G. The angular distribution of directional changes of guided 3T3 cells. *Journal of Cell Biology.* 1979;80(1):53-60.
13. Ivanova OY, Margolis LB. The Use of Phospholipid Film for Shaping Cell Cultures. *Nature.* 1973;242(5394):200-201.
14. Furshpan EJ, MacLeish PR, O'Lague PH, Potter DD. Chemical Transmission between Rat Sympathetic Neurons and Cardiac Myocytes Developing in Microcultures: Evidence for Cholinergic, Adrenergic, and Dual-Function Neurons. *Proceedings of the National Academy of Sciences of the United States of America* 1976;73(11):4225-4229.
15. Hammarback JA, Palm SL, Furcht LT, Letourneau PC. Guidance of neurite outgrowth by pathways of substratum-adsorbed laminin. *Journal of Neuroscience Research.* 1985;13(1-2):213-220.

16. Hammarback JA, McCarthy JB, Palm SL, Furcht LT, Letourneau PC. Growth cone guidance by substrate-bound laminin pathways is correlated with neuron-to-pathway adhesivity. *Developmental Biology.* 1988;126(1):29-39.

17. Wolf S. *Microchip Manufacturing*. Sunset Beach: Lattice Press; 2004.

18. Kleinfeld D, Kahler KH, Hockberger PE. Controlled outgrowth of dissociated neurons on patterned substrates. *Journal of Neuroscience.* 1988;8(11):4098-4120.

19. Britland S, Clark P, Connolly P, Moores G. Micropatterned substratum adhesiveness: A model for morphogenetic cues controlling cell behavior. *Experimental Cell Research.* 1992;198(1):124-129.

20. Spargo BJ, Testoff MA, Nielsen TB, Stenger DA, Hickman JJ, Rudolf AS. Spatially Controlled Adhesion, Spreading, and Differentiation of Endothelial Cells on Self-Assembled Molecular Monolayers. *Proceedings of the National Academy of Sciences of the United States of America.* 1994;91(23):11070-11074.

21. Healy KE, Thomas CH, Rezania A, et al. Kinetics of bone cell organization and mineralization on materials with patterned surface chemistry. *Biomaterials.* 1996;17(2):195-208.

22. Flagello DG. Evolution as applied to optical lithography. Paper presented at: Proceedings of SPIE - The International Society for Optical Engineering; 2008, 2007; Beijing, China.

23. Xia Y, Whitesides GM. Soft lithography. *Annual Review of Materials Science.* 1998;28(1):153-184.

24. Singhvi R, Kumar A, Lopez GP, et al. Engineering cell shape and function. *Science.* 1994;264(5159):696-698.

25. Lahann J, Choi IS, Lee J, Jensen KF, Langer R. A New Method toward Microengineered Surfaces Based on Reactive Coating *Angewandte Chemie International Edition* 2001;40(17):3166-3169.

26. Csucs G, Michel R, Lussi JW, Textor M, Danuser G. Microcontact printing of novel co-polymers in combination with proteins for cell-biological applications. *Biomaterials.* 2003;24(10):1713-1720.

27. Liu WF, Chen CS. Engineering biomaterials to control cell function. *Materials Today.* 2005;8(12):28-35.

28. Tan JL, Liu W, Nelson CM, Raghavan S, Chen CS. Simple Approach to Micropattern Cells on Common Culture Substrates by Tuning Substrate Wettability. *Tissue Engineering.* 2004;10(5-6):865-872.

29. Folch A, Jo B-H, Hurtado O, Beebe DJ, Toner M. Microfabricated elastomeric stencils for micropatterning cell cultures. *Journal of Biomedical Materials Research.* 2000;52(2):346-353.

30. Tourovskaia A, Barber T, Wickes BT, et al. Micropatterns of Chemisorbed Cell Adhesion-Repellent Films Using Oxygen Plasma Etching and Elastomeric Masks. *Langmuir* 2003;19(11):4754-4764.

31. Delamarche E, Bernard A, Schmid H, Michel B, Biebuyck H. Patterned delivery of immunoglobulins to surfaces using microfluidic networks. *Science.* 1997;276(5313):779-781.

32. Patel N, Padera R, Sanders GHW, et al. Spatially controlled cell engineering on biodegradable polymer surfaces. *FASEB Journal.* 1998;12(14):1447-1454.

33. Takayama S, Ostuni E, Qian X, et al. Topographical micropatterning of poly(dimethylsiloxane) using laminar flows of liquids in capillaries. *Advanced Materials* 2001;13(8):570-574.

34. Nelson CM, Lim E, Chen CS. Two to tango: micropatterned substrates to control cell-cell interactions. Paper presented at: Proceedings of the Second Joint EMBS/BMES Conference 2002; Houston.

35. Michel B, Bernard A, Bietsch A, et al. Printing meets lithography: Soft approaches to high-resolution patterning. *Advanced Semiconductor Lithography.* 2001;45(5):697-719.

36. Klebe RJ. Cytoscribing: A method for micropositioning cells and the construction of two- and three-dimensional synthetic tissues. *Experimental Cell Research.* 1988;179(2):362-373.

37. Sanjana NE, Fuller SB. A fast flexible ink-jet printing method for patterning dissociated neurons in culture. *Journal of Neuroscience Methods.* 2004;136(2):151-163.

38. Wilson Jr. WC, Boland T. Cell and organ printing 1: Protein and cell printers *Anatomical Record - Part A Discoveries in Molecular, Cellular, and Evolutionary Biology.* 2003;272(2):491-496.

39. Boland T, Tao X, Damon BJ, et al. Drop-on-demand printing of cells and materials for designer tissue constructs. *Materials Science and Engineering: C.* 2007;27(3):372-376.

40. Radulescu D, Dhar S, Young CM, et al. Tissue engineering scaffolds for nerve regeneration manufactured by ink-jet technology. *Materials Science and Engineering: C.* 2007;27(3):534-539.

41. Falconnet D, Csucs G, Michelle Grandin H, Textor M. Surface engineering approaches to micropattern surfaces for cell-based assays. *Biomaterials.* 2006;27(16):3044-3063.

42. Pirone DM, Chen CS. Strategies for Engineering the Adhesive Microenvironment. *Journal of Mammary Gland Biology and Neoplasia.* 2004;9(4):405-417.

43. Andersson H, Van Den Berg A. Microfabrication and microfluidics for tissue engineering: State of the art and future opportunities. *Lab on a Chip - Miniaturisation for Chemistry and Biology* 2004;4(2):98-103

44. Yap FL, Zhang Y. Protein and cell micropatterning and its integration with micro/nanoparticles assembly. *Biosensors and Bioelectronics.* 2007;22(6):775-788.

45. Shin H. Fabrication methods of an engineered microenvironment for analysis of cell-biomaterial interactions. *Biomaterials.* 2007;28(2):126-133.

46. Buess M, Nuyten D, Hastie T, Nielsen TB, Pesich R, Brown P. Characterization of heterotypic interaction effects in vitro to deconvolute global gene expression profiles in cancer. *Genome Biology.* 2007;8(9):R191.

47. Gurdon JB, Lemaire P, Kato K. Community effects and related phenomena in development. *Cell.* 1993;75(5):831-834.

48. Alberts B, Johnson A, Lewis B, Raff M, Roberts K, Walter P. *Molecular Biology of the Cell*. Fourth ed. New York: Garland Science; 2002.

49. Bhatia SN, Yarmush ML, Toner M. Controlling cell interactions by micropatterning in co-cultures: Hepatocytes and 3T3 fibroblasts. *Journal of Biomedical Materials Research* 1997;34(2):189 - 199.

50. Nelson CM, Raghavan S, Tan JL, Chen CS. Degradation of Micropatterned Surfaces by Cell-Dependent and -Independent Processes. *Langmuir.* 2003;19(5):1493-1499.
51. Bhatia SN, Balis UJ, Yarmush ML, Toner M. Microfabrication of Hepatocyte/Fibroblast Co-cultures: Role of Homotypic Cell Interactions. *Biotechnology Progress.* 1998;14(3):378-387.
52. Kane BJ, Zinner MJ, Yarmush ML, Toner M. Liver-Specific Functional Studies in a Microfluidic Array of Primary Mammalian Hepatocytes. *Analytical Chemistry* 2006;78(13):4291-4298.
53. Morin O, Normand C. Long-term maintenance of hepatocyte functional activity in co-culture: Requirements for sinusoidal endothelial cells and dexamethasone. *Journal of Cellular Physiology.* 1986;129(1):103-110.
54. Zinchenko YS, Coger RN. Engineering micropatterned surfaces for the coculture of hepatocytes and Kupffer cells *Journal of Biomedical Materials Research - Part A.* 2005;75(1):242-248.
55. Revzin A, Rajagopalan P, Tilles AW, Berthiaume F, Yarmush ML, Toner M. Designing a Hepatocellular Microenvironment with Protein Microarraying and Poly(ethylene glycol) Photolithography. *Langmuir.* 2004;20(8):2999-3005.
56. Lee JY, Jones C, Zern MA, Revzin A. Analysis of Local Tissue-Specific Gene Expression in Cellular Micropatterns. *Analytical Chemistry.* 2006;78(24):8305-8312.
57. Khetani SR, Bhatia SN. Microscale culture of human liver cells for drug development. *Nat Biotech.* 2008;26(1):120-126.
58. Yamato M, Kwon OH, Hirose M, Kikuchi A, Okano T. Novel patterned cell coculture utilizing thermally responsive grafted polymer surfaces *Journal of Biomedical Materials Research.* 2001;55(1):137-140.
59. Yamato M, Konno C, Utsumi M, Kikuchi A, Okano T. Thermally responsive polymer-grafted surfaces facilitate patterned cell seeding and co-culture. *Biomaterials.* 2002;23(2):561-567.
60. Okano T, Yamada N, Sakai H, Sakurai Y. A novel recovery system for cultured cells using plasma-treated polystyrene dishes grafted with poly(N-isopropylacrylamide) *Journal of Biomedical Materials Research.* 1993;27(10):1243 - 1251.
61. Matsuda N, Shimizu T, Yamato M, Okano T. Tissue engineering based on cell sheet technology *Advanced Materials.* 2007;19(20):3089-3099.
62. Tsuda Y, Kikuchi A, Yamato M, Chen G, Okano T. Heterotypic cell interactions on a dually patterned surface. *Biochemical and Biophysical Research Communications.* 2006;348(3):937-944.
63. Cheng X, Wang Y, Hanein Y, Böhringer KF, Ratner BD. Novel cell patterning using microheater-controlled thermoresponsive plasma films. *Journal of Biomedical Materials Research Part A.* 2004;70A(2):159-168.
64. Yang IH, Co CC, Ho C-C. Spatially controlled co-culture of neurons and glial cells. *Journal of Biomedical Materials Research - Part A.* 2005;75A(4):976-984.
65. Khademhosseini A, Suh KY, Yang JM, et al. Layer-by-layer deposition of hyaluronic acid and poly--lysine for patterned cell co-cultures. *Biomaterials.* 2004;25(17):3583-3592.
66. Fukuda J, Khademhosseini A, Yeh J, et al. Micropatterned cell co-cultures using layer-by-layer deposition of extracellular matrix components. *Biomaterials.* 2006;27(8):1479-1486.

67. Kidambi S, Lee I, Chan C. Primary neuron/astrocyte co-culture on polyelectrolyte multilay films: A template for studying astrocyte-mediated oxidative stress in neurons. *Advanced Functional Materials* 2008;18(2):294-301.

68. Kaji H, Sekine S, Hashimoto M, Kawashima T, Nishizawa M. Stepwise formation of patterned cell co-cultures in silicone tubing. *Biotechnology and Bioengineering.* 2007;98(4):919-925.

69. Fukuda J, Khademhosseini A, Yeo Y, et al. Micromolding of photocrosslinkable chitosan hydrogel for spheroid microarray and co-cultures. *Biomaterials.* 2006;27(30):5259-5267.

70. Chiu DT, Jeon NL, Huang S, et al. Patterned deposition of cells and proteins onto surfaces by using three-dimensional microfluidic systems. *Proceedings of the National Academy of Sciences of the United States of America.* 2000;97(6):2408-2413.

71. Khademhosseini A, Yeh J, Eng G, et al. Cell docking inside microwells within reversibly sealed microfluidic channels for fabricating multiphenotype cell arrays *Lab on a Chip - Miniaturisation for Chemistry and Biology.* 2005;5(12):1380-1386.

72. Khademhosseini A, Ferreira L, Blumling Iii J, et al. Co-culture of human embryonic stem cells with murine embryonic fibroblasts on microwell-patterned substrates. *Biomaterials.* 2006;27(36):5968-5977.

73. Tan W, Desai TA. Microscale multilayer cocultures for biomimetic blood vessels. *Journal of Biomedical Materials Research Part A.* 2005;72A(2):146-160.

74. Bruzewicz DA, McGuigan AP, Whitesides GM. Fabrication of a modular tissue construct in a microfluidic chip *Lab on a Chip - Miniaturisation for Chemistry and Biology.* 2008;8(5):663-671.

75. Tien J, Nelson CM, Chen CS. Fabrication of aligned microstructures with a single elastomeric stamp. *Proceedings of the National Academy of Sciences of the United States of America.* February 19, 2002 2002;99(4):1758-1762.

76. Leclerc E, El Kirat K, Griscom L. In situ micropatterning technique by cell crushing for co-cultures inside microfluidic biochips. *Biomedical Microdevices.* 2008;10(2):169-177.

77. Nahmias Y, Arneja A, Tower TT, Renn MJ, Odde DJ. Cell Patterning on Biological Gels via Cell Spraying through a Mask. *Tissue Engineering.* 2005;11(5-6):701-708.

78. Gao BZ, Fass JN, Renn MJ, Odde DJ. Nano- and microscale manipulation of biological particles by laser-guided direct writing. Paper presented at: Proceedings of SPIE - The International Society for Optical Engineering 2002; Gaithersburg.

79. Odde DJ, Renn MJ. Laser-guided direct writing for applications in biotechnology. *Trends in Biotechnology.* 1999;17(10):385-389.

80. Narasimhan SV, Goodwin RL, Borg TK, Dawson DM, Gao BZ. Multiple beam laser cell micropatterning system. Paper presented at: Proceedings of SPIE - The International Society for Optical Engineering 2004; Bellingham.

81. Nahmias Y, Schwartz RE, Verfaillie CM, Odde DJ. Laser-guided direct writing for three-dimensional tissue engineering. *Biotechnology and Bioengineering.* 2005;92(2):129-136.

82. Bakken DE, Narasimhan SV, Burg KJL, Gao BZ. Laser Micropatterning of Polylactide Microspheres into Neuronal-Glial Coculture for the Study of Axonal Regeneration. *Macromolecular Symposia.* 2005;227(1):335-344.

83. Rosenbalm RN, Owens S, Bakken DE, Gao BZ. Cell viability test after laser guidance. Paper presented at: Proceedings of SPIE - The International Society for Optical Engineering2006; San Jose.
84. Nahmias Y, Odde DJ. Micropatterning of living cells by laser-guided direct writing: application to fabrication of hepatic-endothelial sinusoid-like structures. *Nat. Protocols.* 2006;1(5):2288-2296.
85. Hui EE, Bhatia SN. From the Cover: Micromechanical control of cell-cell interactions. *Proceedings of the National Academy of Sciences of the United States of America* April 3, 2007 2007;104(14):5722-5726.
86. Rusk N. A gentle touch for cells *Nature Methods.* 2007;4(6):472.
87. Metallo CM, Mohr JC, Detzel CJ, dePablo JJ, VanWie BJ, Palecek SP. Engineering the Stem Cell Microenvironment. *Biotechnology Progress.* 2007;23(1):18-23.
88. Wright D, Rajalingam B, Selvarasah S, Dokmeci MR, Khademhosseini A. Generation of static and dynamic patterned co-cultures using microfabricated parylene-C stencils *Lab on a Chip - Miniaturisation for Chemistry and Biology.* 2007;7(10):1272-1279.
89. Yousaf MN, Houseman BT, Mrksich M. Using electroactive substrates to pattern the attachment of two different cell populations. *Proceedings of the National Academy of Sciences of the United States of America.* 2001;98(11):5992-5996.
90. Li Y, Yuan B, Ji H, et al. A method for patterning multiple types of cells by using electrochemical desorption of self-assembled monolayers within microfluidic channels *Angewandte Chemie - International Edition.* 2007;46(7):1094-1096.
91. Selden C, Khalil M, Hodgson HJF. What keeps hepatocytes on the straight and narrow? Maintaining differentiated function in the liver. *Gut* 1999;44(4):443-446.
92. Woehrling EK, Hill EJ, Coleman MD. Development of a neurotoxicity test-system, using human post-mitotic, astrocytic and neuronal cell lines in co-culture. *Toxicology in Vitro.* 2007;21(7):1241-1246.
93. De Luca M, D'Anna F, Bondanza S, Franzi AT, Cancedda R. Human epithelial cells induce human melanocyte growth in vitro but only skin keratinocytes regulate its proper differentiation in the absence of dermis. *Journal of Cell Biology.* 1988;107(5):1919-1926.
94. Schumm MA, Castellanos DA, Frydel BR, Sagen J. Direct cell-cell contact required for neurotrophic effect of chromaffin cells on neural progenitor cells. *Developmental Brain Research.* 2003;146(1-2):1-13.
95. Li X, Yu X, Lin Q, et al. Bone marrow mesenchymal stem cells differentiate into functional cardiac phenotypes by cardiac microenvironment. *Journal of Molecular and Cellular Cardiology.* 2007;42(2):295-303.
96. Christman KL, Enriquez-Rios VD, Maynard HD. Nanopatterning proteins and peptides. *Soft Matter.* 2006;2(11):928-939.
97. Wood MA, Riehle M, Wilkinson CDW. Patterning colloidal nanotopographies. *Nanotechnology* 2002(5):605.

CHAPTER 4:
PHOTOLABILE MOLECULES AS LIGHT-ACTIVATED SWITCHES TO CONTROL BIOMOLECULAR AND BIOMATERIAL PROPERTIES

Catherine A. Goubko, Nan Cheng, and Xudong Cao

Reprinted with kind permission from Nova Science Publishers, Inc.
***Photochemistry: UV/VIS Spectroscopy, Photochemical Reactions and Photosynthesis*, K. J. Maes, J. M. Willems, Eds. (Nova Publishers, 2011)**
pp. 175-202

The following chapter represents a literature review published as a book chapter providing detailed information on photolabile molecules not covered in Chapter 2. This review is intended to provide the interested reader with information on the roles currently played by photolabile molecules in the field of biological and biomaterial research. Photolabile molecules play a key role in the cell patterning strategy presented in this thesis; caged RGDS peptides allow the HA hydrogel base to be switched from cell non-adhesive to adhesive upon near-UV light exposure. This review will first briefly overview some commonly used photolabile molecules and then examine some of the applications they have found to date in caging biomolecules. This will set the stage for a detailed discussion on how photolabile molecules are incorporated into materials for biological applications and the future potential of these novel strategies in biomedical engineering research and biotechnology.

4.1 Introduction

Photolabile protecting groups, or caging groups, offer researchers involved in the biological sciences a unique tool – a light switch – which can alter material properties at will or even result in the activation of whole biomolecules. These light-responsive caging groups can be covalently bound to a functional group on a molecule of interest. Upon irradiation with light of appropriate energy, the caging group is removed while freeing the functional group in the process. Thanks to the imagination of chemists, biologists, and material scientists alike, this seemingly simple process has brought about a new generation of biological molecules and materials which can be controlled by light in both a spatial and temporal manner. The photolabile protecting group can render a biomolecule unrecognizable to its corresponding receptor, enzyme, or target due to steric hindrance or changes in charge. Biomolecules in a particular location can be re-activated any time during a process or experiment with light. In materials, the photolabile group can mask a functional group which can then be revealed with light in desired regions to allow for further chemical modifications or building of a material. Caging groups can be incorporated into crosslinkers, holding a material together, in order to allow for controlled degradation with light. Removal of caging groups can also result in charge alterations in regions of a material. Caged biomolecules can even be bound to a biomaterial and selectively activated upon irradiation. In these ways,

materials can be fundamentally altered with time, or patterned at - or even below - the micron scale for the fine-tuning of material properties.

Chemists have provided us with a variety of photolabile protecting groups which can be introduced onto biological molecules and materials. The most popular of these groups in the biological sciences are the o-nitrobenzyl derivatives.[1] Figure 4.1 depicts the structure of some commonly used o-nitrobenzyl derivatives as well as the reaction they undergo with light. These derivatives can be covalently bound to a range of functional groups including carboxylates, amines, amides, alcohols, phenols, phosphates and more with relative ease. Despite this, there are several disadvantages associated with their use including the formation of potentially toxic strongly absorbing reaction by-products and relatively slow rates of cage release following excitation.[2] Furthermore, the light required to uncage these molecules is of relatively high energy – in the near-UV range.

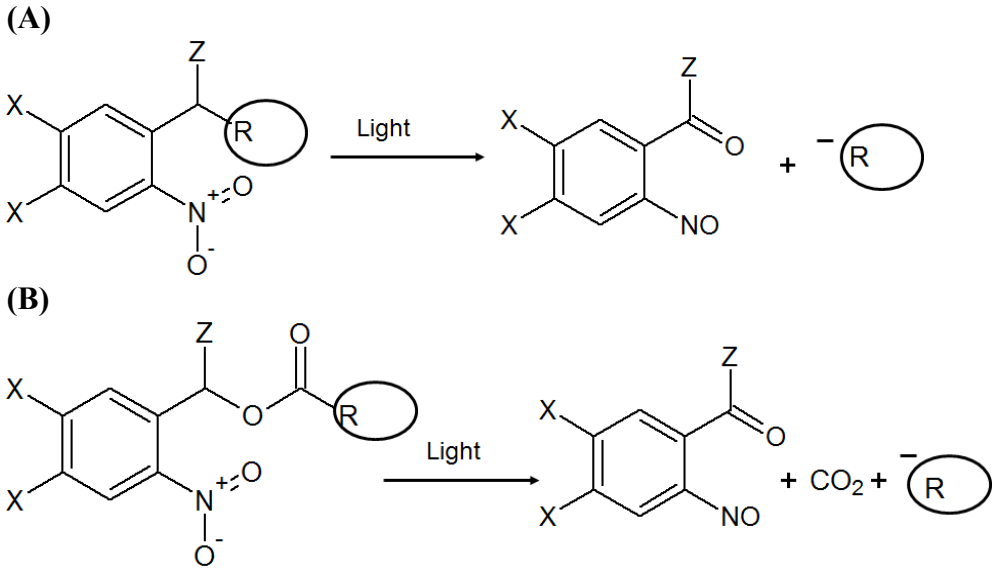

Figure 4.1: General structure of o-nitrobenzyl derivatives and associated light reactions. Some common substituents include: **(A)** X=H, Z=H: o-nitrobenzyl (2-NB); X=H, Z= CH_3: o-nitrophenethyl (NPE), X=H, Z=COOH: α-carboxy-2-nitrobenzyl (CNB); X=OCH_3, Z=H: 4,5-dimethoxy-2-nitrobenzyl (DMNB); X=OCH_3, Z=CH_3: 4,5-dimethoxy-2-nitrophenethyl (DMNPE); **(B)** X=OCH_3, Z=H: 6-nitroveratryloxycarbonyl (NVOC)[2]

A group of newer photolabile cages becoming increasingly more popular are coumarin-4-ylmethyl groups (coumarins). Figure 4.2 depicts the general structure of some coumarins used in the literature as well as the reaction they undergo upon irradiation. These groups have been used to cage phosphates, carboxylates, amines, alcohols, phenols, and carbonyl compounds. Coumarins absorb strongly into the visible light region and demonstrate relatively quick photolysis rates. They have also been shown as well-suited for two-photon photolysis. However, these compounds often suffer from solubility isssues.[3]

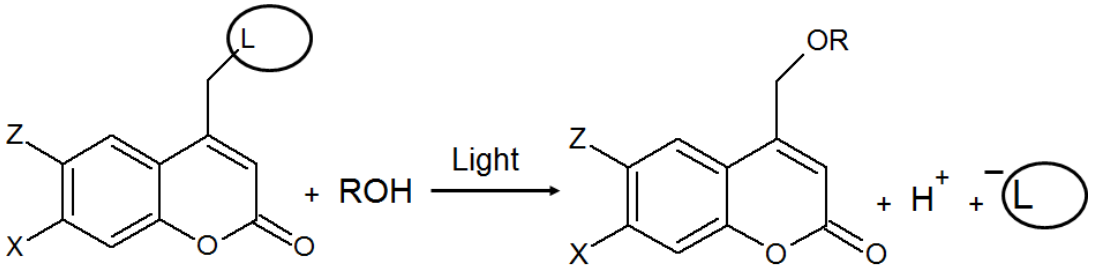

Figure 4.2: General structure of photolabile coumarin-4-yl methyl groups and reaction resulting from irradiation. Some substituents found in the literature include[3]: X=OX' (X'=CH_3, H, CH_3CO, CH_3CH_2CO, or CH_2CO_2H), Z=H: 7-alkoxy group; X=Z=OX' (X'=CH_3, CH_2CO_2H, or CH_2CO_2Et): 6,7-dialkoxy group; X=OX' (X'=H or CH_3CO), Z=Br: 6-bromo-7-alkoxy group; X=NX'_2 (X'=CH_3CH_2, CH_3), Z=H: 7-dialkylamino group

A number of other more minor photolabile caging molecules exist and have been used in biological applications, but are beyond the scope of this review. For more information, please refer to recent comprehensive review articles.[4,5]

A number of issues must be considered when attempting to cage a molecule or material for biological applications. The first is the efficiency of photolysis, which can be considered as the percentage of molecules from which the photolabile cage is removed upon irradiation. This is dependent on the quantity of light absorbed at the wavelength of irradiation, which is related to the molecule's extinction coefficient, as well as the fraction of caged molecules that will react after absorbing a photon, described by the quantum yield.[3] The coumarins absorb strongly, but have low quantum yields.[2] As caged biomolecules often need to be dissolved in aqueous environments, solubility can also be an issue for some cages. Absorption properties and solubility can be altered and improved by carefully choosing the

substituents on the ring structure of these cages. The rate of photolysis should also be considered; coumarin groups show relatively high photolysis rates upon irradiation. Another important consideration is the irradiation wavelength which should be greater than 300 nm to minimize potential damage caused by UV light. At lower wavelengths significant damage to proteins and the nucleic acids that make up cell DNA can be detected.[1] Furthermore, to be useful in biological environments, caged products must not hydrolyze in water to a large degree. Finally, one of the greatest considerations must be the placement of the cage on the biomolecule or material of interest. There must be a functional group to which the caging group can bind, and binding in that particular location must have a significant effect on the molecule. For example, in a large protein, placing the caging group away from the active site may not have any effect on the ability of the protein to function, rendering the light switch useless.

Once a photocaged biomolecule or material is created, the next decision is the nature of the light source for photolysis. UV lamps are inexpensive, readily accessible, and can be attached to filters for selection of specific wavelengths. Photomasks can be placed on surfaces underneath a lamp to allow uncaging only in patterned regions allowing for spatial selectivity. Lasers can be used to deliver light of one specific wavelength corresponding to the maximal absorbance of a caged molecule. Lasers can also be focused onto small areas below the nano scale for spatial selectivity. Two photon lasers are now in use for photolysis of caged biomolecules or materials.[6] Photolabile molecules exposed to such sources absorb two photons at the same wavelength practically simultaneously to undergo photolysis. These two photons together deliver the same quantity of energy to the caged product as a single photon would in another laser. Therefore, the wavelength of light delivered by these lasers is approximately double that used in a single photon laser so infrared light is normally employed for uncaging with two-photon lasers. This is highly beneficial since cells and tissues do not strongly absorb IR light, allowing for greater depth of penetration with less scattering and less damage. Furthermore, two-photon lasers can target a small focal volume within a 3D environment, whereas single-photon lasers lack this 3D selectivity. Coumarins have been found to be much more efficient for two-photon uncaging as compared to o-nitrobenzyl derivatives, which require higher laser powers for uncaging.[3]

The combined efforts of chemists in designing new caging groups with improved properties for use in the biological environment and physicists in designing improved lasers for targeted removal of photolabile caging groups have led to the recent increase in the use of these caging groups in life sciences research and the development of materials for biological applications. To date, much effort has been devoted to developing a variety of caged biomolecules and their applications are ever-growing. Use of these molecules in biomaterials has been gaining in popularity recently and new highly-creative, light-responsive materials have been born and their applications in sensor-design, tissue engineering, and life sciences research are just beginning.

4.2 Caging of Biological Molecules

Over the past thirty years, great effort has been devoted to caging a variety of biological molecules. Initial work involved caging smaller molecules that nonetheless play large roles in biochemistry and moved towards complex macromolecules such as nucleic acids and proteins. Techniques to cage these molecules are well developed in the literature but still require expertise in synthetic chemistry. Nevertheless, there are relatively fewer works dealing with the application of these molecules. Here, we will provide an overview of some key biomolecules that have been bound with photolabile groups, and demonstrate some of the applications they have found.

4.2.1 Small Biologically Relevant Molecules

To date, hundreds of experiments have been conducted employing small caged biomolecules of which a number are currently commercially available. Strong interest in caging biomolecules began with a landmark study by Kaplan et al.[7] In 1978, they synthesized a caged ATP by binding o-nitrobenzyl onto a phosphate group. Caged ATP molecules were introduced into red blood cells where they were used as an energy source upon irradiation to activate cellular Na:K pumps. Caged ATP cannot be hydrolyzed to form ADP - which normally generates energy for cellular processes - until it is activated with light. Caging this molecule thus allows for a number of studies requiring control over energy reserves making caged ATP an excellent research tool still in use today.[8]

Calcium plays a strong role in cellular biochemistry; changes in intracellular calcium levels are linked to muscle contraction, mitosis, and neurotransmitter release among others. Since calcium cannot be covalently bound to a caging group, photo-responsive high affinity calcium chelators were developed having a high affinity for calcium in the caged state. Upon irradiation, affinity for calcium is decreased releasing the inorganic molecule and therefore increasing calcium levels in the cellular environment. A good review of caged calcium by Ellis-Davies exists for interested readers.[9] By employing caged calcium to spatially and temporally control available calcium levels, Gomez and Spitzer were able to determine that transient calcium level elevations control axon growth in the developing spinal cord.[10] Growth cones located at the extending tips of neuronal cells showed transient elevations of calcium as these extensions migrated. Releasing caged calcium chelators accelerated the migration, while reproducing the transient elevations with the photorelease of calcium slowed the growth.

Photolabile molecules which release nitric oxide have also been created. Nitric oxide plays a role in a large number of biological events such as certain neural physiological processes like long term potentiation and depression, constriction of smooth muscle and blood flow control, and NO has been found, under different conditions, to both enhance tumor growth and destroy it.[11] Another important small molecule that has been caged is cAMP which acts as a secondary messenger in eukaryotic cells and as such is involved in the regulation of a vast number of cellular processes.[5] Caging these molecules allows for in-depth investigations into their roles in these widely varied cell processes.

Over the years, there has existed a strong interest in caging neurotransmitters. Caged glutamate is one of the most well-known thanks in part to a 1994 study by Dalva and Katz who investigated the patterns of synaptic connections in a developing visual cortex. Brain slices were irradiated to selectively uncage glutamate and generate action potentials in presynaptic neurons located at the laser focal point.[12] Since this time, new caged derivatives of glutamate have been developed with improved sensitivity to two-photon photolysis allowing for better spatial selectivity during light activation. Some other reported caged neurotransmitters include GABA, glycine, and anandamides.[13] Such caged species have

played important roles in elucidating the processes of neurotransmission and signal transduction.[3]

In an excellent example of an application of a small caged biomolecule, Cambridge et al. designed a gene expression system responsive to light.[14] Their method was based on the "tetracycline-controlled transcriptional activation" system, which can control the transcription of transgenes in an organism or cell culture by the presence of tetracycline antibiotics or doxycycline. The group caged doxycycline so that irradiation would free the antibiotic and induce transcription. Sauers et al also employed a photolabile doxycycline to control cell localization in a co-culture.[15] A culture derived from NIH 3T3 fibroblasts was created that could be induced with light to express Ephrin A5. When expressed in a cell, this molecule causes repulsion towards other cells expressing the receptor, EphA7, and attraction to cells expressing a variant, EphA7-T1. After forming a pattern of Ephrin A5 expression in a monolayer of the 3T3s with light, they found that EphA7-T1-expressing cells preferentially adhered to the patterned area. This method of controlling attractive/repulsive cell cues with light is an exciting and creative way to control the arrangement of cells *in vitro*.

4.2.2 Peptides and proteins

Proteins and peptides play many different roles in our body; enzymes act as chemical catalysts; transporters regulate the cell environment; signaling molecules and hormones send messages across the body to coordinate actions during development and beyond; and the list goes on. These biomolecules are key to the basic processes of life and disease. However, we do not yet fully understand the roles played by many proteins. Now that we have sequenced the human genome, we must come to a better understanding of how these key gene products act in the body. Caging proteins is an often under-used tool in these important studies with the capability to temporally and spatially control protein activity. Much effort has been spent on the technique of inserting a caging group into these biomolecules, but comparatively less effort has been extended to their use in advanced biological studies. We will therefore begin with an overview of some of the key methods employed in caging proteins.

Several methodologies have been developed to synthesize photocaged proteins. Traditionally, caging groups were introduced non-specifically into whole, intact proteins. Various o-nitrobenzyl derivatives were designed to specifically react with functional groups on certain amino acids such as sulfhydryl groups, found on the amino acid cysteine, and amino groups found on lysine.[16-18] These techniques allow for the caging of larger molecules, but suffer certain drawbacks: (a) it is difficult to target a specific residue for caging, (b) the technique is limited to specific types of residues, and (c) typically only surface-exposed residues can be reached for caging. Furthermore, cysteine residues are relatively rare in proteins and may need to be introduced via mutagenesis near a protein active site for this strategy to work.[3] In addition, too many residues caged can result in difficulties reactivating the protein upon irradiation.

In comparison, when a small peptide is involved, a more direct approach to introducing photolabile molecules can be taken. Researchers have been successful in introducing a caging group onto a single amino acid and then introducing this caged unit into a larger peptide via automated solid-phase peptide synthesis (SPPS) procedures. One study has even attempted to add the caging group to the peptide directly during automated SPPS.[19] Many different caged amino acids have been designed including Lys, Tyr, Glu, Asp, Arg, Ser, Gln, and Gly by introducing the caging group on either an amino acid side chain or even the peptide backbone.[20-23] This process allows for much improved control over the placement of the caging group. Often, several different caged amino acids are synthesized to produce peptides caged in different locations. In this manner, the caged peptide which most effectively inhibits activity prior to light exposure- and allows for activation after irradiation - can be selected for use.[20,22,23] However, this method is limited to smaller proteins and synthesis can be very time consuming.

In another synthesis strategy, caged amino acids were introduced directly into proteins via *in vitro* translation. For example, Wu et al. made use of a unique *E. Coli* tRNA/aminoacyl tRNA synthetase pair to incorporate a caged cysteine into proteins synthesized in yeast in response to a nonsense codon, TAG.[24] Others have used a similar methodology to introduce caged lysine into proteins in mammalian cells.[25,26] This system of

caging allows for direct incorporation of a caging group into a large protein, but is fairly complex and requires highly specialized knowledge and techniques to accomplish.

Another approach involves the protein phosphorylation process. Phosphorylation is a common way for cells to regulate protein activity after translation. In one study, the caging group was placed on the phosphate groups needed to activate Smad2, a tumor suppressor protein important in cancer research. The caged Smad2 acted like the unphosphorylated protein, while UV irradiation resulted in activity similar to the phosphorylated Smad2. This strategy could theoretically be used to cage any protein activated through phosphorylation.[27] Another interesting strategy involves ligating a synthetic moiety to the C-terminus of a peptide such that the bond is photocleavable due to the presence of an o-nitrobenzyl derivative. In one example, a photolabile lipid was ligated to a protein resulting in its re-localization mostly within cell membranes. Upon photocleavage, the protein was able to move towards the cytoplasm and nucleus. Therefore, proteins can be deactivated through relocation strategies.[28]

Using the strategies discussed above, a wide variety of peptides and proteins can potentially be caged such that they can be switched on by light at will. Proteins involved in gene expression, from transcription to translation, have even been caged such that they can control the expression of a wide variety of other proteins and gene products. These caged proteins can also offer us further insight into the roles their uncaged versions play in gene expression. To this end, Chou et al. were able to cage an RNA polymerase to render it inactive until near-UV exposure. With this caged enzyme, they were able to control gene function with light in both bacteria and mammalian cells.[29] A variety of caged biomolecules involved in protein translation from RNA have been designed such as caged anisomycin which inhibits protein synthesis by binding to cell ribosomes, caged 4E-BP which is involved in translation of mRNAs with a cap structure on their end, and rapamycin which inhibits mTORC1, a complex involved in translation initiation.[30,31] Growth factors or signaling molecules stimulate certain cell behaviors and can be caged to either study their function, or to control cell behavior experimentally. Miller et al. caged a synthetic epidermal

growth factor sequence and demonstrated its use in controlling cell migration and proliferation upon activation with UV light.[32]

Despite a growing library of caged proteins in the literature, relatively few studies make true use of the advantages of this strategy to control protein expression with precise temporal and spatial control. Using light as a switch to turn on proteins can allow us to target single cells in a culture or multi-cellular organism or even organelles within a cell. The state of a cell is constantly changing with time; cells divide, migrate, differentiate and undergo apoptosis. Different proteins may vary in activity or function during these different times. With light as a switch, we can turn on a particular protein during any point of a cell's life cycle to examine temporal effects.

One excellent example of the spatial control afforded by protein caging is seen in a study by Priestman and Lawrence where they investigated the role played by cofilin, an intracellular protein involved in cell motility. A caged cofilin was injected into cells. After exposing whole cells to irradiation, they found an increase in lamellipod (a cell projection) size and formation time. They then irradiated 3 um spots on single cells and noted that cell protrusions formed near these spots in 80% of the cells. Therefore, they were able to demonstrate that by using caged cofilin proteins, cells could be induced to move in the direction of illumination. In comparison, cells without the caged protein moved randomly.[33]

In a good example of the experimental potential of caged proteins for temporal control of processes, Sinha et al. designed a system for introducing a caged protein into zebrafish embryos. These creatures are ideal for experimentation due to their small size and transparency.[34] Sinha et al. genetically programmed a protein with a small site that was activated by a lipophilic molecule which was caged. The developing embryo was incubated in a solution of this caged inducer molecule that could bind to form a caged protein complex *in vivo.* Caging was accomplished with both o-nitrobenzyl and coumarin derivatives to allow for single photon or two-photon uncaging. This protein could thus be activated in a select group of cells within the zebrafish and at any time, offering an exciting method to study the activity of a protein at specific time points in embryonic development.

4.2.3 Nucleotides and Nucleic Acids

Another way to achieve photo-control over gene expression is the direct caging of nucleic acids (i.e. DNA or RNA). To this end, photocages have been introduced on nucleotide bases, backbone phosphates, and hydroxyl groups on ribose sugar rings.[35] Ando et al. developed a process to cage the phosphate backbone of mRNA with a coumarin such that approximately 30 caged sites were generated per kb of RNA.[36] Eng2a mRNA was caged, which codes for a transcription factor, Engrailed2a. Embryos with the caged mRNA showed normal eye development, while those irradiated in the head region at a certain time during development to uncage the mRNA developed an eyeless phenotype. In this way, caged mRNA can be used to investigate the impact of certain genes on development.

DNA has also been caged. In the past, plasmid DNA has been caged non-specifically on the phosphate backbone. Yamaguchi et al. introduced a site-specific caging group into a plasmid attached to biotin. Streptavidin selectively binds to the biotin to provide additional steric hindrance during caging which assures the inability of transcription factors to bind to the plasmid. Irradiation cleaves the biotin thus freeing the plasmid for gene expression and subsequent transcription.[37] Caging groups have also been used to exert spatial and temporal control over the activation of small interfering RNAs (siRNAs). A little over a decade ago, it was discovered that double stranded RNA, namely siRNAs, could silence the expression of a particular gene and this process was termed RNA interference. Caging groups have been introduced onto siRNAs to disrupt their interaction with a protein complex, the RISC, necessary for gene silencing. Irradiation of caged siRNAs at a time point during an experiment leads to the silencing of a particular gene product. For more information on this topic, please refer to an excellent review paper by Casey et al.[38] Caging of nucleic acids has occurred more recently in comparison to proteins and as such fewer studies are available. It was only a little over ten years ago, when in 1999, gene expression was first controlled with a caged nucleic acid - a plasmid coding for luciferase.[39] As a result, more applications are expected as knowledge of these techniques become more widespread.

4.2.4 Drugs

Caging drug molecules could lead to effective targeting strategies; theoretically, free drug could be localized in irradiated areas of the body allowing for minimal side effects elsewhere. This could be particularly exciting for tumor targeting. Therapeutic antibodies have been developed to target tumors, but unfortunately, are often not specific enough leading to dangerous side-effects. Caging such antibodies to render them inactive and irradiating the tumor for local release of active antibody could lead to another level of specificity increasing their safety. It is theorized that visible areas of the body such as the skin, eye, mouth and those accessible with endoscopes or areas open during surgeries could be treated with such caged drugs.[40] Skwarczynski et al. developed a prodrug of paclitaxel bound to a coumarin derivative and demonstrated that the drug could be regenerated upon light exposure. This drug is commonly used in the treatment of a variety of cancers.[41] In another study, Reinhard and Schmidt synthesized and investigated o-nitrobenzyl photocaged derivatives of phosphoramide mustards, which are also used in cancer therapy. These compounds have an alkylating activity that allows them to attack proliferating cells.[42] Insulin, for the treatment of diabetes, has also been caged for improved temporal control over its release; researchers envisioned its use in a glucose sensor armed with a small UV lamp to activate and release specific doses in response to blood glucose levels.[43] While the caging of drug molecules is very promising for improved targeting through controlled irradiation, as well as temporal control in response to need, many issues still remain to be addressed. New light sources that can access other areas of the body are needed, and the laser light must be able to significantly penetrate tissues without damage. We must consider moving away from the higher energy near-UV light required by the popular o-nitrobenzyl derivatives and towards potentially safer lower-energy wavelengths. Hopefully, multiphoton laser technologies will eventually satisfy these needs.

4.3 Photolabile Molecules in Biological Devices and Biomaterials

The caged biomolecules discussed in the previous section can be incorporated into biomaterials to create powerful new biotechnologies. In addition to the direct caging of biomolecules, traditional photolabile caging groups have been more directly implemented in materials, in creative ways, for the development of biological devices on solid surfaces and biomaterials that can respond dynamically to light.

4.3.1 Patterning Biomolecules and Cells on Solid Surfaces

Solid surfaces modified with caged compounds hold great promise for various biotechnological and biomedical applications. They can be used as a platform to make chips for drug and biomarker discovery, mapping protein-protein interactions, DNA screening and analysis of cellular processes.[44,45] One strategy in the development of materials for such applications is to create a substrate capable of responding to an external stimulus. Light as the external stimulus, combined with photocleavable caging molecules, has the advantage of high resolution - both spatial and temporal - and leaves no residue post reaction which could cause unexpected side effects on the development of these chips. Light-induced surface chemistry is crucial in the production of microchips for the microelectronics industry, so it is natural that such strategies be translated to the creation of chips for biological applications. Currently, a popular application of photocleavable surfaces is DNA screening and *in situ* synthesis. DNA probe arrays are useful tools in biomedical research and diagnostics because of their ability to simultaneously address large numbers of genes.[46]

The photocleavable molecules in these designs aid in DNA synthesis; they are used to temporarily protect the terminal groups of nucleotide monomers, which are often assembled on glass or metal surfaces. They block the DNA polymerase enzyme from incorporating additional nucleotides to a growing nucleic acid strand after each "cycle" of nucleotide incorporation. Irradiation and the use of appropriate photomasks could allow the deprotection of specific terminal groups and control over the DNA sequence and size produced. Seo et al., in 2004, reported a successful DNA sequencing approach based on DNA synthesis using photocleavable fluorescent nucleotides on a solid surface.[46] They attached azido-labeled DNA onto alkyne-modified glass. The goal was to identify the DNA

sequence of interest via the synthesis of its complimentary strand. A series of nucleotide analogues bound to different fluorescent dyes through an o-nitrobenzyl linker were exposed to the DNA to be sequenced. By observing which dye was incorporated, the identity of the unknown nucleotide could be established. They showed that near-UV irradiation leads to efficient release of the fluorophore and demonstrated the feasibility of performing the DNA polymerase reaction on the solid surface. They expected to be able to sequence at least 25 bases per spot on their chip. Their DNA sequencing technology has the potential for use in whole genome sequencing and can be applied to pharmacogenetics. So far, limited success with photochemical approaches has been reported but several caging groups have been studied and demonstrated fast and efficient photo deprotection of the hydroxyl group for DNA microarray synthesis,[47] such as coumarins,[35] indoline, and quinoline. The ability to produce high-density oligonucleotide arrays (GenChip®probe arrays) has been utilized in DNA sequencing technology.[48] Photocleavable protecting groups can also be used in the synthesis of other biomolecules on solid surfaces; Fodor et al. reported the generation of a successful array of 1024 peptides using an o-nitrobenzyl derivative.[49]

The basic challenge for the fabrication of protein and cell microarrays is the ability to label proteins with high resolution on a substrate. To achieve this, a high density of individual, isolated reactive protein sites are required. Light as a trigger, can induce instantaneous photoreactions on surfaces to control immobilization of biomolecules without chemical reagents.[50,51] Several studies have already been done to demonstrate the feasibility of applying different photocleavable molecules on different functionalized solid surfaces and have investigated their advantages. Basically, the caged molecules are attached to a solid substrate and irradiated through a mask or using laser lithography. Deprotection happens selectively on the molecules exposed to the light and free functional groups are generated ready to react with a second molecule, which is usually a biomolecule.[51] This technique can lead to the development of biosensors and offers certain potential advantages, including reduced operation time, parallel detection of multiple targets, and small sample requirements.

Sundberg et al fabricated a heterogeneous surface with two different antibodies on a solid substrate in 1996.[52] An o-nitrobenzyl derivative was used to create a caged biotin analogue which was immobilized to a glass surface. UV light exposure through a photomask yielded regions of deprotected biotin. These regions can bind specifically to the molecule streptavidin to which biotinylated macromolecules could subsequently be linked. They achieved two different biotinylated antibodies immobilized on different regions of a planar substrate. Alonso et al. created a photosensitive silane based on NVOC chemistry.[53] They assembled tetraethylene glycol, a typical protein repellent, on a silica surface bound by a NVOC terminal group. By UV irradiation, they could achieve highly selective deprotection of amine groups and site-specific immobilization of tris-nitrilotriacetic acid (tris-NTA) for His-tagged protein attachment and biotin for streptavidin attachment (Figure 4.3). In their system, the oligoethylene glycol was introduced to the substrate to decrease non-specific binding between the substrate and undesirable proteins.

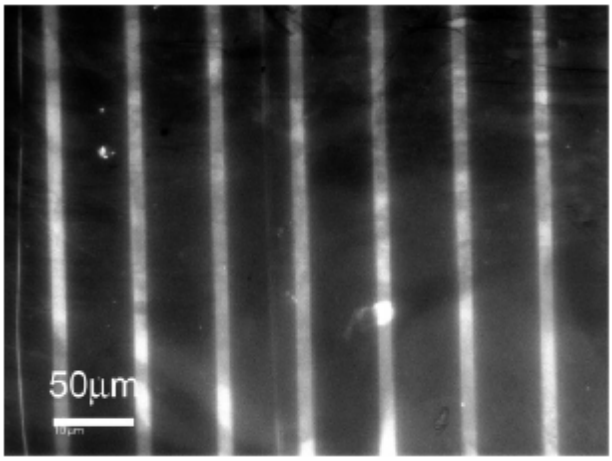

Figure 4.3: Fluorescence image of a patterned substrate after coupling biotin, then streptavidin, followed by fluorescently labelled biotin. Reprinted with permission.[53] Copyright 2010 American Chemical Society.

Lee et al. developed a maskless photolithography process to control protein patterns with NVOC molecules.[54] They fabricated a two dimensional micro mirror array, where they used digital micro mirrors as a virtual photomask to create a biotin pattern. Most recently, Grunwald et al. applied photocleavable surfaces to capture and recognize viruses.[55] They created a photo-activatable tris-NTA via a nitrobenzyl linker. The photo-activatable tris-

NTAs were self-inactivated by His-tagged proteins. Irradiation could activate the affinity by cleaving a tethered intramolecular ligand and arming a multivalent chelator head. In their study, different strategies were applied to create site-specific protein patterns, including mask patterning, laser lithography, and successive activation of different areas using *in situ* laser scanning lithography. Furthermore, they demonstrated the ability of their system to capture virus-specific very low-density lipoprotein receptors, which made it a highly flexible platform for detection and analysis of clinically relevant virus particles. Until now, many different solid surface-based systems using photocleavable caging groups have been developed and most of them used o-nitrobenzyl derivatives to control protein specific binding to the solid support.[56-60] Achieving control over the size of patterns and avoiding non-specific binding of proteins is still a big challenge for protein patterning techniques based on photochemistry.

Cell microarrays are important platforms for the study of cellular processes and cell behaviour. It is thus important to spatially control cell adhesion on substrates for cell culture. Using light as a stimulus and developing functional substrates that can respond to irradiation to switch surface properties from cell non-adhesive to adhesive is a powerful method to realize such technologies. Several researchers have already created cell patterns either on glass or silicon-based surfaces using self-assembled monolayers (SAMs).[61,62] For example, Nakanishi et al. developed a method to control site-specific cell adhesion on a SAM spatiotemporally.[45] In their study, an o-nitrobenzyl derivative was used to create a photocleavable SAM surface based on an alkylsiloxane. Bovine serum albumin (BSA) was adsorbed onto the surface to prevent cell adhesion. Selective irradiation led to the binding of fibronectin to create cell adhesive regions. By controlling the size of the irradiated region, they could reduce the pattern to smaller than a single cell. Their results showed that the cells formed nodal structures corresponding to pattern size and shape. At the same time, by sequential irradiation of the substrate, they could control cell migration and proliferation from one patterned region to another. Their technique is a potential research tool for the manipulation of cells in biological studies. Dillmore et al. provided a method to pattern ligands and cells on SAMs made up of alkane-thiols on gold using an o-nitrobenzyl derivative (Figure 4.4).[63] Their method began with a NVOC-hydroquinone containing

monolayer on gold. Irradiation revealed the hydroquinone, which following oxidation, provided a site for the immobilization of cell adhesive peptides. Finally, the designed surface could generate circular patterns of attached cells corresponding to the photomask applied.

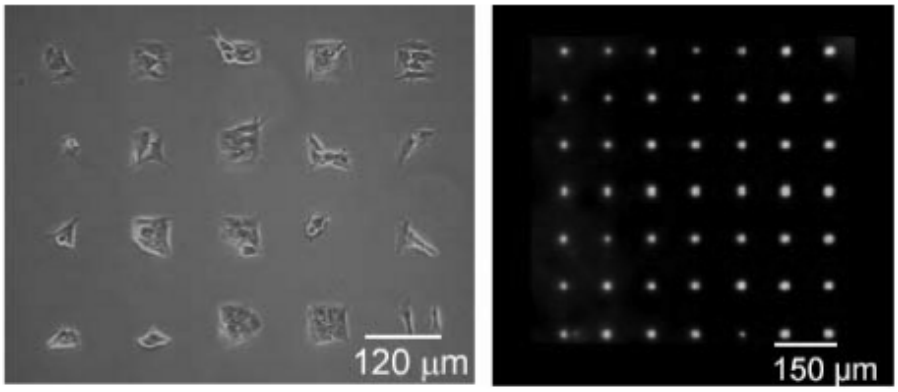

Figure 4.4: Swiss 3T3 fibroblast cells selectively attached to a SAM. Reprinted with permission.[63] Copyright 2010 American Chemical Society.

Park et al. also developed a protein and cell pattern on thiolated gold SAM surfaces using o-nitrobenzyl derivates.[64] Their strategy resulted in the immobilization of a variety of cell adhesive peptides containing a ketone group. At the same time, they showed the sequential immobilization of two fluorescent dyes in a pattern and also the immobilization of ligands in gradients. Our group also developed a photoactive substrate based on an alkane-thiol SAM on gold.[65] Poly(ethylene glycol) (PEG) was introduced to a gold SAM surface to initially create a cell repulsive surface via a photocleavable o-nitrobenzyl functional group. The cell repulsive surface was subsequently rendered cell adhesive by UV-irradiation to cleave the photoactive o-nitrobenzyl group and allow for the further immobilization of cell adhesive peptides onto the irradiated regions. Control of cell attachment was shown on the surfaces before and after UV-irradiation and the efficient control of cell attachment lasted up to 5 days in culture. Kikuchi et al. were able to photocage a variety of functional groups on a glass substrate and use their technology to pattern multiple cell types together on one surface at the single cell level.[66] Furthermore, there exist studies of photocleavable substrates to develop other technologies such as microfluidics devices[44] and devices for protein purification.[67]

Photocleavable molecules applied on solid supports are a promising platform to develop microarrays for DNA analysis and diagnostics, protein-protein interactions and the study of cell processes, drug screening and other biomedical applications. A solid flat support can minimize any topographical influence on the development of microarray chips and can also tolerate harsher operating or reaction conditions like organic solvent exposures and high temperatures, which are usually problematic for biomaterials.

4.3.2 Biomaterials for Controlled Release

The development of materials employing photolabile molecules destined for use in the human body is a much more recent area of research. One major application is for controlled release of drug molecules. Introducing photolabile molecules into the material design can potentially allow for release upon light exposure in a particular area of the body where it is needed and when it is needed. Previously, we had discussed the caging of actual drug molecules. These strategies, conversely, concentrate on caging a delivery vehicle which once developed, could hold any number of different drugs.

One such body of work has focused on the development of light-activated micelles for drug release. Micelles are aggregates formed in aqueous solutions such that a hydrophilic exterior surrounds and protects a mostly hydrophobic interior. Within this interior, drugs or bioactive molecules can be stored. In their pioneering work, Jiang et al. created a copolymer consisting of hydrophilic and hydrophobic blocks. The hydrophobic blocks, which ultimately form the micelle interior, contained a photolabile chromophore. Upon UV irradiation, the chromophore pendant group broke off from the polymer chain transforming its associated hydrophobic block to a hydrophilic one. This transformation ultimately led to the dissociation of the micelle and release of the hydrophobic cargo in its interior.[68] This group later modified their strategy to employ an o-nitrobenzyl derivative as the photolabile moiety in the co-block polymer seen in Figure 4.5. They were able to study the photo-controlled release of a model dye molecule and demonstrated release via two-photon irradiation, which unfortunately required longer irradiation times to achieve release.[69] In another drug delivery strategy, micelles were created containing a hydrophilic contrast agent in the interior detectable by MRI.[70] The hydrophobic component of the micelle contained an

o-nitrobenzyl derivative. Upon UV-irradiation, the photolabile groups could leave resulting in the formation of exposed carboxylic acids whose polar nature increased the hydrophilicity of the polymer micelle causing it to undergo a rearrangement and releasing its cargo in the process. Xie et al. employed a similar strategy but designed the o-nitrobenzyl containing polymer micelles to be biodegradable allowing for effective elimination from the body after release.[71] Such a strategy shows great potential to control the delivery of hydrophilic drugs with light.

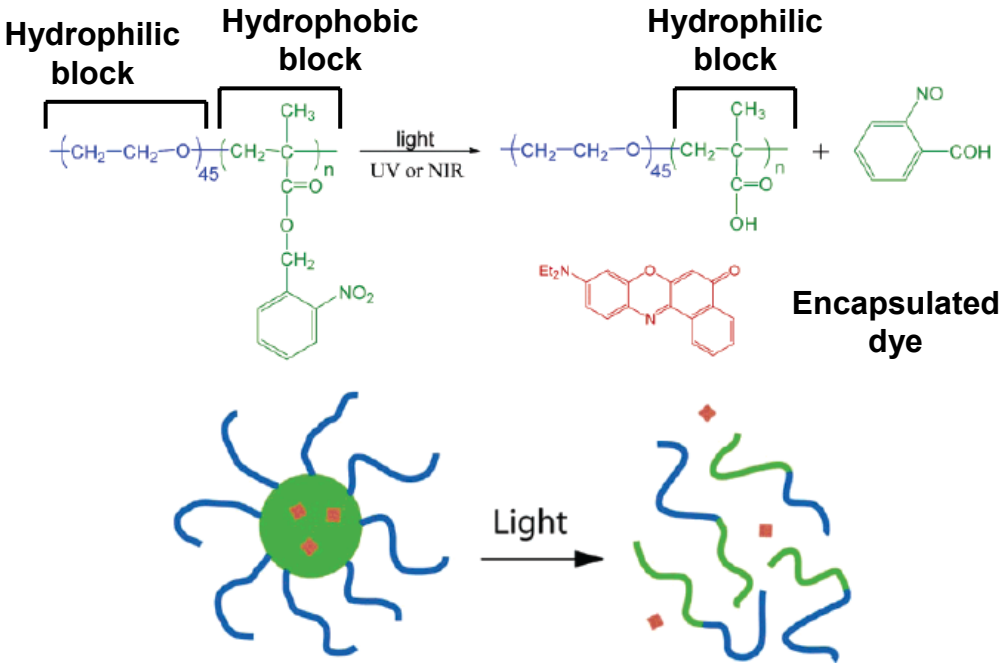

Figure 4.5: Structure of a block copolymer which forms a light-responsive micelle and the release of a representative encapsulated material after light exposure. Reprinted with permission,[69] Copyright 2010 American Chemical Society.

Similar to the micelle systems, Li et al. employed dendrimers made of poly(amidoamine) bound to an o-nitrobenzyl group for photo-responsive drug delivery (Figure 4.6). Dendrimers are large synthetic molecules possessing nanoscale internal cavities and having surfaces with bound functional groups of controllable quantities. Drugs can be encapsulated in the internal cavities. In this study, the 2-NB groups form the dendrimer shell keeping the drug molecules, salicylic acid and adriamycin, encased in the dendrimer. UV-induced cleavage of these photolabile groups allowed for drug escape.[72] Park et al. had previously designed dendrimers incorporating photo-activatable groups for light induced

release of model dye molecules and developed strategies for encapsulating hydrophilic molecules in the watery interior of the dendrimer as well as hydrophobic molecules in the membrane of the particles.[73]

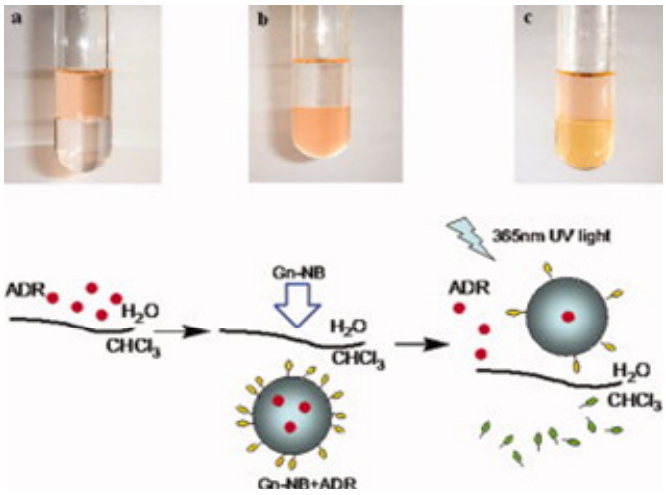

Figure 4.6: (A) Free Adriamycin (ADR) represented as dots is first dissolved in water and is encapsulated into the dendrimers (Gn-NB) in the chloroform phase upon addition. Note the presence of 2-NB drawn on the surface shell of the dendrimer in **(B)**. Irradiation causes the disintegration of the shell with freed 2-NB groups shown in the chloroform causing release of the ADR molecules into aqueous solution in **(C)**. Reprinted with permission.[72] Copyright 2010 John Wiley & Sons, Inc.

In their work, Murayama and Kato employed hydrogels as a drug delivery system.[74] The hydrogels encapsulated proteins and degraded upon near-UV light exposure. Degradation was controlled by introducing a photolabile group in the hydrogel crosslinker causing the crosslinkers to break apart upon irradiation. The group demonstrated that enzyme activity could be preserved by encapsulation in the hydrogel whereby released enzymes presented strong activity levels after UV irradiation making their delivery system ideal for bioactive proteins, which are easily degraded in the body and thus often difficult to use as drugs.

Another interesting avenue of controlled drug release research focuses on directly binding the caging group to a drug material and embedding the drug in a polymeric scaffold to form a delivery device. In the previous studies with micelles, the bioactive molecules of

interest were released at once in a relatively uncontrolled fashion upon micelle disintegration. Binding the photocage directly to a drug molecule, by comparison, has the potential to better control the quantity of drug released. McCoy et al. bound several model drugs such as acetyl salicylic acid, ibuprofen, and ketoprofen to a photolabile group, 3,5-dimethyoxybenzoin. The bound compounds were quite hydrophobic and when incorporated into a methyl methacrylate hydrogel, they remained encased in the matrix. Upon irradiation, the photolabile groups were removed rendering the drug molecules more hydrophilic and able to diffuse through aqueous solution in the hydrogel and freeing the drugs for delivery.[75]

In a unique strategy, Mizukami et al. created photoresponsive liposomes (Figure 4.7). However, instead of inserting the cage into the liposome structure, they caged an activator molecule that could create pores in the liposome upon UV irradiation.[76] This molecule was an antimicrobial peptide and they designed the liposome, which carries the biomolecules of interest in its interior, to be of similar composition to bacterial membranes. Using this methodology, they were able to visualize the release of a fluorescent dye from their system post irradiation.

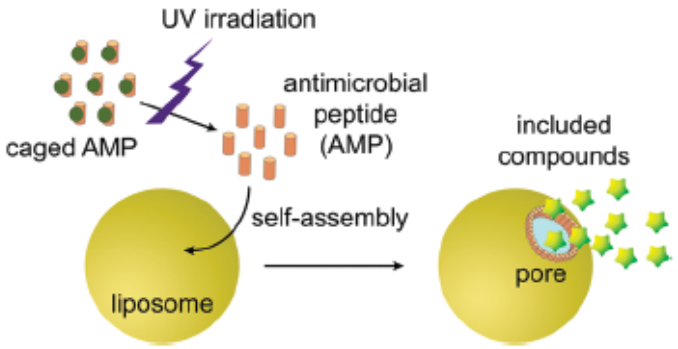

Figure 4.7: Diagram of a photorelease system based on a caged antimicrobial peptide which is activated upon irradiation to create pores in a liposome carrying molecules of interest. Reprinted with permission.[76] Copyright 2010 American Chemical Society.

Targeted drug delivery devices are currently in great demand to avoid the side effects associated with active drug freely circulating the body, targeting healthy tissues and cells and causing unwanted side effects. This is an area where traditional caging chemistry can be incorporated into new designs with biomaterials to provide effective solutions. The designs

discussed here have mostly been conceived over the past five years showing the beginnings of a new area of research which promises to grow stronger with time.

4.3.3 Controlling Biomaterial Physical Properties

In the previous section, we saw examples of how materials can be designed with traditional caging groups to control the release of a bioactive molecule for drug delivery. For applications such as tissue engineering or cell studies, it would be ideal to have tools which can afford a high level of control over biomaterial physical properties, such as material degradation, formation, or strength.

In one study to control bulk gel degradation, an o-nitrobenzyl derivative was introduced into a peptide amphiphile.[77] Peptide amphiphiles contain a short peptide sequence, which is often bioactive and relatively hydrophilic, connected to a hydrophobic segment. In solution, the molecules act like surfactants presenting the hydrophilic peptide sequences on the surface and burying the hydrophobic faces. These amphiphiles assemble spontaneously to form nanofibres which can be interconnected to form gels.[78] Löwik et al. inserted a photolabile o-nitrobenzyl derivative between the hydrophilic peptide and hydrophobic block of an amphiphile. Near UV-light exposure served to cleave the hydrophobic block away destabilizing the amphiphile leading to degradation of the biomaterial. The group suggested that not only could bulk degradation be performed, but that photomasks could potentially be used to spatially control degradation.[77]

Gels incorporating photolabile o-nitrobenzyl derivatives have also been designed to respond to more than one stimulus - both light and temperature. Gels were designed to undergo a transition from solution state to gel at higher temperatures and could be degraded upon exposure to near-UV light which cleaved a pendant 2-nitrobenzyl group leaving behind a free carboxylic acid. This caused a hydrophobic block of the polymer to become hydrophilic which served to increase the sol-gel transition temperature. Thus, the degraded gels could even be induced to gel again, but at a higher temperature.[79] This group had previously designed o-nitrobenzyl containing micelles also responsive to both light and temperature.[80]

Gels have also now been designed to degrade in a controlled fashion in select regions. Kloxin et al. created a photodegradable PEG hydrogel by incorporating a novel light-responsive monomer into the material.[81] PEG formed the base of the monomer which was attached to a photolabile o-nitrobenzyl derivative and acrylate end groups to facilitate polymerization (Figure 4.8A). This modified PEG monomer was copolymerized with PEG acrylate monomers to create the final photoresponsive hydrogel. In regions exposed to light, the modified monomer broke off from the polymer network causing gel degradation while leaving the material intact in non-exposed regions (Figure 4.8B). In this way, photomasks were used to control gel degradation for patterned erosion. The group demonstrated that live cells could be encapsulated in the gel and that controlled degradation could be used to manipulate cell movement by allowing for migration in eroded areas.

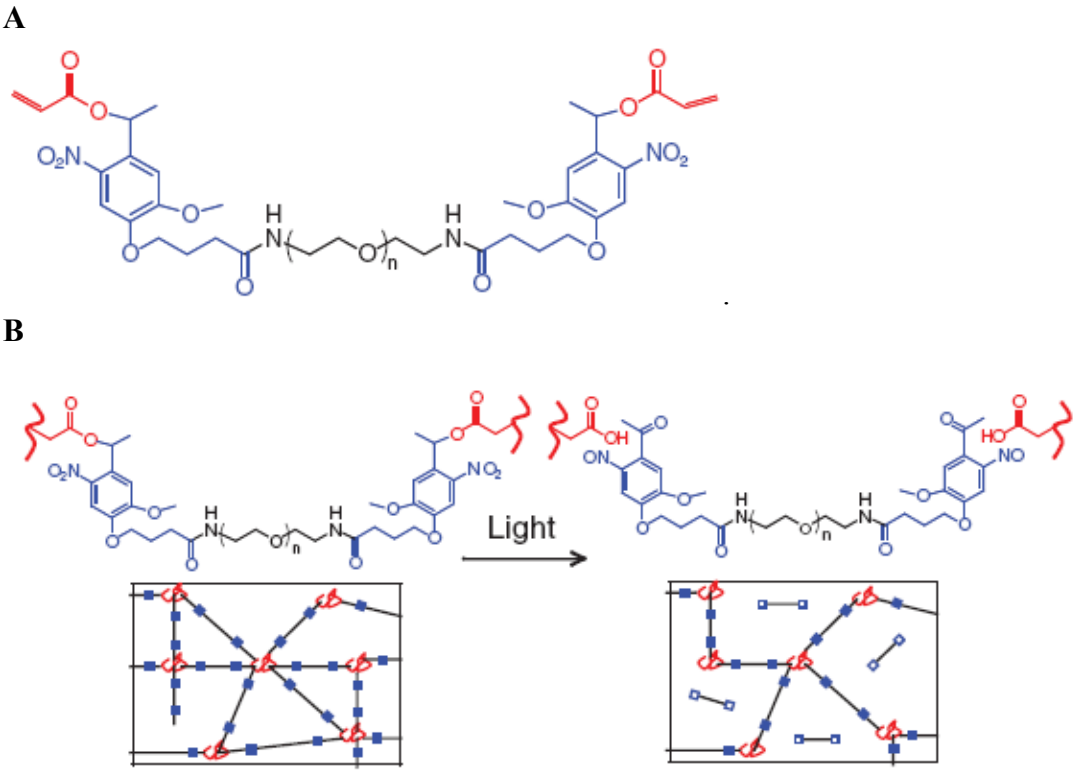

Figure 4.8: (A) Monomer used in the formation of photodegradable hydrogels **(B)** Method of light catalyzed polymer degradation where PEG polymer chains (coils) are crosslinked with PEG (lines) containing photolabile nitrobenzyl groups (squares) [81] Reprinted with permission from AAAS.

The group further studied this material system to characterize the degradation kinetics.[82] This ability to predict mass loss within a material can allow for control over the hydrogel's crosslinking density with irradiation time. The group was further able to vary the degree of degradation within the gel to create controlled gradients in both the x-y plane and z-direction. Material strength, which is related to the degree of crosslinking, is known to impact cell morphology and differentiation.[83,84] Towards such applications, human mesenchymal stem cells were successfully encapsulated within their degradable gels which were irradiated to create a gradient in the z-direction. Cells were found to spread within the material in areas of decreased crosslinking density demonstrating the biocompatibility of their system in addition to the ability to control stem cell behavior with light.

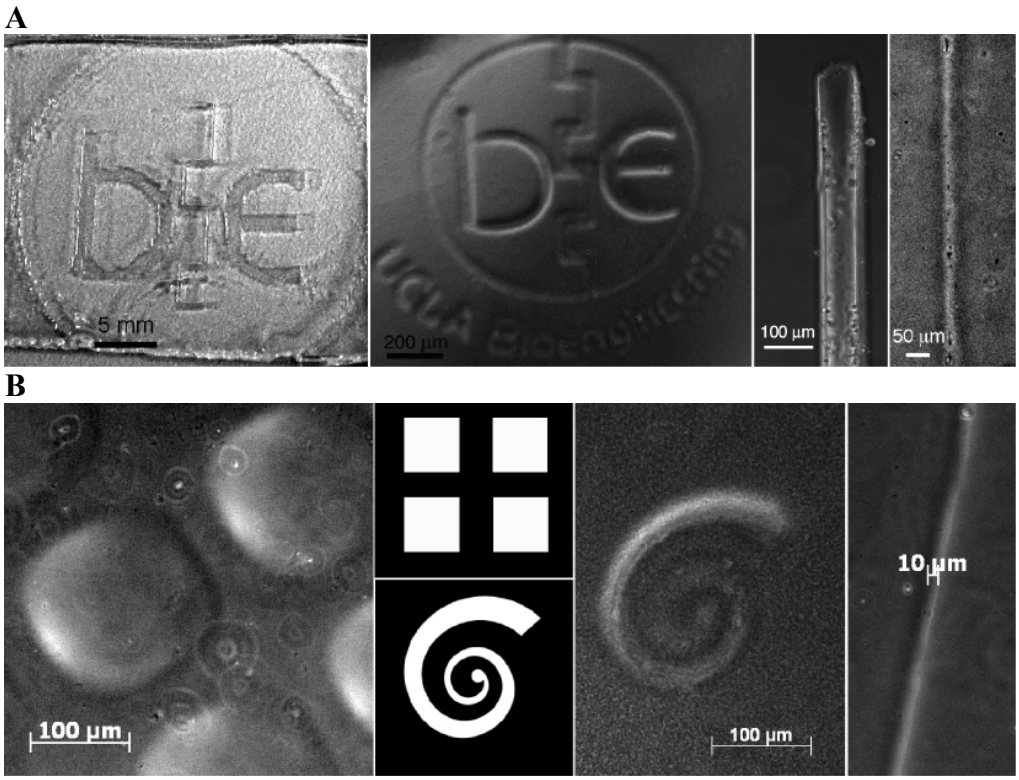

Figure 4.9: (A) Degraded features patterned in a hydrogel **(B)** Raised features patterned in a hydrogel. Reprinted with permission.[85] Copyright 2010 American Chemical Society.

The controllable degradation of this material was further used to produce patterned features in the hydrogel.[85] Negative, or recessed, features were created by exposing the gel to light through a photomask resulting in degradation in the exposed areas (Figure 4.9 A) while positive, or raised, features were created by decreasing the crosslinking density in light-

exposed regions without complete erosion of the material. This led to increased swelling of the hydrogel in these areas generating material patterns such as those seen in Figure 10 B. In addition, they were able to demonstrate degradation via two-photon photolysis. Since two-photon laser technology has the capability to focus light in three-dimensions, this leads to the possibility of forming a wide range of three dimensional patterns that do not necessarily need to be interconnected.

Materials with potential biological applications can not only be degraded with light, but also be induced to form with the help of photolabile switches. The ability to form hydrogels using light as a trigger can be very useful in biomedical applications. A liquid material could be injected into a body cavity and induced to gel at a pre-determined time point through irradiation allowing the gel to take the shape of the local environment. Haines et al. designed a peptide that can spontaneously fold in solution to self-assemble into a hydrogel. The peptide forms into a folded hairpin structure whereby one face of the hairpin is hydrophobic and the other hydrophilic. Since hydrophobic interactions were key to hydrogel self-assembly, the group hypothesized that introducing a negative charge on the hydrophobic side via a photolabile o-nitrobenzyl derivative could disrupt peptide folding. The group was able to successfully induce folding of the peptides upon near-UV light exposure.[86] Biocompatibility of the material was demonstrated by the adhesion and migration of 3T3 fibroblasts. Muraoka et al. similarly designed photoresponsive self-assembling peptides with the ability to gel upon irradiation and in one such peptide they were able to incorporate the well-known cell-adhesive peptide sequence Arg-Gly-Asp-Ser (RGDS).[87,88] Their material was also shown to support a 3T3 fibroblast culture in 3D where the cells developed focal adhesions on the gelled material indicative of cell attachment and spreading.

Traditional caging groups can thus be incorporated into soft biocompatible materials to control their degradation dynamically and spatially to produce high resolution patterns. Gelation can even be brought under temporal control using light as a switch. These techniques offer new tools for improved control over biomaterial properties for new tissue engineering solutions and applications in the study of cell biology.

4.3.4 Controlling Biomaterial Chemical Properties: Patterning Biomolecules and Cells

Another exciting application for traditional photolabile caging groups in biomaterial design is the generation of protein and cell patterns using light as a switch. One effective strategy to generate a peptide pattern for cell patterning is to cage an adhesive peptide and then bind it to a non-adhesive biomaterial. This creates a cell non-adhesive material prior to light exposure. Uncaging the peptide upon irradiation in a pattern leads to adhesive spots on the biomaterial to which cells can selectively bind. Our group utilized caged RGDS peptides bound to a non-adhesive hyaluronic acid hydrogel material to create such a cell pattern.[89] Figure 4.10 shows lined patterns of cells at various times post irradiation. We were later able to demonstrate the patterning of two cell types on the same surface to generate a patterned co-culture.[90] Petersen et al. and Ohmuro-Matsuyama utilized a similar caged peptide strategy to pattern 3T3s on solid-surfaces.[91,92]

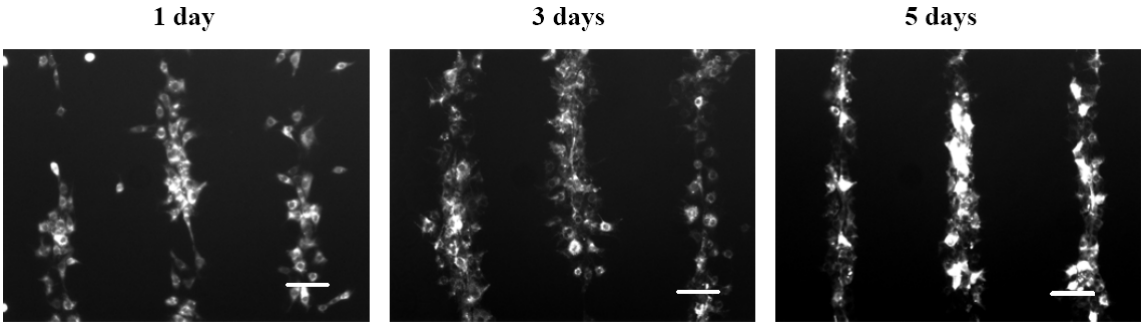

Figure 4.10: Fluorescence micrographs depicting line patterns of 3T3 fibroblasts dyed with CellTracker™ Red and grown on a HA hydrogel bound with patterned caged and uncaged R[G]DS peptide over five days post seeding. Scale bars = 100 μm.[90]

Gu and Yang developed a novel technique to create coordinated physical and chemical patterns in a biocompatible PEG hydrogel using a photolabile group and an enzyme.[93] Their technique relies on a unique crosslinker which contains a peptide sequence that can be cleaved by specific protease enzymes. However, the cleavage sequence is initially caged via an o-nitrobenzyl derivative so that it is inaccessible to the enzymes. Initial patterns are thus created by irradiating the crosslinked PEG gel to remove the photolabile group to create free peptide sequences in a desired pattern. Exposure to proteases then dissolves the gel in the irradiated regions to create a physical pattern. Protease degradation furthermore results in the formation of free reactive amine groups which can be used to bind

bioactive molecules in the physically patterned regions to create chemical patterns as well. Using this methodology, the group was able to create cell patterns on the single cell level in a hydrogel. They patterned circular wells 20 μm in diameter separated by 20 μm and 500 μm in depth and chemically patterned antibodies in the wells to trap β-cells.

There is a great deal of interest in guiding cells through a 3D environment. Patterning cells in 3D would allow for improved re-creations of the natural cellular microenvironment. In an exciting study, Shoichet's group was able to guide neuronal cells in three dimensions employing photolabile o-nitrobenzyl derivatives. The base materials they developed included an optically transparent agarose hydrogel and hyaluronic acid hydrogel through which cells could migrate. They modified the hydrogels to contain sulfhydryl groups protected by the o-nitrobenzyl derivative. With a laser, they were able to create a channel of free sulfhydryl groups which could subsequently be used to bind bioactive, adhesive peptides. They chose RGDS as the peptide and discovered that neurons could indeed be guided along these adhesive channels through the bulk of the gel (Figure 4.11).[94,95] In subsequent studies, this group attempted 3D patterning via two photon microscopy.[96,97] The two photon laser can potentially be used to form much more complex patterns to perhaps approach those complex biochemical cues found in natural tissue. Since nitrobenzyl-based photolabile groups have often been seen in the literature to be inefficiently removed with two-photon irradiation, the group decided to use a 6-bromo-7-hydroxycoumarin group in its place. They were able to demonstrate the formation of three dimensional patterns in the volume of the hydrogel (Figure 4.12) formed by two-photon irradiation by binding a dye to the freed sulfhydryl groups for pattern visualization. In a very recent study utilizing a similar patterning strategy, they were able to create gradients of a vascular endothelial growth factor in an agarose hydrogel bound with adhesive RGDS peptides to guide the migration of endothelial cells in 3D and induce the formation of tubule-like structures.[98]

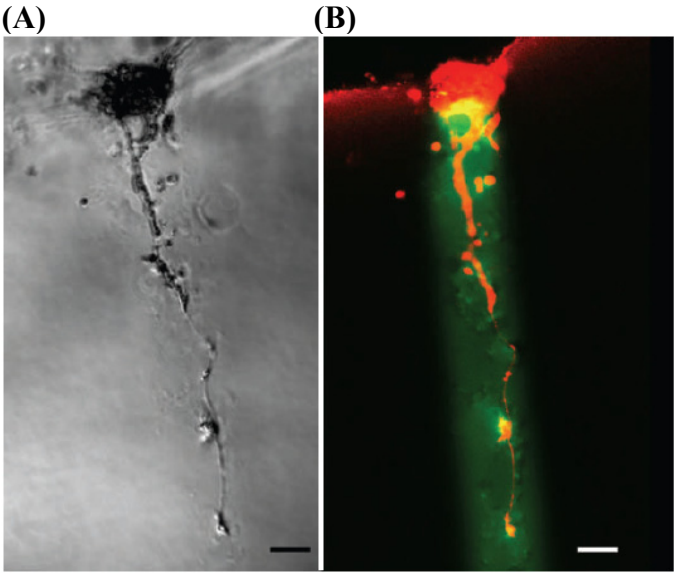

Figure 4.11: (A) Dorsal root ganglion cells growing within an agarose channel patterned with GRGDS peptides via photolabile 2-NB groups **(B)** Fluorescent micrograph of patterned agarose channel dyed green with fluorescein and cells labeled red. Reprinted by permission from Macmillan Publishers Ltd.: *Nature Materials*,[94] copyright 2010.

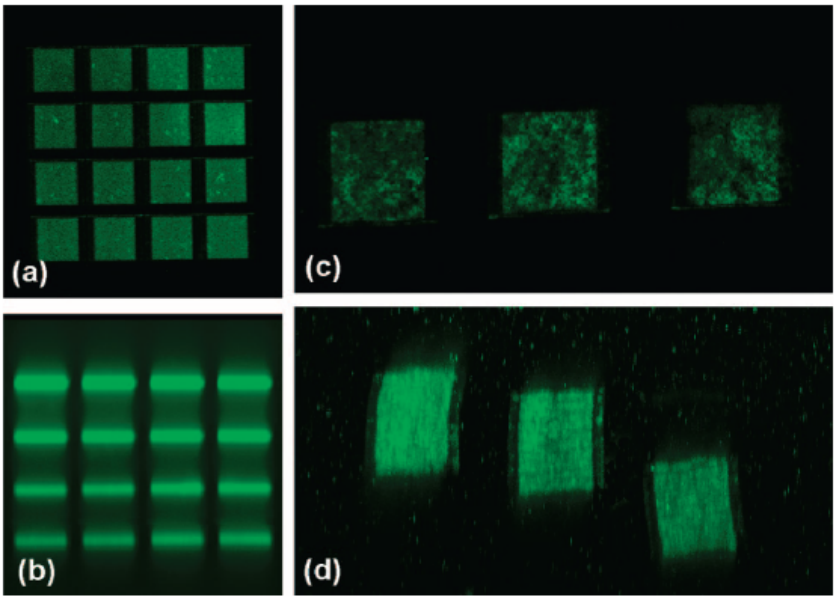

Figure 4.12: (A) Top view and **(B)** side view of two photon patterned squares in a hydrogel and **(C)** top view and **(D)** side view of rectangular volumes patterned in a hydrogel visualized with AF488-Mal dye. Reprinted with permission.[96] Copyright 2010 American Chemical Society.

4.4 Conclusion

Since the late 1970s, the caging of biomolecules and the design of biomaterials incorporating traditional photolabile caging groups has grown into a great body of highly creative research with huge potential. With the technology to cage small activators, proteins, and nucleic acids, the potential to control virtually any gene product or biochemical pathway with a light switch is within our grasp. With this power, we can hope to expand our current knowledge in the biological sciences and come to improved understandings of a variety of disease states. However, we appear to be sitting in the beginning stages of this technology's development. While we are amassing growing libraries of caged biomolecules, the number of purely application-based research papers taking advantage of the unique spatial and temporal control afforded by these techniques is limited. The application of these traditional photolabile caging molecules for light-activated control over the design of solid-surface biotechnologies and biomaterial properties is relatively newer. Many of the studies discussed were published within the last five years, or even the current year at the time of this writing. Material engineers and scientists have harnessed these molecules to make truly creative dynamic, light-responsive materials which could be developed into biochips, drug delivery devices, tissue engineered constructs and more. We have the power to carve channels and features into biomaterials, modify their strength and degradation, dictate gel formation, and create cell and protein patterns all spatially and temporally controlled with light. On or within these materials, cells can be exposed to changing conditions under our control to monitor or direct their behavior. However, once again, these materials are mostly in purely developmental stages. Caging biomolecules and designing these complex materials often requires a high level of specialized technical skills and such training may not be available to the end-users of these creations. To take all of these technologies employing photocaged molecules to the next step, the chemists, material scientists and engineers who have become design experts in these areas must form close ties with biologists, biochemists, and medical experts. Physicists and electrical engineers should also be consulted in the design of optimal lasers or other light sources for these different applications, which may involve laser access to areas of the body for drug delivery, creating a patterned exposure, or irradiating small focal volumes in three dimensions for local uncaging. As long as we can work together, the use of photolabile caging molecules has the potential to bring about leaps in understanding

in the biological sciences and a new generation of highly tunable and responsive biomaterials.

4.5 References

1. Young DD, Deiters A. Photochemical control of biological processes *Organic and Biomolecular Chemistry.* 2007;5(7):999-1005.

2. Pelliccioli AP, Wirz J. Photoremovable protecting groups: Reaction mechanisms and applications *Photochemical and Photobiological Sciences.* 2002;1(7):441-458

3. Goeldner M, Givens R. *Dynamic studies in biology : phototriggers, photoswitches and caged biomolecules*. Weinheim: Wiley-VCH; 2005.

4. Pelliccioli AP, Wirz J. Photoremovable protecting groups: Reaction mechanisms and applications. *Photochemical and Photobiological Sciences.* 2002;1(7):441-458.

5. Yu H, Li J, Wu D, Qiu Z, Zhang Y. Chemistry and biological applications of photo-labile organic molecules *Chemical Society Reviews.* 2010;39(2):464-473

6. Denk W, Strickler JH, Webb WW. Two-Photon Laser Scanning Fluorescence Microscopy. *Science.* 1990;248(4951):73-76.

7. Kaplan JH, Forbush B, Hoffman JF. Rapid photolytic release of adenosine 5'-triphosphate from a protected analog: utilization by the sodium:potassium pump of human red blood cell ghosts. *Biochemistry.* 1978;17(10):1929-1935.

8. Jun B, Kim S. Real-time Structural Transitions Are Coupled to Chemical Steps in ATP Hydrolysis by Eg5 Kinesin. *Journal of Biological Chemistry.* 2010;285(15):11073-11077.

9. Ellis-Davies GCR. Development and application of caged calcium. *Methods in Enzymology.* Vol 360: Academic Press; 2003:226-238.

10. Gomez TM, Spitzer NC. In vivo regulation of axon extension and pathfinding by growth-cone calcium transients. *Nature.* 1999;397(6717):350-355.

11. Pavlos CM, Hua X, Toscano JP. Photosensitive Precursors to Nitric Oxide. *Current Topics in Medicinal Chemistry.* 2005;5(7):637-647.

12. Dalva MB, Katz LC. Rearrangements of Synaptic Connections in Visual Cortex Revealed by Laser Photostimulation. *Science.* 1994;265(5169):255-258.

13. Kramer RH, Fortin DL, Trauner D. New photochemical tools for controlling neuronal activity. *Current Opinion in Neurobiology.* 2009;19(5):544-552.

14. Cambridge SB, Geissler D, Keller S, Cürten B. A caged doxycycline analogue for photoactivated gene expression. *Angewandte Chemie - International Edition* 2006;45(14):2229-2231.

15. Sauers DJ, Temburni MK, Biggins JB, Ceo LM, Galileo DS, Koh JT. Light-Activated Gene Expression Directs Segregation of Co-cultured Cells in Vitro. *ACS Chemical Biology.* 2010;5(3):313-320.

16. Bayley H. Pore-Forming Proteins with Built-in Triggers and Switches. *Bioorganic Chemistry.* 1995;23(4):340-354.

17. Chang C-y, Niblack B, Walker B, Bayley H. A photogenerated pore-forming protein. *Chemistry and Biology.* 1995;2(6):391-400.

18. Marriott G. Caged Protein Conjugates and Light-Directed Generation of Protein Activity: Preparation, Photoactivation, and Spectroscopic Characterization of Caged G-Actin Conjugates. *Biochemistry.* 1994;33(31):9092-9097.

19. Nandy SK, Agnes RS, Lawrence DS. Photochemically-Activated Probes of Protein Protein Interactions. *Organic Letters.* 2007;9(12):2249-2252.

20. Bourgault S, Létourneau M, Fournier A. Development of photolabile caged analogs of endothelin-1. *Peptides.* 2007;28(5):1074-1082.

21. Wood JS, Koszelak M, Liu J, Lawrence DS. A Caged Protein Kinase Inhibitor. *Journal of the American Chemical Society.* 1998;120(28):7145-7146.

22. Tatsu Y, Nishigaki T, Darszon A, Yumoto N. A caged sperm-activating peptide that has a photocleavable protecting group on the backbone amide. *FEBS Letters.* 2002;525(1-3):20-24.

23. Hiraoka T, Hamachi I. Caged RNase: photoactivation of the enzyme from perfect off-state by site-specific incorporation of 2-nitrobenzyl moiety. *Bioorganic & Medicinal Chemistry Letters.* 2003;13(1):13-15.

24. Wu N, Deiters A, Cropp TA, King D, Schultz PG. A Genetically Encoded Photocaged Amino Acid. *Journal of the American Chemical Society.* 2004;126(44):14306-14307.

25. Gautier A, Nguyen DP, Lusic H, An W, Deiters A, Chin JW. Genetically Encoded Photocontrol of Protein Localization in Mammalian Cells. *Journal of the American Chemical Society.*132(12):4086-4088.

26. Chen PR, Groff D, Guo J, et al. A facile system for encoding unnatural amino acids in mammalian cells. *Angewandte Chemie - International Edition.* 2009;48(22):4052-4055

27. Hahn ME, Muir TW. Photocontrol of Smad2, a Multiphosphorylated Cell-Signaling Protein, through Caging of Activating Phosphoserines. *Angewandte Chemie - International Edition.* 2004;43(43):5800-5803.

28. Pellois J-P, Muir TW. A ligation and photorelease strategy for the temporal and spatial control of protein function in living cells *Angewandte Chemie - International Edition.* 2005;44(35):5713-5717.

29. Chou C, Young DD, Deiters A. Photocaged T7 RNA polymerase for the light activation of transcription and gene function in pro- and eukaryotic cells. *ChemBioChem.* 2010;11(7):972-977.

30. Sadovski O, Jaikaran ASI, Samanta S, et al. A collection of caged compounds for probing roles of local translation in neurobiology. *Bioorganic & Medicinal Chemistry.* 2010;In Press, Corrected Proof.

31. Goard M, Aakalu G, Fedoryak OD, et al. Light-Mediated Inhibition of Protein Synthesis. *Chemistry and Biology.* 2005;12(6):685-693.

32. Miller DS, Chirayil S, Ball HL, Luebke KJ. Manipulating cell migration and proliferation with a light-activated polypeptide *ChemBioChem.* 2009;10(3):577-584.

33. Priestman MA, Lawrence DS. Light-mediated remote control of signaling pathways. *Biochimica et Biophysica Acta (BBA) - Proteins & Proteomics.* 2010;1804(3):547-558.

34. Sinha DK, Neveu P, Gagey N, et al. Photocontrol of protein activity in cultured cells and zebrafish with one- and two-photon illumination. *ChemBioChem.* 2009;11(5):653-663

35. Furuta T, Watanabe T, Tanabe S, Sakyo J, Matsuba C. Phototriggers for nucleobases with improved photochemical properties. *Organic Letters.* Nov 2007;9(23):4717-4720.

36. Ando H, Furuta T, Tsien RY, Okamoto H. Photo-mediated gene activation using caged RNA/DNA in zebrafish embryos. *Nature Genetics.* 2001;28(4):317.

37. Yamaguchi S, Chen Y, Nakajima S, Furuta T, Nagamune T. Light-activated gene expression from site-specific caged DNA with a biotinylated photolabile protection group. *Chemical Communications.* 2010;46(13):2244-2246.

38. Casey JP, Blidner RA, Monroe WT. Caged siRNAs for Spatiotemporal Control of Gene Silencing. *Molecular Pharmaceutics.* 2009;6(3):669-685.

39. Monroe WT, McQuain MM, Chang MS, Alexander JS, Haselton FR. Targeting Expression with Light Using Caged DNA. *Journal of Biological Chemistry.* 1999;274(30):20895-20900.

40. Thompson S, Self AC, Self CH. Light-activated antibodies in the fight against primary and metastatic cancer. *Drug Discovery Today.* 2010;15(11-12):468-473.

41. Skwarczynski M, Noguchi M, Hirota S, et al. Development of first photoresponsive prodrug of paclitaxel. *Bioorganic & Medicinal Chemistry Letters.* 2006;16(17):4492-4496.

42. Reinhard R, Schmidt BF. Nitrobenzyl-Based Photosensitive Phosphoramide Mustards: Synthesis and Photochemical Properties of Potential Prodrugs for Cancer Therapy. *Journal of Organic Chemistry.* 1998;63(8):2434-2441.

43. Li L-S, Babendure JL, Sinha SC, Olefsky JM, Lerner RA. Synthesis and evaluation of photolabile insulin prodrugs. *Bioorganic & Medicinal Chemistry Letters.* 2005;15(17):3917-3920.

44. Lim M, Rothschild KJ. Photocleavage-based affinity purification and printing of cell-free expressed proteins: Application to proteome microarrays. *Analytical Biochemistry.* 2008;383(1):103-115.

45. Nakanishi J, Kikuchi Y, Takarada T, Nakayama H, Yamaguchi K, Maeda M. Spatiotemporal control of cell adhesion on a self-assembled monolayer having a photocleavable protecting group. *Analytica Chimica Acta.* Sep 2006;578(1):100-104.

46. Seo TS, Bai XP, Ruparel H, Li ZM, Turro NJ, Ju JY. Photocleavable fluorescent nucleotides for DNA sequencing on a chip constructed by site-specific coupling chemistry. *Proceedings of the National Academy of Sciences of the United States of America.* 2004;101(15):5488-5493.

47. Afroz F, Barone AD, Bury PA, et al. Photo-removable protecting groups for in situ DNA microarray synthesis. *Clinical Chemistry.* 2004;50(10):1936-1939.

48. Chee M, Yang R, Hubbell E, et al. Accessing genetic information with high-density DNA arrays. *Science.* 1996;274(5287):610-614.

49. Fodor SPA, Read JL, Pirrung MC, Stryer L, Lu AT, Solas D. Light-Directed, Spatially Addressable Parallel Chemical Synthesis. *Science.* 1991;251(4995):767-773.

50. Mrksich M. Using self-assembled monolayers to model the extracellular matrix. *Acta Biomaterialia.* 2009;5(3):832-841.

51. Pelliccioli AP, Wirz J. Photoremovable protecting groups: reaction mechanisms and applications. *Photochemical & Photobiological Sciences.* 2002;1(7):441-458.

52. Sundberg SA, Barrett RW, Pirrung M, Lu AL, Kiangsoontra B, Holmes CP. Spatially-addressable immobilization of macromolecules on solid supports. *Journal of the American Chemical Society.* 1995;117(49):12050-12057.

53. Alonso JM, Reichel A, Piehler J, del Campo A. Photopatterned surfaces for site-specific and functional immobilization of proteins. *Langmuir.* 2008;24(2):448-457.

54. Lee KN, Shin DS, Chung WJ, Lee YS, Kim YK. Photochemical selective surface modification using micromirror array for biochip fabrication. In: Karam JM, Yasaitis J, eds. *Micromachining and Microfabrication Process Technology Vii.* Vol 4557 2001:352-359.

55. Grunwald C, Schulze K, Reichel A, et al. In situ assembly of macromolecular complexes triggered by light. *Proceedings of the National Academy of Sciences of the United States of America.*107(14):6146-6151.

56. Mancini RJ, Li RC, Tolstyka ZP, Maynard HD. Synthesis of a photo-caged aminooxy alkane thiol. *Org Biomol Chem.* 2009;7(23):4954-4959.

57. Veiseh M, Zareie MH, Zhang MQ. Highly selective protein patterning on gold-silicon substrates for biosensor applications. *Langmuir.* 2002;18(17):6671-6678.

58. Banala S, Arnold A, Johnsson K. Caged substrates for protein labeling and immobilization. *Chembiochem.* 2008;9(1):38-41.

59. Nakagawa M, Ichimura K. Photopatterning of self-assembled monolayers to generate aniline moieties. *Colloids and Surfaces a-Physicochemical and Engineering Aspects.* 2002;204(1-3):1-7.

60. Ito Y, Nogawa M, Takeda M, Shibuya T. Photo-reactive polyvinylalcohol for photo-immobilized microarray. *Biomaterials.* 2005;26(2):211-216.

61. Chen SY, Smith LM. Photopatterned Thiol Surfaces for Biomolecule Immobilization. *Langmuir.* 2009;25(20):12275-12282.

62. Nakayama H, Nakanishi J, Shimizu T, et al. Silane coupling agent bearing a photoremovable succinimidyl carbonate for patterning amines on glass and silicon surfaces with controlled surface densities. *Colloids and Surfaces B-Biointerfaces.* 2010;76(1):88-97.

63. Dillmore WS, Yousaf MN, Mrksich M. A photochemical method for patterning the immobilization of ligands and cells to self-assembled monolayers. *Langmuir.* 2004;20(17):7223-7231.

64. Park S, Yousaf MN. An interfacial oxime reaction to immobilize ligands and cells in patterns and gradients to photoactive surfaces. *Langmuir.* 2008;24(12):6201-6207.

65. Cheng N, Cao XD. Photoactive SAM surface for control of cell attachment. *Journal of Colloid and Interface Science.* 2010;348(1):71-79.

66. Kikuchi Y, Nakanishi J, Shimizu T, et al. Arraying Heterotypic Single Cells on Photoactivatable Cell-Culturing Substrates. *Langmuir.* 2008;24(22):13084-13095.

67. Besson E, Gue AM, Sudor J, Korri-Youssoufi H, Jaffrezic N, Tardy J. A novel and simplified procedure for patterning hydrophobic and hydrophilic SAMs for microfluidic devices by using UV photolithography. *Langmuir.* 2006;22(20):8346-8352.

68. Jiang J, Tong X, Zhao Y. A New Design for Light-Breakable Polymer Micelles. *Journal of the American Chemical Society.* 2005;127(23):8290-8291.

69. Jiang J, Tong X, Morris D, Zhao Y. Toward Photocontrolled Release Using Light-Dissociable Block Copolymer Micelles. *Macromolecules.* 2006;39(13):4633-4640.

70. Lepage M, Jiang J, Babin J, Qi B, Tremblay L, Zhao Y. MRI observation of the light-induced release of a contrast agent from photo-controllable polymer micelles. *Physics in Medicine and Biology.* 2007;52:N249–N255.

71. Zhigang X, Xiuli H, Xuesi C, Guojun M, Jing S, Xiabin J. A Novel Biodegradable and Light-Breakable Diblock Copolymer Micelle for Drug Delivery. *Advanced Engineering Materials.* 2009;11(3):B7-B11.

72. Li Y, Jia X, Gao M, He H, Kuang G, Wei Y. Photoresponsive nanocarriers based on PAMAM dendrimers with a o-nitrobenzyl shell. *Journal of Polymer Science Part A: Polymer Chemistry.* 2010;48(3):551-557.

73. Park C, Lim J, Yun M, Kim C. Photoinduced Release of Guest Molecules by Supramolecular Transformation of Self-Assembled Aggregates Derived from Dendrons. *Angewandte Chemie - International Edition.* 2008;47(16):2959-2963.

74. Murayama S, Kato M. Photocontrol of Biological Activities of Protein by Means of a Hydrogel. *Analytical Chemistry.* 2010;82(6):2186-2191.

75. McCoy CP, Rooney C, Edwards CR, Jones DS, Gorman SP. Light-Triggered Molecule-Scale Drug Dosing Devices. *Journal of the American Chemical Society.* 2007;129(31):9572-9573.

76. Mizukami S, Hosoda M, Satake T, et al. Photocontrolled Compound Release System Using Caged Antimicrobial Peptide. *Journal of the American Chemical Society.* 2010;132(28):9524-9525.

77. Löwik DWPM, Meijer JT, Minten IJ, et al. Controlled disassembly of peptide amphiphile fibres. *Journal of Peptide Science.* 2008;14(2):127-133.

78. Cui H, Webber MJ, Stupp SI. Self-assembly of peptide amphiphiles: From molecules to nanostructures to biomaterials. *Peptide Science.* 2010;94(1):1-18.

79. Woodcock JW, Wright RAE, Jiang X, O'Lenick TG, Zhao B. Dually responsive aqueous gels from thermo- and light-sensitive hydrophilic ABA triblock copolymers. *Soft Matter.* 2010;6(14):3325-3336.

80. Jiang X, Lavender CA, Woodcock JW, Zhao B. Multiple Micellization and Dissociation Transitions of Thermo- and Light-Sensitive Poly(ethylene oxide)-b-poly(ethoxytri(ethylene glycol) acrylate-co-o-nitrobenzyl acrylate) in Water. *Macromolecules.* 2008;41(7):2632-2643.

81. Kloxin AM, Kasko AM, Salinas CN, Anseth KS. Photodegradable Hydrogels for Dynamic Tuning of Physical and Chemical Properties. *Science.* 2009;324(5923):59-63.

82. Kloxin AM, Tibbitt MW, Kasko AM, Jonathan AF, J.A., Anseth KS. Tunable Hydrogels for External Manipulation of Cellular Microenvironments through Controlled Photodegradation. *Advanced Materials.* 2010;22(1):61-66.

83. Lutolf MP, Gilbert PM, Blau HM. Designing materials to direct stem-cell fate. *Nature.* 2009;462(7272):433-441.

84. Leipzig ND, Shoichet MS. The effect of substrate stiffness on adult neural stem cell behavior. *Biomaterials.* 2009;30(36):6867-6878.

85. Wong DY, Griffin DR, Reed J, Kasko AM. Photodegradable Hydrogels to Generate Positive and Negative Features over Multiple Length Scales. *Macromolecules.* 2010;43(6):2824-2831.

86. Haines LA, Rajagopal K, Ozbas B, Salick DA, Pochan DJ, Schneider JP. Light-Activated Hydrogel Formation via the Triggered Folding and Self-Assembly of a

Designed Peptide. *Journal of the American Chemical Society.* 2005;127(48):17025-17029.

87. Muraoka T, Cui H, Stupp SI. Quadruple Helix Formation of a Photoresponsive Peptide Amphiphile and Its Light-Triggered Dissociation into Single Fibers. *Journal of the American Chemical Society.* 2008;130(10):2946-2947.

88. Muraoka T, Koh C-Y, Cui H, Stupp SI. Light-Triggered Bioactivity in Three Dimensions. *Angewandte Chemie International Edition.* 2009;48(32):5946-5949.

89. Goubko C, Majumdar S, Basak A, Cao X. Hydrogel cell patterning incorporating photocaged RGDS peptides. *Biomedical Microdevices.* 2010;12(3):555-568.

90. Goubko CA, Majumdar S, Basak A, Cao X. Novel cell patterning platform employing photocaged RGDS peptides on a hydrogel. *AIChE Annual Meeting, Conference Proceedings*. Nashville, TN 2009.

91. Petersen S, Alonso JM, Specht A, Duodu P, Goeldner M, del Campo A. Phototriggering of Cell Adhesion by Caged Cyclic RGD Peptides. *Angewandte Chemie International Edition.* 2008;47(17):3192-3195.

92. Ohmuro-Matsuyama Y, Tatsu Y. Photocontrolled Cell Adhesion on a Surface Functionalized with a Caged Arginine-Glycine-Aspartate Peptide. *Angewandte Chemie International Edition.* 2008;47(39):7527-7529.

93. Gu Z, Tang Y. Enzyme-assisted photolithography for spatial functionalization of hydrogels. *Lab on a Chip.* 2010;10(15):1946-1951.

94. Luo Y, Shoichet MS. A photolabile hydrogel for guided three dimensional cell growth and migration. *Nature Materials.* 2004;3:249-253.

95. Musoke-Zawedde P, Shoichet MS. Anisotropic three-dimensional peptide channels guide neurite outgrowth within a biodegradable hydrogel matrix *Biomedical Materials.* 2006;1(3):162-169.

96. Wosnick JH, Shoichet MS. Three-dimensional Chemical Patterning of Transparent Hydrogels. *Chemistry of Materials.* 2008;20(1):55-60.

97. Wylie RG, Shoichet MS. Two-photon micropatterning of amines within an agarose hydrogel. *Journal of Materials Chemistry.* 2008;18(23):2716-2721.

98. Aizawa Y, Wylie R, Shoichet M. Endothelial Cell Guidance in 3D Patterned Scaffolds. *Advanced Materials.* 2010.

CHAPTER 5:
HYDROGEL CELL PATTERNING INCORPORATING PHOTOCAGED RGDS PEPTIDES

Catherine A. Goubko, Swapan Majumdar, Ajoy Basak, Xudong Cao

Reprinted with kind permission from Springer Science and Business Media
Biomed Microdevices
12, 555 (2010)

The following paper represents the first full length research paper published for this thesis. Herein, we discuss the chemical synthesis and photoactive properties of caged RGDS peptides as well as the subsequent binding of these peptides to our hydrogel base. We further demonstrate the ability of this modified hydrogel material to pattern 3T3 fibroblast cells on the micron scale using near-UV light exposure through a patterned photomask to selectively switch areas of the hydrogel surface from cell non-adhesive to cell adhesive. The cells are found to adhere and proliferate along the developed line patterns for at least 2.5 days. When this thesis work began, photocaging of an RGD peptide had not been carried out previously in the literature. During this thesis (as began in 2007), two communication papers were released whereby different RGD peptides (i.e. cyclo(-Arg-Gly-Asp-D-Phe-Val-) and YAVTGRGDSPASS) were caged to control cell adhesion.[1,2] With this publication, we released the first full-length paper detailing the use of photocaged RGD peptides to form cell patterns. This work was also novel in the respect that patterning with the photocaged RGD peptides was demonstrated on a hydrogel material. Furthermore, the patterned fibroblasts were shown to remain on-pattern longer in comparison to the previously referenced studies (i.e. 2.5 days at which fibroblasts peeled from the surface vs. 6 hours at which fibroblasts moved significantly off-pattern).[1,3]

5.1 Introduction

The nature of the microenvironment surrounding cells has a substantial impact on cell behavior.[4-7] In the body, complex tissue architectures exist with carefully crafted microenvironments to guide cell behavior. As a result, techniques are needed to gain *in vitro* design control over the cell microenvironment to allow for the creation of improved cell-based devices and to assist researchers in advancing our current knowledge of cell biology. In traditional culture methods, cells are seeded randomly on a surface. In contrast, cell patterning systems can allow for control over the degree of contact that cells make with an underlying material substrate and with neighboring cells.[8-10] These parameters can then be manipulated to optimize or explore cell functions while the high degree of control attained can allow for improved experimental reproducibility and lower variability in cell-based devices. As such, the potential applications for cell patterning systems are numerous. For

example, cell patterning has demonstrated that the multicellular organization of cells determines their growth pattern[11] and that cell shape can influence whether cells grow or die.[8] Spatially defined neural networks have been patterned and will ultimately lend to a greater understanding of the nervous system organization and its function in information processing.[12-14] In the field of tissue engineering, epithelial cells have been patterned and organized atop human lens capsules towards the development of a retinal implant,[15] and patterned materials have been developed to maintain chondrocyte phenotype for cartilage regeneration.[16] Numerous other examples can be found in the literature and the future will undoubtedly bring more fascinating and far-reaching applications.

The majority of cell patterning methods developed to date have relied heavily on either photolithography or soft lithography techniques.[4,17-20] While commonly used, these techniques suffer drawbacks in practice. For example, photolithography - originally developed for the semi-conductor industry - utilizes toxic solvents which can hinder the use of easily denatured biomolecules and requires specialized clean rooms and expensive equipment. This makes it inaccessible to most life scientists. Soft lithography, while much gentler towards the biomolecules used for cell patterning, often depends on adsorption as opposed to covalent binding of biomolecules to a surface in creating cell patterns, which can limit pattern longevity. In this study, we report a novel cell patterning platform based on a hydrogel which makes use of extracellular matrix (ECM) materials in order to closely mimic the natural cell microenvironment and employs methods accessible to life scientists. Patterning is performed with light, and thus has the potential to eventually obtain resolutions near the single cell level (i.e. pattern sizes in the 15 μm range for animal cells).[21] Additionally, the biomolecules involved in our pattern formation are covalently bound to the base of the pattern to maximize longevity.

An overview of our cell patterning methodology can be seen in Figure 5.1. The base of the design is a non-adhesive crosslinked hyaluronic acid (HA) hydrogel. RGDS peptides were bound to the hydrogel to create a cell-adhesive layer. This sequence is naturally found in the ECM as a recognition site within the cell-adhesive protein fibronectin and binds to integrin receptors located on the surfaces of cells.[22] In order to allow for pattern creation, a

photo-labile caging group, 2-nitrobenzyl (2-NB), was covalently bound to the RGDS peptides to disrupt integrin recognition and thus cell binding. Therefore, the photocaged-RGDS peptides immobilized to the HA base create a surface that is cell non-adhesive. The 2-NB photocage can be selectively removed from RGDS upon near-UV light exposure through a patterned photomask to produce adhesive RGDS regions on an otherwise cell non-adhesive background. In this manner, a cell pattern can be formed as dictated by the photomask used.

In this work, the photocaged RGDS peptide was synthesized such that the 2-NB group was attached to the nitrogen atom of the backbone amide group between the Arg and Gly residues (designated as R[G]DS) as indicated by the symbol [G]. Such binding of a photocage group to a peptide backbone and its biochemical use have been recently demonstrated in the literature.[23-25] In selecting where along the peptide to bind the cage, it was noted that substituting the Gly residue with Ala - where the only structural difference is a single methyl group - has been shown to knock out RGD binding activity.[22,26] Therefore, we hypothesized that the introduction of a bulky group, such as 2-NB, would serve to severely disrupt the adhesive properties of the RGDS sequence. Furthermore, the stability of the bond that could be formed at this location on the peptide appeared superior to other possible sites such as the carboxylic acid group on the Asp residue[27] or the guanidinium group on the Arg residue.[28]

During the course of this study, a couple of other research groups have independently reported the development of photoresponsive RGD-based peptides in communication papers with Petersen et al. being the first to do so.[29,30] Both works were able to demonstrate significantly decreased cell adherence to caged RGD-modified surfaces versus RGD- or uncaged RGD- modified surfaces. In addition, Petersen et al. showed the formation of a preliminary cell pattern with NIH 3T3 fibroblasts. However, cells showed significant off-pattern binding only 6 h after seeding. The strategy of Petersen et al. relied on an oligo(ethylene glycol) (OEG) linker to both tether the caged RGD-based peptide onto a solid silica-based surface and act as a cell non-adhesive background. Similarly, Ohmuro-Matsuyama and Tatsu used a poly(ethylene glycol) (PEG) linker to create a non-adhesive

background on a poly-L-lysine coated culture dish.[2] Our strategy, in contrast, is based on a hydrogel of crosslinked ECM molecules in place of a solid synthetic surface to which peptides were bound with a zero-length crosslinker (i.e. the peptides were bound to the hydrogel directly with the crosslinker adding no spacer in-between). Hydrogels based on natural materials have demonstrated great potential for biological and medical applications due to their biocompatibility.[31] As such, the development of a technique to spatially localize cells on such a material has increased potential for future tissue engineering applications.

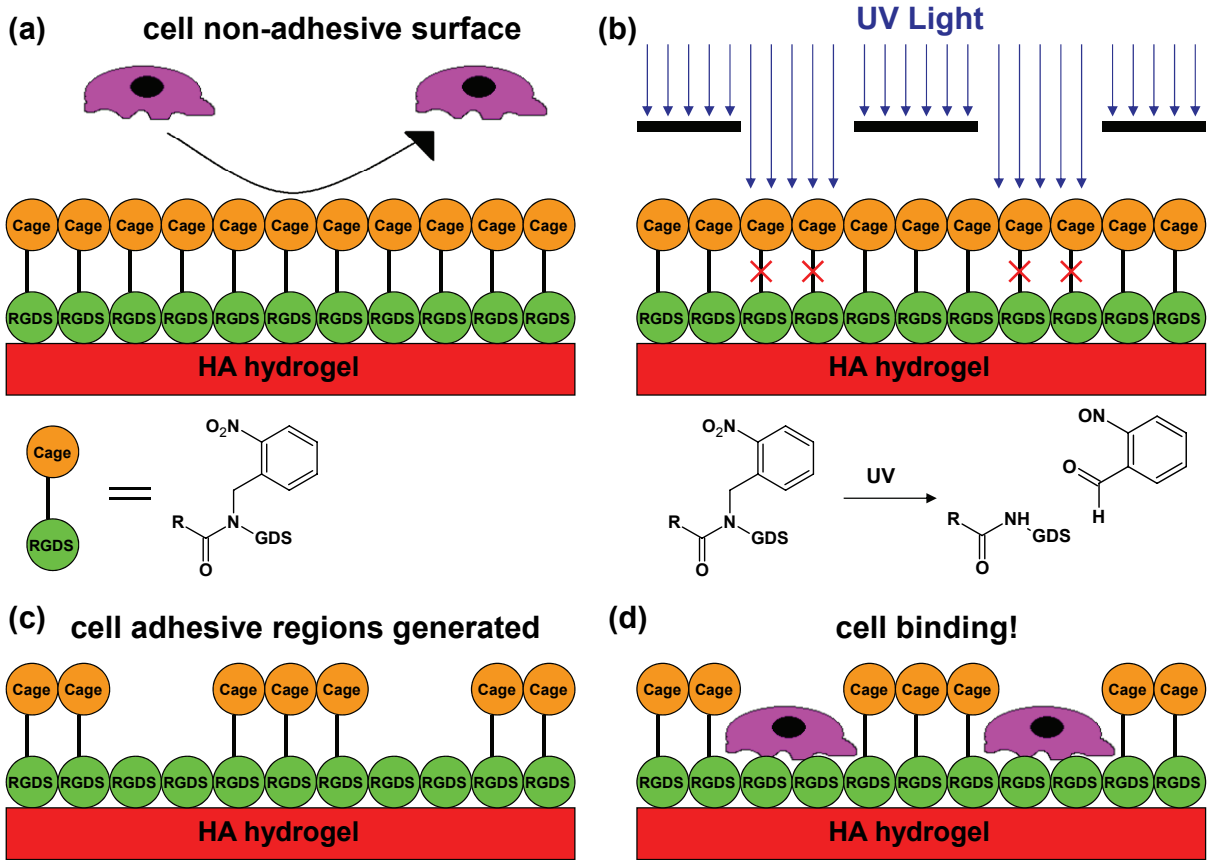

Figure 5.1: Strategy to create a patterned surface: **(a)** Adhesive RGDS peptides are caged and bound to a non-adhesive HA hydrogel to produce a cell non-adhesive surface. **(b)** Caging groups are removed upon exposure to UV light through a photomask **(c)** leaving patterned, exposed regions of RGDS **(d)** to which cells can bind.

This paper outlines the development of our cell patterning strategy including the development of the HA hydrogel base, along with the synthesis and analysis of the R[G]DS peptides. Finally, we demonstrate that cell patterns can be formed on our novel hydrogel surface which demonstrates significantly increased pattern longevity from those previously reported employing similar photocaged peptides.

5.2 Materials and Methods

5.2.1 Materials

Peptide coupling reagents, i.e. N,N'-diisopropylcarbodiimide (DIC), 4-dimethylaminopyridine (DMAP), 2-(1H-7-Azabenzotriazol-1-yl)-1,1,3,3-tetramethyl uranium hexafluorophosphate methanaminium (HATU), and N,N-diisopropylethylamine (DIPEA) were purchased from Applied Biosystems (Framingham, MA). For peptide synthesis, protected amino acids, Boc-Arg(Pbf)-OH, H-Gly-OMe·HCl, Boc-Asp(OBu^t)-OH and H-Ser(Bu^t)-OBu^t were bought from ChemImpex International (Wooddale, IL) and Bachem Inc. (Torrance, CA). All other chemicals were purchased from Sigma-Aldrich (St. Louis, MO) unless otherwise indicated. All chemicals were used as received.

5.2.2 Preparation of HA Hydrogels

A final *Streptococcus equi* fermentation-derived hyaluronic acid sodium salt (avg. MW 1,200 kDa, research grade) solution of 4 mg/mL concentration in sterile distilled and deionized water (dd-water) was used to make HA gels. To prepare the crosslinked HA gel substrate, a solution of adipic acid dihydrazide (ADH, 15 mg) in 0.5 mL of sterile dd-water was filtered through a 0.45 μm filter and added to 10 mL of aqueous HA solution. The resulting solution was adjusted to pH 3.5 by slowly adding 1 M HCl. This was followed by the addition of 16.5 mg of filtered 1-ethyl-3-(3-dimethylaminopropyl) carbodiimide (EDC) in 1 mL of sterile dd-water with vigorous agitation. To the wells of a 12-well polystyrene tissue culture plate, 1.4 mL of the resulting reaction solution was transferred to let set. To prevent premature crosslinking, the reaction solution was cooled prior to EDC addition. Gelation was allowed to occur overnight at room temperature. The resulting gels were then washed in sterile phosphate-buffered saline (PBS) solution at pH 7.4 (Invitrogen) for 24

hours with light agitation, followed by a 24 hour wash with dd-water. This initial HA layer was air dried for several days and two more layers of gel were deposited atop the first in the same fashion as that outlined above. Prior to use, gels were rehydrated to equilibrate in sterile PBS.

5.2.3 Peptide Synthesis

The two tetrapeptides, caged RGDS **(1)** and native RGDS **(2)** (chemical structures shown in Figure 5.2(a), were synthesized stepwise via liquid phase and solid phase peptide chemistry methods, respectively. Figure 5.3 outlines the synthesis of the caged RGDS peptide **(1)**. The preparation of native RGDS peptide (steps not shown) was accomplished by normal HATU/DIPEA mediated Fmoc based solid phase chemistry as described earlier.[32] For the caged peptide **(1)**, a 2-NB group was linked to the backbone amide nitrogen between the Arg and Gly residues. To achieve this, N-α-2'-nitrobenzyl-glycine methyl ester **(3)** was first prepared from o-nitro benzaldehyde by coupling it with glycine methyl ester in alkaline solution in the presence of sodium bicarbonate followed by reduction with sodium borohydride, as shown in Figure 5.2(b). Specifically, o-nitro benzaldehyde (3.02 g, 0.02 mol) in methanol (50 ml) was added to 50 ml cold Gly-OMe·HCl (0.02 mol) $NaHCO_3$ solution (2%, w/v) under agitation, and the reaction mixture continued to be stirred for an additional 1h while the temperature was kept below 4^{o}C. Subsequently, $NaBH_4$ (0.800 g, 0.021 mol) was slowly added to the reaction while maintaining the temperature between 0-5^{o}C. After stirring for another 2h, the resultant solution was dried under vacuum to evaporate methanol, and the residue was extracted with ether (3 x 50 ml) at low temperature. The combined organic layer was washed with brine solution, dried over anhydrous Na_2SO_4 and fully evaporated under vacuum to obtain **(3)** as a dry brown gummy residue (1.2 g, not optimized). The caged tetrapeptide R[G]DS was then synthesized using this intermediate according to the scheme shown in Figure 5.3**.** To a stirred, cold mixture of Boc-Arg(Pbf)-OH (1 mmol) and **(3)** (1.1 mmol) in dichloromethane (15 ml), DIC (182 mg, 1.2 mmol) was added followed by DIPEA (200mg, 1.5mmol) and a catalytic amount of DMAP.

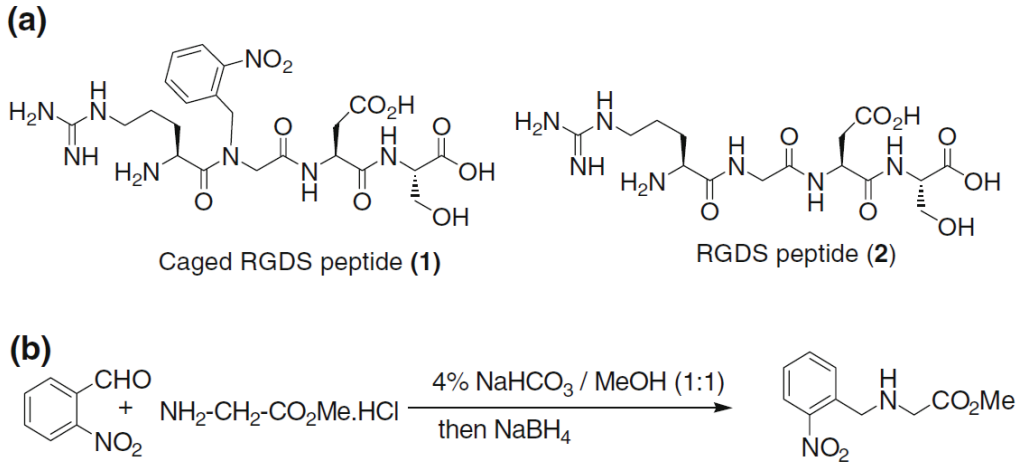

Figure 5.2: (a) Chemical structures of caged and native tetrapeptides used in the present study and **(b)** chemical steps involved in the synthesis of caged Gly residue.

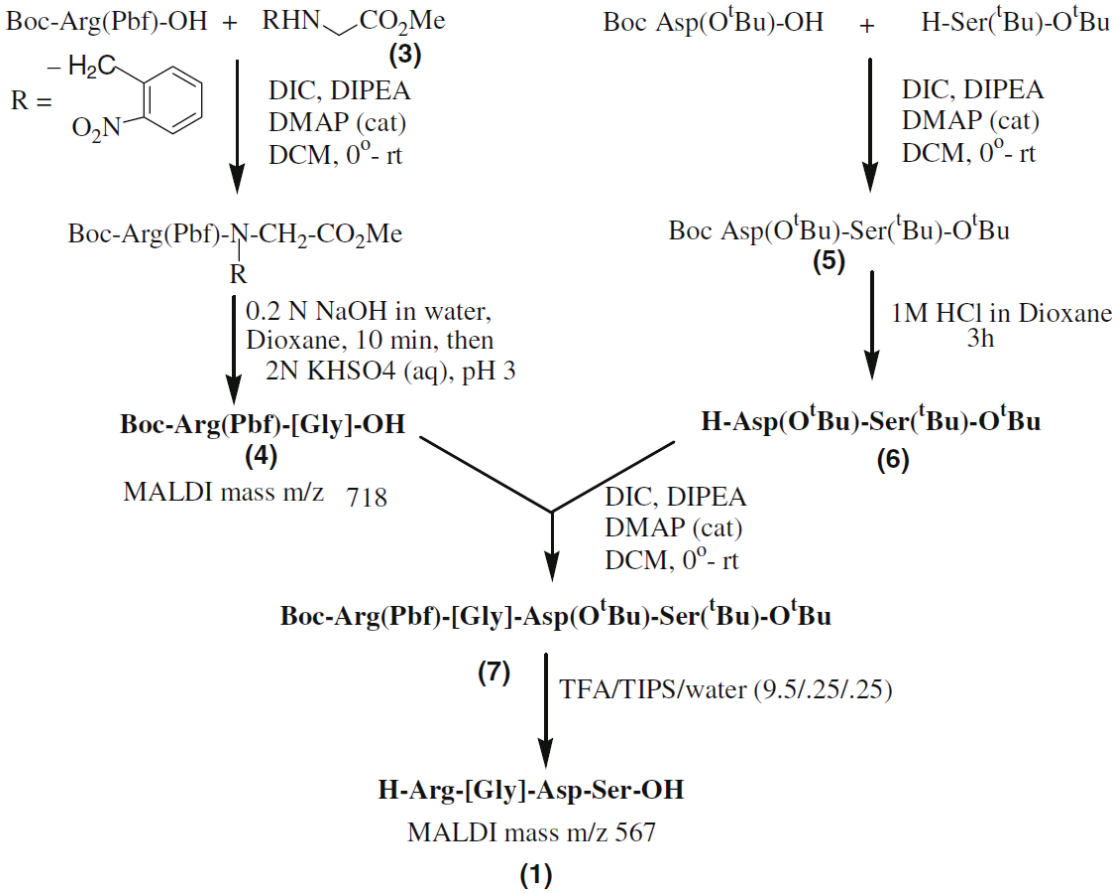

Figure 5.3: Complete schematic diagram showing various steps involved in the synthesis of caged RGDS tetrapeptide using liquid phase peptide chemistry.

After completion of the reaction, as revealed by thin layer chromatography (TLC), dichloromethane was removed using a rotary evaporator, and ethyl acetate (25 ml) was added. The white precipitate (i.e. byproduct from DIC) formed was filtered off and washed with ethyl acetate (20 ml). The combined organic layer was evaporated and dried under vacuum. The white powder thus obtained was dissolved in dioxane (20 ml) and cooled to 0^oC in an ice bucket. A 0.2 M aqueous NaOH (10 ml) was added dropwise for hydrolysis of the ester bond. After completion of the reaction (~ 10 min) as revealed by TLC, dioxane was removed by rotary evaporation. The obtained residue was re-dissolved in 50 ml water and pH adjusted to 3.0 by 2M aqueous $KHSO_4$. The reaction mixture was extracted with ethyl acetate (3 x 20 ml) in a separatory funnel. The combined organic layer was dried over anhydrous Na_2SO_4 and evaporated to dryness under vacuum to afford Boc-Arg(Pbf)-[Gly]-OH **(4)** as a thick yellow powder with molecular m/z of 718 (MALDI-tof MS), consistent with its chemical structure. Similarly, Boc-Asp(OBu^t)-OH and H-Ser(Bu^t)-O^tBu were coupled together under the same reagent conditions as mentioned above to produce the protected dipeptide Boc-Asp(OBu^t)-Ser(Bu^t)-O^tBu **(5)**. The Boc group was then selectively deprotected using 1M HCl in dioxane for 1h, as checked by MALDI-tof mass spectrometry (m/z 388 in agreement with the chemical structure) to produce H-Asp(OBu^t)-Ser(Bu^t)-O^tBu **(6)**.

Coupling of the two dipeptides, Boc-Arg(Pbf)-[Gly]-OH **(4)** (amino acid within the second bracket indicates the caged residue) and H-Asp(OBu^t)-Ser(Bu^t)-O^tBu **(6),** was then achieved using the same coupling procedure as described above leading to the formation of protected caged tetrapeptide **(7).** Finally, all protecting groups were cleaved by treating **(7)** at room temperature for 3 h with a mixture of trifluoroacetic acid (TFA)/triisopropylsilane (TIPS)/water (95 / 2.5 / 2.5). Subsequently, the TFA was removed under vacuum, and the crude peptide was precipitated by cold ether at ~0^oC. The precipitate was collected by centrifugation and the product was lyophilized after dissolving in 0.1% TFA in water. The crude caged peptide **(1)** was then purified by RP-HPLC and fully identified by MALDI-tof mass (m/z 567) and proton NMR spectroscopy.

5.2.4 Photolysis

Near-UV irradiation from a 365 nm Longwave UV Lamp (Black-Ray B-100 Longwave UV lamp, 100 W, UVP, Upland, CA) was used to remove the 2-NB caging group from the R[G]DS peptide. Samples containing R[G]DS were irradiated on a platform 10 cm from the light source. Gels containing bound R[G]DS were irradiated for 10-12 minutes. For patterning experiments, a line-patterned mask was placed on the gel surface during UV exposure.

5.2.5 ^{1}H NMR Spectrum of Caged and Uncaged RGDS Peptides

^{1}H NMR characterizations of the R[G]DS peptide before and after exposure to near-UV irradiation were conducted to examine the uncaging event. Two mg of the caged peptide was dissolved in deuterium oxide (D_2O) and analyzed by ^{1}H NMR employing a Bruker AVANCE 500 MHz Wide Bore spectrometer. The R[G]DS peptide solution was subsequently exposed to near-UV light for one hour and the ^{1}H-NMR spectrum was recorded again. The ^{1}H NMR spectrum of caged R[G]DS peptide (Supplemental Figure 5.1) indicates that there are possibly two different R[G]DS conformational states based on the appearance of two sets of doublets in δ 4-5.5 ppm region with significantly higher coupling constants (J ~ 16-18 Hz) for the two benzylic geminal CH_2-protons. This is also supported by the observed splitting profiles of aromatic protons. ^{1}H NMR for caged R[G]DS peptide (500 MHz, D_2O): δ 8.23 (0.5H, d, J = 8.2 Hz), 8.11 (0.5H, d, J = 8.2 Hz), 7.79 (0.5H, t, J = 7.5Hz), 7.71 (1H, t, J = 7.5Hz), 7.64 (1H, t, J = 7.5 Hz), 7.59 (0.5H, t, J = 7.5 Hz), 7.51 (0.5H, d, J = 7.8Hz), 7.47 (0.5H, d, J = 7.8Hz), 5.27 (0.5H, d, J = 17.2) and 5.16 (0.5H, benzylic, d, J = 15.8), 4.98 (1H, one Gly αH), 4.52-4.43 (m, 3H, second Gly αH, Asp and Ser αH), 4.21 (0.5H, d, J = 18 Hz) and 4.16 (0.5H, benzylic, d, J = 16.6 Hz), 3.96-3.83 (m, 2H, Ser βH, + HOD formed due to solvent exchange), 3.21-3.16 (m, 2H, Arg δH), 3.09-3.05 (m, αH), 2.96-2.90 (m, αH), 2.87-2.69 (m, 2H, Asp βH), 1.96-1.88 (m, 2H, βH of Arg) and 1.71-1.60 (m, 2H, γH of Arg). The proton integrations of some of the signals have been found to be half of a single proton suggesting that the above peptide exists in two conformational forms in D_2O solvent. The large coupling constants with J ~ 15 – 18 Hz for benzylic protons are consistent with the geminal nature of the protons. It may be pointed out

that some of the proton assignments, particularly those of α-protons of amino acids, are tentative and may be interchanged.

Upon UV irradiation, the aromatic protons consisting of two sets of doublets at δ 8.23 and 8.11 ppm, two sets of triplets at δ 7.64 and 7.59 ppm, and another two sets of doublets at δ 7.51 and δ 7.47 all disappeared completely as expected (Supplemental Figure 2), indicating the loss of the aromatic 2-NB group. Instead, additional aromatic peaks appeared at δ 7.85 – 7.72 for 2H and δ 7.35 – 7.25 for another 2H due to the formation of 2-nitroso benzaldehyde following UV-irradiation. The formation of the latter product was further confirmed by the appearance of a singlet at δ 8.25 for aldehydic proton (CHO). The peaks at δ 5.27 ppm (0.5H, d, J = 17.2 Hz), 5.16 (0.5H, d, J = 15.8), 4.21 ppm (0.5H, d, J = 18 Hz), and 4.16 (0.5H, d, J = 16.6 Hz) correspond to the benzylic protons of two conformational states of caged peptide which also disappeared as expected following the irradiation, indicating a regeneration of RGDS peptide.

5.2.6 Photolysis Reaction Rate Investigation

To further study the R[G]DS photolysis reaction, the kinetics of the disappearance of R[G]DS upon UV irradiation was investigated. To this end, 1 mg/mL solutions of the caged peptide were prepared in PBS (pH 7.4) and exposed to near-UV light for varying times (n=2). The irradiated solutions were analyzed by RP-HPLC to determine, as a function of exposure time, the percentage of R[G]DS reacted based on the peptide's predetermined retention time. The chromatographic separation of the reaction products was performed with a Waters 2695 Separation Module using a reversed phase column (Waters XBridge BEH 130 C_{18}, 3.5 μm) employing a mobile phase in gradient elution mode with a flow rate of 1 mL/min at room temperature. Initially, a mobile phase consisting of 95% water (0.1% TFA (Pierce)) and 5% acetonitrile (Fisher) with 0.1% TFA was delivered, and after 5 minutes the solvent ratios were linearly decreased to 5% water (0.1% TFA): 95% acetonitrile (0.1% TFA) over a period of 35 minutes. UV absorbance was recorded for wavelengths ranging from 190 nm to 500 nm using a Waters 2996 Photodiode Array Detector.

5.2.7 Peptide Binding to the Hydrogel

To bind peptides (both RGDS and R[G]DS) to the HA gel, a solution consisting of 25 mg/mL EDC and 15 mg/mL N-hydroxysuccinimide (NHS) (Pierce) in 0.1 M 2-(*N*-morpholino) ethanesulfonic acid (MES) (Fisher) buffer was prepared. Subsequently, 1 mL of this solution was added to each HA gel that was previously transferred to and crosslinked in wells of a 12-well plate. The reaction was carried out at room temperature for 15 minutes to activate the carboxyl groups in HA for peptide binding. The gels were then washed once in PBS (pH 7.4) to get rid of unreacted chemical residuals. The desired peptide solution was subsequently added to the gels and allowed to react for 2 h. Finally, the resulting gels were washed in PBS overnight. In order to visualize the immobilized peptide, fluorescent bovine serum albumin (BSA) was used as a model biomolecule to demonstrate the immobilization of peptide/protein to the HA gel. This reaction was carried out using 0.3 mg of FITC-BSA in bulk solution per gel as per the above procedure and the resulting gels were subsequently washed for 22 hours to remove unbound protein.

5.2.8 Cell Adhesion Tests *In Vitro*

To test the relative cell adhesiveness of the peptide modified HA surfaces, NIH 3T3 fibroblasts were used as model adherent cells. The cells were routinely maintained in medium containing Dulbecco's Modified Eagle's Medium (DMEM) (Invitrogen) supplemented with 10% fetal bovine serum (FBS) (Invitrogen), 100 U/mL Penicillin (Invitrogen), and 0.1 mg/mL Streptomycin (Invitrogen), and kept in T-75 flasks at 37˚C in a humidified environment containing 5% CO_2. Prior to cell seeding on the experimental surfaces, cells were trypsinized, centrifuged to a pellet, re-suspended in culture medium (with serum) and counted using a hemocytometer. The cells were subsequently seeded onto the experimental surfaces at a density of $1X10^4$ cells/cm^2. Cells plated onto the experimental surfaces were initially maintained for 24 h, after which the surfaces were gently (and carefully) washed twice with sterile PBS (pH 7.4) to remove non-adherent cells. The adherent cells were then detached from the hydrogel surface using enzymatic digestion and collected. The surfaces were subsequently washed several times with culture medium to collect the rest of the cells, and the collected cells were pooled and centrifuged to a pellet.

Live/dead cell counts were performed using trypan blue staining followed by a hemocytometer count.

For cell culture on patterned HA surfaces, cells were plated onto the patterned surfaces in a similar fashion as described above except that the non-adherent cells were not washed away until pre-determined time points when the cultures were examined using an inverted phase contrast microscope (Olympus 1X81 F), and the observations were documented using Image-Pro Plus (Media Cybernetics, Silver Spring, MD).

5.2.9 Cell staining

CellTracker™ Red CMTPX (Invitrogen) was used to label the fibroblasts in this study according to the vendor's protocol. A 10 mM stock solution of the dye in DMSO was prepared. This solution was subsequently dissolved in DMEM to produce a 2.5 μM working solution. One milliliter of the working solution was added to wells containing adherent cells in 12-well plates and allowed to incubate for 45 minutes at 37ºC. The staining solution was then replaced with pre-warmed fresh media and allowed to incubate for another 30 minutes at 37ºC. Cells were then washed in PBS (pH 7.4) followed by incubation in fresh media. The stained cells were used in cell adhesion and cell patterning studies, as outlined in Section 5.2.8, and visualized with fluorescence microscopy.

5.3 Results and Discussion

5.3.1 Hydrogel Development

HA hydrogels were developed to form the base of the cell pattern. HA was an ideal choice because (a) it is a component of the ECM in the natural cell microenvironment known to regulate cell proliferation and adhesion,[33-36] (b) in its native state, HA is naturally cell non-adhesive so it could prevent the background binding of cells located off-pattern,[37] and (c) it contains easily functionalized carboxylic acid groups for crosslinking to form stable hydrogels as well as for the covalent addition of biomolecules.[38-40] To form a stable HA gel, HA molecules were crosslinked in such a way that the material remained non-adherent to cells.

First, HA gel was prepared. Gelation was determined by inverting the tube in which the gels formed to verify that the material would maintain its shape. Gels were formed by joining HA chains via ADH crosslinkers which formed covalent bonds to carboxylic acid groups on the HA polymer chains, as shown in Figure 5.4(a). Similar crosslinking approaches using ADH in HA have been described elsewhere.[41-43] To further confirm the incorporation of ADH into the HA polymer chains (i.e. crosslinking reaction), solid-state ^{13}C NMR analysis of the hydrogel after crosslinking was carried out. The spectrum of the crosslinked sample as well as that of the native HA before crosslinking (data not shown here – see Chapter 9, Figure 9.2) matched results previously reported by Pouyani et al.,[44] suggesting the success of the crosslinking reaction.

To evaluate these HA gels for cell-adhesiveness, 3T3 fibroblasts were first seeded onto single-layered gel surfaces. One day after the initial cell seeding, the gels were gently washed and subsequently observed. As seen in Figure 5.4(b), a significant number of fibroblast cells remained adherent to the gel; however, it was also evident that the cells could not spread well onto the hydrogel. Fibroblasts were round in shape and had grouped together to form distinct clusters. Filopodia could be seen extending from the clusters anchoring the cells to the underlying HA gel, preventing the cells from removal upon washing.

It is known that increasing the fractional surface coverage of HA can reduce cell adhesion.[37] Therefore, the concentration of HA in the hydrogel was increased in order for the pattern base to better repel cells. To achieve this, the original hydrogel layer was dried and new hydrogel layers were deposited onto its surface to create a dried, layered gel which was subsequently rehydrated. Such gels were visibly less swollen than the original single-layered gels, due to the dehydration/rehydration process, and as a result of this decrease in gel volume, contain a higher concentration of HA molecules. As seen in Figure 5.4(c), when seeded with 3T3 fibroblasts, these layered gels exhibited significantly improved cell repulsion capabilities since virtually no cells were found to adhere one day post seeding. This layered gel configuration was used for the rest of the studies in this report.

5.3.2 Binding of Peptide to the Gel

In developing the cell patterns on the HA hydrogel, both native RGDS and caged R[G]DS peptides were covalently bound to the gel via carboxyl groups on HA. Merely adsorbing RGD peptides onto surfaces leads to poor cell attachment,[22] and such peptides are more easily dislodged, negatively impacting pattern longevity. We confirmed that peptides could be covalently bound to the gel surface using fluorescent (FITC-labeled) bovine serum albumin (BSA) as a model molecule (for ease of detection). The gel shown in Figure 5.4(d) was treated with both FITC-BSA and a peptide coupling agent, EDC, and displayed strong fluorescence over the entire gel surface. In comparison, the control gel in Figure 4(e) exposed only to FITC-BSA exhibited significantly less fluorescence intensity. An additional control in which FITC-BSA was omitted in the reaction exhibited no autofluorescence (result not shown). Since the fluorescence images were obtained using identical exposure times, the sharp contrast in fluorescence demonstrated that the gels exposed to EDC were able to covalently immobilize a significant amount of peptides while the controls were not, resulting in the adsorbed peptides mostly being washed away in the extensive washing steps.

Similarly, RGDS peptides were bound to the HA gel. Figure 5.4(f) shows the resulting morphology of fibroblasts grown on the HA hydrogel bound with RGDS 24 h after seeding. It is evident that the immobilization of RGDS drastically increased the adhesiveness of the HA hydrogel (*cf.* Figures 5.4(c) and 5.4(f)). Cells assumed a well-spread and flattened morphology with numerous extensions, exhibiting a similar morphology to that of cells grown on the control polystyrene tissue culture plate, as shown in Figure 5.4(g).

5.3.3 Peptide Characterization

In developing the cell patterned surfaces, it was important to synthesize the caged peptide, R[G]DS, with a high purity since any RGDS contaminants could potentially bind cells thus allowing for off-pattern binding. However, our first attempts to synthesize the R[G]DS using a solid phase peptide synthesis approach resulted in a relatively low yield, with the occurrence of significant side reactions. The reasons for these side reactions are still under investigation. Alternatively, liquid phase synthesis was attempted with success. We were able to prepare high purity R[G]DS in sufficient quantities.

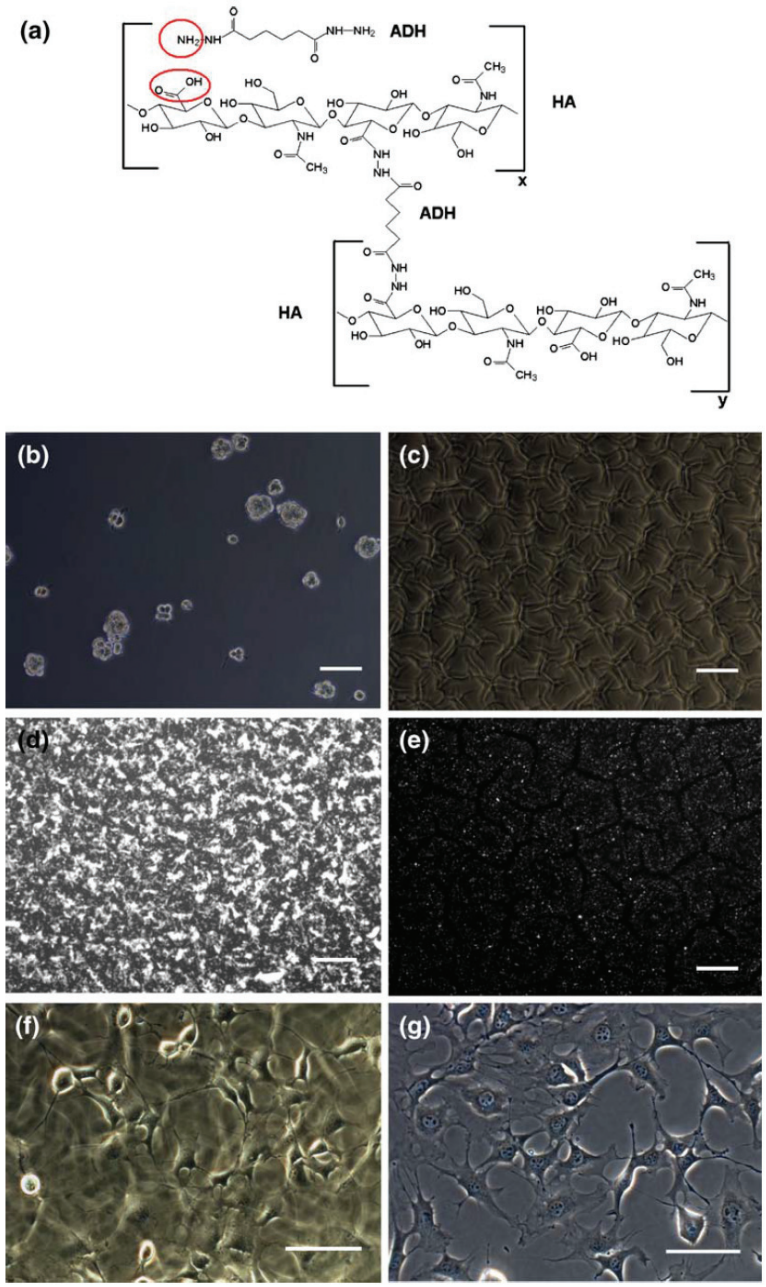

Figure 5.4 (a) Structure of ADH-crosslinked HA polymers with the functional groups involved in coupling the two molecules highlighted in red. **(b)** Single layer of HA gel one day post seeding of 3T3 fibroblasts onto the surface (image obtained by phase contrast). **(c)** Layered HA gel one day post seeding of 3T3 fibroblasts onto the surface (image obtained by phase contrast). Note the cracks in the gel formed during the rehydration process in the preparation of the layered gel **(d)** Fluorescence image of FITC-BSA bound to HA hydrogel facilitated by EDC and **(e)** control HA hydrogel exposed to FITC-BSA in the absence of EDC after 22 hours of washing. **(f)** Phase contrast image of 3T3 fibroblasts adhering to a layered HA gel bound with RGDS one day post seeding. **(g)** Phase contrast image 3T3 fibroblasts adhering to a polystyrene tissue culture plate one day post seeding. Scale bars = 100 μm and images were obtained using an Olympus 1X81 F microscope.

The synthetic peptides, both RGDS and R[G]DS, were fully characterized by MALDI-tof mass spectrometry as well as ^{1}H NMR spectroscopy (see Section 5.2).

5.3.3.1 Molecular Modeling

A 3D energy minimized molecular modeling structure for each peptide was developed using Hyperchem software (Hypercube Inc., Gainesville, FL). These theoretically derived structures in Figure 5.5 suggested that the introduction of a 2-NB group at the backbone amide nitrogen atom of the Gly residue led to a significant change in the geometry of the molecule. Thus, the caged RGDS peptide appeared to possess a more compact structure compared to regular RGDS tetrapeptide which exhibited a β-turn structure at the R-G amide bond. These significantly different structural features provide, at least in part, the rationale for this patterning approach and perhaps explain the cell patterning results as shown below.

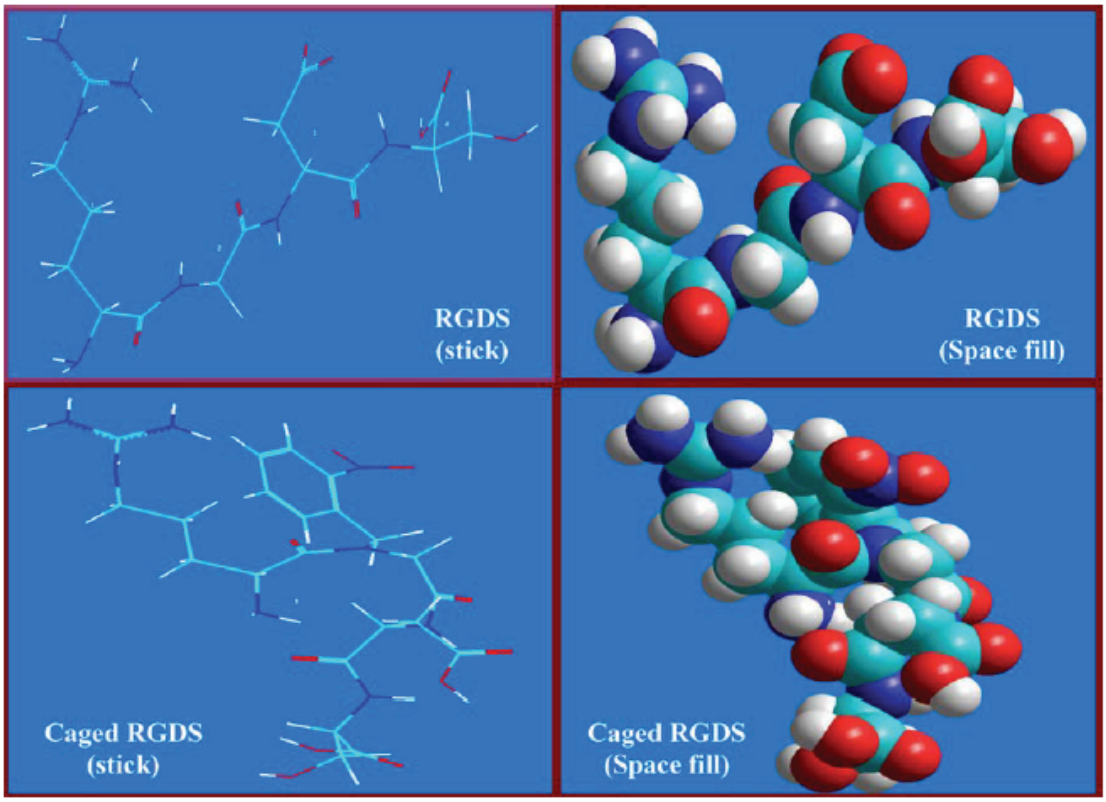

Figure 5.5: Hyperchem generated theoretical energy minimized molecular model structures of RGDS and caged R[G]DS peptides.

5.3.3.2 Photolysis Reaction

To investigate the kinetics of the R[G]DS photolysis reaction, the rate of disappearance of the caged peptide upon UV exposure was evaluated using RP-HPLC. Figure 5.6(a) is a plot of absorbance versus wavelength for various irradiation times corresponding to the R[G]DS peptide elution peak on the RP-HPLC chromatogram. The R[G]DS peptide exhibited an absorption maxima at 266 nm, but absorbed light with a wavelength up to approximately 370 nm. This observation agrees well with that reported by Zhang et al. who found that 2-NB caged 5-fluorouracel prodrugs had maximum absorbances of around 265 nm in acetonitrile/water systems.[45] As expected, the absorbance at this elution time decreased with increasing UV irradiation time due to the removal of the strongly absorbing 2-NB group from the R[G]DS peptide. Despite the maximum absorption found at 266 nm, uncaging reactions were carried out with a 365 nm light source to ensure the safety of our biomolecule-based system. It has been established in the literature that, in general, exposure to irradiation above 350 nm is relatively safe for work in biological systems.[46,47] Figure 5.6(b) plots the percentage of R[G]DS reacted as a function of irradiation time, as determined from measuring the area under the R[G]DS peak in the HPLC chromatograms. It can be seen that after 10-12 minutes of irradiation, 60-70% of the R[G]DS had reacted, and over 90% of the caged peptide disappeared after 30 min. This is encouraging since it indicates that the majority of the R[G]DS will react upon UV irradiation at 365 nm in 30 min. ^{1}H NMR data supported the regeneration of the RGDS peptide (see Section 5.2). A plot of $\ln[C]/[C]_o$ versus time (where [C] represents the concentration of R[G]DS peptide and $[C]_o$ the initial concentration) showed a linear relationship, which indicated that first order reaction kinetics could be used to describe the 2-NB photolysis as seen previously.[48] Furthermore, from Figure 5.6(c) the apparent first order uncaging reaction rate constant was calculated to be 1.6×10^{-3} s^{-1}. In comparison, values reported by Kim and Diamond for 2-NB ester compounds ranged from 1-9 $\times 10^{-4}$ s^{-1}.[48] Differences in the values may be attributed to the increased light intensity used in this paper compared to Kim and Diamond's work (7 mW/cm^2 vs 1.6 mW/cm^2 respectively) which would be expected to increase the rate constant, and differences in the solvent systems used in the experiments.[48]

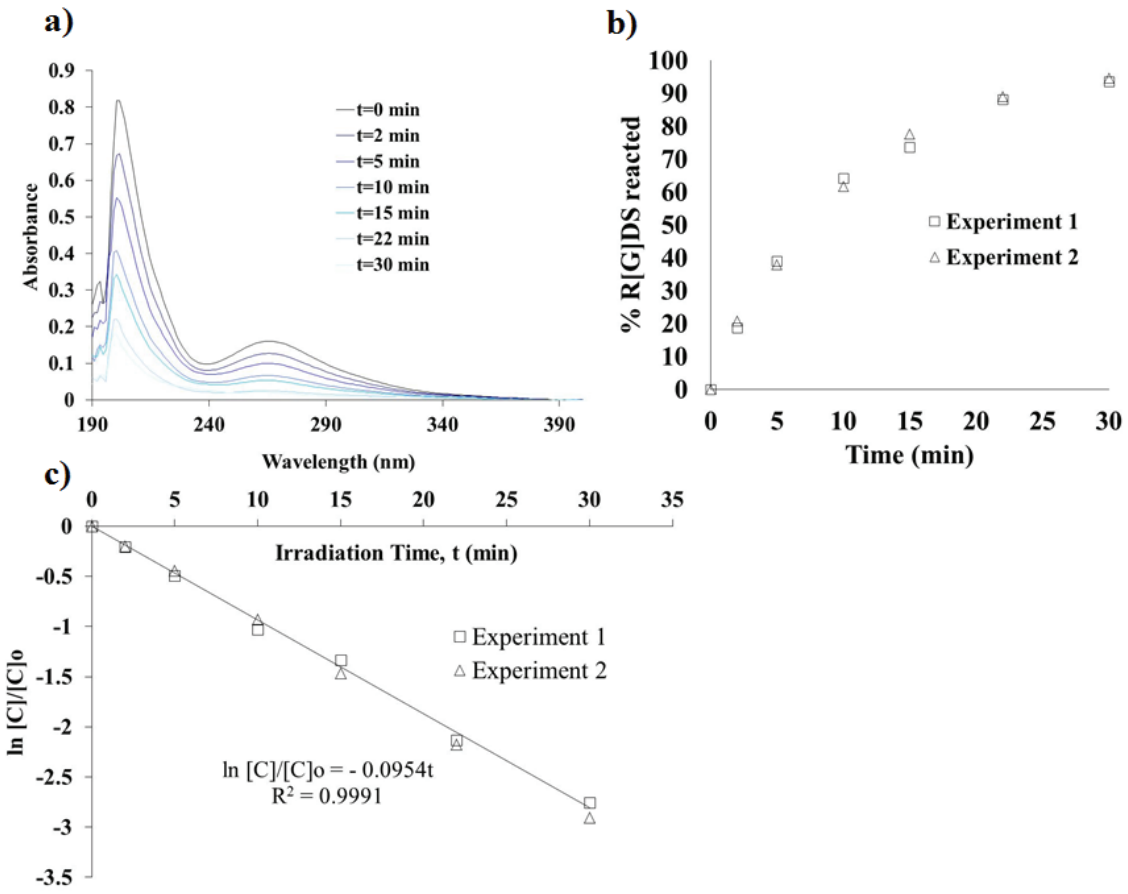

Figure 5.6: (a) The absorbance of the R[G]DS elution peak versus wavelength following UV irradiation for the indicated times from an RP-HPLC chromatogram. **(b)** The percentage of R[G]DS reacted with UV irradiation time (n=2). **(c)** Plot of ln[C]/[C]o versus irradiation time, t (n=2).

5.3.4 Cell Binding Studies

In order to examine all of the various surfaces that will ultimately make up the cell patterning platform, several homogenous surfaces were created for cell seeding to test their relative surface adhesiveness. These surfaces include a pure, layered crosslinked HA gel, HA gel bound to RGDS, HA gel bound to R[G]DS, HA gel bound to R[G]DS exposed to near-UV light for 12 minutes, and a control polystyrene tissue culture surface. All of the gels were created with equimolar quantities of the different peptides in bulk solution (0.3 mg of R[G]DS peptide) and seeded with stained 3T3 fibroblasts. From Figure 5.7, it can be seen that virtually no cells adhered to the surface of the pure HA gel or to the surface of the HA gel bound with the caged peptide, R[G]DS. This cell non-adhesive background is crucial for

cell patterning to take place – the surface of the gel prior to exposure to near-UV light must be completely cell repellant to prevent against off-pattern binding. On the other hand, the HA gel bound to RGDS and the HA gel bound to R[G]DS uncaged with near-UV light both supported cell adhesion. Moreover, both surfaces supported cells with similar morphologies. Cells appeared well-spread and morphologically comparable to those grown on the control tissue culture plate. This suggests that the uncaging of R[G]DS took place upon near-UV exposure and regenerated RGDS peptides on the HA gel surface, converting a cell non-adhesive surface to a cell adhesive one to allow for cell attachment. The cell counts based on Figure 5.7(f) showed similar numbers on the HA-RGDS surface as on the tissue culture plate. This suggests a high degree of biocompatibility for the developed HA material. The biocompatibility of the material is also supported by the fact that very few dead cells were counted on any of the surfaces.

It is interesting to note that fewer cells were adherent to the HA-R[G]DS surface exposed to near-UV light prior to cell seeding, suggesting that not all of the R[G]DS peptides became uncaged during near-UV light exposure. Virtually no cells were counted on the caged R[G]DS-HA surfaces and on HA gel surfaces (see Figure 5.7(f)) which suggests that positioning the caging group on the peptide backbone between the Arg and Gly residues of the RGDS sequence does indeed inhibit cell binding to the sequence, most likely through disrupting integrin recognition of the RGDS sequence. This is consistent with our prediction.

X-ray structure analysis performed to study the interactions of an integrin receptor (i.e. $\alpha_V\beta_3$) and a bound RGD ligand (i.e. c(-RGDf[NMe]V-)) showed that the Gly residue was directly positioned on the integrin surface, suggesting its direct involvement in hydrophobic interactions with the integrin.[49,50] In addition, it has been further suggested that this hydrophobic interaction may add to the stability of the RGD-integrin binding complex.[49] We can thus speculate that the introduction of a bulky group such as 2-NB on the peptide backbone by Gly would, to some degree, disrupt the ability of the Gly residue to interact with the integrin surface. It has also been suggested that close contact between the polar amide groups adjacent to Gly and the integrin receptor is essential for integrin mediated cell attachment.[51]

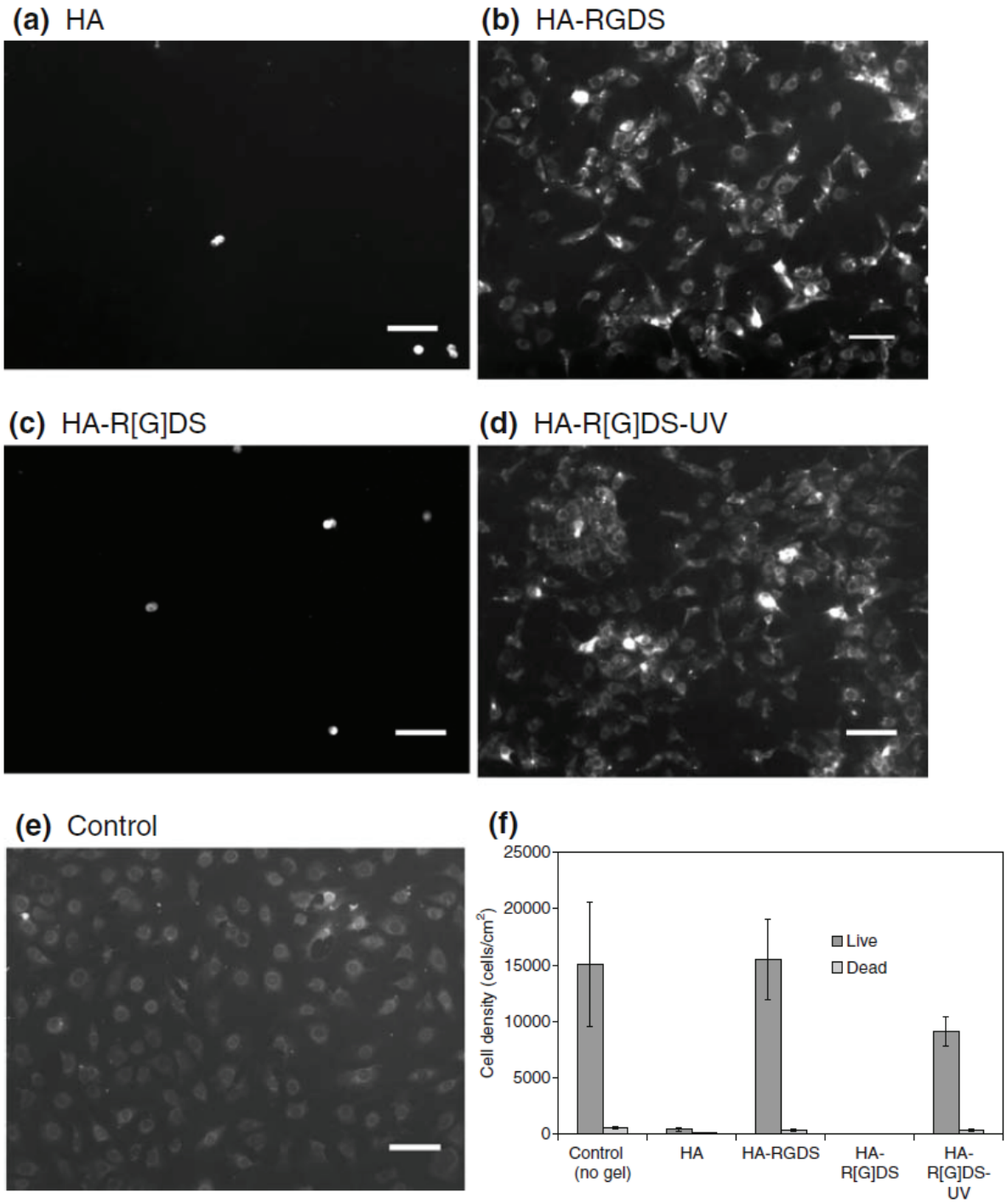

Figure 5.7: 3T3 Fibroblasts 24 h post seeding on **(a)** pure layered ADH-crosslinked HA hydrogel, **(b)** HA gel bound to RGDS peptide (HA-RGDS) **(c)** HA gel bound to a caged R[G]DS peptide (HA-R[G]DS) **(d)** HA gel bound to a caged R[G]DS peptide exposed to near-UV light (HA-R[G]DS-UV) and **(e)** a control in which cells were grown on a polystyrene 12-well plate (no gel) **(f)** Number of live and dead cells harvested after 24 hours of culture on the indicated surfaces with *error bars* representing one standard deviation from the mean with a sample size of three gels. Scale bars = 100 μm

Since our caging group is covalently linked to one of such amide groups, it would certainly serve to disrupt any such receptor binding at this location. Another explanation for the inhibition of cell binding to our R[G]DS peptide could be that the introduction of the caging group drastically changes the conformation of the RGDS peptide. This was noted in our modeling studies.

In order to further demonstrate that cell binding is RGD-dependent, cells were seeded on HA-R[G]DS surfaces after UV exposure in the presence of free RGDS peptides. Preliminary results (not shown) demonstrate that 1 mg/mL of free RGDS peptides present during cell seeding can almost completely inhibit 3T3 binding to the surface. This would seem to indicate that binding is integrin dependent - as the free RGDS peptides would serve to bind and block cell integrin receptors preventing their participation in surface binding - and not mediated by other mechanisms involving non-specific protein adsorption or unpredicted UV modifications to the surface after exposure. These findings ultimately suggest that the caged R[G]DS-HA surface could indeed be converted from cell non-adhesive to adhesive upon exposure to near-UV light, which supported the notion that this system could be used for cell patterning.

5.3.5 Cell Patterning

To produce cell patterns on the HA hydrogel surfaces, photomasks with line patterns were placed overtop R[G]DS-HA gels, and near-UV light was shone onto the surfaces to generate patterns of adhesive RGDS. Gels were then sterilized with ethanol and washed overnight. Subsequently, 3T3 fibroblasts were seeded onto the patterned gels. Figures 5.8(a)-(c) show fluorescent micrographs of the fibroblasts stained with CellTracker^{TM} Red one day post seeding on the pattern as well as the mask used. Cells can be seen adherent to the surface in distinct lines matching the pattern on the photomask. Figures 5.8(d)-(g) is a compilation of phase contrast images showing fibroblasts adhering to line patterns from 12 h to 2.5 days post seeding. Over the 2.5 days post seeding, it was noted that cells appeared to spread and grow, increasing in density along the patterned regions. Significantly, the cell pattern was well maintained as few cells could be seen growing off-pattern even after 2.5

days in culture. It was quite interesting that even during proliferation, cells remained aligned to the underlying pattern.

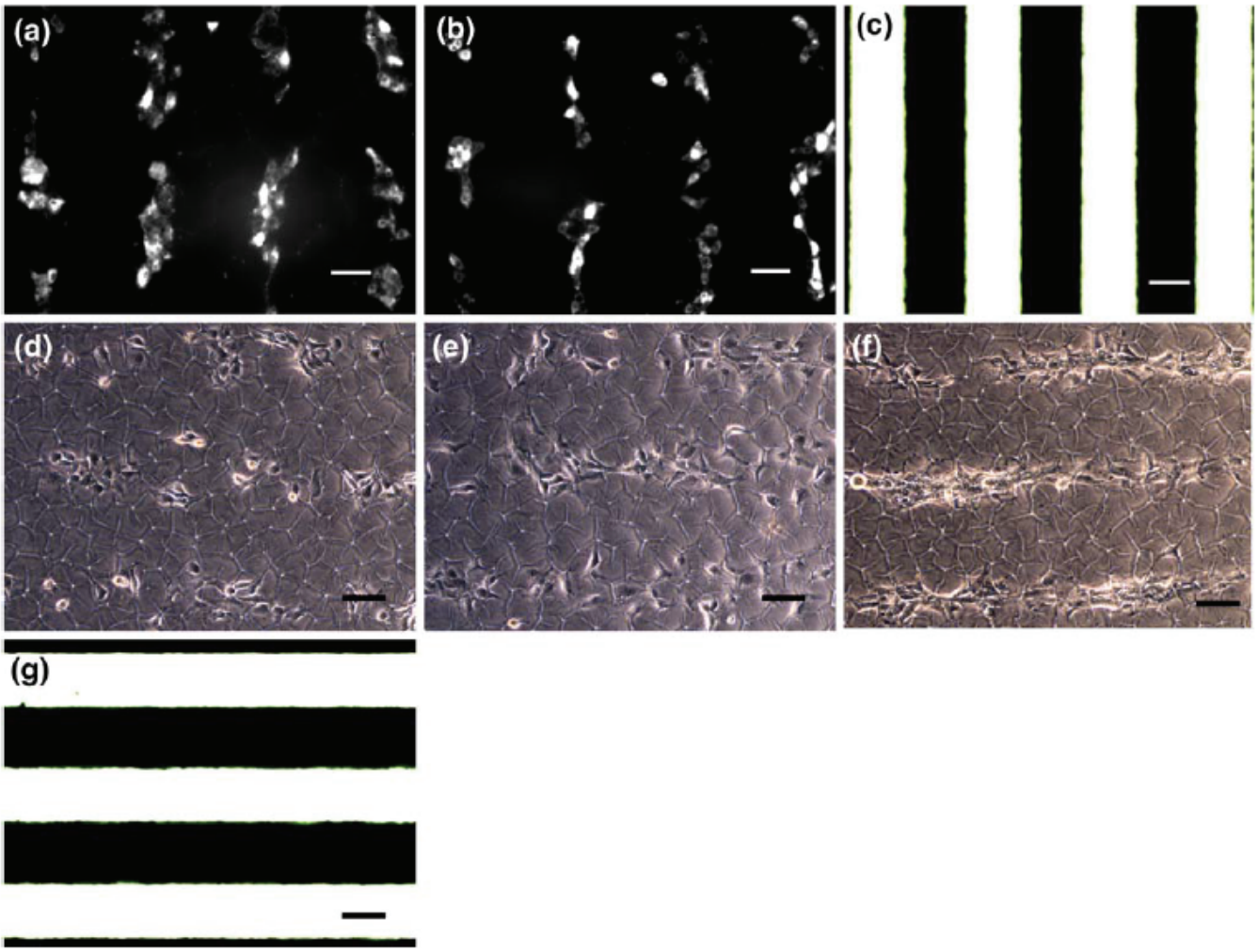

Figure 5.8: (a,b) Fluorescent micrographs depicting line patterns of 3T3 fibroblasts stained with CellTracker™ Red and grown on a HA hydrogel bound with patterned caged and uncaged R[G]DS peptides one day post seeding. **(c)** Mask used to generate the line pattern. Phase contrast images of line patterns of 3T3 fibroblasts grown on a HA hydrogel bound with patterned caged and uncaged R[G]DS peptides at **(d)** 12 hours, **(e)** one day and **(f)** 2.5 days post seeding. **(g)** Mask used to generate the line patterns. Scale bars = 100 μm.

One potential concern with this current patterning strategy based on light exposure is that ambient light and light exposure from microscopy techniques may serve to uncage the R[G]DS peptide and degrade the pattern over time. However, this did not seem to be an issue over the 2.5 days the pattern was monitored in our study as the cells did not appear to

move significantly off-pattern despite routine examination of the surface using phase contrast and fluorescence microscopy.

In comparison with previous studies using caged RGD peptides for cell patterning, we were able to achieve increased pattern longevity; this study demonstrated pattern stability for at least 2.5 days in culture. In contrast, a study by Petersen et al., also employing 3T3 fibroblasts as in the current study, reported significant off-pattern deviations just 6 hours post seeding.[29] While there may be many other reasons for the significantly improved cell pattern longevity achieved in this study, we attribute our success to two chief reasons: 1) the use of a strongly non-adhesive HA base to provide a non-adhesive background, and 2) the use of a zero-length crosslinker to bind the R[G]DS to the gel surface. As mentioned, previous works with caged RGD relied on flexible OEG or PEG chains to link the peptides to a solid surface and provide a non-adhesive background.[29,30] Flexible chains acting as spacers are often used to link RGD peptides to surfaces to enhance access of cell integrin receptors to the peptide sequence and thus enhance cell adhesion.[52,53] It was hypothesized that the use of a zero-length crosslinker would limit the flexibility of the caged RGDS peptide to undergo such conformational changes which could otherwise potentially permit partial binding to integrins on cell surfaces, and therefore the zero-length crosslinker may assist in maintaining the cell non-adhesive background essential to cell patterning.

Our design is not only functional, but also quite versatile. The potential exists to pattern a wide variety of cell types since the RGD peptide sequence employed is one of the most widely recognized sequences to support cell-surface adhesion. There is also the potential to form a wide variety of patterns through the use of different photomasks. Furthermore, it is felt that our strategy could eventually allow for patterning at the single cell level since resolution is only theoretically limited by the density of peptide coverage on the underlying surface, which can be readily manipulated. Numerous potential applications exist for our unique patterning approach. The spatial control that it affords over cell positioning on a biocompatible surface makes it an excellent platform for more controlled studies in cell biology. Since our patterned design is based on a natural hydrogel material, we envision great potential for future applications in tissue engineering. HA has been incorporated into

numerous tissue engineering scaffolds,[54] and HA polymers modified with RGD peptides have also found several tissue engineering applications.[42,55,56] Our design is especially interesting because it has been shown to not only support the adhesion of cells onto a pattern, but new cell growth was also directed along the patterned lines. This characteristic behavior could be harnessed in the future to direct the growth of cells along desired routes *in vivo*. Our current design therefore holds much potential and future refinement in resolution promises to bring new and exciting applications.

5.4 Conclusions

We have developed a novel cell patterning platform in patterning a hydrogel surface with a photocaged RGDS tetrapeptide. Our surface and pattern base consist of cell non-adhesive hyaluronic acid, a material naturally found in the extracellular matrix. An RGDS peptide attached to a 2-NB cage via the peptide backbone amide nitrogen atom was synthesized, fully characterized and bound to the hydrogel base. We were able to demonstrate that this peptide was efficiently bound to the gel via covalent binding. Moreover, the generated surface was non-adhesive to cells, but could be switched to become cell adhesive upon exposure to near-UV light. In this way, a pattern of cell adhesive regions on an otherwise cell repellant hydrogel surface was created by shining near-UV light through a patterned photomask. We have demonstrated the creation of line patterns of cells using this novel method. Cells were also shown to proliferate along the created line patterns, adhering to the patterns for at least 2.5 days, demonstrating increased longevity compared to previous reports.

5.5 Acknowledgements

The authors would like to acknowledge financial support from the Natural Sciences and Engineering Research Council of Canada (NSERC) (XC) and the Canadian Institutes of Health Research (CIHR) (AB). Catherine A. Goubko is supported by an NSERC Canada Graduate Scholarship and Dr. Swapan Majumdar is supported by a CIHR-HOPE fellowship. SM is thankful to Tripura University, India for leave of absence.

5.6 References

1. Petersen S, Alonso JM, Specht A, Duodu P, Goeldner M, del Campo A. Phototriggering of Cell Adhesion by Caged Cyclic RGD Peptides. *Angewandte Chemie International Edition.* 2008;47(17):3192-3195.

2. Ohmuro-Matsuyama Y, Tatsu Y. Photocontrolled Cell Adhesion on a Surface Functionalized with a Caged Arginine-Glycine-Aspartate Peptide. *Angewandte Chemie International Edition.* 2008;47(39):7527-7529.

3. Goubko C, Majumdar S, Basak A, Cao X. Hydrogel cell patterning incorporating photocaged RGDS peptides. *Biomedical Microdevices.* 2010;12(3):555-568.

4. Liu WF, Chen CS. Engineering biomaterials to control cell function. *Materials Today.* 2005;8(12):28-35.

5. Rosso F, Giordano A, Barbarisi M, Barbarisi A. From Cell-ECM interactions to tissue engineering. *Journal of Cellular Physiology.* 2004;199(2):174-180.

6. Yamada S, Nelson WJ. Synapses: Sites of Cell Recognition, Adhesion, and Functional Specification. *Annual Review of Biochemistry.* 2007;76(1):267-294.

7. Sands RW, Mooney DJ. Polymers to direct cell fate by controlling the microenvironment. *Current Opinion in Biotechnology.* 2007;18(5):448-453.

8. Chen CS, Mrksich M, Huang S, Whitesides GM, Ingber DE. Geometric Control of Cell Life and Death. *Science.* 1997;276(5317):1425-1428.

9. Nelson CM, Chen CS. Cell-cell signaling by direct contact increases cell proliferation via a PI3K-dependent signal. *FEBS Letters.* 2002;514(2-3):238-242.

10. Goubko CA, Cao X. Patterning multiple cell types in co-cultures: A review. *Materials Science and Engineering: C.* 2009;29(6):1855-1868.

11. Nelson CM, Jean RP, Tan JL, et al. Emergent patterns of growth controlled by multicellular form and mechanics. *Proceedings of the National Academy of Sciences of the United States of America.* 2005;102(33):11594-11599.

12. Morin F, Nishimura N, Griscom L, et al. Constraining the connectivity of neuronal networks cultured on microelectrode arrays with microfluidic techniques: A step towards neuron-based functional chips. *Biosensors and Bioelectronics.* 2006;21(7):1093-1100.

13. Vogt AK, Brewer GJ, Decker T, et al. Independence of synaptic specificity from neuritic guidance. *Neuroscience.* 2005;134(3):783-790.

14. Vogt AK, Wrobel G, Meyer W, Knoll W, Offenhausser A. Synaptic plasticity in micropatterned neuronal networks. *Biomaterials.* 2005;26(15):2549-2557.

15. Lee CJ, Blumenkranz MS, Fishman HA, Bent SF. Controlling Cell Adhesion on Human Tissue by Soft Lithography. *Langmuir.* 2004;20(10):4155-4161.

16. Petersen EF, Spencer RGS, McFarland EW. Microengineering neocartilage scaffolds. *Biotechnology and Bioengineering.* 2002;78(7):802-805.

17. Kleinfeld D, Kahler KH, Hockberger PE. Controlled outgrowth of dissociated neurons on patterned substrates. *Journal of Neuroscience.* 1988;8(11):4098-4120.

18. Singhvi R, Kumar A, Lopez GP, et al. Engineering cell shape and function. *Science.* 1994;264(5159):696-698.

19. Falconnet D, Csucs G, Michelle Grandin H, Textor M. Surface engineering approaches to micropattern surfaces for cell-based assays. *Biomaterials.* 2006;27(16):3044-3063.

20. Shin H. Fabrication methods of an engineered microenvironment for analysis of cell-biomaterial interactions. *Biomaterials.* 2007;28(2):126-133.

21. Kikuchi Y, Nakanishi J, Shimizu T, et al. Arraying Heterotypic Single Cells on Photoactivatable Cell-Culturing Substrates. *Langmuir.* 2008;24(22):13084-13095.

22. Hersel U, Dahmen C, Kessler H. RGD modified polymers: biomaterials for stimulated cell adhesion and beyond. *Biomaterials.* 2003;24(24):4385-4415.

23. Tatsu Y, Nishigaki T, Darszon A, Yumoto N. A caged sperm-activating peptide that has a photocleavable protecting group on the backbone amide. *FEBS Letters.* 2002;525(1-3):20-24.

24. Rhee H, Lee J-S, Lee J, Joo C, Han H, Cho M. Photolytic Control and Infrared Probing of Amide I Mode in the Dipeptide Backbone-Caged with the 4,5-Dimethoxy-2-nitrobenzyl Group. *Journal of Physical Chemistry B.* 2008;112(7):2128-2135.

25. Nandy SK, Agnes RS, Lawrence DS. Photochemically-Activated Probes of Protein-Protein Interactions. *Organic Letters.* 2007;9(12):2249-2252.

26. Cherny RC, Honan MA, Thiagarajan P. Site-directed mutagenesis of the arginine-glycine-aspartic acid in vitronectin abolishes cell adhesion. *Journal of Biological Chemistry* 1993;268(13):9725-9729.

27. Bourgault S, Létourneau M, Fournier A. Development of photolabile caged analogs of endothelin-1. *Peptides.* 2007;28(5):1074-1082.

28. Wood JS, Koszelak M, Liu J, Lawrence DS. A Caged Protein Kinase Inhibitor. *Journal of the American Chemical Society.* 1998;120(28):7145-7146.

29. Petersen S, Alonso JM, Specht A, Portia Duodu P, Goeldner M, del Campo A. Phototriggering of Cell Adhesion by Caged Cyclic RGD Peptides. *Angewandte Chemie International Edition.* 2008;47(17):3192-3195.

30. Ohmuro-Matsuyama Y, Tatsu Y. Photocontrolled Cell Adhesion on a Surface Functionalized with a Caged Arginine-Glycine-Aspartate Peptide13. *Angewandte Chemie International Edition.* 2008;47(39):7527-7529.

31. Peppas NA, Hilt JZ, Khademhosseini A, Langer R. Hydrogels in Biology and Medicine: From Molecular Principles to Bionanotechnology. *Advanced Materials.* 2006;18(11):1345-1360.

32. Basak A, Mitra A, Basak S, Pasko C, Chrétien M, Seaton P. A Fluorogenic Peptide Containing the Processing Site of Human SARS Corona Virus S-Protein: Kinetic Evaluation and NMR Structure Elucidation. *ChemBioChem.* 2007;8(9):1029-1037.

33. Alberts B, Johnson A, Lewis B, Raff M, Roberts K, Walter P. *Molecular Biology of the Cell*. Fourth ed. New York, New York: Garland Science; 2002.

34. Yamane S, Iwasaki N, Majima T, et al. Feasibility of chitosan-based hyaluronic acid hybrid biomaterial for a novel scaffold in cartilage tissue engineering. *Biomaterials.* 2005;26(6):611-619.

35. Stern R, Asari AA, Sugahara KN. Hyaluronan fragments: An information-rich system. *European Journal of Cell Biology.* 2006;85(8):699-715.

36. Collins M, Birkinshaw C. Comparison of the effectiveness of four different crosslinking agents with hyaluronic acid hydrogel films for tissue-culture applications. *Journal of Applied Polymer Science.* 2007;104(5):3183-3191.

37. Morra M, Cassineli C. Non-fouling properties of polysaccharide-coated surfaces. *Journal of Biomaterials Science - Polymer Edition.* 1999;10(10):1107.

38. Park YD, Tirelli N, Hubbell JA. Photopolymerized hyaluronic acid-based hydrogels and interpenetrating networks. *Biomaterials.* 2003;24(6):893-900.
39. Lee JY, Spicer AP. Hyaluronan: a multifunctional, megaDalton, stealth molecule. *Current Opinion in Cell Biology.* 2000;12(5):581-586.
40. Hu M, Sabelman EE, Tsai C, Tan J, Hentz VR. Improvement of Schwann Cell Attachment and Proliferation on Modified Hyaluronic Acid Strands by Polylysine. *Tissue Engineering.* 2000;6(6):585-593.
41. Vercruysse KP, Marecak DM, Marecek JF, Prestwich GD. Synthesis and in Vitro Degradation of New Polyvalent Hydrazide Cross-Linked Hydrogels of Hyaluronic Acid. *Bioconjugate Chemistry.* 1997;8(5):686-694.
42. Cui F, Tian W, Hou S, Xu Q, Lee IS. Hyaluronic acid hydrogel immobilized with RGD peptides for brain tissue engineering. *Journal of Materials Science: Materials in Medicine.* 2006;17(12):1393-1401.
43. Hou S, Tian W, Xu Q, et al. The enhancement of cell adherence and inducement of neurite outgrowth of dorsal root ganglia co-cultured with hyaluronic acid hydrogels modified with Nogo-66 receptor antagonist in vitro. *Neuroscience.* 2006;137(2):519-529.
44. Pouyani T, Harbison GS, Prestwich GD. Novel Hydrogels of Hyaluronic Acid: Synthesis, Surface Morphology, and Solid-State NMR. *Journal of the American Chemical Society.* 1994;116(17):7515-7522.
45. Zhang Z, Hatta H, Ito T, Nishimoto S-I. Synthesis and photochemical properties of photoactivated antitumor prodrugs releasing 5-fluorouracil *Organic and Biomolecular Chemistry.* 2005;3(4):592-596.
46. Sigrist H, Collioud A, Clemence J-F, et al. Surface immobilization of biomolecules by light. *Optical engineering.* 1995;34(8):2339-2348.
47. Furuta T, Noguchi K. Controlling cellular systems with Bhc-caged compounds. *TrAC Trends in Analytical Chemistry.* 2004;23(7):511-519.
48. Kim MS, Diamond SL. Photocleavage of o-nitrobenzyl ether derivatives for rapid biomedical release applications. *Bioorganic & Medicinal Chemistry Letters.* 2006;16(15):4007-4010.
49. Gottschalk K-E, Kessler H. The Structures of Integrins and Integrin-Ligand Complexes: Implications for Drug Design and Signal Transduction. *Angewandte Chemie International Edition.* 2002;41(20):3767-3774.
50. Marinelli L, Lavecchia A, Gottschalk K-E, Novellino E, Kessler H. Docking Studies on αvβ3 Integrin Ligands: Pharmacophore Refinement and Implications for Drug Design. *Journal of Medicinal Chemistry.* 2003;46(21):4393-4404.
51. Dechantsreiter MA, Planker E, Matha B, et al. N-Methylated Cyclic RGD Peptides as Highly Active and Selective αvβ3 integrin antagonists. *Journal of Medicinal Chemistry.* 1999;42(16):3033-3040.
52. Beer JH, Springer KT, Coller BS. Immobilized Arg-Gly-Asp (RGD) peptides of varying lengths as structural probes of the platelet glycoprotein IIb/IIIa receptor. *Blood.* January 1, 1992 1992;79(1):117-128.
53. Nishi M, Kobayashi J, Pechmann S, et al. The use of biotin-avidin binding to facilitate biomodification of thermoresponsive culture surfaces. *Biomaterials.* 2007;28(36):5471-5476.

54. Allison DD, Grande-Allen KJ. Review. Hyaluronan: A Powerful Tissue Engineering Tool. *Journal of Histochemistry and Cytochemistry.* 2006;12(8):2131-2140.

55. Shu XZ, Ghosh K, Liu Y, et al. Attachment and spreading of fibroblasts on an RGD peptide-modified injectable hyaluronan hydrogel. *Journal of Biomedical Materials Research Part A.* 2004;68A(2):365-375.

56. Glass JR, Dickerson KT, Stecker K, Polarek JW. Characterization of a hyaluronic acid-Arg-Gly-Asp peptide cell attachment matrix. *Biomaterials.* 1996;17(11):1101-1108.

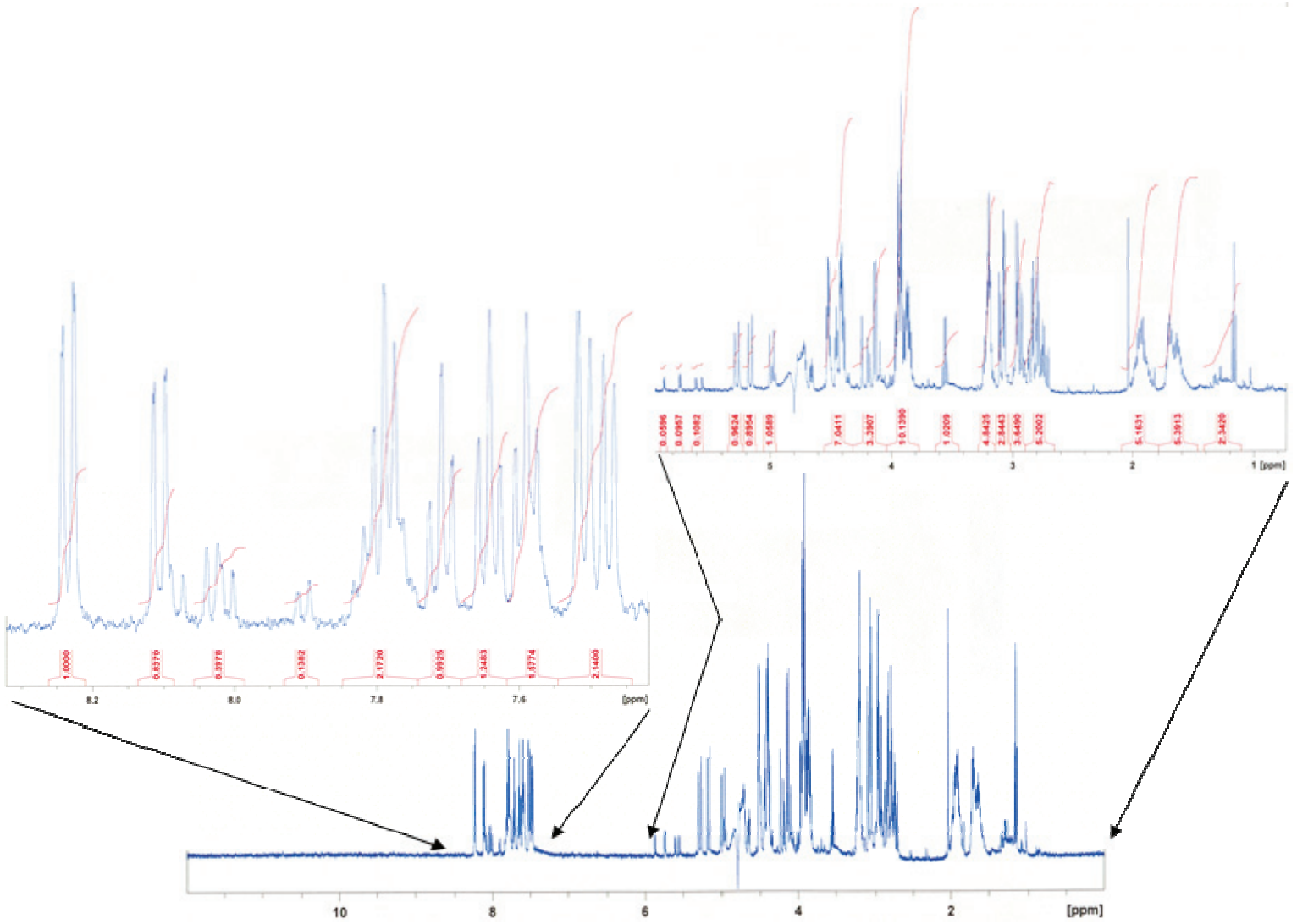

Supplemental Figure 5.1: ^{1}H NMR spectrum of caged R[G]DS tetrapeptide in D_2O with expanded portions within the insets.

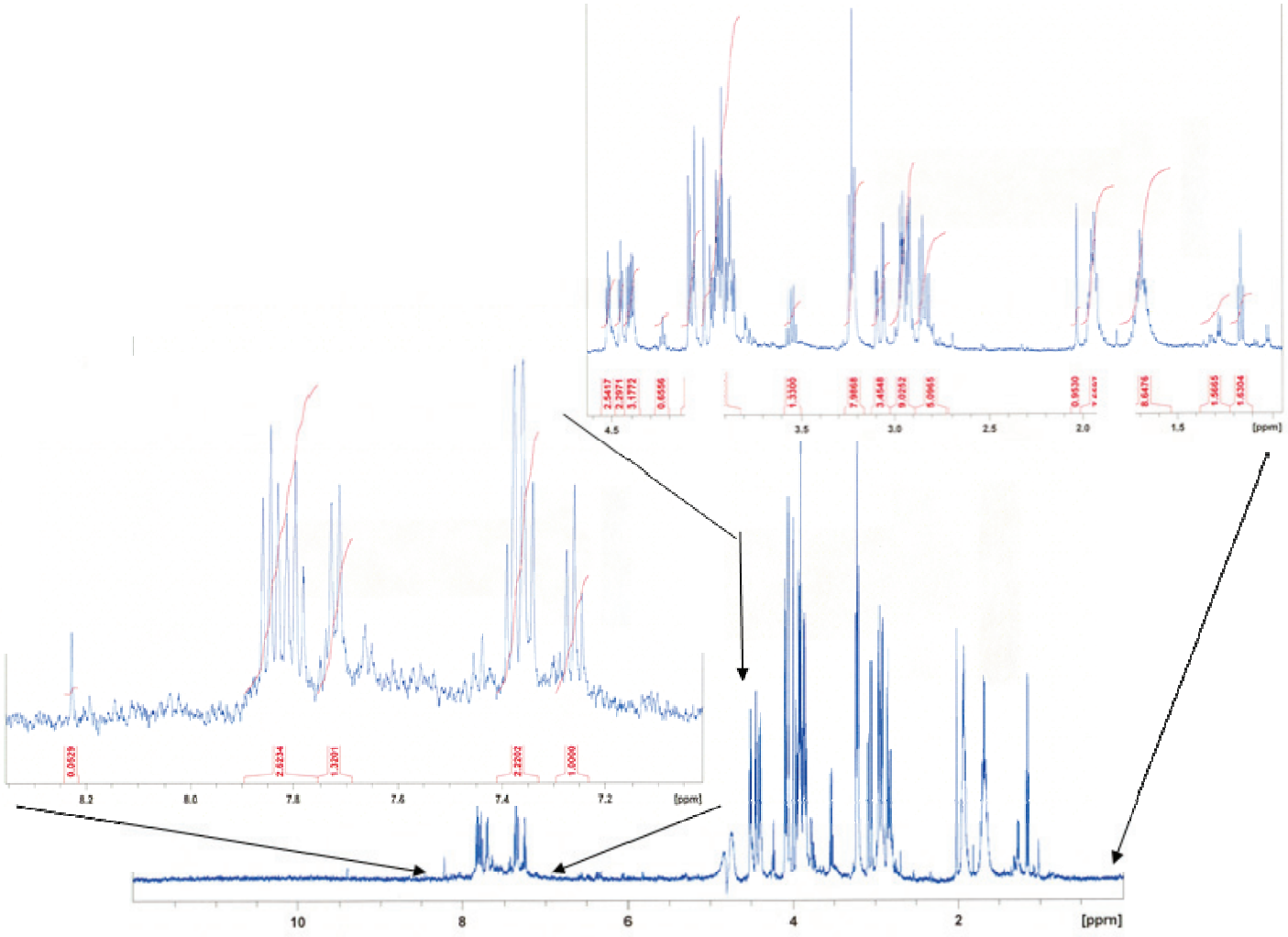

Supplemental Figure 5.2: ^{1}H NMR spectrum of R[G]DS in D_2O following UV-irradiation with expanded portions within the inset.

CHAPTER 6:
COMPARATIVE ANALYSIS AND MODELING OF PHOTOCAGED ARG-GLY-ASP-SER (RGDS) PEPTIDES FOR CELL PATTERNING

Catherine A. Goubko, Ajoy Basak, Swapan Majumdar, Harold Jarrell, Nam Khieu, Xudong Cao

Reprinted with permission from John Wiley and Sons
Journal of Biomedical Materials Research - Part A
101A, 787 (2013)

The following paper represents the second full length research paper published for this thesis with a focus on studying photocaged RGDS peptides. After achieving preliminary cell patterns with an RGDS peptide caged on the Arg-Gly backbone amide nitrogen atom as seen in Chapter 5, it was desired to synthesize another RGDS peptide caged in a different location, deemed promising through modeling studies, and compare properties of importance for cell pattern formation in order to potentially improve our cell patterning strategy. In addition, synthesized caged RGD ligands had been used by two other groups in the literature to control cell adhesion (including one caged on the Arg-Gly backbone amide nitrogen[1] like that used in our previous studies and one caged on the Asp side chain carboxyl[2]) and it was of interest to compare those used to date in the literature. Herein, we prepared RGDS peptide photocaged either on the Arg-Gly backbone amide nitrogen atom (R[-]GDS) or Asp side chain carboxyl (RG[D]S). Note that this work uses the symbol R[-]GDS in place of R[G]DS (found in Chapter 5). This is so that R[-]GDS can be distinguished from a peptide caged on the peptide backbone adjacent to Gly, but on the Gly-Asp backbone (RG[-]DS) which will be discussed in relation to modeling, and it is a more representative symbol since the caging group appears not on a side chain (of which Gly has none), but between amino acids on the peptide backbone.

This work was novel in that it carried out, for the first time, a critical comparison of the photocaged RGD peptides' chemical and physiological properties relevant for biological applications as follows. It was observed that RG[D]S was synthesized more readily via automated solid-phase synthesis, underwent uncaging with a rate constant 3-fold higher than R[-]GDS, and was more stable in aqueous solution. Automated docking studies were performed to examine the interactions of various caged RGDS peptides with cell surface integrin receptor to identify suitable locations for the photosensitive 2-nitrobenzyl (NB) group for biological applications. A competitive binding ELISA method compared the ability of various peptides to bind to $\alpha_V\beta_3$ cell integrin receptors and the data was found to be consistent with the modeling predictions. This work was novel in suggesting the use of docking software as a method to assess various caging locations within in a peptide. Furthermore, the difference in binding affinity to an integrin receptor between the caged and irradiated, uncaged, state of R[-]GDS was found to be the greatest, which justified its future use in our patterning studies.

6.1 Introduction

Photocaged peptides incorporated into biocompatible materials create an exciting design opportunity towards the formation of photoresponsive biomaterials. Caging allows for the regulation of peptide bioactivity and associated cell signaling pathways with light.[3] It involves attaching a photoactive protecting group onto a key amino acid residue essential for bioactivity to essentially deactivate the peptide. Reactivation occurs upon irradiation with light, which breaks the bond between the photosensitive group and the original peptide.[4] By merely shining light onto the peptide of interest, one can potentially switch it from an inactive to an active state. In this way, light can be used to control the activity of biomolecules temporally and spatially within a material to create a dynamic microenvironment for biological applications.

Despite showing great promise, this technique faces several challenges. One of which is finding an effective location for the photocaging group, which must be predicted prior to synthesis.[5] Finding a location which effectively disrupts the interaction between biomolecule and target can prove challenging.[6] In fact, it is often necessary to prepare a variety of peptides caged on different locations within the peptide chain and compare the efficacy of each which can be time consuming and costly.[7,8] In the present work, synthesis was combined with automated molecular docking studies which were found to be useful to identify effective caging locations.

We are particularly interested in caging the RGD peptide sequence which binds with cell surface integrin receptors. Since the identification of RGD in 1980s and its role in enhancing cell adhesion, this small peptide sequence has played an enormous role in the development of new biomaterials.[9] The ability to cage RGD peptides to render them physiologically inactive until exposure with near-UV light leads to a number of exciting applications. Others have caged RGD peptides to successfully gain spatial or temporal control over cell adhesion. Petersen et al. caged RGD on the Asp side chain carboxyl (RG[D]) and Ohmuro-Matsuyama and Tatsu caged on the Arg-Gly amide backbone nitrogen atom (R[-]GD) in the course of their studies.[1,2,10] Previously, we also caged RGDS at the Arg-Gly backbone amide position to control the spatial localization of cells to produce patterns on a hyaluronic acid hydrogel.[11] Controlling the location of cell adhesion in biomaterials could allow one to optimize cell behavior towards producing a new

generation of medical devices such as guiding neurons towards appropriate targets or guiding the formation of new blood vessels for vascularization within materials.[12,13]

This paper is a comparative study of caged RGDS peptides. It describes their design, synthesis, modeling, and comparative binding affinities to an integrin receptor. We prepared two RGDS peptides caged at locations of interest in the literature as discussed above by synthesizing caged Fmoc Asp and caged Fmoc Gly and incorporating these caged amino acids into the RGDS tetrapeptide to generate RG[D]S and R[-]GDS, respectively. We then carefully measured and compared their chemical and biological properties. These included synthesis routes (since efficient synthesis routes may promote more wide-spread usage of these caged molecules), photolysis reaction kinetics (where a faster reaction rate is desirable), hydrolysis reaction kinetics (where hydrolysis in an aqueous environment could impede function of the caged molecules), modeled binding affinities and conformations to an integrin receptor, and experimental comparative binding affinities to an integrin receptor (ultimately, it is desirable that the caged peptides show a low affinity for binding to integrin receptors, but that the photolysis reaction product show a return of activity and high affinity for binding to integrin receptors). This information may aid to determine the ideal caged peptide for use in various biomaterial applications and to obtain a more in depth understanding of the activity of these important caged molecules.

6.2 Experimental

6.2.1 Synthesis of Caged Fmoc Aspartic Acid

Fmoc-Asp-OtBu (1 mol eq), 2-nitrobenzyl (2-NB) alcohol (1.1 mol eq), diisopropyl carbodiimide (DIC) (1.25 mol eq), and 4-dimethylaminopyridine (DMAP) (0.10 mol eq) were reacted overnight in dichloromethane (DCM) at room temperature (RT) under a nitrogen atmosphere. Precipitated material was filtered out and solvent removed under vacuum. The crude product was then treated with 1:1 DCM:trifluoroacetic acid (TFA) (such that the material was dissolved in a minimum volume of DCM) at RT for 1h to remove the tBu protecting group. Solvent was evaporated under vacuum. The residual material thus obtained was washed repeatedly with cold ether to remove all non-polar impurities. The white crystal thus obtained

was fully characterized by ^{1}HNMR and mass spectrometry. ^{1}HNMR (400 MHz, DMSO-d_6) δ, ppm: 8.11 (1H , d, J_{HH} 10.8 Hz, 2-NB ortho aromatic), 7.88 (2H, d, J_{HH} 10.0 Hz, Fmoc aromatic), 7.80 (1H, d, J_{HH} 11.3 Hz, 2-NB meta aromatic), 7.70 (2H, Fmoc aromatic), 7.67 (1H, 2-NB aromatic), 7.61 (1H, t, J_{HH} 10 Hz, 2-NB aromatic), 7.40 (2H, t, J_{HH} 9.6 Hz, Fmoc aromatic) 7.30 (2H, t, J_{HH} 9.2 Hz, Fmoc aromatic), 5.46 (2H, s, benzylic), 4.41 (1H, q, α-carbon), 4.30 and 4.21 (3H, Fmoc non-aromatic), 3.16 (12H, s, isopropyl group from DIC by-product, N,N'-diisopropylurea), 2-3 (1H, β-carbon). Note that some of the proton assignments are tentative and may be interchanged. SELDI-TOF MS using a Ciphergen Protein chip® instrument showed a strong peak at *m/z* 492 which correlated well with the calculated molecular mass.

6.2.2 Synthesis of Caged Fmoc Glycine

Potassium carbonate (2.5 mol eq), 2-nitrobenzylamine hydrochloride (1 mol eq) and tert-butyl bromoacetate (1 mol eq) dissolved in dimethylformamide (DMF) were reacted at 60-70^{o}C for 2h after which precipitated materials were filtered. The crude material was dried, re-dissolved in cold ether, and polar impurities were extracted with water. The organic phase was dried and concentrated under vacuum. The product was purified via silica gel column chromatography using ethyl acetate and hexane mixtures for the mobile phase. This product was subsequently employed in the synthesis of caged peptide by a liquid phase method as reported earlier by us,[11] or a solid phase method. For the solid phase method, an Fmoc protecting group was introduced to the terminal amino group of caged Gly as reported elsewhere.[14] The tBu protecting group was removed from the terminal carboxyl by treatment with 1:1 TFA:DCM (such that the material was dissolved in a minimum volume of DCM) for 3h followed by solvent removal under vacuum. The product was treated with aqueous $NaHCO_3$ until bubbling ceased. The aqueous soluble product was washed with cold ether to remove impurities, and then precipitated upon acid addition and dried. ^{1}HNMR indicated the formation of two conformational forms of caged Fmoc Gly. ^{1}HNMR (400 MHz, DMSO-d_6) δ, ppm: 8.10 and 8.02 (1H, d, J_{HH} 10.4 Hz, 2-NB ortho aromatic), 7.77 (1H, d, J_{HH} 10.1 Hz, aromatic), 7.65 1H, (2H, d, J_{HH} 10.6 Hz, Fmoc aromatic), 7.60 – 7.17 (19H, Fmoc and 2-NB aromatic), 4.89 and 4.80 (2H, s, benzylic), 4.62 and 4.56 (2H, d, J_{HH} 7-8 Hz, Fmoc non-aromatic CH_2OCOO), 4.25 and 4.18 (1H, t, J_{HH} 7-8 Hz, Fmoc non-aromatic cyclic), 4.10 and 3.86 (2H, s, Gly αH). Note that some of the proton assignments are tentative and may be interchanged. MALDI-tof MS revealed a strong molecular ion peak at *m/z*

432 consistent with the calculated molecular mass in addition to peaks at *m/z* 415, 455 and 471 owing to the loss of NH_2 and formation of adducts with sodium and potassium respectively.

6.2.3 Peptide Synthesis

Caged and native RGDS peptides were prepared by automated solid phase chemistry using an Intavis AG Bioanalytical Multipep Instrument (Germany) with normal HATU/DIEA mediated Fmoc chemistry as described earlier.[15] Products were analyzed by SELDI-tof MS which showed a peak at *m/z* 565 for R[-]GDS and *m/z* 561 for RG[D]S which correlated well with the expected molecular weights. The final crude peptide was also analyzed and purified by reversed phase HPLC (RP-HPLC) (Varian Prostar) using a Phenomenex Synergi semi-preparative column (Hydro-RT, 750x10 mm, 4 μm pore size) and a UV-detector at 215 nm. Two solvent systems consisting of water with 0.1% TFA (solvent A) and acetonitrile with 0.1% TFA (solvent B) were used. Initially, 90% solvent A + 10% solvent B was used and after 5 min the solvent ratios were linearly changed to 20% solvent A + 80% solvent B at a gradient of 1% B/min.

6.2.4 Photolysis

Exposure at 365 nm from a long wave UV Lamp (100 W) was employed for photolysis of caged RGDS peptides. Samples were irradiated 10 cm from the light source to produce an intensity of ~7 mW/cm^2, as measured by a calibrated radiometer.

6.2.5 Photolysis Reaction Rate Comparison

Caged peptides at 0.1 mg/ml in 1xPBS buffer (pH 7.4) were irradiated for varying lengths of time. Resulting solutions were analyzed by RP-HPLC to determine the % of caged peptide reacted as a function of exposure time. This was based on each peptide's predetermined retention time (verified by MS) and the change in area under this peak with exposure time. Reaction products were separated with a RP-HPLC column (Waters XBridge BEH 130, 4.6x75 mm, C_{18}, 3.5 μm pores) and a mobile phase in gradient elution mode with a flow rate of 1 ml/min at RT. Initially, 95% solvent A + 5% solvent B was delivered and after 5 minutes the solvent ratio was linearly decreased by 1% A/min. Absorbance at 190 nm – 500 nm was recorded.

6.2.6 Hydrolysis Reaction Rate Comparison

To compare the rate of hydrolysis of caged RGDS peptides, 0.1 mg/ml solutions of caged peptide were prepared in sterile 1xPBS buffer (pH 7.4) and incubated at 37°C in the dark for a period of up to 4 weeks. The reaction was analyzed at various time points for the disappearance of the caged peptide using RP-HPLC in the same manner as described above.

6.2.7 Molecular Modeling and Automated Docking

Docking calculations were carried out with AutoDock 4.0.1 (The Scripps Research Institute)[16,17] which has been used previously to study $\alpha_V\beta_3$ integrin-ligand interactions.[18] The peptide backbone atoms were superimposed onto those in the known X-ray structure, in order to position the peptide properly in the binding site as a docking starting point. Docking runs were conducted such that the ligand undergoes no translational or molecular rotational motions out of this binding pocket since the binding mode of the ligand within the pocket was known from X-ray crystal structure data and it allowed for much improved convergence of docking calculations. The search method used was the Lamarckian Genetic Algorithm and for each ligand, 100 independent docking runs were simulated with an initial population of 150 randomly placed individuals, a maximum of 25 million energy evaluations and 27 000 generations. The mutation rate was set to 0.02 with a cross over rate of 0.8 and an elitism value of 1. The protein-ligand complexes obtained after docking were visualized using PyMOL (The PyMOL Molecular Graphics System, 2007 DeLano Scientific LLC) and the result with the lowest free energy of binding was identified after verifying that it represented a well-populated cluster containing protein-ligand complexes with root mean square distances of 2.0 Å.

The ligands utilized for docking were cyclo(-RGDf[NMe]V-), linear RGD, and RGDS peptides. The cyclo(-RGDf[NMe]V-) was chosen for modeling because it was the only RGD ligand found with X-ray crystal structure information available showing the ligand bound to integrin, and as such makes an excellent control.[19] Linear RGD was chosen since its binding structure could be modeled by merely deleting the extraneous function groups from cyclo(-RGDf[NMe]V-), and finally linear RGDS was modeled as it is the peptide of interest in this thesis work although no binding conformation information was found for the terminal Ser residue. The cyclo(-RGDf[NMe]V-) structure was retrieved from the protein data bank in

complex with $\alpha_V\beta_3$ integrin receptor (ID 1l5g),[19] and was isolated using Sybyl software (Tripos International). Caging groups were added with the standard fragment library from Sybyl. Linear RGD was constructed from cyclo(-RGDf[NMe]V-) by deleting extraneous functional groups. For RGDS peptide, Ser was added using Sybyl. Structures were imported into Autodock Tools where all hydrogens were added, Gasteiger charges calculated, and non-polar hydrogens merged. During the docking process, the peptide backbone was held rigid while all other rotatable bonds were treated as flexible. The Ser residue of RGDS was treated as flexible since no detailed experimental results were found describing its integrin-bound conformation. The $\alpha_V\beta_3$ integrin receptor was imported into Autodock Tools where all hydrogens were added, Kollman partial charges assigned, and non-polar hydrogens merged. Mn^{2+} ions were manually assigned a charge of +2.[20] Grid maps were calculated with AutoGrid, and chosen to encompass residues directly involved in the peptide binding sites, as well as a significant portion of the integrin receptor residues around the binding site of cyclo(-RGDf[NMe]V-) based on the solved crystal structure. Grid maps with 60 X 76 X 60 points with a 0.375 Å grid-point spacing were employed.

6.2.8 ELISA for Measuring Binding Efficiencies of Caged and Native RGDS Peptides to an Integrin Receptor

Recombinant human integrin $\alpha_V\beta_3$ (R&D Systems, 3050-AV) was diluted to 2.5 μg/ml in 1xPBS buffer and 100 μl of this was coated onto the wells of an amine-binding maleic anhydride 96-well plate overnight at 4°C. Unreacted groups were blocked with 1% BSA in 1xPBS for 3h at RT. A 10 nM solution of recombinant human fibronectin (Fn) in binding buffer (50 mM Tris, 100 mM NaCl, 2 mM $CaCl_2$, and 2 mM $MgCl_2{\cdot}6H_2O$) was prepared. Solutions containing equivalent amounts of Fn were incubated with or without the specified peptide at a fixed molar ratio to Fn (5,000:1, 500:1, 50:1, and 5:1 peptide:Fn). Bound Fn was detected with anti-human Fn antibody (Sigma Aldrich, F3648) diluted 1:5,000 and incubated for 2h at RT followed by incubation with Anti-rabbit IgG conjugated to horseradish peroxidase (Sigma Aldrich, A6154) diluted 1:1,000 for 1 h. Secondary antibody was detected with a TMB substrate kit (Thermo Fisher Scientific, 34021) as per product instructions. Absorbance readings at 450 nm were recorded.

6.3 Results and Discussion

6.3.1 Caged Peptide Synthesis

R[-]GDS and RG[D]S caged peptides were successfully synthesized using a combination of liquid and solid phase chemistry. It was desired to compare their synthesis schemes since an efficient synthetic route can promote more wide-spread use of these molecules in biomaterials. First, individual amino acids were caged (Supplementary Figure 6.1). To our best understanding, the synthetic scheme as proposed by us in this study for caged Gly has not been reported, and in that respect it is novel. In the second stage of synthesis, these caged amino acids were incorporated at the proper location in an RGDS peptide chain via automated Fmoc-solid phase chemistry.[15] This incorporation often presents challenges in the generation of caged peptides. Bourgeault et al. were the first to successfully cage an Asp residue but failed to incorporate it into their full endothelin-1 peptide chain.[7] Tatsu et al. have reported the successful synthesis of a caged Gly-containing-peptide with 2-NB group.[8] However, it required a large excess of coupling agent (10 fold). Others have attempted automated synthesis of backbone caged peptides with mixed results.[21,22]

Standard solid phase peptide synthesis methods were successfully modified to incorporate caged Asp into the RGDS chain. Thus, the time for the base-catalyzed Fmoc deprotecting steps was minimized to half the standard time, to 3.5 minutes (with 2 deprotecting steps/cycle of amino acid addition), after the addition of caged amino acid to prevent removal of the 2-NB caging group. The other modification was the introduction of quadruple coupling steps for all amino acids except that of caged amino acid. Figure 6.1A shows the RP-HPLC profile of crude RG[D]S peptide. The major Peak "A" showed an intense peak in the mass spectrum at *m/z* 560 consistent with its calculated mass, while Peak "B" at *m/z* 474 is likely due to the formation of deletion peptide RG[D] as a minor by-product. In comparison, the synthesis of R[-]GDS peptide was found to be much less clean as demonstrated by the presence of multiple peaks in the RP-HPLC profile of its crude product (Figure 6.1B). Peak "A" was attributed to the peptide RGDS (*m/z* 433), missing the caging group. Peak "B" was due to the formation of [-]GDS peptide (*m/z* 417) while peak "C" represented another deletion peptide, R[-]GS (*m/z* 458). The last eluting peak (minor), "D" was identified as the desired R[-]GDS peptide – NH_2 (*m/z*= 555). Thus, the major product in the synthesis was [-]GDS indicating the absence of Arg which failed

to couple after the caged Gly addition. This is consistent with previously reported observations by others.[21,22] Because the desired product is produced in extremely low amounts, this method of automated solid-phase synthesis is not suitable. Since further modification of the solid phase method did not improve the synthesis, an alternate liquid phase method was followed as previously outlined which led to an efficient yield of the correct peptide.[11] Therefore, RG[D]S synthesis is more straightforward, and can be accomplished via a more accessible automated solid-phase synthesis route.

6.3.2 Uncaging Reaction

The rates of photolysis of the caged peptides were analyzed and compared. The % of peptide uncaged with 365 nm light was followed by RP-HPLC. Peptide peaks were identified by MS and by HPLC comparison to pure peptides prior to irradiation. As expected, the R[-]GDS and RG[D]S peak intensities in the RP-HPLC chromatograms decreased consistently with exposure time. Both caged peptides exhibited absorption maxima at a wavelength of 266 nm, but absorb light even up to ~375 nm as expected due to the presence of the same caging group, 2-NB.[23] We used 365 nm light for uncaging studies since it was shown to be effective, and was found to be relatively safe for biological systems which could be subjected to these caged peptides.[24]

Figure 6.2A plots the % of R[-]GDS and RG[D]S reacted after exposure to 365 nm light. A plot of $\ln[C]/[C]_o$ versus time (where [C] represents the concentration of caged RGDS peptide and $[C]_o$ the initial concentration) in Figure 6.2B showed a linear decrease indicating first order rate kinetics as expected since the 2-NB uncaging reaction has been previously described as apparent first order.[25] The rate constant was calculated as $-0.00139 \pm 0.00004\ s^{-1}$ (95% confidence interval) for R[-]GDS and $-0.00404 \pm 0.00039\ s^{-1}$ (95% confidence interval) for RG[D]S. Thus, RG[D]S reacts significantly faster than R[-]GDS upon irradiation at a 95% confidence level, and its rate constant value suggests this being 3-fold higher. This lends advantage to the use of RG[D]S peptide, as less energy is required for the uncaging process, which equates to lower light exposure times. Less energy input required also presents less potential for side-reactions or disruptions to any biological systems to which the caged peptides are applied.

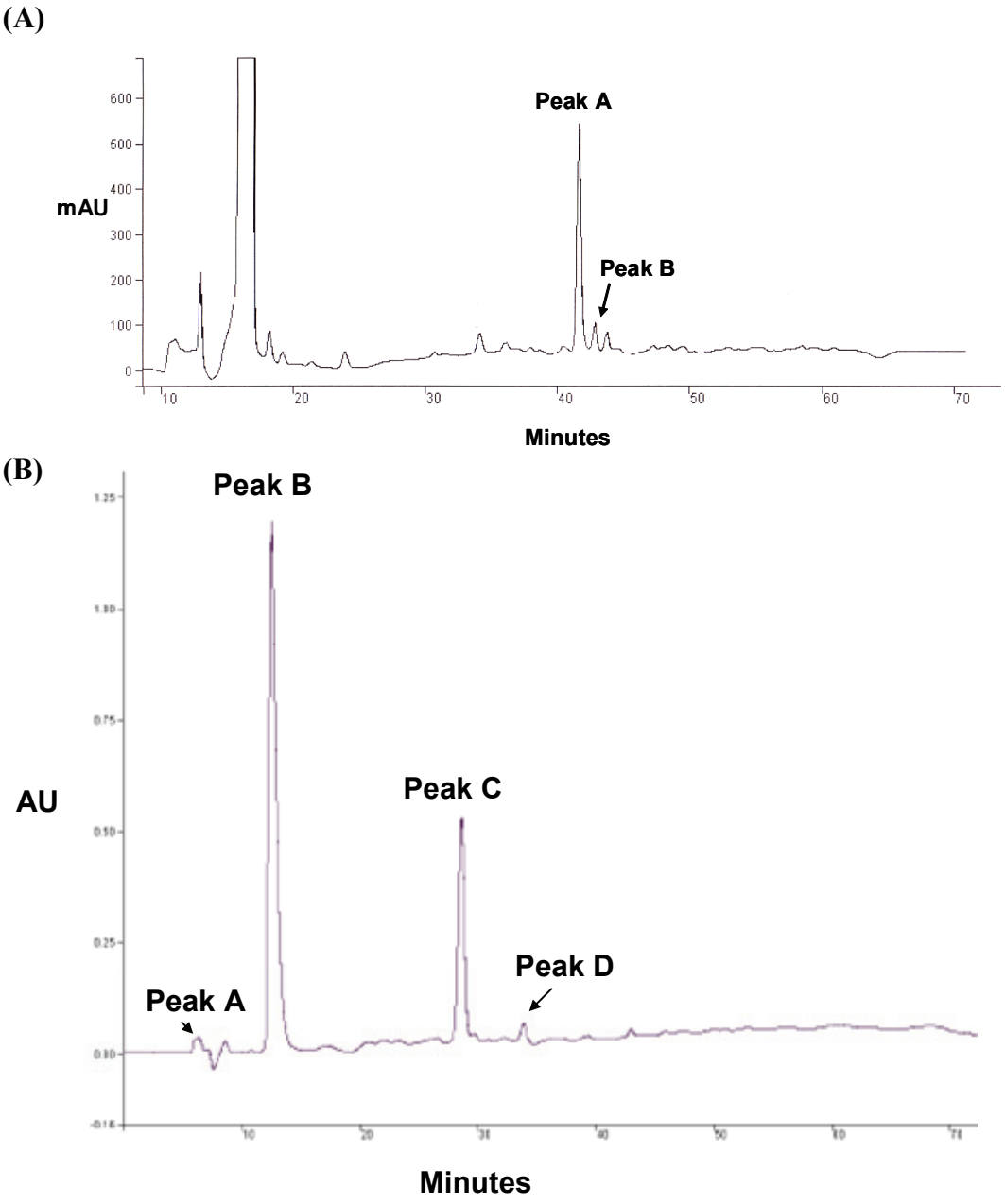

Figure 6.1: (A) HPLC chromatogram profiles of RG[D]S and **(B)** R[-]GDS peptides following their syntheses by an automated Fmoc solid-phase method.

(A)

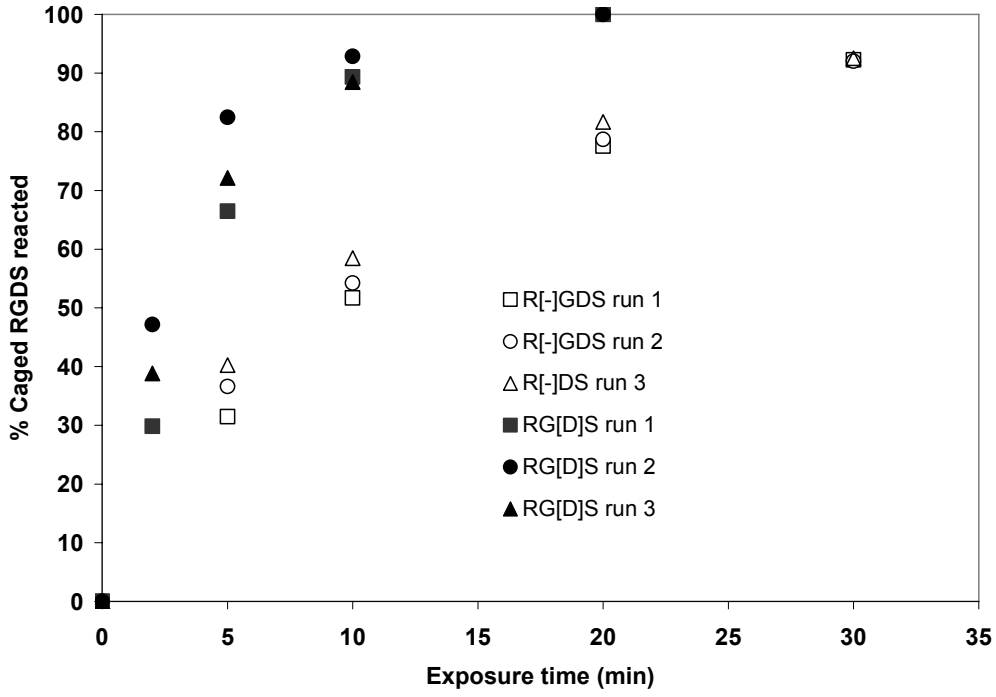

(B)

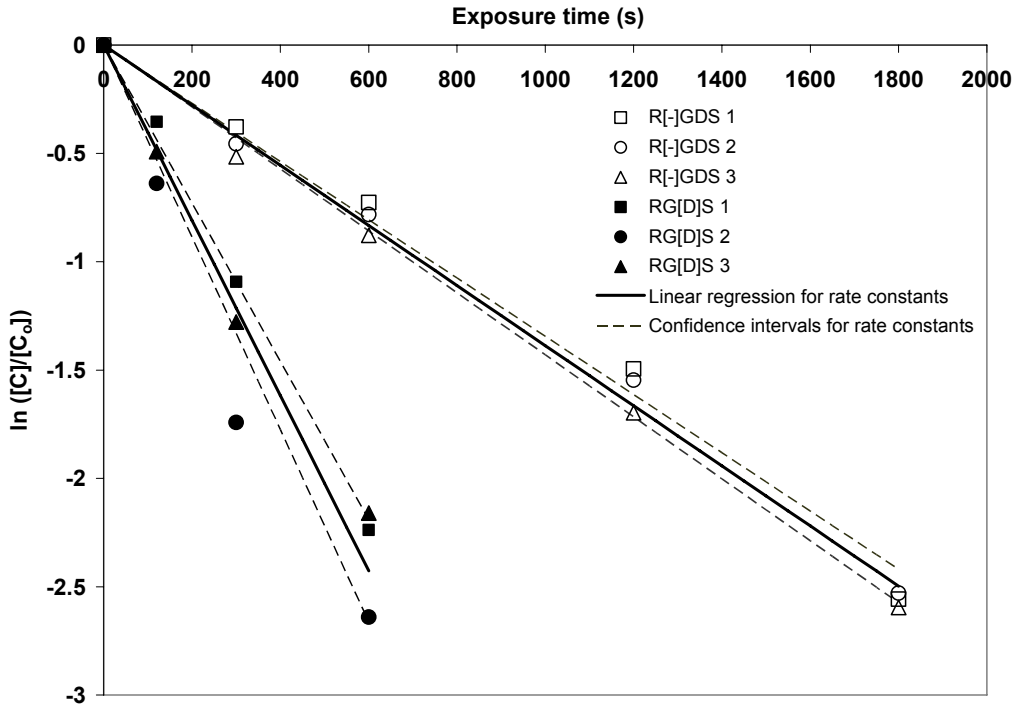

Figure 6.2: (A) Plot of percent peptide reacted vs near-UV light exposure time. **(B)** Plot of ln ([C]/[C_0]) as a function of exposure time. [C]= Concentration of caged peptide present at any time; [C_0]= Concentration of caged peptide originally present. 95% confidence intervals represented.

RGDS regeneration could not be followed by HPLC, since RGDS eluted in the column void fraction, which is an issue also reported by others.[26] Therefore, ^{1}HNMR spectroscopy was used to confirm the removal of the photocage moiety from the caged peptides after UV exposure. A solution of caged RG[D]S in D_2O was analyzed via proton NMR before and after 1h UV exposure. Peaks associated with peptide protons were largely unchanged between the two spectra, providing evidence that the peptide chain itself remained similar after light exposure. However, as expected, the benzylic proton peak (2H, δ=5.45 ppm) disappeared after light exposure, due to the removal of the caging group. In addition, a new aldehyde proton peak (δ=9.3 ppm) appeared after light exposure. The expected product of uncaging is a nitroso-aldehyde which provides further evidence that the peptide is uncaged upon near-UV light exposure to regenerate RGDS. A similar analysis was performed earlier by us for R[-]GDS.[11]

6.3.3 Stability of Caged Peptides to Hydrolysis

The solubility of caged peptides in aqueous medium is highly desirable for use in biological systems. Fortunately, both caged R[-]GDS and RG[D]S were found to be highly soluble in aqueous medium. However, it is equally important that caged peptides do not undergo significant hydrolysis in this environment in the absence of near-UV light. Since stability during experimental time frames is crucial for their successful implementation in biomaterials,[27] we set out to compare the susceptibility to hydrolysis of our two caged RGDS peptides under physiological conditions. The experimental results (Figure 6.3) showed significant differences between the two caged peptides. After one day, almost half of the caged R[-]GDS had reacted and by day 3, over 90% of the peptide had degraded. In contrast, the RG[D]S peptide was shown to be quite stable over the entire study period leading to <15% degradation at four weeks. It is clear that RG[D]S is significantly more stable in aqueous solution than R[-]GDS.

To investigate the instability of R[-]GDS in more detail, overlaid HPLC chromatograms of R[-]GDS in aqueous solution after predetermined time points are shown in Figure 6.4A. Mass spectrometry confirmed that peak “A” represents the original R[-]GDS (*m/z* 566) peptide which disappeared with time while Peak “B” grew in intensity and was analyzed by MS to have a molecular weight of 350. The max absorbance of this peak was seen at 265 nm similar to the 2-NB caging group.

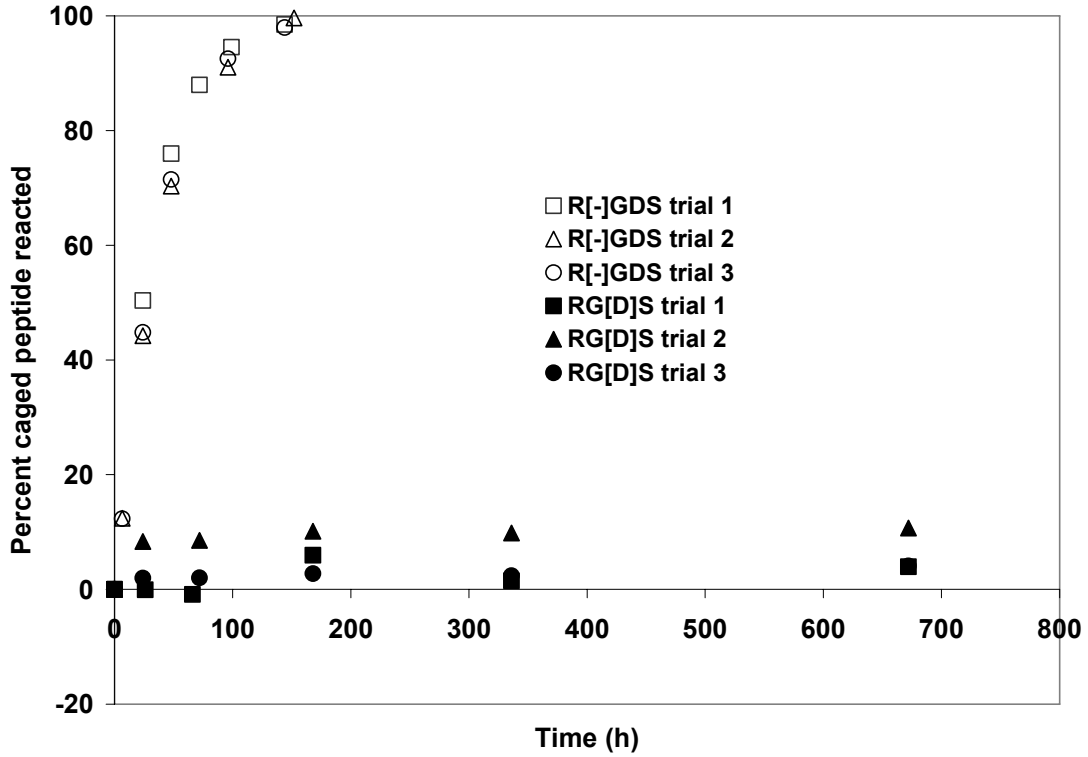

Figure 6.3: Comparative hydrolysis (disappearance) of caged RGDS peptides with time at 37°C in 1xPBS (pH 7.4) buffer. The reaction is monitored by the disappearance of the caged peptide RP-HPLC chromatogram peak.

We hypothesized that this peak represents an Arg-Gly cyclic dipeptide with 2-NB caging group on the amide backbone nitrogen (shown in Figure 6.4B as "dipeptide diketopiperazine"). Bogdanowich-Knipp et al. studied the degradation pathways of RGD peptides, and found that the mechanism primarily involves the Asp residue, which can attack and cleave the peptide backbone to form the dipeptide Arg-Gly.[26] It is therefore likely that a similar reaction also occurs with R[-]GDS, but the presence of a strongly electron withdrawing 2-NB caging group could make the peptide more susceptible to attack (see Figure 6.4B). In the proposed mechanism, a diketopiperazine (DKP) is formed, since dipeptide esters readily cyclize to produce DKPs.[28] The expected molecular weight of this DKP (349) correlates well with MS data for Peak B (m/z=350) in Figure 6.4A. Our data therefore indicated that caged RG[D]S peptide possesses increased stability. By caging the carboxyl group on the Asp, we protect the most reactive group on the RGDS peptide which should increase stability.

(A)

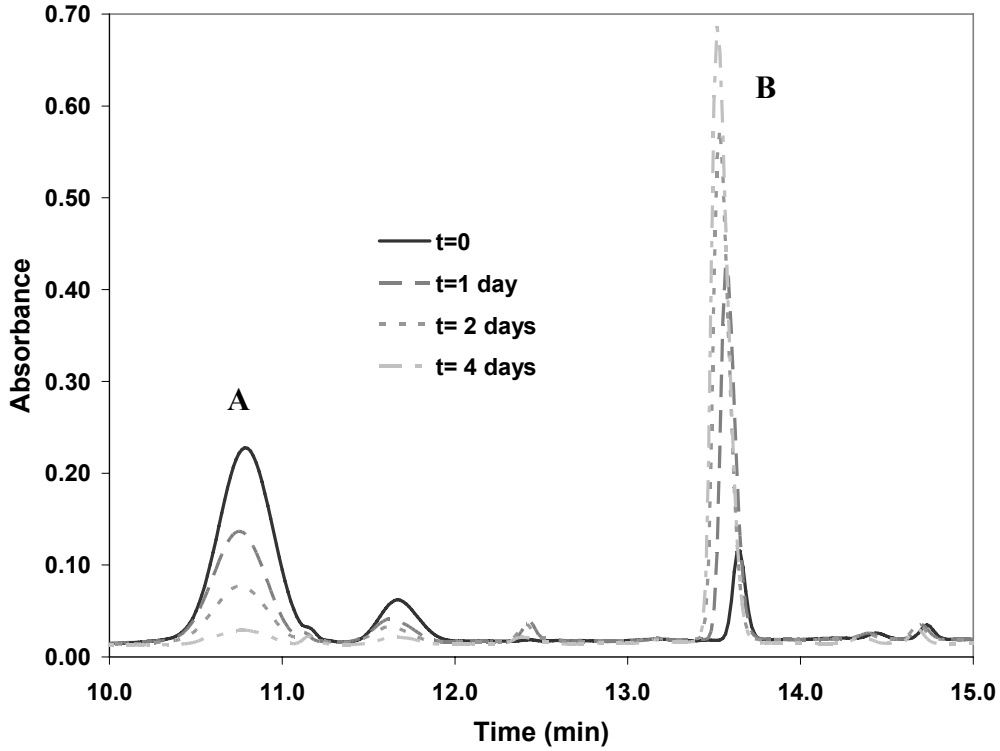

(B)

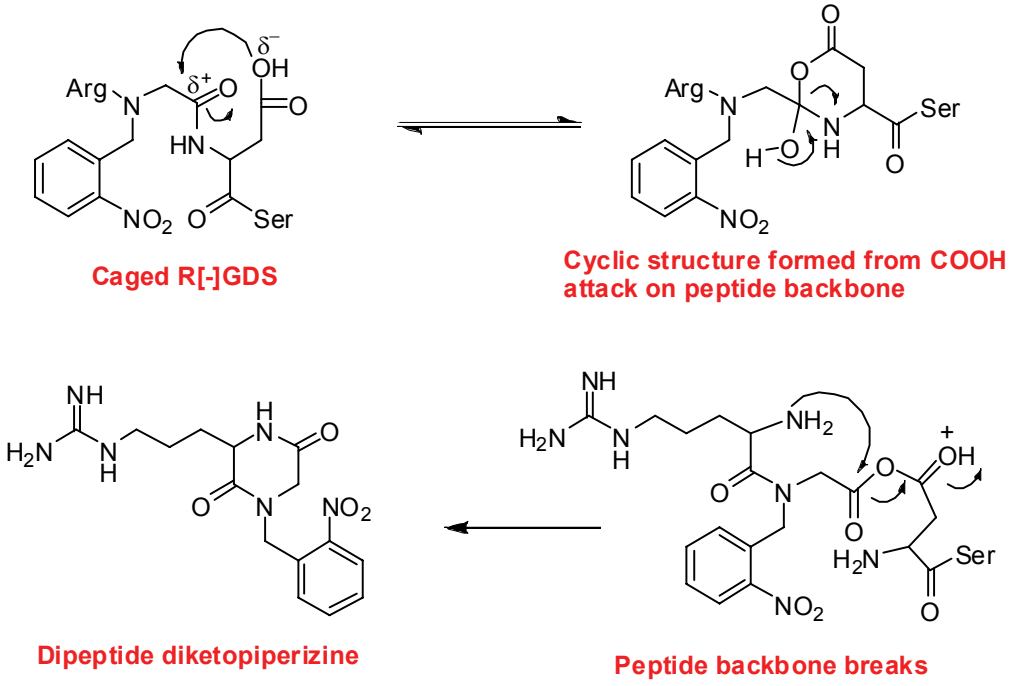

Figure 6.4: (A) Overlaid RP-HPLC chromatograms of R[-]GDS peptide in solution (1xPBS buffer, 37°C) at various time points. **(B)** Proposed degradation scheme for the hydrolysis of R[-]GDS.

6.3.4 Modeling Study

Three RGD ligands - cyclo(-RGDf[NMe]V-) (Cilengitide, Figure 6.5E), RGD, and RGDS - both native and caged with 2-NB at various sites (Figure 6.5), were subjected to automated docking with $\alpha_V\beta_3$ integrin receptor to compare their interactions and explore effective locations to bind a 2-NB caging group. The study was based on known X-ray structure data of cyclo(-RGDf[NMe]V-) bound to $\alpha_V\beta_3$ integrin.[19] Table 6.1 shows the estimated free energy of binding of these various ligands with $\alpha_V\beta_3$ integrin receptor and suggests that placing a 2-NB caging group at different locations within the RGD sequence disrupts integrin binding to varying degrees. Integrins bind in clusters, and ultimately the combined binding energy of a large number of integrin-RGD complexes anchor a cell to a surface - Benedetto et al. identified $3x10^3$-$1.4x10^4$ α_v /cell and $5.3x10^2$-$1.1x10^4$ β_3/cell. It is therefore likely that even small increases in binding energy between an RGD-integrin pair will be significant.[29]

As a control, we first reproduced the known X-ray crystal structure by successfully docking cyclo(-RGDf[NMe]V-) with $\alpha_V\beta_3$ integrin. The position of the ligand after docking differed from the binding conformation of the X-ray crystal structure by only 0.90 Å (Figure 6.6A) suggesting that the docking conditions used for analysis were reasonable (since the original X-ray crystal structure resolution from the Protein Data Bank was given to be 3 Å). Figure 6.6B shows the overlapped image of three native RGD ligands with integrin receptor. Docking studies predicted (Table 1) that the order of binding affinity to the integrin receptor would be cyclo(-RGDf[NMe]V-)>RGDS>RGD which correlates well to the literature.[9,30] The best controlled automated docking studies will ultimately be those involving cyclo(-RGDf[NMe]V-) due to the availability of the X-ray crystal structure for the bound conformation. For modeling the linear peptides, we assumed that the Arg, Gly, and Asp residue backbones bound in a mode similar to cyclo(-RGDf[NMe]V-). When Xiong et al. discovered this crystal structure of $\alpha_V\beta_3$ integrin in complex with cyclo(-RGDf[NMe]V-) they cited evidence which suggested that their crystal structure could serve as a basis for understanding the interaction of integrins with other RGD ligands.[19] Though there may exist differences in reality, this assumption may still provide some useful information concerning linear RGD and RGDS, which are often incorporated in biomaterials.

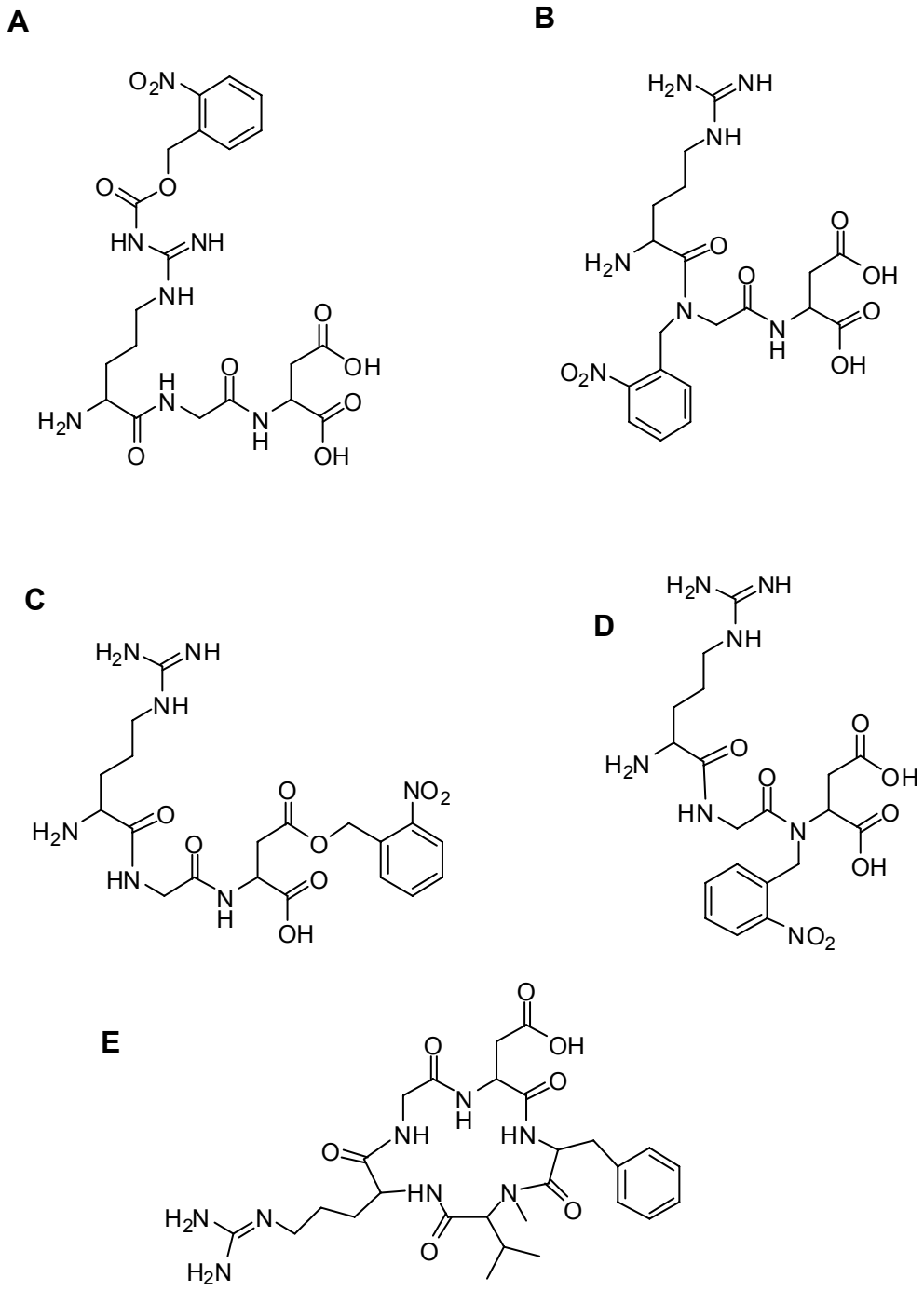

Figure 6.5: Chemical structure of RGD ligands caged with a 2-NB function in various locations as used in the docking studies. Linear RGD ligand is shown caged for illustrative purposes. **(A)** Caged [R]GD; **(B)** Caged R[-]GD; **(C)** Caged RG[D]; **(D)** Caged RG[-]D where brackets [] indicate the position of the 2-NB group **(E)** Structure of cyclo(-RGDf[NMe]V-).

Table 6.1: Calculated binding energies of the final docked conformations for the native non-caged and caged cyclo(-RGDf[NMe]V-), linear RGD, and linear RGDS peptides interacting with the $\alpha_V\beta_3$ integrin receptor

Ligand	Free energy of binding (kcal/mol)	Difference in free energy of binding from native non-caged ligand	Decrease in quantity of integrin-ligand complexes formed compared to non-caged ligand
cyclo R[-]GD	+0.38	+6.55	No binding
cyclo RG[-]D	-1.95	+4.22	1250X
cyclo RG[D]	-2.98	+3.19	220X
non-caged cyclo RGD	*-6.17*	*0*	
cyclo [R]GD	-7.43	-1.26	
RG[-]D	+0.02	+4.18	No binding
RG[D]	-0.78	+3.38	300X
R[-]GD	-2.88	+1.28	9X
[R]GD	-3.0	+1.16	7X
non-caged RGD	*-4.16*	*0*	
RG[-]DS	-0.77	+4.42	1750X
RG[D]S	-2.82	+2.37	55X
R[-]GDS	-3.3	+1.89	24X
non-caged RGDS	*-5.19*	*0*	
[R]GDS	-5.77	-0.58	

Automated docking revealed that for the RGD peptides studied, placing the caging group at the end of an amino acid side chain was not as disruptive as placing it directly on the backbone. Binding the 2-NB cage to a nitrogen atom on the peptide backbone resulted in the highest binding energy to the integrin receptor. Previous experimental work with a different caged peptide similarly found backbone caging more effective in knocking out peptide function.[8] The cyclo R[-]GD peptide was found to bind with the least affinity to integrin compared to any other caged circular RGD molecules with a positive binding energy. Figure 6.6C shows the final docked binding conformations of all three ligands caged at the peptide backbone between Arg and Gly. Docking predicted that for all ligands, caging at this location would interrupt integrin binding. In the literature, Dechantsreiter et al. suggested that for the RGD sequence, close contact between the polar amide groups of the peptide backbone adjacent to Gly and the integrin receptor is essential for integrin-mediated cell attachment.[30] Furthermore, RGD ligands caged at this location have been used to control cell adhesion which supports this prediction.[1,11]

Placing a 2-NB caging group on the nitrogen atom of the Gly-Asp peptide bond was found by automated docking calculations to produce the second highest binding energy to $\alpha_V\beta_3$ integrin for circular ligands, and the highest binding energy (i.e. lowest binding affinity) for the linear ligands. The intermolecular energy between the final bound conformation of these backbone caged ligands and the integrin receptor is significantly increased as compared to the non-caged native ligands and appears to be mostly the result of highly positive van der Waals forces between the integrin and 2-NB cage. Therefore, synthesis of such a caged ligand could make for exciting future work since caging in this location is likely to severely interrupt integrin binding.

The Asp residue participates extensively in integrin binding with its side-chain carboxyl group that co-ordinates with a divalent cation in the binding pocket. So, it was hypothesized that caging the carboxyl group on its side chain would cause significant binding disruption.[2,7] Although the cage did interfere with integrin binding, caging the Asp residue never produced the highest free energy of binding (i.e. lowest binding affinity) to the integrin for any ligand. Docking results predicted a stabilizing interaction between the $-NO_2$ group of the cage and the divalent cation in the integrin binding pocket. Figure 6.6D shows the docked conformations of the caged Asp ligands.

The crucial Arg residue is known to make strong physical contacts with the integrin receptor; its side chain inserts into a narrow groove on the receptor surface, where it forms salt bridges with integrin residues. Despite these contributions to binding, caging the Arg side chain did not produce any significant increase in the free energy of binding with the integrin receptor by automated docking. The flexibility of the Arg side chain seemed to allow it to relocate on the integrin surface to form energetically favorable contacts despite the presence of the caging group, and therefore caging the Arg residue is not recommended.

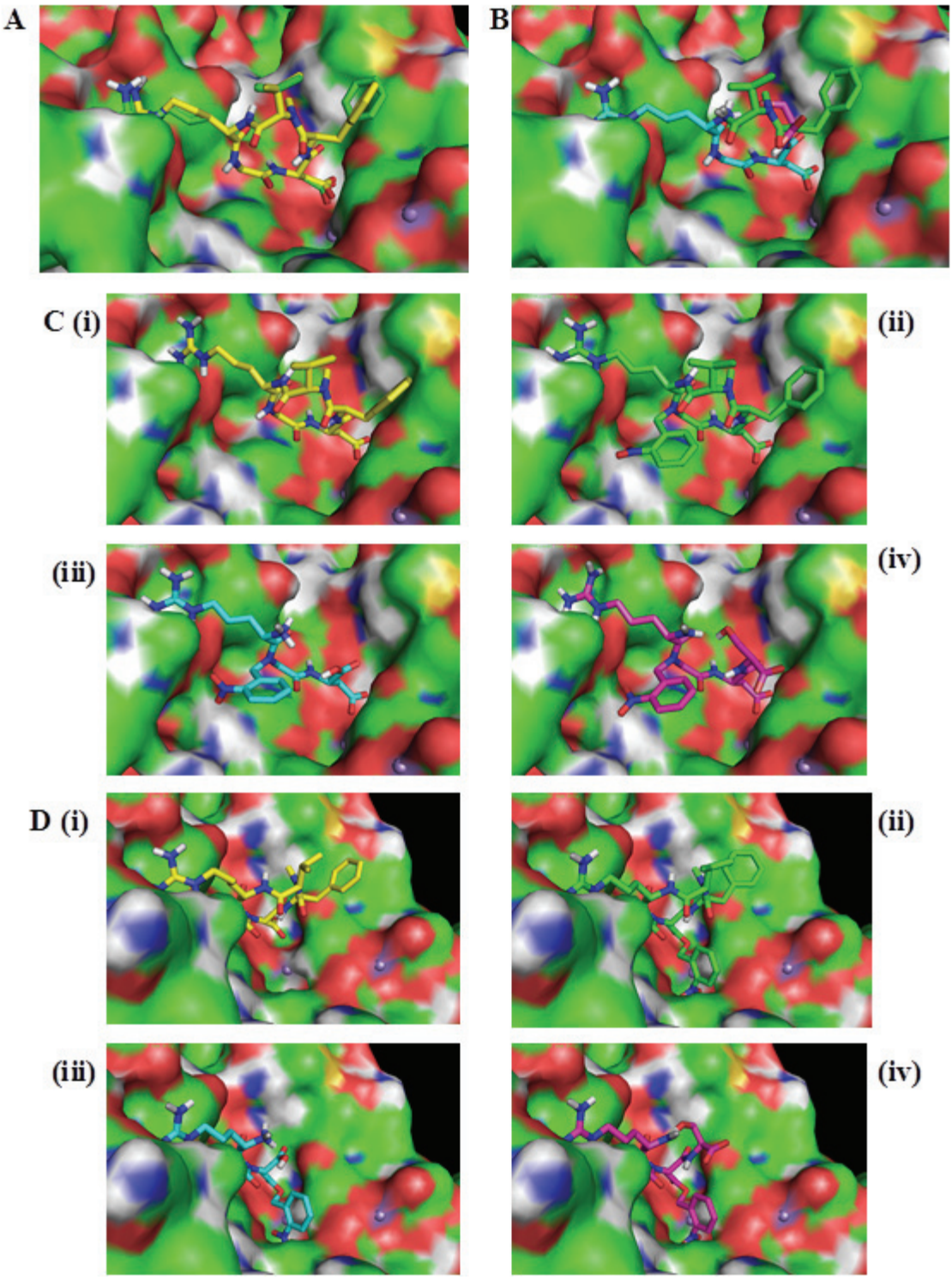

Figure 6.6: PyMOL images of the $\alpha_V\beta_3$ integrin receptor surface and various docked RGD ligands: (yellow = x-ray crystal structure of cyclo(-RGDf[NMe]V-), green = cyclo(-RGDf[NMe]V-), blue = RGD, magenta = RGDS) **(A)** control **(B)** overlapped native non-caged ligands **(C)** ligands caged on backbone between Arg and Gly **(D)** ligands caged on Asp side chain carboxyl.

6.3.5 Binding of RGDS Peptides to Integrin Receptor

To determine the comparative affinity of binding for the caged versus native RGDS peptides to an integrin receptor, a competitive binding ELISA assay was used based on protocols by others.[31,32] In the assay, the RGDS peptides competed with fibronectin for $\alpha_V\beta_3$ integrin binding. RGDS is a sequence within fibronectin that binds integrin. At a certain excess, RGDS can displace Fn binding. The assay produced absorbance readings which correlate to increased Fn binding or, equivalently, less peptide binding. Results are depicted in Figures 6.7 A-D. The control consisted of Fn only which was allowed to bind to integrin receptors. As expected, RGDS bound to the integrin receptor when present at 5 000 to 50-fold molar excess to Fn, resulting in decreased ELISA absorbance values compared to the control. At only a 5-fold excess, RGDS could not compete with Fn for binding. Even at 5 000x excess to Fn, the control peptide RGES did not bind to integrin (Figure 6.7A), suggesting that integrin binding is highly sequence specific. Both caged peptides, R[-]GDS or RG[D]S, were shown to inhibit Fn binding only at 5 000x excess to Fn, but not at lower concentrations. This suggests that both peptides are capable of binding partially to the integrin receptor, in agreement with docking results. However, at 50-500X excess, RGDS inhibited Fn binding, while the caged RGDS peptides could not. This demonstrated experimentally that the presence of a 2-NB cage on either the Asp side chain or Arg-Gly peptide backbone amide do inhibit integrin binding. Since these results are largely consistent with the automated docking predictions, Autodock was shown to be a useful tool to predict the efficacy of caged peptides in inhibiting binding to their associated receptor or target protein.

While it is important that caged peptides possess a low binding affinity to their associated receptor as explored in the modeling work and this ELISA assay, it is also very important that the irradiated peptides maintain a high binding affinity to their associated receptor. Ultimately, to employ caged RGDS peptides in a cell patterning strategy it is essential to have a large difference in binding energy with integrin receptors between the caged and uncaged/irradiated states. Interestingly, our data revealed a significant difference in the binding of uncaged peptide to the integrin receptor. While irradiation increased binding of R[-]GDS samples, as expected, no such difference was observed with RG[D]S ($p>0.05$).

A 50 µM Peptides (5 000X excess to Fn)

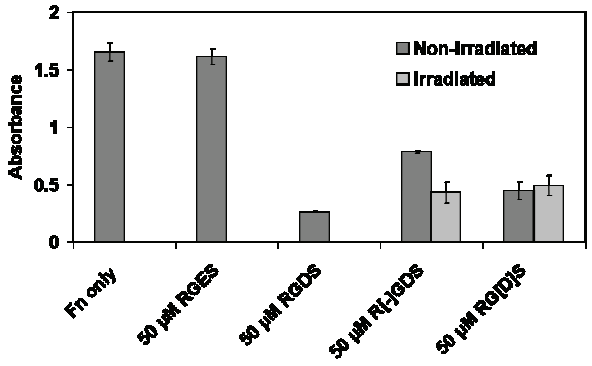

B 5 µM Peptides (500X excess to Fn)

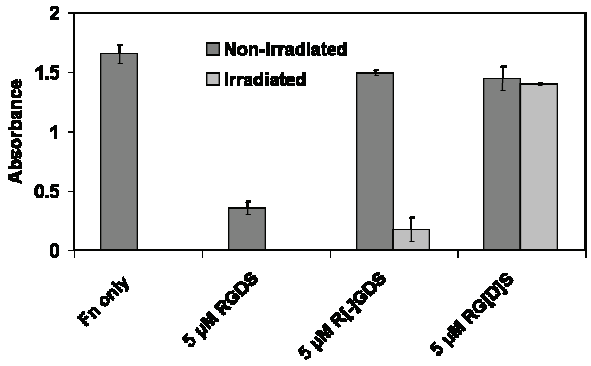

C 0.5 µM Peptides (50X excess to Fn)

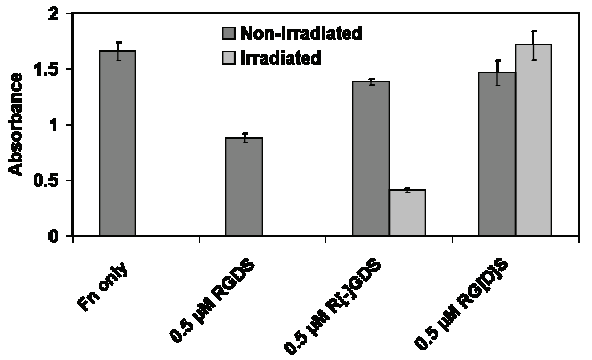

D 0.05 µM Peptides (5X excess to Fn)

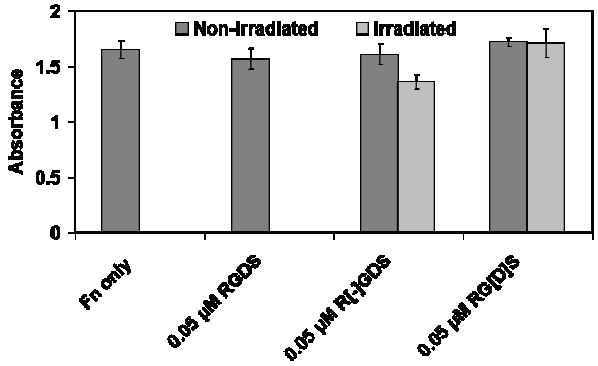

E Use of Cys for quenching, 5 µM Peptides (500X excess to Fn)

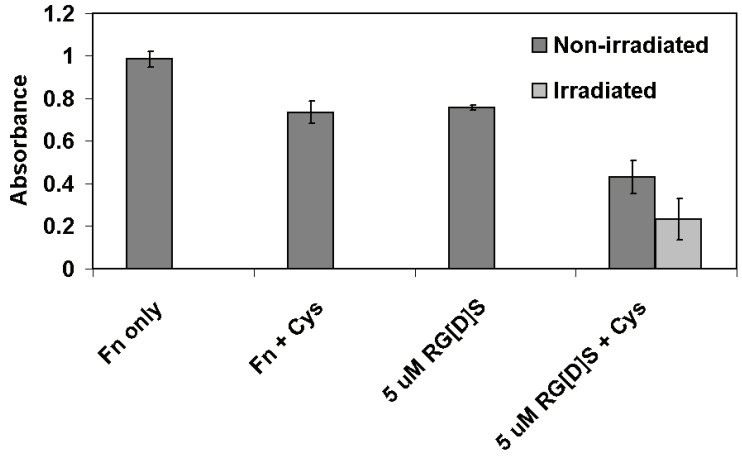

Figure 6.7: ELISA assay results shown for various caged and native non-caged RGDS peptides under varying conditions. Absorbance intensity at 450 nm after incubation of Fn + RGDS peptide at various concentrations with bound $\alpha_V\beta_3$ integrin receptor was plotted and compared to control with Fn only (no peptide added). Error bars represent +/- one standard deviation from the mean, n=3.

So, cysteine (100 mM) was added to the reaction mixture in order to quench the reactive photo by-product, nitrosoaldehyde, along with a decreased light exposure time (6 min).[27] Although Cys was found to interfere somewhat with Fn binding to integrin, the decrease in absorbance from caged to uncaged RG[D]S in the presence of Cys was found to be significant at a 95% confidence level demonstrating the binding of uncaged RG[D]S to integrin. To further support the ability of a caged Asp to regenerate an RGD ligand, Petersen et al. have successfully used such a caged species to control cell adhesion.[2]

6.3.6 Cell Patterning with R[-]GDS

One important application of these photocaged RGDS peptides is that they can be used to control cell adhesion on biomaterials. In Figure 6.8, NIH 3T3 fibroblasts were patterned in 100 μm circles using R[-]GDS, bound to a hyaluronic acid hydrogel following previously published protocols.[11] The bound peptide was exposed to 365 nm light through a photo mask (made with clear 100 μm circles on an otherwise dark background) to create circular adhesive spots of uncaged RGDS on a background of cell non-adhesive R[-]GDS peptide bound to the hydrogel. The desired circular pattern (previously unpublished) was achieved and lasted for at least 3 days in culture.

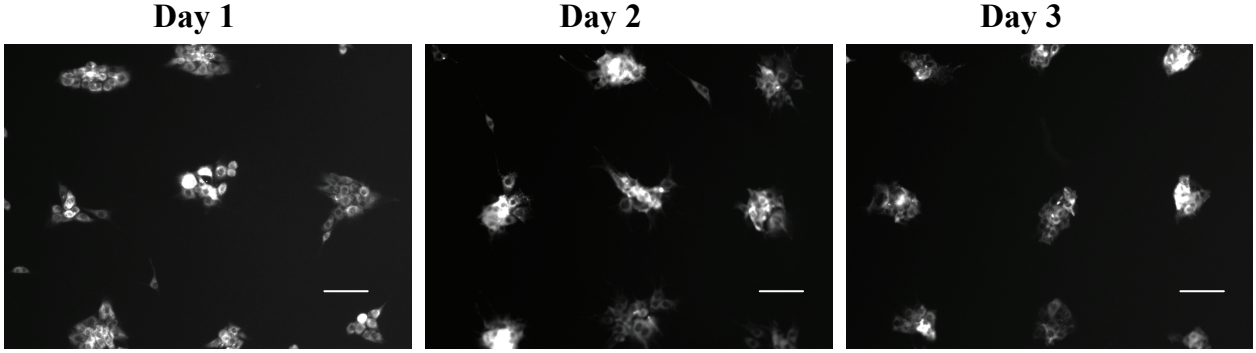

Figure 6.8 Cell pattern of 3T3 fibroblasts dyed with CellTracker Red™ on a hyaluronic acid hydrogel. Hydrogel was patterned with a photomask consisting of 100μm clear circles separated by 200μm dark spaces. Scale bars = 100 μm.

6.4 Conclusions

RGD peptides have been used extensively in biomaterials and so the ability to control their function with light through photocaging is an exciting tool to have at our disposal. We have demonstrated that such peptides can be used to control cell adhesion on a biomaterial for cell patterning. We also used, for the first time, automated docking software to predict effective location/s for positioning a caging group within a peptide to disrupt bioactivity. Autodock provided useful information concerning the interactions of caged RGDS with $\alpha_V\beta_3$ integrin receptor that were largely consistent with ELISA binding results. We prepared two RGDS peptides caged at locations of interest in the literature in order to compare properties which will impact their use in biological applications and biomaterials. Our data revealed that RG[D]S was more readily uncaged with 365 nm light, and was more stable to hydrolysis compared to R[-]GDS. In addition, RG[D]S was synthesized efficiently by solid phase peptide synthesis while R[-]GDS required a more laborious liquid phase route. However, the competitive ELISA assay indicated that RG[D]S regenerates RGDS with less ease and may require the use of a quenching agent. Therefore, R[-]GDS is recommended for use in short term experiments and where system exposure to increased irradiation is not of great importance. In contrast, RG[D]S is recommended to be used for other types of applications, but closer attention must be paid to the conditions of uncaging to regenerate RGDS. A quenching agent should be employed in this case.

6.5 Acknowledgements

We thank A. Chen and F. Sirois for their technical assistance, M. Gagne for initiating the modeling work, and the Molecular Graphics Lab, Department of Molecular Biology at the Scripps Research Institute for the Autodock program. This study was supported by a NSERC Discovery Grant to X. Cao, a NSERC Discovery grant and Heart & Stroke Foundation grant to A. Basak and a CIHR-HOPE fellowship grant to S. Majumdar and A. Basak.

6.6 References

1. Ohmuro-Matsuyama Y, Tatsu Y. Photocontrolled Cell Adhesion on a Surface Functionalized with a Caged Arginine-Glycine-Aspartate Peptide13. *Angew. Chem., Int. Ed.* 2008;47(39):7527-7529.

2. Petersen S, Alonso JM, Specht A, Duodu P, Goeldner M, del Campo A. Phototriggering of Cell Adhesion by Caged Cyclic RGD Peptides. *Angew. Chem., Int. Ed.* 2008;47(17):3192-3195.

3. Yu H, Li J, Wu D, Qiu Z, Zhang Y. Chemistry and biological applications of photo-labile organic molecules *Chem. Soc. Rev.* 2010;39(2):464-473

4. Young DD, Deiters A. Photochemical control of biological processes. *Org. Biomol. Chem.* 2007;5(7):999-1005.

5. Shigeri Y, Tatsu Y, Yumoto N. Synthesis and application of caged peptides and proteins. *Pharmacol. Ther.* 2001;91(2):85-92.

6. Ellis-Davies GCR. Caged compounds: photorelease technology for control of cellular chemistry and physiology. *Nat Meth.* 2007;4(8):619-628.

7. Bourgault S, Létourneau M, Fournier A. Development of photolabile caged analogs of endothelin-1. *Peptides.* 2007;28(5):1074-1082.

8. Tatsu Y, Nishigaki T, Darszon A, Yumoto N. A caged sperm-activating peptide that has a photocleavable protecting group on the backbone amide. *FEBS Lett.* 2002;525(1-3):20-24.

9. Hersel U, Dahmen C, Kessler H. RGD modified polymers: biomaterials for stimulated cell adhesion and beyond. *Biomaterials.* 2003;24(24):4385-4415.

10. Wirkner M, Alonso JM, Maus V, et al. Triggered Cell Release from Materials Using Bioadhesive Photocleavable Linkers. *Adv. Mater.* 2011;23:3907-3910.

11. Goubko C, Majumdar S, Basak A, Cao X. Hydrogel cell patterning incorporating photocaged RGDS peptides. *Biomedical Microdevices.* 2010;12(3):555-568.

12. Luo Y, Shoichet MS. A photolabile hydrogel for guided three-dimensional cell growth and migration. *Nat Mater.* 2004;3(4):249-253.

13. Moon JJ, Hahn MS, Kim I, Nsiah BA, West JL. Micropatterning of poly(ethylene glycol) diacrylate hydrogels with biomolecules to regulate and guide endothelial morphogenesis. *Tissue Eng Part A.* 2009;15(3):579(577).

14. Myers AG, Gleason JL, Yoon T, Kung DW. Highly Practical Methodology for the Synthesis of d- and l-α-Amino Acids, N-Protected α-Amino Acids, and N-Methyl-α-amino Acids. *Journal of the American Chemical Society.* 1997;119(4):656-673.

15. Basak A, Mitra A, Basak S, Pasko C, Chrétien M, Seaton P. A Fluorogenic Peptide Containing the Processing Site of Human SARS Corona Virus S-Protein: Kinetic Evaluation and NMR Structure Elucidation. *ChemBioChem.* 2007;8(9):1029-1037.

16. Morris GM, Goodsell DS, Halliday RS, et al. Automated docking using a Lamarckian genetic algorithm and an empirical binding free energy function. *J. Comput. Chem.* 1998;19(14):1639-1662.

17. Huey R, Morris GM, Olson AJ, Goodsell DS. A semiempirical free energy force field with charge-based desolvation. *J. Comput. Chem.* 2007;28(6):1145-1152.

18. Marinelli L, Lavecchia A, Gottschalk KE, Novellino E, Kessler H. Docking Studies on αVβ3 Integrin Ligands: Pharmacophore Refinement and Implications for Drug Design. *J. Med. Chem.* 2003;46(21):4393-4404.

19. Xiong J-P, Stehle T, Zhang R, et al. Crystal Structure of the Extracellular Segment of Integrin αVβ3 in Complex with an Arg-Gly-Asp Ligand. *Science.* 2002;296(5565):151-155.

20. Cheng F, Oldfield E. Inhibition of Isoprene Biosynthesis Pathway Enzymes by Phosphonates, Bisphosphonates, and Diphosphates. *Journal of Medicinal Chemistry.* 2004;47(21):5149-5158.

21. Johnson E, Kent S. Synthesis, stability and optimized photolytic cleavage of 4-methoxy-2-nitrobenzyl backbone-protected peptides. *Chem. Commun.* 2006(14):1557-1559.

22. Nandy SK, Agnes RS, Lawrence DS. Photochemically-activated probes of protein-protein interactions. *Org. Lett.* 2007;9(12):2249-2252.

23. Zhang Z, Hatta H, Ito T, Nishimoto S-I. Synthesis and photochemical properties of photoactivated antitumor prodrugs releasing 5-fluorouracil *Org. Biomol. Chem.* 2005;3(4):592-596.

24. Furuta T, Noguchi K. Controlling cellular systems with Bhc-caged compounds. *TrAC, Trends Anal. Chem.* 2004;23(7):511-519.

25. Kim MS, Diamond SL. Photocleavage of o-nitrobenzyl ether derivatives for rapid biomedical release applications. *Bioorg. Med. Chem. Lett.* 2006;16(15):4007-4010.

26. Bogdanowich-Knipp SJ, Chakrabarti S, Williams TD, Dillman RK, Siahaan TJ. Solution stability of linear vs. cyclic RGD peptides. *J. Pept. Res.* 1999;53(5):530-541.

27. Goeldner M, Givens R. *Dynamic studies in biology : phototriggers, photoswitches and caged biomolecules*. Weinheim: Wiley-VCH; 2005.

28. Goolcharran G, Borchardt RT. Kinetics of Diketopiperazine Formation Using Model Peptides. *J. Pharm. Sci.* 1997;87(3):283-288.

29. Benedetto S, Pulito R, Crich SG, et al. Quantification of the expression level of integrin receptor αVβ3 in cell lines and MR imaging with antibody-coated iron oxide particles. *Magn. Reson. Med.* 2006;56(4):711-716.

30. Dechantsreiter MA, Planker E, Matha B, et al. N-Methylated Cyclic RGD Peptides as Highly Active and Selective alpha(V)beta(3) Integrin Antagonists. *J. Med. Chem.* 07/24/ 1999;42(16):3033-3040.

31. Bowditch RD, Halloran CE, Aota S, et al. Integrin αIIbβ3 (platelet GPIIb-IIIa) recognizes multiple sites in fibronectin. *J. Biol. Chem.* 1991;266(34):23323-23328.

32. Bowditch RD, Hariharan M, Tominna EF, et al. Identification of a novel integrin binding site in fibronectin. *J. Biol. Chem.* 1994;269(14):10856-10863.

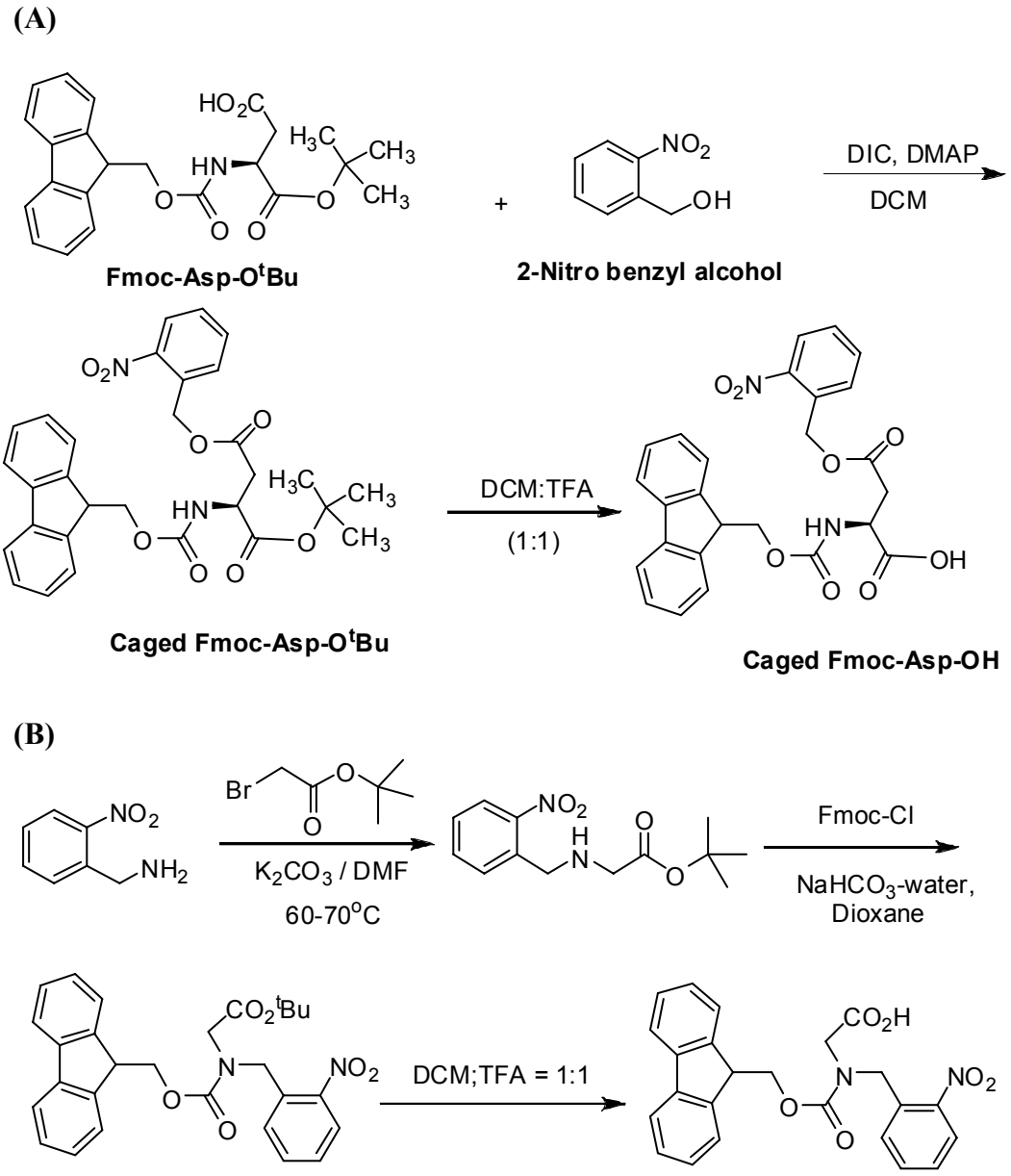

Supplementary Figure 6.1: (A) Synthetic scheme for the preparation of Fmoc 2-nitrobenzyl caged aspartic acid and (B) Fmoc 2-nitrobenzyl caged glycine to be used for incorporation into RGDS peptides.

CHAPTER 7:
NOVEL CELL PATTERNING PLATFORM EMPLOYING PHOTOCAGED RGDS PEPTIDES ON A HYDROGEL

Catherine A. Goubko, Swapan Majumdar, Ajoy Basak, Xudong Cao

AIChE Annual Meeting, Conference Paper
Nashville, TN (2009)

Chapter 7: Novel cell patterning platform employing caged RGDS peptides on a hydrogel

The following work represents a conference paper published for this thesis in the *2009 AIChE Annual Meeting, Conference Proceedings*. The work found in Chapter 8 is built from the work presented in the following. The subject of this work is single cell micropatterning with control experiments to investigate whether cell adhesion to the pattern occurs in an RGD-dependent manner, and the development of a co-culture pattern on an HA hydrogel. In this work, we were able to increase the longevity of our patterning strategy from the paper presented in Chapter 5 (2.5 days to 5 days). This was accomplished by storing gels dehydrated at 4ºC, and using directly after rehydration in 1XPBS. This work demonstrated for the first time that photocaged small adhesive peptides, such as a caged RGDS molecule, could be used to create co-culture patterns, and such patterning could be accomplished on a hydrogel material.

Cell behaviors, including proliferation, differentiation, and migration, are known to be influenced to a large extent by the nature of the surrounding microenvironment. Cell micropatterning platforms provide us with tools to control the spatial localization of cells on biomaterial constructs. To date, the vast majority of cell micropatterning techniques focus on the patterning of a single cell type. However, in order to truly fabricate the highly controlled microenvironments found in multicellular organisms, it becomes necessary to develop simple, accessible techniques to control the spatial localization of multiple cell types on a single construct. Herein we demonstrate our ability to create single cell type and co-culture patterns on a hyaluronic acid hydrogel material using photo-active RGDS peptides. As a proof of concept, NIH 3T3 fibroblasts are shown to adhere to patterned regions over five days, and human umbilical vein endothelial cells (HUVEC) are shown co-patterned with fibroblasts.

7.1 Introduction

In the body, cells grow within carefully defined tissue architectures, and not in the randomly placed fashion realized with traditional cell culture techniques. Studies are showing that the tissue architecture itself can regulate tissue development, maintenance, and function.[1] It is therefore necessary that we continue to develop tools that will enable us to reconstruct important aspects of tissue architecture *in vitro* for implementation in the next generation of cell-based devices. Achieving control over the spatial localization of multiple cell types within a material construct is imperative for such design. By manipulating the properties of patterned co-cultures we can also hope to optimize cell behavior to fit desired applications. For example, liver-specific functions of hepatocytes were optimized for a drug toxicity testing device by employing a patterned co-culture with fibroblasts and varying pattern dimensions.[2] Being able to control the geometry of two cell types relative to one another and in relation to an underlying material offers increased design parameters for optimization when creating cell-based devices.

Figure 7.1 provides an overview of our strategy for patterning two cell types on the same hydrogel surface. The base of our design is a hyaluronic acid (HA) hydrogel. HA is a natural component of the extracellular matrix and, in its native state, it is non-adhesive to cells which can assist in the prevention of off-pattern cell binding. Adhesive RGDS (Arg-Gly-Asp-Ser) peptides bound with a photolabile 2-nitrobenzyl (NB) caging group on the amide of the peptide backbone between the Arg and Gly residues (designated as R[-]GDS in this study) were covalently bound to the hydrogel. The presence of this caging group interferes with the ability of cells to recognize and bind the RGDS sequence. The photolabile cage can be removed upon near-UV light exposure. Patterning of a single cell type was accomplished by shining near-UV light on select regions of the functionalized hydrogel surface through a mask to create a pattern of exposed RGDS peptides on an otherwise cell non-adhesive background. Once the initial cell type was seeded, the non-adhesive background was subsequently switched to become cell adhesive by shining near-UV light over the entire surface. This allowed for the seeding of a second cell type on the patterned surface. Recently, work with caged RGD peptides for cell adhesion control has been documented through a couple of communication studies.[3,4] This work shall examine some

of the details of our patterning strategy and demonstrate how single cell-type patterns and co-culture patterns were developed.

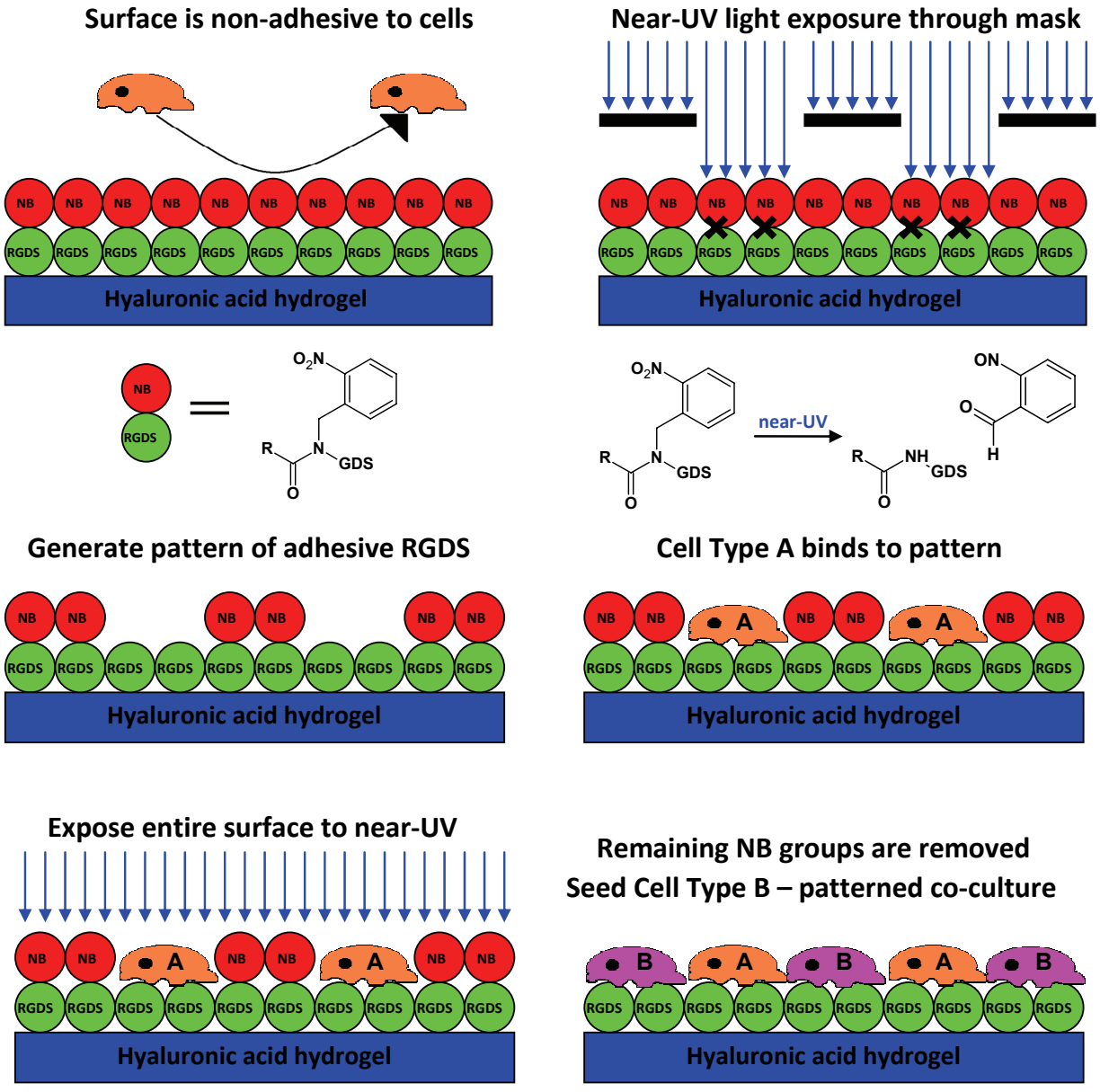

Figure 7.1: Strategy to create a patterned co-culture: RGDS peptides are caged with a photolabile NB group and bound to a HA hydrogel to produce a cell non-adhesive surface. Exposure to near-UV light through a mask selectively removes the NB cage to form a pattern of exposed RGDS peptides to which a cell type, A, can bind. Subsequently, the entire surface can be exposed to near-UV light to remove the remaining NB caging groups and allow the seeding of a second cell type, B.

7.2 Materials and Methods

7.2.1 Preparation of HA Hydrogels with Bound Peptide

A final fermentation-derived 4 mg/mL HA sodium salt solution (Sigma) in sterile distilled water was prepared. A solution of 15 mg adipic acid dihydrazide in 0.5 mL of sterile distilled water was filtered through a 0.45 μm filter and added to 10 mL of aqueous HA solution. The pH was adjusted to 3.5 through the addition of 1 M HCl. Subsequently, 16.5 mg of filtered 1-ethyl-3-(3-dimethylaminopropyl) carbodiimide (EDC) in 1 mL of sterile distilled water was added with vigorous agitation. To the wells of a 12-well polystyrene tissue culture plate, 1.4 mL of the reaction solution was transferred to let set. Gelation was allowed to occur overnight at room temperature. The resulting gels were then washed in sterile phosphate-buffered saline (PBS, pH 7.4) (Invitrogen) for 24 hours with light agitation, followed by a 24 hour wash with sterile distilled water. Gels were then air dried for several days and two more layers of gel were deposited atop the first in the same fashion as that outlined above. Prior to use, gels were rehydrated to equilibrate in sterile PBS (pH 7.4).

RGDS and R[-]GDS peptides were synthesized using solid-phase and liquid-phase peptide chemistry methods, respectively. To bind peptides to the HA gel, a 1 mL solution containing 25 mg/mL EDC and 15 mg/mL N-hydroxysuccinimide (NHS) in 0.1 M 2-(*N*-morpholino) ethanesulfonic acid (MES) buffer was added to each HA gel. The reaction was carried out at room temperature for 15 minutes to activate the HA carboxyl groups for peptide binding. This procedure was repeated twice more. The gels were then washed once in PBS (pH 7.4) to remove unreacted chemical residuals. A solution containing 0.3 mg R[-]GDS or an equimolar quantity of RGDS in 0.1 M MES was subsequently added to the gels and allowed to react for 2 hours, after which the gels were washed in PBS overnight.

7.2.2 Photolysis

Near-UV light from a 365 nm Longwave UV Lamp (Black-Ray B-100 Longwave UV lamp, 100 W) was used in all UV irradiation experiments. All samples were irradiated on a platform 10 cm from the light source. For single cell type patterning experiments, gels

containing bound R[-]GDS were covered with a patterned mask and irradiated for 12 minutes. Following exposure, gels were rinsed with PBS and sterilized with 70% ethanol. To pattern a second cell type, the entire single cell type patterned surface (two days post 3T3 cell seeding) was irradiated for 12 minutes in PBS (pH 7.4) followed by washing with cell culture media.

7.2.3 Cell Culture

NIH 3T3 fibroblast cells (3T3s) and human umbilical vein endothelial cells (HUVECs) were seeded on the experimental surfaces. 3T3 cells were routinely maintained in medium containing Dulbecco's Modified Eagle's Medium (DMEM) supplemented with 10% fetal bovine serum (FBS), 100 U/mL Penicillin (Invitrogen), and 0.1 mg/mL Streptomycin. HUVECs and media were kindly provided by Dr. Suuronen at the Ottawa Health Research Institute. Both cell lines were kept in T-75 flasks at 37˚C in a humidified environment containing 5% CO_2. Prior to cell seeding on the experimental surfaces, cells were trypsinized, centrifuged to a pellet, re-suspended in culture medium and counted using a hemacytometer. 3T3 cells were subsequently seeded onto the experimental surfaces at a density of $1X10^4$ cells/cm^2 and HUVECs at $5X10^4$ cells/cm^2. For peptide incubation studies, cells were seeded with 1 mg/mL soluble RGDS peptide. Live/dead cell counts were performed using trypan blue staining followed by a hemacytometer count. CellTracker^{TM} Red CMTPX and Green BODIPY (Invitrogen) were used to label the fibroblasts and HUVECs, respectively, according to the vendor's protocol. Cultures were examined using an inverted phase contrast and fluorescence microscope (Olympus IX81 F), and the observations were documented using Image-Pro Plus (Media Cybernetics).

7.3 Results and Discussion

The base of our cell patterning platform consists of a HA hydrogel crosslinked with adipic acid dihydrazide. Cell culture studies demonstrated that 3T3 fibroblasts could not adhere to this material. RGDS peptides were subsequently bound to the material to create an adhesive layer; after this modification, 3T3 fibroblasts were found to adhere and spread on the HA-RGDS material. Next, NB caging groups were bound to the RGDS peptides and then covalently bound to the hydrogel to create a photo-responsive material, HA-R[-]GDS. As

hypothesized, cells were unable to bind to the HA-R[-]GDS material. However, near-UV light exposure rendered the HA-R[-]GDS adhesive to the fibroblasts which was thought to be due to the removal of the photolabile NB caging groups to reveal freed adhesive RGDS peptides on the gel surface. These studies on homogenous surfaces suggested that the developed HA-R[-]GDS platform could indeed be manipulated to form cell patterns.[5]

It was necessary to demonstrate that the adherence of cells to the HA-R[-]GDS surface exposed to near-UV light (denoted HA-R[-]GDS-UV) was due to cell recognition of an uncaged RGDS peptide and not some other alteration to the surface brought on by near-UV light exposure. The RGDS sequence is an epitope of the extracellular matrix protein fibronectin, and cells recognize and bind to it through integrin receptors located on their surfaces. If cell binding to the HA-R[-]GDS-UV surface is RGDS-integrin mediated, then free RGDS peptides in solution should be able to compete with the uncaged RGDS bound to the underlying gel. These free peptides should adhere to integrin receptors to decrease cell adhesion to the gel. As a control, we seeded cells on an HA-RGDS surface in the presence or absence of free RGDS peptides. As predicted, cells did not adhere significantly to the surface in the presence of 1 mg/mL free RGDS peptides, while they bound readily in the absence of free peptide. Note that on non-RGDS containing surfaces such as tissue culture plates, cells were shown to adhere regardless of the presence of free RGDS peptide in the media since binding could occur in a non-RGD dependent fashion (results not shown). Cells were shown not to bind to the HA-R[-]GDS-UV surfaces in the presence of 1 mg/mL free RGDS peptide, while they were shown to bind in the absence of these peptides (Figure 7.2). This served as an indication that binding to our experimental cell patterning surfaces was indeed mediated specifically by uncaged RGDS presented on the gel and not any other factors introduced by the near-UV light exposure.

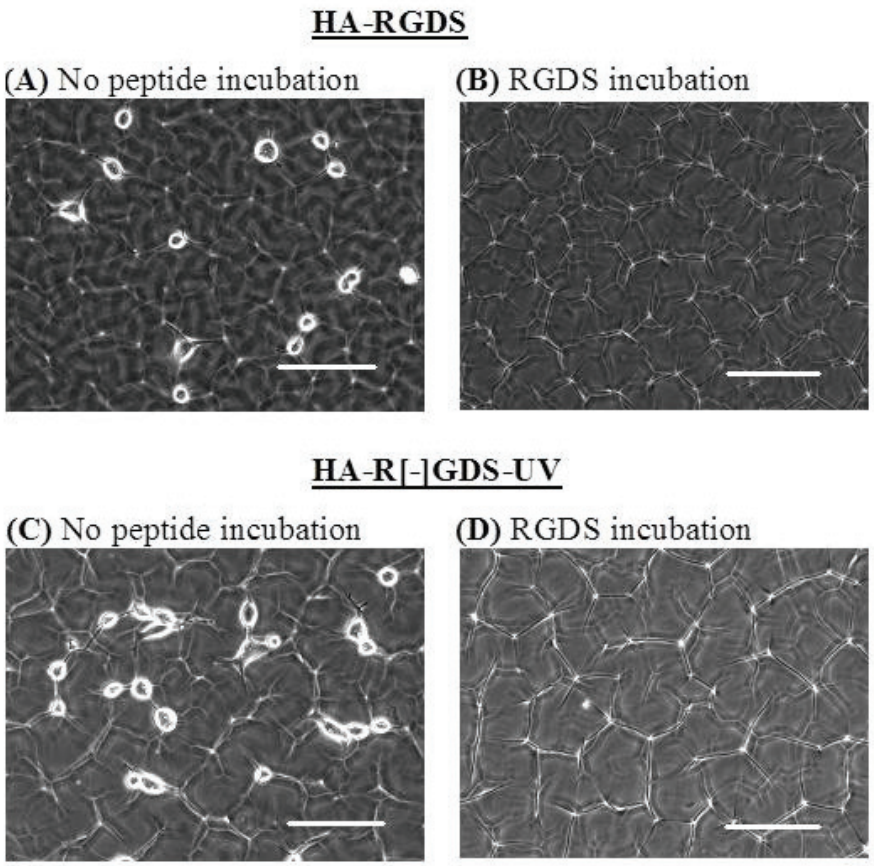

(E)

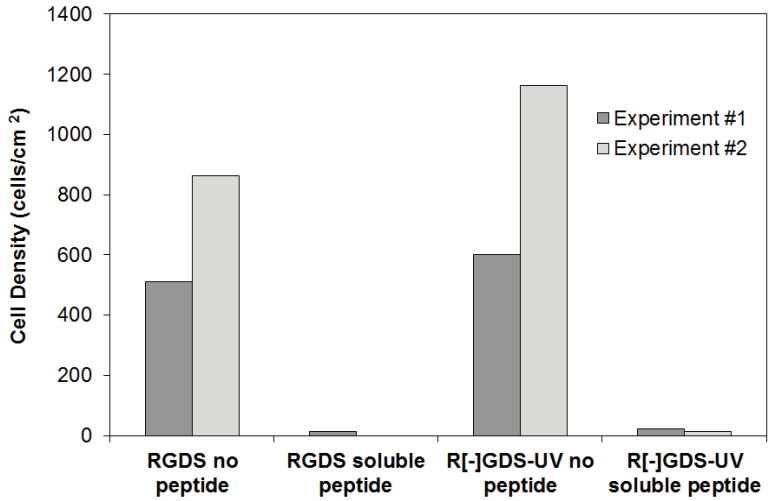

Figure 7.2: (A) Phase contrast images of 3T3s on an HA-RGDS surface two hours post seeding in the absence of soluble RGDS peptide and **(B)** in the presence of 1 mg/mL soluble RGDS peptide. **(C)** 3T3s on an HA-R[-]GDS surface irradiated with near-UV light two hours post seeding in the absence of soluble RGDS peptide and **(D)** in the presence of 1 mg/mL soluble RGDS peptide. **(E)** Cell densities two hours post seeding, n=2 (where "no peptide" indicates no soluble RGDS peptide present during cell seeding on the indicated functionalized HA surface). Scale bars = 100 μm.

The HA-R[-]GDS surfaces developed were patterned by exposing the surface to near-UV light through a line-patterned mask. 3T3 fibroblasts were subsequently seeded on the surface and were found to adhere to the pattern over five days as shown in Figure 7.3. By the fifth day, fibroblasts had reached confluence on the pattern and were beginning to peel off in confluent cell sheets. Our experience has shown that some cells typically remain after peeling and can repopulate the surface. We have created a number of other cell patterns of differing shapes and dimensions with 3T3s (results not shown). With the ability to create patterns of a single cell type on our hydrogel surface established, it was desired to pattern a second cell type on the same surface. To achieve this, we exposed a whole 3T3 fibroblast-patterned surface to near-UV light to render the non-adhesive regions of the pattern adhesive. UV light is known to damage cells; however near-UV light at wavelengths above 300 nm, such as that used in this study (~365 nm) is considered less likely be absorbed and thus cause damage to biological systems.[6] Nevertheless, 3T3s were exposed to near-UV light under the same conditions as the co-culture experiments for various amounts of time and live/dead cell counts were performed one hour and three days after exposure to see if there was an observable effect on cell survivability and proliferation.

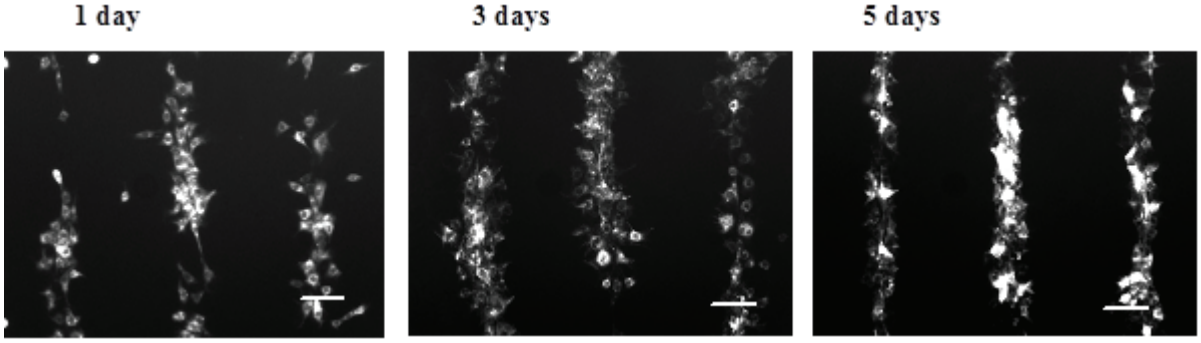

Figure 7.3: Fluorescence micrographs depicting line patterns of 3T3 fibroblasts dyed with CellTracker™ Red and grown on a HA hydrogel bound with patterned caged and uncaged R[-]GDS peptide over five days post seeding. Scale bars = 100 μm.

Results in Figure 7.4 show that for the near-UV light exposure conditions investigated, no detrimental effects on 3T3 cell survival or proliferation were seen. Therefore, the 3T3 cell pattern seen in Figure 7.5(A) was exposed to near-UV light and immediately afterwards, HUVECs were seeded onto the surface where they began to adhere around the original 3T3 cells to create a patterned co-culture. Figures 7.5(B)-(E) show the co-culture at various times after near-UV light exposure and seeding of the HUVECs. It can be seen that after one day, the cell pattern is becoming disorganized. Since the second near-UV irradiation step exposed the entire surface to light, the entire hydrogel surface is expected to be rendered cell-adhesive. Therefore, there is no longer a pattern of cell non-adhesive regions which allows the cells to freely migrate over the entire hydrogel and off the original single-cell pattern.

We are currently working towards improving this co-culture strategy. It is desired to obtain an increased amount of control over the positioning of the second cell type seeded. With our current approach, this second cell type is limited to adhering around the initially seeded cells. By aligning a second mask to the original cell pattern, or using another technology to control the location of light exposure on the surface, we could create a unique pattern for the spatial localization of the second cell type. By repeating this process, it is theoretically possible to seed more than just two cell types. Furthermore, by only exposing select non-adhesive regions of the hydrogel to near-UV light for the seeding of a second cell type, we can better ensure the protection of the initially seeded cells. While our initial experiments suggest that cell viability is not impacted by the light exposure, more in-depth work would be needed to ensure that other aspects of cell behavior are not affected by the light exposure using our current cell co-culture patterning strategy.

(A)

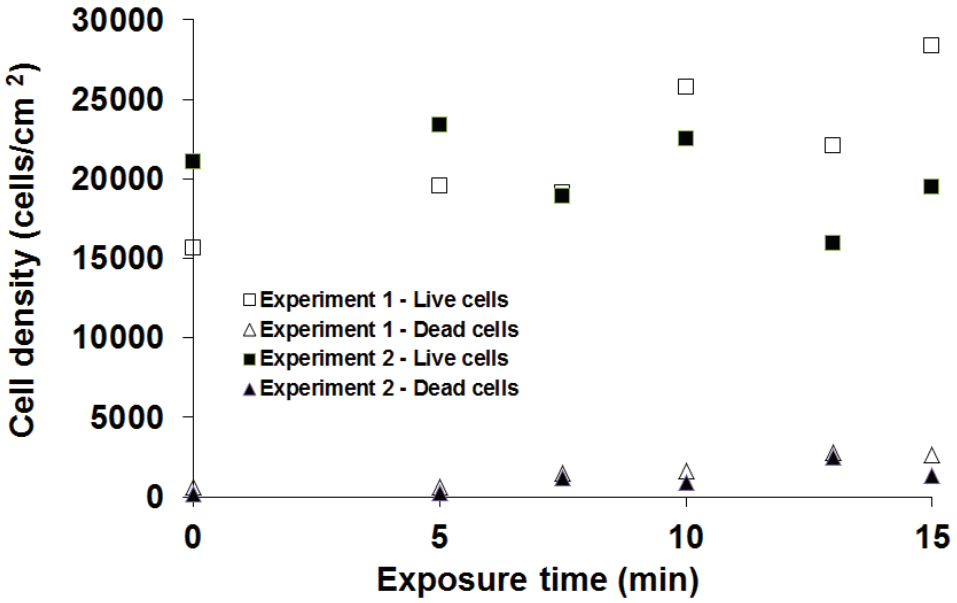

(B)

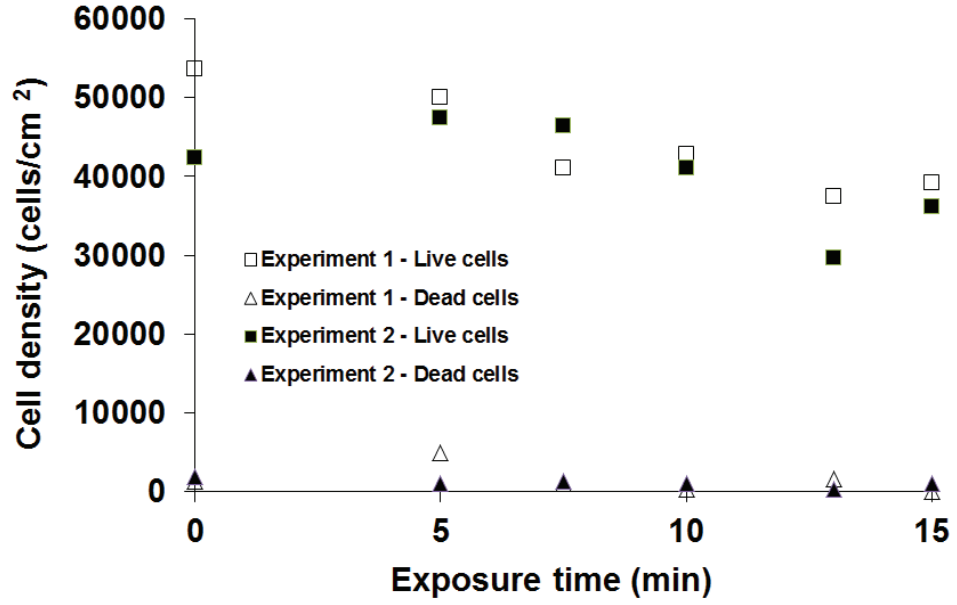

Figure 7.4: (A) 3T3 cell density on the surface of 12-well plates one hour post near-UV exposure versus near-UV exposure time (n=2). **(B)** 3T3 cell density on the surface of 12-well plates three days post near-UV exposure versus near-UV exposure time (n=2).

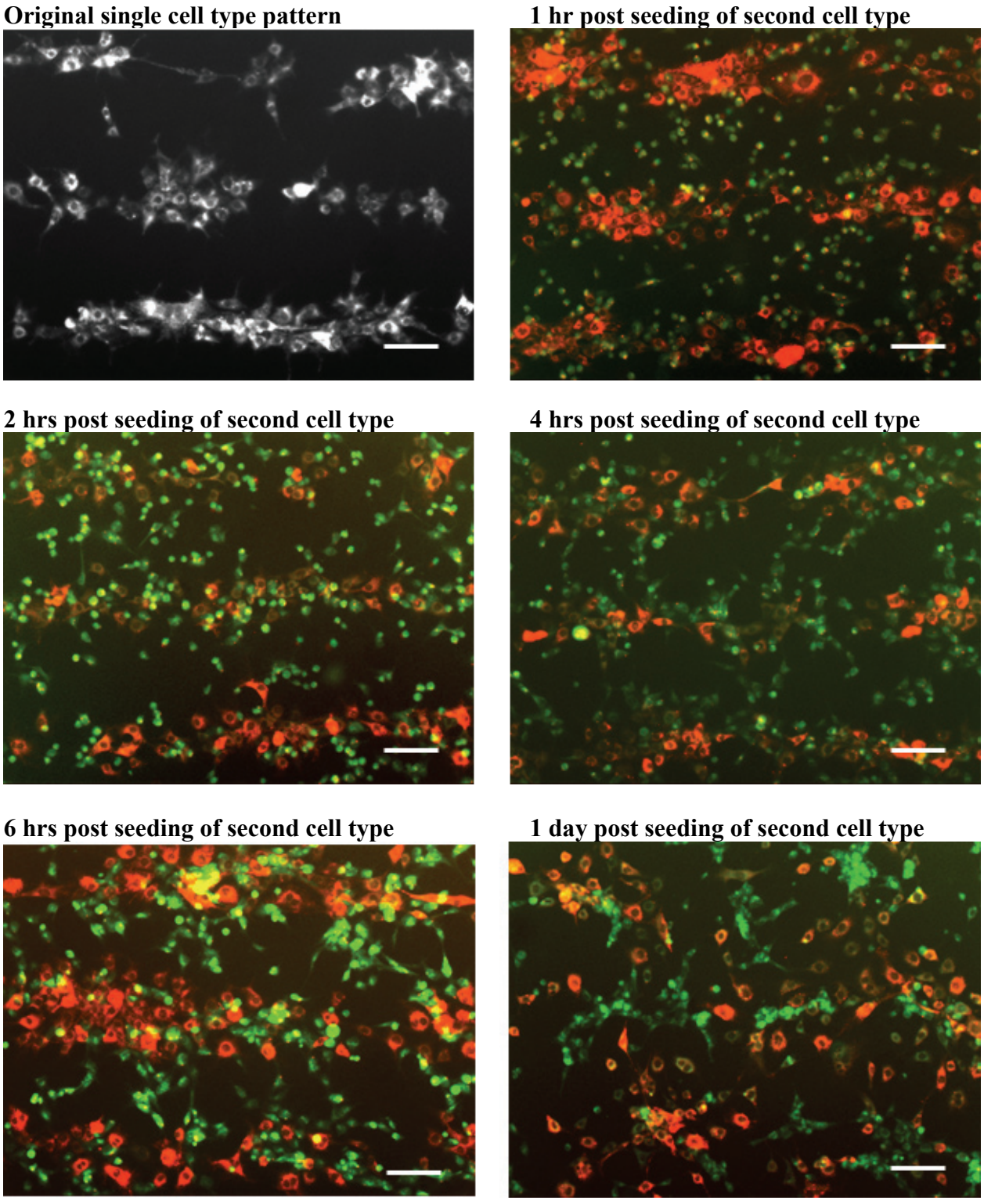

Figure 7.5: Fluorescence micrographs of the original pattern of 3T3 fibroblasts prior to the seeding of HUVECs and patterned co-culture of 3T3s (red) and HUVECs (green) at various indicated times post-seeding of the HUVECs. Scale bars = 100 μm.

One great advantage of our cell patterning strategy is that it is based on biocompatible materials. HA, which forms the base of our pattern, can be found naturally in almost all body fluids and tissues, and has been used extensively in the design of tissue engineered devices.[7,8] The RGD amino acid sequence can be found in a number of proteins naturally mediating cell adhesion.[9] Though the NB caging molecule is synthetic, caging groups have been bound to a number of naturally occurring molecules which have been subsequently and successfully uncaged within biological systems for experimentation into temporal biological phenomena.[10] Due to the inherent biocompatibility of the components of our cell patterning platform, our strategy is well adapted for use in tissue engineering or for highly controlled studies in cell biology. To be able to control the spatial localization of multiple cell types in a hydrogel is an exciting tool that could lead to optimization of cell behavior through controlled cell placement and controlled interactions between cell types within a material suitable for tissue engineering. In the future, we will be looking towards new light sources for uncaging, such as a two-photon laser. It has the potential to uncage peptides in three dimensions, which could form the basis of a three dimensional patterning platform, a truly powerful tissue engineering tool. We are also working towards using our 2-D hydrogel patterned surfaces as platforms to study interactions between biologically relevant pairs of cell types. Such a biocompatible platform with the ability to spatially localize multiple cell types can allow for studies to be conducted with a much higher degree of control than that obtained with traditional cell culture where cells are randomly seeded on a surface.

7.4 Conclusions

We have developed a cell patterning platform employing photocaged RGDS peptides on a hyaluronic acid hydrogel with the capability to pattern a single cell type up to five days, and the flexibility to pattern multiple cell types on the same surface. This strategy holds great promise for more controlled studies in cell biology and future applications in tissue engineering.

7.5 References

1. Rivron NC, Rouwkema J, Truckenmüller R, Karperien M, De Boer J, Van Blitterswijk CA. Tissue assembly and organization: Developmental mechanisms in microfabricated tissues. *Biomaterials.* 2009;30(28):4851-4858.

2. Khetani SR, Bhatia SN. Microscale culture of human liver cells for drug development. *Nat Biotech.* 2008;26(1):120-126.

3. Petersen S, Alonso JM, Specht A, Duodu P, Goeldner M, del Campo A. Phototriggering of Cell Adhesion by Caged Cyclic RGD Peptides. *Angewandte Chemie International Edition.* 2008;47(17):3192-3195.

4. Ohmuro-Matsuyama Y, Tatsu Y. Photocontrolled Cell Adhesion on a Surface Functionalized with a Caged Arginine-Glycine-Aspartate Peptide. *Angewandte Chemie International Edition.* 2008;47(39):7527-7529.

5. Goubko C, Majumdar S, Basak A, Cao X. Hydrogel cell patterning incorporating photocaged RGDS peptides. *Biomedical Microdevices.* 2010;12(3):555-568.

6. Pelliccioli AP, Wirz J. Photoremovable protecting groups: Reaction mechanisms and applications *Photochemical and Photobiological Sciences.* 2002;1(7):441-458

7. Collins M, Birkinshaw C. Comparison of the effectiveness of four different crosslinking agents with hyaluronic acid hydrogel films for tissue-culture applications. *Journal of Applied Polymer Science.* 2007;104(5):3183-3191.

8. Allison DD, Grande-Allen KJ. Review. Hyaluronan: A Powerful Tissue Engineering Tool. *Journal of Histochemistry and Cytochemistry.* 2006;12(8):2131-2140.

9. Hersel U, Dahmen C, Kessler H. RGD modified polymers: biomaterials for stimulated cell adhesion and beyond. *Biomaterials.* 2003;24(24):4385-4415.

10. Shigeri Y, Tatsu Y, Yumoto N. Synthesis and application of caged peptides and proteins. *Pharmacol. Ther.* 2001;91(2):85-92.

CHAPTER 8:
DYNAMIC CELL PATTERNING OF PHOTORESPONSIVE HYALURONIC ACID HYDROGELS

Catherine A. Goubko, Ajoy Basak, Swapan Majumdar, Xudong Cao

Reprinted with kind permission from John Wiley and Sons
Journal of Biomedical Materials Research - Part A
Article in press (2013), published online May 2013

The following paper represents the third full length research paper published for this thesis. This work follows from that presented in Chapters 6 and 7. In Chapter 6, it was found that R[-]GDS peptides, in comparison to RG[D]S peptides, showed the greatest difference in binding energy to $\alpha_V\beta_3$ integrin receptors between their pre- and post-irradiation states. This property is very important in patterning as it will influence the difference in the ability of cells to bind to patterned adhesive vs. non-adhesive regions. However, in this work, it was desired that cell patterns be maintained over a period of weeks, and it was found previously that R[-]GDS can degrade due to hydrolysis with the proposed degradation scheme shown in Figure 6.4. This scheme depends on a flexible peptide possessing a free terminal amine group. Our cell patterning strategy binds the peptide's terminal amine group to an HA hydrogel base, so it is not free, and because the peptide is bound directly to the hydrogel, it has limited flexibility. Because of these factors, degradation should be less likely when the R[-]GDS peptide is bound to the hydrogel. For these reasons, it was decided to continue with R[-]GDS peptides for the cell patterning work in this chapter.

In Chapter 7, preliminary experiments using soluble RGDS peptides were performed to ensure that cell adhesion to the hydrogels was the result of biospecific interactions between cell integrin receptors and the RGDS sequence. Further experiments were conducted in this work using control RGES peptides to provide more conclusive evidence. Experiments were also performed to examine the quantity of peptide binding to HA hydrogels, and attempts were made to increase binding.

Therefore, in Chapter 8, we have developed and enhanced a hydrogel cell patterning strategy based on photoactive caged RGDS peptides incorporated into a HA hydrogel, which can be subsequently activated with near-UV light to create cell-adhesive regions within an otherwise non-adhesive hydrogel. Furthermore, with this strategy, we have been able to pattern multiple cell populations - either in contact with one another or held apart - on an underlying chemically patterned HA hydrogel. The hydrogel cell pattern could be altered with time, even two weeks after initial seeding, to create additional adhesive regions to regulate the direction of cell growth and migration. These dynamic hydrogel cell patterns,

created with a standard fluorescence microscope, were shown to be robust and lasted at least three weeks *in vitro*.

Overall this work is novel in its development of a method to chemically pattern cells on a hydrogel material, using photocaged small adhesive peptides (i.e. RGDS), such that multiple cell populations can be patterned on this same hydrogel and cell patterns can be spatio/temporally controlled so that additional adhesive regions can be created at desired times on the cell-seeded material to control cell growth and/or migration.

8.1 Introduction

The ability to pattern cells on biocompatible materials is an exciting tool for the development and optimization of devices for tissue engineering and biological research. In the body, cells are organized into complex tissue architectures, and not in a random fashion as achieved with traditional cell culture. In order to study and then reproduce these architectures for tissue engineering applications, it is necessary to develop techniques that can spatially localize or "pattern" multiple cell populations. Additionally, in the development of tissues and organs, the microenvironment surrounding the cells evolves with time. Therefore it is of great interest to develop cell patterning techniques that are dynamic and can thus be manipulated temporally to better replicate such events.[1]

Of the materials investigated for applications in tissue engineering, hydrogels are especially attractive due to their high water content in addition to their ideal mechanical and chemical properties mimicking those of body tissues.[2] Hydrogels consisting of hyaluronic acid (HA), a natural biocompatible material, have generated great interest for use in tissue repair applications.[3] HA is an immunoneutral polysaccharide found throughout the human body, and has been used in commercial medical applications since the 1960s.[4] It is a natural choice for use as a base in cell patterning applications, since it is characteristically non-adhesive in its native form, which is beneficial to prevent cells from binding off-pattern.

Various techniques have been explored to generate cell patterns within or on hydrogels including soft lithography methods[5] such as micromoulding,[6] microcontact printing,[7] soft embossing,[8] and microfluidics,[9] which has even been used to create co-culture patterns.[10-12] In addition, methods using laser printing[13] and inkjet printing[14] have deposited cells directly onto gels in a systematic manner. Techniques inspired by photolithography have generated patterned polyethylene glycol (PEG) hydrogel structures with encapsulated cells.[15,16] Additionally, some creative patterning strategies involving layer-by-layer hydrogel deposition techniques[17] and stereolithography[18,19] among others,[20,21] have formed patterned co-cultures in a hydrogel.

Many patterning techniques employ external stimuli such as electric fields[22] or temperature changes[23] to generate the cell patterns. Photopatterning harnesses light to create cell-adhesive regions on hydrogels. Light can be controlled both spatially and temporally with high precision and resolution using sources, such as lasers, making it an ideal choice for pattern generation. Light-controlled biomolecule patterning techniques have created static 3D hydrogel cell patterns.[24-28] Dynamic patterns have also been created with light to spatially pattern a biomolecule in a hydrogel which could be subsequently and selectively removed.[29]

In this work, we combined a HA hydrogel with photocaged RGDS peptides to generate a dynamic patterned hydrogel which can be altered with time to support multiple cell populations or guide cell growth and migration. Figure 8.1 summarizes our strategy. The base material is a crosslinked and cell non-adhesive HA hydrogel that can be rendered cell adhesive by conjugation with RGDS peptides. However, the peptides covalently linked to the gel were caged via a 2-nitrobenzyl group (2-NB) bound to the nitrogen atom of the Arg-Gly peptide backbone (referred to as R[-]GDS herein) to render the RGDS sequence unrecognizable to cell-surface integrin receptors therefore preventing cell binding. The 2-NB group has been used extensively in biological systems and has demonstrated compatibility with fragile biomolecules such as DNA and proteins.[2] In fact, the 2-NB group is the most commonly used caging group for caging biomolecules primarily due to ease of synthesis and ease of binding to target molecules, such as peptides.[30] Patterned cell adhesive regions were

created on the otherwise non-adhesive HA-R[-]GDS hydrogel material by exposing selected areas to near-UV light to remove the caging group. This was accomplished in one of the following two ways – using a patterned photomask or a standard fluorescence microscope with a UV filter focused on selected areas of the hydrogel. Subsequent light exposures using a UV lamp or the microscope allow for the patterns to be changed with time creating additional adhesive regions to seed multiple cell populations or guide cell growth and migration of the original cell population.

To date, there is a lack of techniques capable of patterning hydrogels in a dynamic manner to achieve patterns that can change with time and can spatially localize multiple cell populations. The development of such techniques brings us closer to better mimicking *in vivo* tissue properties in research laboratories for advanced cell biology studies with the hope of future translation into optimized tissue engineering devices for implantation with control over cell positioning, migration, and growth. In previous work, pioneers in caging RGDS to control cell adhesion, Petersen et al. and Ohmuro-Matsuyama and Tatsu created single cell patterns on solid surfaces over one day in culture.[31,32] Recently, we created a static pattern of cells on a hydrogel for up to 2.5 days based on caged RGDS peptides.[33] In this work, we have further advanced our hydrogel patterning strategy such that we can create a patterned co-culture and other dynamic patterns on a HA hydrogel that last several weeks in culture demonstrating the great versatility and relevance of this technique in the growing field of hydrogel cell patterning.

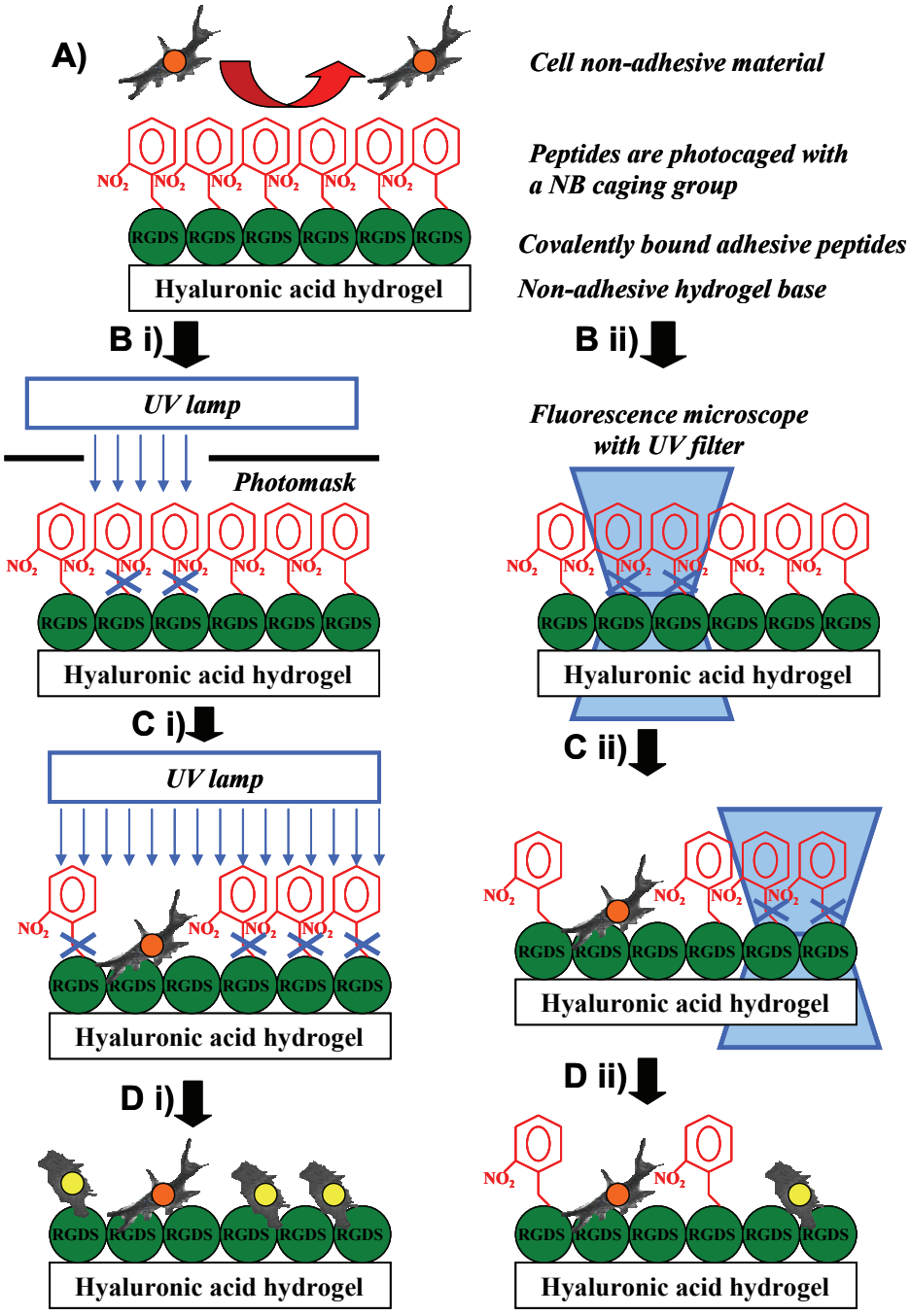

Figure 8.1: Hyaluronic acid hydrogel patterning strategy. **(A)** RGDS is covalently bound to a HA hydrogel but is photocaged to prevent cell recognition and binding to the hydrogel. **(Bi)** The 2-NB caging group is removed from selective regions of the hydrogel via light from a UV lamp through a photomask or **(Bii)** via light focused with a fluorescence microscope through a UV filter. Cells are able to adhere to the newly exposed RGDS regions and additional cell adherent regions are created by either **(Ci)** exposing the entire hydrogel under a near-UV lamp or **(Cii)** exposing select regions identified and then focused on with the fluorescence microscope which results in **(Di)** a co-culture pattern with the entire hydrogel surface rendered adhesive or **(Dii)** a pattern that can be changed with time with only select adhesive regions on an otherwise non-adhesive gel.

8.2 Materials and Methods

8.2.1 Preparation of HA Hydrogels

Hyaluronic acid sodium salt produced via fermentation (purchased from Sigma Aldrich, St. Louis, MO) was dissolved in sterile distilled water to a final solution concentration of 4 mg/mL and allowed to mix overnight. For crosslinking, a filtered (0.45 μm pore size) solution of adipic acid dihydrazide (ADH, 15 mg) in 0.5 mL of sterile distilled water was added to 10 mL of aqueous HA solution which was subsequently adjusted to pH 3.5 with 1 M HCl and cooled on ice to prevent premature crosslinking. This was followed by the addition of 16.5 mg of filtered 1-ethyl-3-(3-dimethylaminopropyl) carbodiimide (EDC) in 1 mL of sterile distilled water with vigorous agitation. To the wells of a 12-well polystyrene tissue culture plate (TCP), 1.4 mL of the resulting reaction solution was transferred to let set. Gelation was allowed to occur overnight at room temperature. The resulting gels were then washed in sterile phosphate-buffered saline (PBS) solution at pH 7.4 (Invitrogen) for 24 h with light agitation, followed by a 24 h wash with sterile distilled water. This initial HA layer was air dried for several days and prior to use, gels were rehydrated to equilibrate in sterile PBS buffer (pH 7.4). Three hydrogel layers were created for all experiments except for those involving patterning with the fluorescence microscope, which involved a single hydrogel layer to limit light scattering through the hydrogel. For cell culture experiments, gels were soaked in 70% aqueous ethanol for at least 30 min for sterilization.

8.2.2 Peptide Synthesis

Caged RGDS and RGES peptides (denoted as R[-]GDS and R[-]GES, respectively) were synthesized via a liquid phase route as described previously.[34] RGDS and RGES peptides were prepared by automated solid phase chemistry using an Intavis AG Bioanalytical Multipep Instrument with normal HATU/DIEA mediated Fmoc chemistry as described earlier.[35]

8.2.3 Peptide Binding

To bind peptides to the HA gel, a solution consisting of 25 mg/mL EDC and 15 mg/mL N-hydroxysuccinimide (NHS) (Pierce) in 0.1 M 2-(*N*-morpholino) ethanesulfonic

acid (MES) buffer was prepared. Subsequently, 1 mL of this solution was added to each HA gel in wells of a 12-well plate at room temperature for 15 minutes to activate the HA carboxyl groups for peptide coupling. The gels were then washed once in PBS (pH 7.4) to remove unreacted material. The desired peptide solution was subsequently added to the gels and allowed to react for 2 h. The peptide analysis study used 0.1 mg (0.17 μmol) of R[-]GES per gel (i.e. 26μg/cm^2). The quantity of all other peptides used in the peptide analysis study was equivalent to the molar quantity of R[-]GES added to the gels (i.e. 0.17 μmol). For other studies, 0.25 mg of R[-]GDS per hydrogel (i.e. 66μg/cm^2) was used. Finally, the resulting gels were washed in PBS (pH 7.4) overnight.

8.2.4 Analysis of Bound Peptide

A standard curve of caged R[-]GDS absorption at 300 nm versus concentration was determined and a linear relationship identified. The initial and final concentrations of caged R[-]GDS in solution before and after immobilization were determined using this relationship. Concentrations of R[-]GDS in three subsequent overnight wash steps were also determined. The subtraction of the peptide known to have washed off the hydrogel minus the initial amount of peptide was found and expressed as a percentage of the original caged R[-]GDS solution.

8.2.5 Light Exposure

Unless otherwise mentioned, exposure at 365 nm from a long wave UV Lamp (Black-Ray B-100 Longwave UV lamp, 100W, UVP, Upland, CA) was employed for photolysis of caged R[-]GDS and R[-]GES peptides. Samples were irradiated 10 cm from the light source to produce an intensity of ~7 mW/cm^2 as measured by a radiometer. For experiments where a fluorescence microscope was indicated as the source of radiation, an Olympus IX81 F microscope was used with Olympus U-N31013-FL Filter Cube which emits excitation light at a wavelength of 365 nm. By adjusting the size of the iris at the field diaphragm in the fluorescent light path, the area of the hydrogel sample exposed to this near-UV light could be controlled.

8.2.6 Cell Culture

In this study, NIH 3T3 fibroblasts (3T3s) were used as model adherent cells. The cells were routinely maintained in medium containing Dulbecco's Modified Eagle's Medium (DMEM) supplemented with 10% fetal bovine serum (FBS), 100 U/mL Penicillin, and 0.1 mg/mL Streptomycin. Human umbilical vein endothelial cells (HUVEC) and media (Medium 199 with 10% FBS, 1% L-glutamine, 2 μg/mL sodium heparin, 1% Penicillin/Streptomycin, 30 μg/mL Endothelial Growth Supplement, pH 7.2) used in co-culture studies were kindly provided as a gift by Dr. Suuronen at the Ottawa Health Research Institute. Both cell types were kept in T-75 flasks at 37˚C in a humidified environment containing 5% CO_2, and prior to cell seeding on the experimental surfaces, cells were trypsinized, centrifuged to a pellet, re-suspended in culture medium and counted using a hemocytometer. 3T3s were subsequently seeded onto the experimental surfaces at a density ~ $1X10^4$ cells/cm^2, and for co-culture studies, HUVEC at ~ $5X10^4$ cells/cm^2. In 3T3 and HUVEC co-culture studies, the co-culture was maintained in HUVEC cell culture media. Unless otherwise stated, cells plated onto the experimental surfaces were initially maintained for 12 h, after which the surfaces were gently (and carefully) washed with fresh media to remove non-adherent cells. Cultures were examined using an inverted phase contrast and fluorescence microscope (Olympus 1X81 F), and observations were documented using Image-Pro Plus (Media Cybernetics, Silver Spring, MD).

CellTracker™ Red CMTPX and Green CMFDA (Invitrogen) were used to label cells in this study according to the vendor's protocol. Briefly, a 10 mM stock solution of the dye in DMSO was prepared and subsequently dissolved in DMEM to produce a 2.5 μM working solution. Adherent cells were incubated for 45 minutes at 37ºC before removing the staining solution and replacing it with fresh media for 30 minute at 37ºC. Cells were then washed in PBS (pH 7.4) followed by incubation in fresh media.

Live/dead staining was carried out with the Invitrogen Live/Dead Viability/Cytotoxicity Kit for mammalian cells (L3224) according to vendor's protocol. Briefly, a working solution containing 1 μM calcein AM and 2 μM ethidium homodimer in serum-free DMEM was prepared and 1 mL was added to each well containing hydrogel in a

12-well plate and allowed to incubate for 30 minutes at 37°C followed by washing and addition of cell culture media.

Cells were counted by staining nuclei with Hoechst (Invitrogen, 34580). The number of adherent cells per sample was determined by counting cells in 9 fields of view per sample and taking the average.

MTT assays were conducted as a measure of cellular metabolic activity, and were carried out using a Molecular Probes Vybrant® MTT Cell Proliferation Assay Kit (V13154) as per product instructions. Briefly, 12 mM stock solutions of MTT in sterile 1XPBS buffer were prepared, and 500 μL of 10% (v/v) MTT in clear media (no phenol red) was added to each well in 12-well TCPs containing 3T3 cells and allowed to incubate for 4 h at 37°C. Afterwards, media was removed and 1 mL DMSO was added to each well and incubated at 37°C for 15 minutes followed by mixing until crystals were fully dissolved. A plate reader measured absorbance at 540 nm.

8.3 Results and Discussion

8.3.1 Peptide Analysis

Our cell patterning strategy was designed to make use of the biospecific interaction between cell integrin receptors and the RGDS sequence to control cell adhesion. Our previous study demonstrated that cells adhere well to our HA-RGDS hydrogels.[33] Therefore, in this study we sought to verify that these specific interactions were the predominant mechanism behind cell binding. In Figures 8.2A-B, it can be seen that 3T3 fibroblast cells did not adhere to the crosslinked HA hydrogel when there was no RGDS peptide bound even after near-UV light irradiation. Therefore, light exposure did not alter the base gel's adhesive properties towards the cells. In addition, it was shown that cells failed to bind to the control hydrogel bound with R[-]GDS peptide, but did bind after near-UV irradiation (that serves to uncage R[-]GDS) which is the main principle for this patterning methodology.

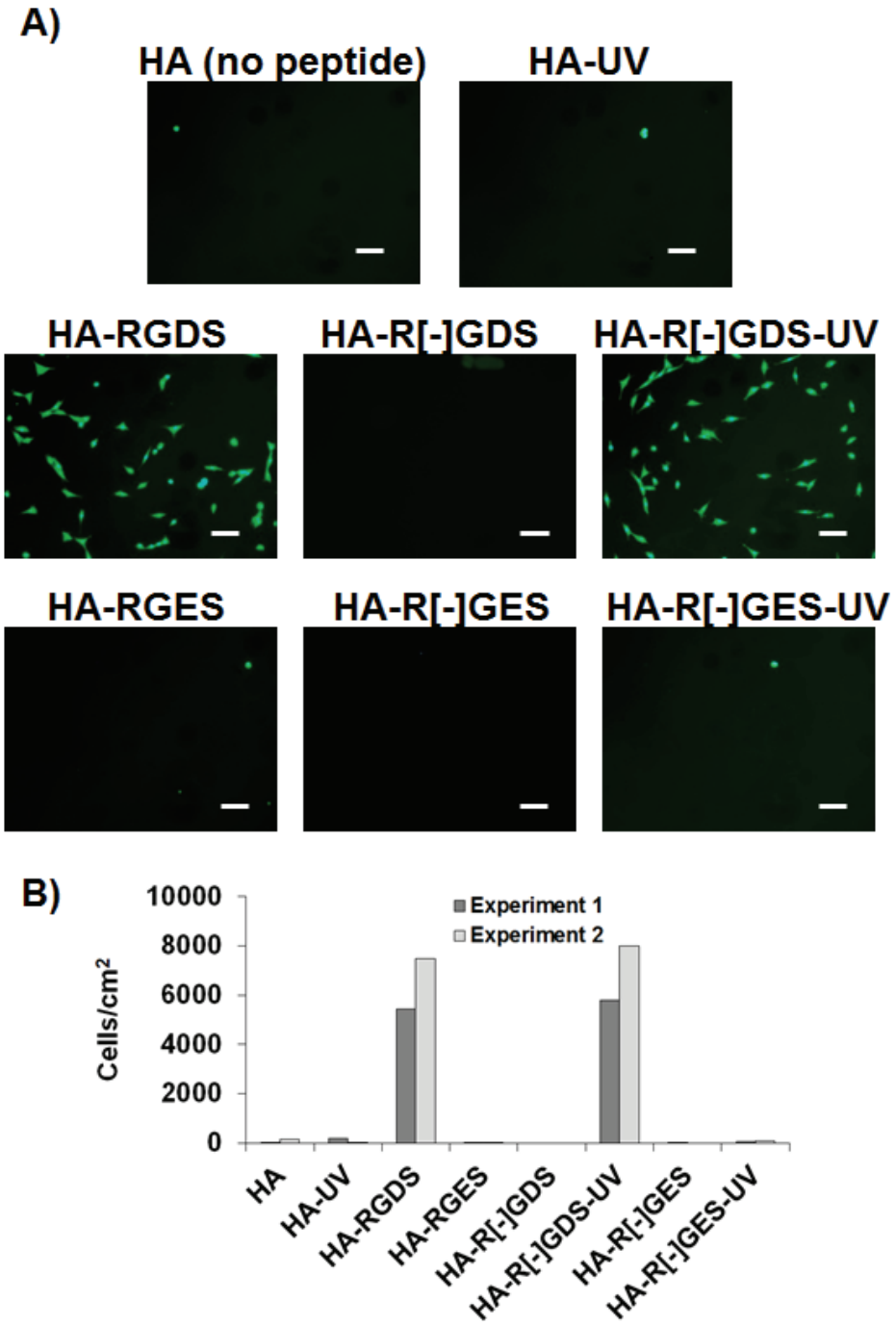

Figure 8.2: (A) Fluorescence micrographs 12 hours post seeding of 3T3 fibroblast cells dyed with live (Calcein AM, green) /dead (Ethidium homodimer, red) stain, and Hoechst bound to the HA hydrogels with or without bound peptide or exposure to near-UV light as indicated. Scale bars equal 100 μm. **(B)** Density of cells adhering to the various HA hydrogel samples 12 h post seeding (n=2).

To examine the possibility that cell binding to the irradiated HA-R[-]GDS sample was the result of changes to hydrogel surface chemistry after light exposure and not specific uncaged RGDS-integrin interactions, experiments with RGES were carried out. The peptide sequence RGES differs from RGDS in having only one additional methyl group on the side chain of an amino acid, so bound surface chemistries are essentially identical. However, changing the Asp (D) to Glu (E) is known to abolish the cell adhesive properties of the RGDS sequence.[36] Therefore, RGES and a photocaged RGES (i.e. R[-]GES) with 2-NB bound to the same functional group as the photocaged R[-]GDS were synthesized. Figure 8.2A shows that RGES bound to the hydrogel did indeed fail to promote cell adhesion, and similarly cells failed to bind to photocaged R[-]GES. After irradiating the photocaged R[-]GES, cells still failed to bind, which strongly suggested that cell binding is the result of specific interactions between cell surface receptors and the RGDS sequence itself and not changes in non-specific surface chemistries or other artifacts resulting from the irradiation. In Figure 8.2B, the results were demonstrated in a quantitative manner.

The cells were subjected to Live/Dead staining, and as shown in Figure 8.2A, the mostly green color of the live Calcein AM stained fibroblasts bound to the uncaged HA-R[-]GDS-UV hydrogel surface which indicated that the cells were alive. This observation provided evidence towards the *in vitro* biocompatibility of the material.

We then conducted experiments for a preliminary estimation of the level of R[-]GDS peptide actually bound to the hydrogel. We initially exposed 65 $\mu g/cm^2$ of R[-]GDS peptide to the EDC/NHS activated hydrogel, but we ultimately estimated that at least 80% of this amount was removed in subsequent washing steps. It was of interest to determine if higher RGDS surface density could result in increased pattern resolution. Furthermore, a material's RGDS density is known to impact cell adhesion, and migration.[37] The HA hydrogel used in these studies was crosslinked with ADH via carboxyl groups on the HA polymer chain. Peptide binding also occurred on HA carboxyl groups; EDC/NHS chemistry was used to activate the carboxyl groups and subsequently bind RGDS peptides via their terminal amine group. Therefore, decreases in crosslinking density may theoretically leave more carboxyl groups available for peptide binding and increase the quantity of RGDS that can be bound.

However, varying the hydrogel crosslinking density from 1 mol HA monomer (with 1 mol of –COOH group) : 0.25 mol ADH crosslinker to 1 mol HA-COOH group: 1.5 mol ADH in order to attempt to vary the number of free -COOH groups available for coupling with the peptide failed to enhance the amount of R[-]GDS that could be bound (data not shown). Despite the inefficiency of this EDC/NHS reaction step for peptide coupling, sufficient cell adhesion occurred for cell patterning. Another important gel property impacting cell behavior is the substrate stiffness, which can theoretically be modified by varying the degree of crosslinking. Varying material stiffness, such as the elasticity of HA gels, has been shown to impact cell adhesion, migration, proliferation and differentiation, and response varies with cell type.[38,39] Since the degree of crosslinking in the range studied was not found to impact peptide binding, this property could potentially be independently varied from RGDS surface density in the future to attempt to modify cell behavior (e.g. migration) on our cell patterning platform towards a specific application.

8.3.2 Co-culture Studies

Since the photoactive HA-R[-]GDS hydrogel could be rendered adhesive through near-UV light exposure, it was hypothesized that multiple cell types could be patterned on the same hydrogel by implementing successive light exposure steps. Initially, circular patterns of 3T3 fibroblasts (Figure 8.3) 100μm in diameter separated by 200 μm non-adhesive spaces were created via near-UV lamp light exposure through a corresponding photomask to create circular adhesive regions of uncaged R[-]GDS for cell binding. To adhere a second cell population, the initial cell pattern was exposed to near-UV light to render the entire hydrogel surface cell adhesive. Immediately afterwards, HUVECs were seeded and they were found to adhere around the initial 3T3 island patterns. Over one day, cells moved off their original circular pattern since there no longer existed an underlying chemical pattern on the hydrogel to prevent migration. Creating an initial pattern of multiple cell types and then allowing for their free migration will make it possible to study cell-cell interactions and cellular response to different microenvironments with varying pattern geometries. It could also provide a technique to study cell self-assembly of tissue architectures.

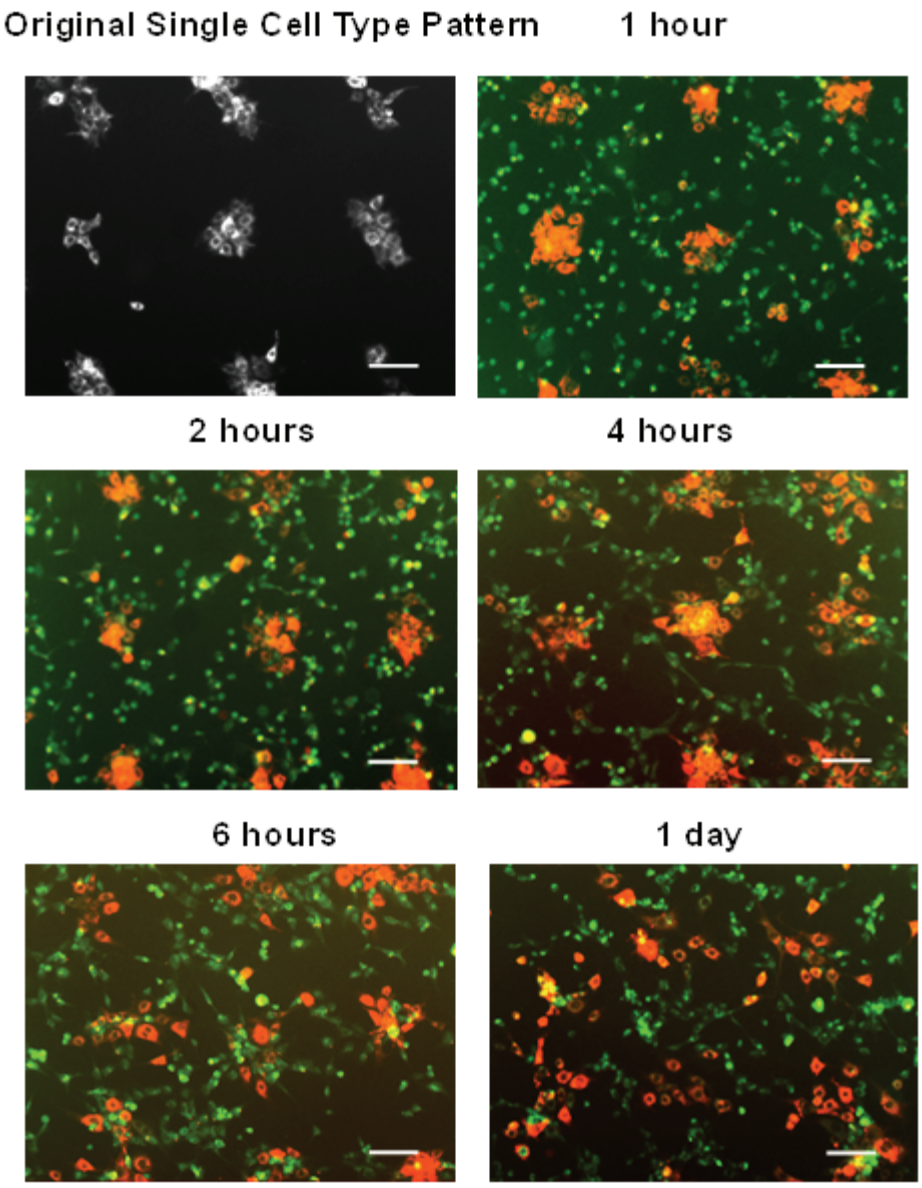

Figure 8.3 Patterned co-culture of 3T3 fibroblasts dyed with CellTracker™ Red, seeded initially onto a near-UV patterned HA-R[-]GDS hydrogel (100μm adhesive islands separated by 200μm non-adhesive space) and HUVEC dyed with CellTracker™ Green seeded after entire gel exposure to near-UV light at various time points past this second irradiation. Scale bars equal 100 μm.

8.3.3 Impact of Near-UV Light Exposure on Initially Seeded Cells

Our original co-culture strategy involved exposure of the initially patterned fibroblast cells to near-UV light at 365 nm. Light at wavelengths greater than 350 nm is generally considered cytocompatible,[40,41] but this is dependent on dose and intensity so the impact of such exposure was studied. In our previously published work it was noted that for

approximately 70% of caged R[-]GDS molecules in solution to react, a 12-minute exposure time was required (for a dose of 5 J/cm^2 at the surface of the hydrogel), and this time was used in cell patterning experiments. For a near complete reaction of caged R[-]GDS, 30 min exposure was sufficient.[33] Therefore, 3T3s grown on TCPs were exposed to 365 nm near-UV light from a lamp for 0, 5, 12, and 30 min and the number of live and dead cells were counted after 6 h to examine the immediate effects of UV exposure (Figure 8.4A) and after 24 h to allow time for apoptosis (Figure 8.4B). An MTT assay was also performed to evaluate any possible impact on cell metabolism (Figure 8.4C).

As shown in Figure 8.4A, at 6 h post exposure, the majority of cells exposed for 30 min are dead. It is worthwhile to note that in comparison with the controls (i.e. no UV exposure) there is no significant decrease in the number of live cells for cells exposed up to 12 minutes. However, at 12 minutes exposure, the MTT assay shows a significant decrease in cell metabolism. In comparison, at one day post exposure (Figure 8.4B), there is a significant decrease in the number of live cells at 12 min exposure as well and MTT assay results showed a significant decrease in cell metabolism (which is positively correlated to absorbance values) compared to controls for even a 5 minute exposure. This demonstrates that cells exposed to the near-UV light for both 5 and 12 min did not die directly after initial exposure, but for a 12 min exposure, some of the population had undergone cell death by one day post-exposure, likely via apoptosis, while cells exposed for 5 min remained alive. Live/dead staining (Figure 8.4D) at one day post exposure visibly showed that while a number of cells remain alive after the 12 min exposure shown by the mostly green color of the live calcein AM stained fibroblasts, cell density is decreased compared to the non-exposed control. For 20 or 30 min exposure, all cells appear dead as evidenced by the absence of green dye and the presence of red-dyed nuclei from ethidium homodimer. These data indicate that the initially patterned cells are definitely impacted by the dose of near-UV light required for effective uncaging. Therefore, we attempted to modify our technique such that the initially patterned cells would not be exposed to near-UV light once seeded on the hydrogel.

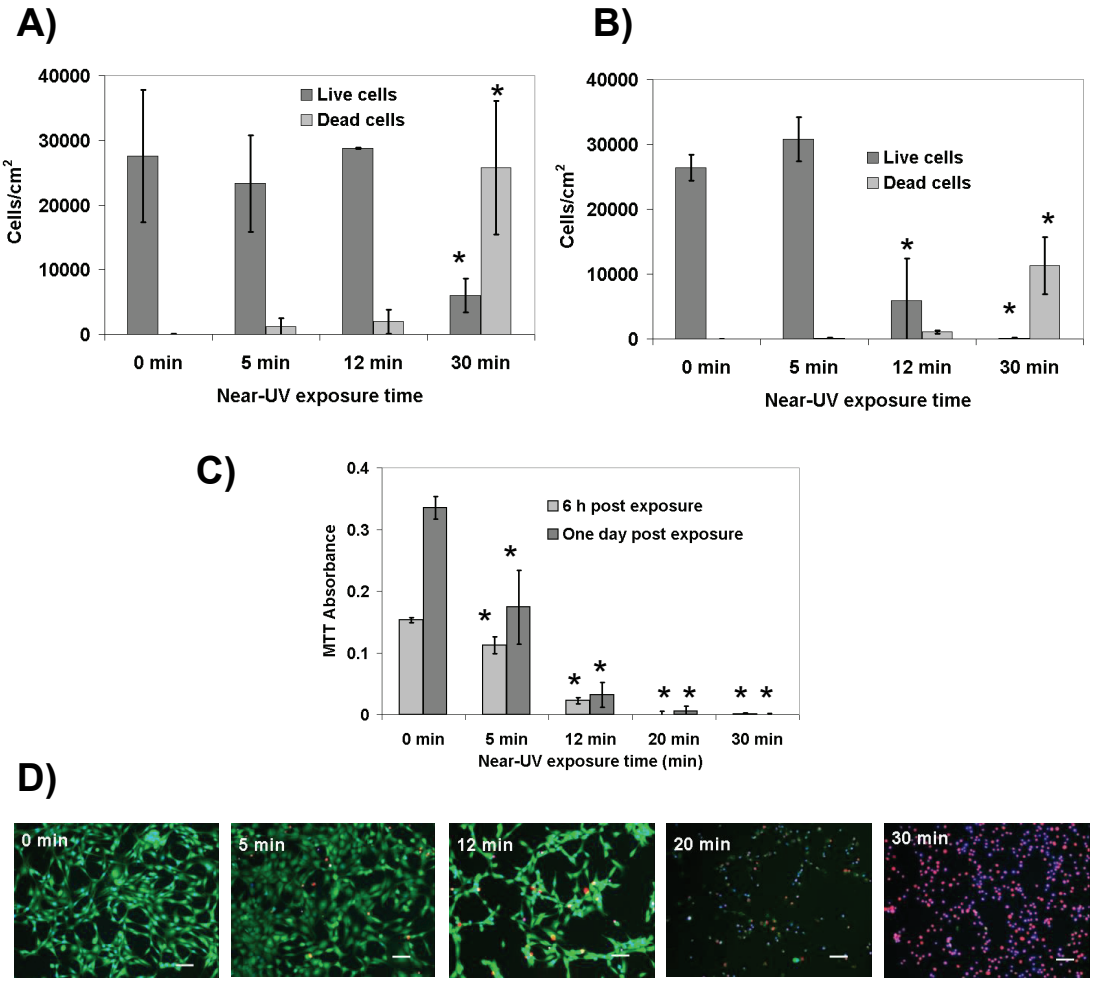

Figure 8.4: Density of live and dead cells counted on a TCP surface **(A)** 6 h post and **(B)** one day post near-UV exposure at 365 nm for various exposure times. **(C)** MTT assay absorbance values at 540 nm of fibroblast populations exposed to 365 nm light for various exposure times. Error bars represent +/- one standard deviation of duplicate samples. A * indicates a significant difference from control, 95% confidence. **(D)** Fluorescence images of live/dead stained fibroblasts one day post exposure for various exposure times. Scale bars equal 100 μm.

8.3.4 Fluorescence Microscope Patterning of Multiple Cell Types

The goal of the following experiments was to form patterns of cell adhesive islands supporting different cell populations, separated and isolated from one another by surrounding non-adhesive regions. This underlying chemical pattern should prevent the different cell populations from moving away from their initial pattern geometries. The use of photomasks was avoided since the mask needs to be placed on or very near to the surface of

a hydrogel to form a clear pattern and friction from the mask would disrupt initially patterned cells. Furthermore, alignment to the initial pattern while maintaining sterility was experimentally difficult. A fluorescence microscope with a 365 nm near-UV filter for uncaging presented a viable alternative. The initial cell pattern, stained, could be observed via microscopy using a different, red-shifted filter or through light microscopy allowing for alignment of the second cell pattern to the first. A second cell pattern could be generated by adjusting the microscope's field diaphragm opening size to create an adhesive spot of similar size on the hydrogel where the microscope is focused followed by seeding of a second cell population. Figure 8.5 shows two cell adhesive islands created on the HA hydrogel by exposing the gel to light from the fluorescence microscope with the field diaphragm opened to different degrees which demonstrates that the microscope can be used to create different sized cell adhesive regions. The smallest adhesive island that could be generated using our Olympus 1X81 F fluorescence microscope was approximately 300 μm.

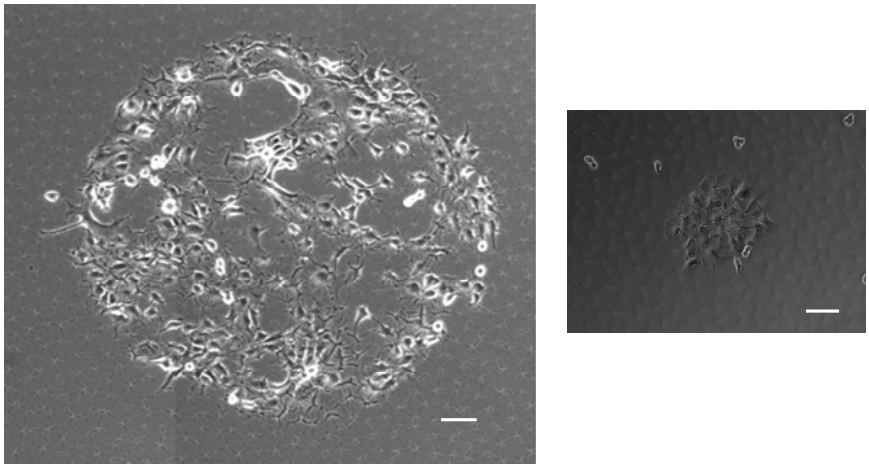

Figure 8.5: Phase contrast micrographs of different sized circular island patterns of 3T3 fibroblast cells formed on a photoactive HA hydrogel patterned using light from a fluorescence microscope with UV filter. Scale bars equal 100 μm.

Figure 8.6A(i) shows the size and geometry of the near-UV light beam from the inverted fluorescence microscope with the diaphragm at its smallest opening. This image shows a population of fibroblasts growing on the surface of a TCP with a dotted white circle drawn on to indicate the size of the field diaphragm at its smallest opening. Figure 8.6A(ii) shows the result of using this light source to pattern fibroblasts on the surface of a HA-R[-

]GDS hydrogel whereby the light path goes through the base of the TCP and through the hydrogel volume to reach its surface. The cell patterned island is seen to be approximately the same size as that in Figure 8.6A(i) even though the near-UV light for patterning had to first travel through the bulk hydrogel. A dotted white line has been overlaid on images in Figures 8.6 and 8.7 to compare the final cell pattern sizes to the original field diaphragm opening size (note that the line does not indicate the exact location of light exposure during patterning). Furthermore, it was observed that if the gel was irradiated for more than 1.5 minutes, cells adhered well beyond the intended pattern boundary throughout the gel. This suggested a possible occurrence of light scattering due to the hydrogel matrix during irradiation resulting in significant off-pattern uncaging at high doses of light.

Additionally, in order to achieve the patterned co-culture of different fibroblast populations, cells on the initial adhesive island needed to reach confluence to prevent the second cell population from mixing with the first. Note that in Figure 8.6A(ii), the cells are not confluent as some space exists between cells on the island. As a result, in Figure 8.6A(iii), when the second population of green cells was seeded, some adhered and mixed with the initial pattern made up of red-dyed fibroblasts. Moreover, when the adhesive islands were produced too close together, the resulting cell patterns were able to merge. This demonstrates some of the limitations noted with our co-culture patterning technique.

Therefore, to improve the resulting patterns, as shown in Figure 8.6B, the initially patterned fibroblasts, dyed red, were allowed to reach confluence and the two populations were held further apart (approximately 2 mm apart). It can be seen that this technique was successful in subsequently seeding multiple cell populations, the first dyed red and the second green, on the same hydrogel material held in place on a chemical pattern of caged and uncaged R[-]GDS. In Figure 8.6C, a pattern of two different cell populations was created and held apart in the μm range (only approximately 250 μm apart).

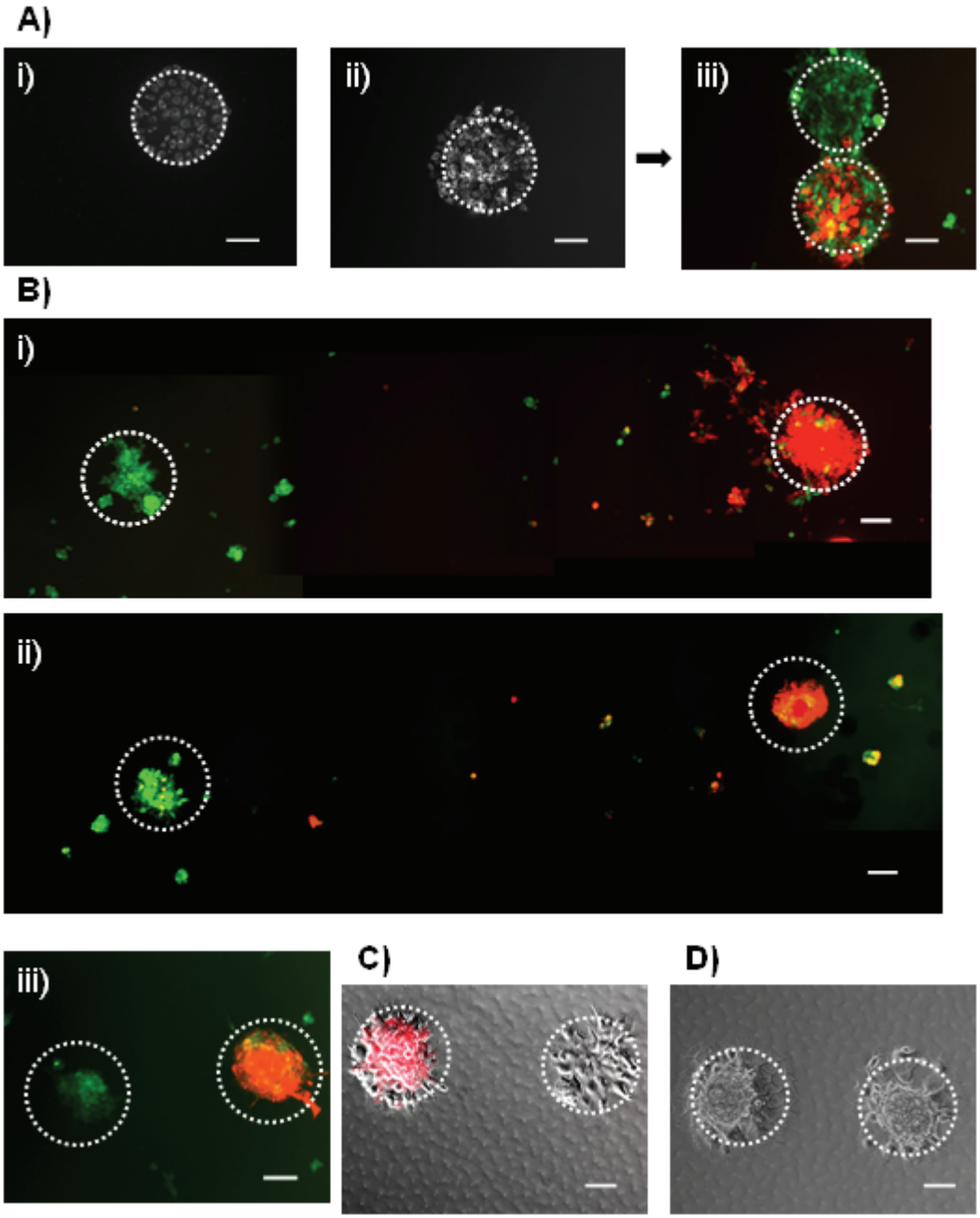

Figure 8.6: (A) (i) Fluorescence micrograph of TCP surface covered with CellTracker™ Red-dyed fibroblasts as seen with smallest field diaphragm opening size with white dashed lines drawn surrounding this area. The remaining images show HA-R[-]GDS hydrogels patterned with the fluorescence microscope having the field diaphragm opening at the same size to produce circular-island patterns of fibroblasts with initially seeded populations dyed with CellTracker™ Red and the second with CellTracker™Green. (ii) One cell island pattern and (iii) second patterned cell population added to the first. **(B)** (i-iii) Fluorescence micrographs of two separately patterned cell populations. **(C)** Phase contrast image with the initially patterned cell population shown in red by the overlay of a fluorescence micrograph and **(D)** the same patterned cell populations 25 days post seeding. Scale bars equal 100 μm.

Occasionally when reaching a dense confluence, the initially patterned fibroblasts would peel from the hydrogel if agitated thereby preventing the ability to form of a co-culture pattern. Therefore, washing steps after the second seeding had to be done extremely carefully and, in fact, the timing of the second seeding had to be immediately after confluence was reached. In addition, this patterning technique can only be successfully used if the two cells populations chosen for patterning do not adhere atop one another. Our result shows some minor degree of mixing of the two fibroblast cell populations regardless of the distance at which the two populations were held apart, which we found to be unavoidable.

In Figures 8.6C and 8.6D, it can be seen that the underlying chemical pattern adhering and separating two cell populations on the HA hydrogel was able to prevent the two cell islands from merging with one another over a period of 25 days. In Figure 8.6C, the phase contrast image is overlaid with a fluorescence micrograph to indicate that the two cell populations are different, with only one being dyed with CellTracker^{TM}Red. This image was taken one day after seeding the second cell population. Figure 8.6D is a phase contrast image only of the same cell populations since the dye was found to fade with time. Although cells in the center of the adhesive islands appear overgrown by 25 days post seeding of the second cell population, the two cell-adhesive islands remain physically separate.

In this study, we have limited our pattern geometry to circular adhesive islands. Kikuchi et al. have shown that patterns can be created at a surface by positing a photomask at the field diaphragm of a microscope.[42] Using this technique and an upright microscope to shine the patterned light directly on the hydrogel surface in order to avoid light scattering through the gel may allow for the formation of a larger variety of pattern geometries using a simple fluorescence microscope. In general, the use of a standard fluorescence microscope for producing patterns of multiple cell populations makes this technique accessible to many laboratories dealing with biological or biomedical studies.

8.3.5 Manipulating the Pattern of A Single Cell Type with Time

To further explore the dynamic aspect of this cell patterning technique, cell patterns were changed with time to increase the area of the underlying hydrogel adhesive region, but

without seeding additional cells. To do so, light from the fluorescence microscope with near-UV filter irradiated a spot directly beside, but not on, the initially seeded cells six days post seeding when cells were confluent on the original pattern (Figure 8.7A). Over a number of days, the cells migrated and grew to fill the newly created adhesive region of the pattern as imaged at 14 days post initial seeding. Growth and subsequent directed migration of the existing cells must be assumed since no additional cells were added to the pattern and the larger adhesive region became confluent with fibroblasts.

To demonstrate the validity of this technique, we applied three subsequent light exposure steps to guide cell migration and growth over 21 days (Figure. 8.7B). Our results demonstrated that the dynamic hydrogel patterns can last at least three weeks and that additional adhesive regions can be created to properly direct cell growth and/or migration even two weeks after initial seeding. Note that very few cells adhere away from the patterned region even after 21 days post seeding. Figure 8.7C, a control, shows that cells seeded on a single adhesive island without subsequent light exposure steps did not migrate or grow significantly off the island pattern during the progress of the experiment.

Others have incorporated photoactive functionalities or ligands into gels so that after selective light exposure to "activate" the material, additional reaction steps can be performed to bind a peptide, protein or other bioactive molecule to the hydrogel in a planned geometry.[24,25,27,28] These techniques offer the advantage of a wide selection of biomolecules for hydrogel incorporation, but the additional reaction steps required after light exposure could impact cells previously seeded on the hydrogel limiting dynamic patterning. Our technique, by comparison, requires no additional reaction steps after irradiation removes the caging group. In this respect, our patterning strategy may better lend itself to applications requiring the culture of multiple cell populations or types or patterns that are to be changed with time in a dynamic fashion. Though our pattern is limited to the use of RGDS to form adhesive islands, this peptide has been found to bind a wide range of cell types in the literature including neurons, hepatocytes, fibroblasts, and endothelial cells among others.[37]

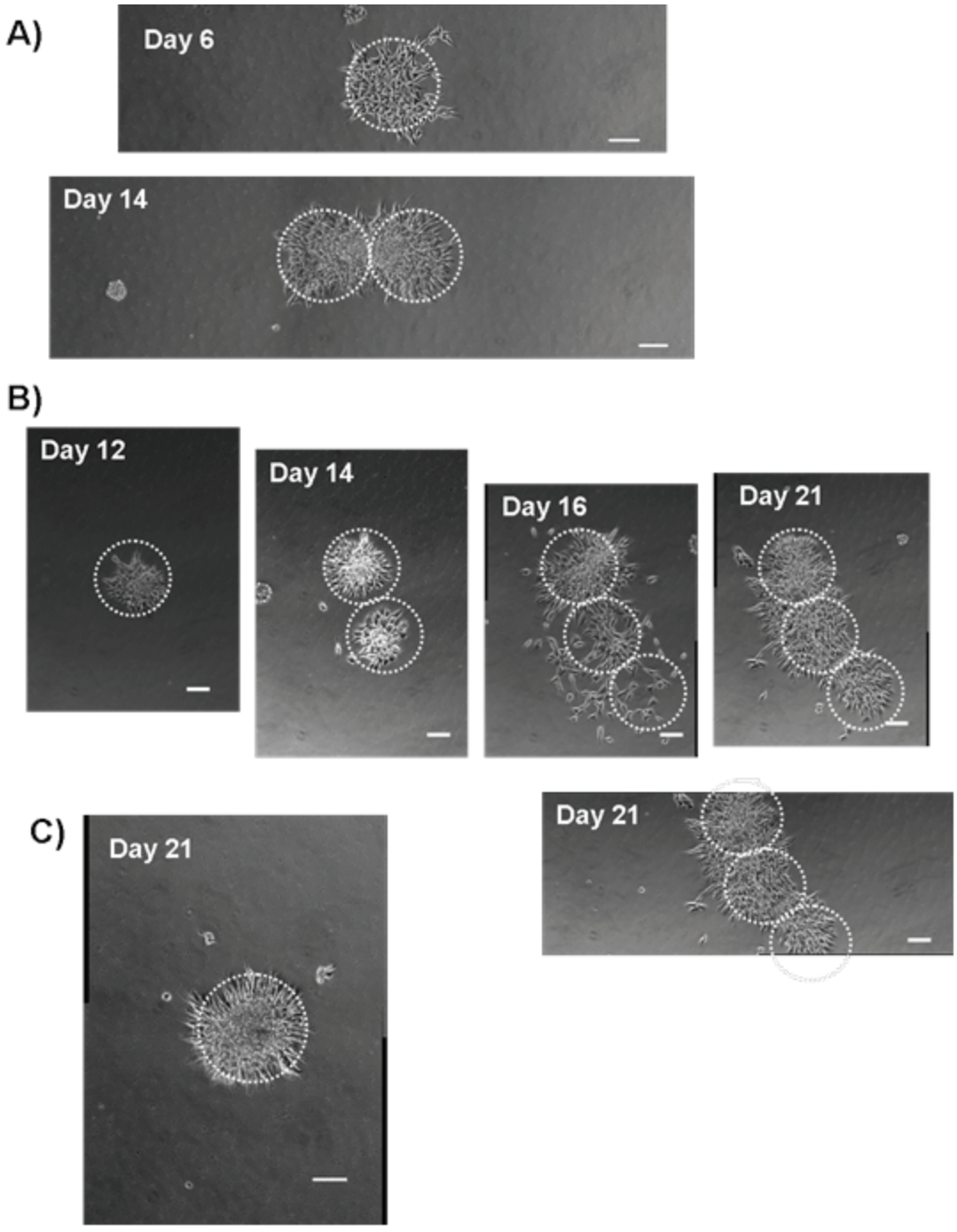

Figure 8.7: Phase contrast micrographs of fibroblasts adhering to adhesive islands on an otherwise nonadhesive HA hydrogel patterned using light from a fluorescence microscope with UV filter. (A) By day 6 post seeding cells fill the initial adhesive island pattern and another adhesive island is patterned adjacent to the first. By day 14 cells fill the second pattern. (B) On day 12 and 14 post seeding of cells, additional adhesive islands are patterned adjacent to the original patterns and cells grow and migrate to fill the new patterns. (C) Cells adhering to a single control adhesive island at 21 days post seeding. Scale bars equal 100 μm.

8.4 Conclusions

Our work demonstrated that hydrogels could be patterned with near-UV light by incorporating a photocaged RGDS peptide with a 2-nitrobenzyl group bound to the peptide backbone nitrogen between Arg (R) and Gly (G) to produce patterned co-cultures and cell patterns that could be dynamically altered and so change deliberately with time. Patterns were shown to last at least three weeks in culture. This patterning technique is accessible to average laboratories involved in biological study, since hydrogel synthesis and liquid phase peptide synthesis can be carried out without specialized equipment and a standard fluorescence microscope was shown to be adequate to generate basic patterns. The ability to pattern multiple cell types and to change the pattern with time on a biocompatible hydrogel material allows for a high degree of control over the cell microenvironment which can aid in future studies investigating cell-cell interactions or devices for tissue regeneration. Modification of this technique also presents the possibility for 3D patterning by merely incorporating the peptide throughout the hydrogel volume instead of on the surface and utilizing a light source such as a 2-photon laser able to focus light in a 3D volume, which would further this versatile technique's exciting potential in the field of tissue engineering.

8.5 Acknowledgements

We thank A.Chen for technical assistance, Dr. Suuronen and D. Kuraitis for generously donating HUVEC and media. This study was supported by a NSERC Discovery Grant to X.Cao, a NSERC Discovery grant and Heart & Stroke Foundation grant to A. Basak and a CIHR-HOPE fellowship grant to S. Majumdar and A. Basak.

8.6 References

1. Rivron NC, Rouwkema J, Truckenmüller R, Karperien M, De Boer J, Van Blitterswijk CA. Tissue assembly and organization: Developmental mechanisms in microfabricated tissues. *Biomaterials.* 2009;30(28):4851-4858.

2. Tomatsu I, Peng K, Kros A. Photoresponsive hydrogels for biomedical applications. *Adv. Drug Delivery Rev.* 2011;63:1257–1266.

3. Burdick JA, Prestwich GD. Hyaluronic Acid Hydrogels for Biomedical Applications. *Adv. Mat.* 2011;23(12):H41-H56.

4. Chong BF, Blank LM, McLaughlin R, Nielsen LK. Microbial hyaluronic acid production. *Appl. Microbiol. Biotechnol.* 2005;66(4):341-351.

5. Zhang H, Hanson Shepherd JN, Nuzzo RG. Microfluidic contact printing: a versatile printing platform for patterning biomolecules on hydrogel substrates. *Soft Matter.* 2010;6(10):2238-2245.

6. Tang MD, Golden AP, Tien J. Molding of Three-Dimensional Microstructures of Gels. *J. Am. Chem. Soc.* 2003;125(43):12988-12989.

7. Hynd MR, Frampton JP, Dowell-Mesfin N, Turner JN, Shain W. Directed cell growth on protein-functionalized hydrogel surfaces. *J. Neurosci. Methods.* 2007;162(1â€“2):255-263.

8. Kobel S, Limacher M, Gobaa S, Laroche T, Lutolf MP. Micropatterning of Hydrogels by Soft Embossing. *Langmuir.* 2009;25(15):8774-8779.

9. Kunze A, Bertsch A, Giugliano M, Renaud P. Microfluidic hydrogel layers with multiple gradients to stimulate and perfuse three-dimensional neuronal cell cultures. *Procedia Chem.* 2009;1(1):369-372

10. Hammoudi TM, Lu H, Temenoff JS. Long-term spatially defined coculture within three-dimensional photopatterned hydrogels. *Tissue Engineering - Part C: Methods.* 2010;16(6):1621-1628.

11. Bruzewicz DA, McGuigan AP, Whitesides GM. Fabrication of a modular tissue construct in a microfluidic chip *Lab Chip.* 2008;8(5):663-671.

12. Trkov S, Eng G, Di Liddo R, Parnigotto PP, Vunjak-Novakovic G. Micropatterned three-dimensional hydrogel system to study human endothelial–mesenchymal stem cell interactions. *J. Tissue Eng. Regener. Med.* 2010;4(3):205-215.

13. Chen CY, Barron JA, Ringeisen BR. Cell patterning without chemical surface modification: Cell-cell interactions between printed bovine aortic endothelial cells (BAEC) on a homogeneous cell-adherent hydrogel. *Appl. Surf. Sci.* 2006;252(24):8641-8645.

14. Xu T, Gregory CA, Molnar P, et al. Viability and electrophysiology of neural cell structures generated by the inkjet printing method. *Biomaterials.* 2006;27(19):3580-3588.

15. Liu VA, Bhatia SN. Three-dimensional photopatterning of hydrogels containing living cells. *Biomed. Microdevices.* 2002;4(4):257-266.

16. Hahn MS, Taite LJ, Moon JJ, Rowland MC, Ruffino KA, West JL. Photolithographic patterning of polyethylene glycol hydrogels. *Biomaterials.* 2006;27(12):2519-2524.

17. Sala A, Hänseler P, Ranga A, et al. Engineering 3D cell instructive microenvironments by rational assembly of artificial extracellular matrices and cell patterning. *Integr. Biol.* 2011;3(11):1102-1111.

18. Chan V, Zorlutuna P, Jeong JH, Kong H, Bashir R. Three-dimensional photopatterning of hydrogels using stereolithography for long-term cell encapsulation. *Lab Chip.* 2010;10(16):2062-2070

19. Zorlutuna P, Jeong JH, Kong H, Bashir R. Stereolithography-Based Hydrogel Microenvironments to Examine Cellular Interactions. *Adv. Funct. Mater.* 2011;21(19):3642-3651.

20. Fukuda J, Khademhosseini A, Yeo Y, et al. Micromolding of photocrosslinkable chitosan hydrogel for spheroid microarray and co-cultures. *Biomaterials.* 2006;27(30):5259-5267.

21. Vermesh U, Vermesh O, Wang J, et al. High-Density, Multiplexed Patterning of Cells at Single-Cell Resolution for Tissue Engineering and Other Applications. *Angew. Chem., Int. Ed.* 2011;50(32):7378-7380.

22. Albrecht DR, Underhill GH, Mendelson A, Bhatia SN. Multiphase electropatterning of cells and biomaterials. *Lab Chip.* 2007;7(6):702-709.

23. Tekin H, Tsinman T, Sanchez JG, et al. Responsive Micromolds for Sequential Patterning of Hydrogel Microstructures. *J. Am. Chem. Soc.* 2011;133(33):12944-12947.

24. Hahn MS, Miller JS, West JL. Three-Dimensional Biochemical and Biomechanical Patterning of Hydrogels for Guiding Cell Behavior. *Adv. Mater.* 2006;18:2679-2684.

25. Musoke-Zawedde P, Shoichet MS. Anisotropic three-dimensional peptide channels guide neurite outgrowth within a biodegradable hydrogel matrix *Biomed. Mater.* 2006;1(3):162-169.

26. Aizawa Y, Wylie R, Shoichet M. Endothelial Cell Guidance in 3D Patterned Scaffolds. *Adv. Mater.* 2010;22(43):4831-4835.

27. Gu Z, Tang Y. Enzyme-assisted photolithography for spatial functionalization of hydrogels. *Lab Chip.* 2010;10(15):1946-1951

28. Seidlits SK, Schmidt CE, Shear JB. High-Resolution Patterning of Hydrogels in Three Dimensions using Direct-Write Photofabrication for Cell Guidance. *Adv. Funct. Mater.* 2009;19(22):3543-3551.

29. DeForest CA, Anseth KS. Photoreversible Patterning of Biomolecules within Click-Based Hydrogels. *Angew. Chem., Int. Ed.* 2012;51(8):1816-1819.

30. Young DD, Deiters A. Photochemical control of biological processes *Org. Biomol. Chem.* 2007;5(7):999-1005.

31. Petersen S, Alonso JM, Specht A, Duodu P, Goeldner M, del Campo A. Phototriggering of Cell Adhesion by Caged Cyclic RGD Peptides. *Angew. Chem., Int. Ed.* 2008;47(17):3192-3195.

32. Ohmuro-Matsuyama Y, Tatsu Y. Photocontrolled Cell Adhesion on a Surface Functionalized with a Caged Arginine-Glycine-Aspartate Peptide13. *Angew. Chem., Int. Ed.* 2008;47(39):7527-7529.

33. Goubko C, Majumdar S, Basak A, Cao X. Hydrogel cell patterning incorporating photocaged RGDS peptides. *Biomed. Microdevices.* 2010;12(3):555-568.

34. Goubko CA, Basak A, Majumdar S, Jarrell H, Huan Khieu N, Cao X. Comparative analysis of photocaged RGDS peptides for cell patterning. *Journal of Biomedical Materials Research - Part A* 2013;101 A (3):787-796.

35. Basak A, Mitra A, Basak S, Pasko C, Chrétien M, Seaton P. A Fluorogenic Peptide Containing the Processing Site of Human SARS Corona Virus S-Protein: Kinetic Evaluation and NMR Structure Elucidation. *ChemBioChem.* 2007;8(9):1029-1037.

36. Cherny RC, Honan MA, Thiagarajan P. Site-directed mutagenesis of the arginine-glycine-aspartic acid in vitronectin abolishes cell adhesion. *J. Biol. Chem.* 1993;268(13):9725-9729.

37. Hersel U, Dahmen C, Kessler H. RGD modified polymers: biomaterials for stimulated cell adhesion and beyond. *Biomaterials.* 2003;24(24):4385-4415.

38. Discher DE, Janmey P, Wang Y-l. Tissue Cells Feel and Respond to the Stiffness of Their Substrate. *Science.* 2005;310(5751):1139-1143.

39. Hachet E, Van Den Berghe H, Bayma E, Block MR, Auzély-Velty R. Design of Biomimetic Cell-Interactive Substrates Using Hyaluronic Acid Hydrogels with Tunable Mechanical Properties. *Biomacromolecules.* 2012;13(6):1818-1827.

40. Furuta T, Noguchi K. Controlling cellular systems with Bhc-caged compounds. *TrAC, Trends Anal. Chem.* 2004;23(7):511-519.

41. Sigrist H, Collioud A, Clemence J-F, et al. Surface immobilization of biomolecules by light. *Opt. Eng.* 1995;34(8):2339-2348.

42. Kikuchi Y, Nakanishi J, Shimizu T, et al. Arraying Heterotypic Single Cells on Photoactivatable Cell-Culturing Substrates. *Langmuir.* 10/16/ 2008;24(22):13084-13095.

CHAPTER 9:
DISCUSSION AND CONCLUSION

Within this chapter, research conducted and presented in the published works from Chapters 3-8 will be discussed within the context of the major goals of this thesis, and the novelty of the work will be highlighted as well as conclusions derived from the work. Supplementary explanations and additional data not found in Chapters 3-8 have been added within this discussion for increased clarity.

9.1 Literature Review and Hypothesis Development

Study for this thesis began by investigating the various methods available for cell patterning. It was noted that relatively few patterning methods allowed for cell patterns that could be deliberately manipulated over time to alter the original pattern or to pattern multiple cell types. Therefore, a comprehensive literature review was conducted of works involving multiple cell patterning, or patterned co-cultures. This review was published and presented in Chapter 3. To the best of our knowledge, this review paper was the first published with a focus on co-culture patterning techniques. During the course of the review it was noted that while a variety of creative cell patterning methods had been developed, in the majority of co-culture patterns formed, the patterns were limited. The initial cell pattern was often designed to take on a variety of geometric shapes, but the second cell population seeded merely filled in the spaces between the original cell pattern. This meant the two cell patterns could not be separated from one another. Some strategies did not employ an underlying chemical pattern to bind cells meaning cells were free to migrate after seeding, and would not necessarily hold the cell pattern for any length of time. Other methods employed complex 3D patterns in PDMS stamps and microfluidics channels for co-culture. However, such strategies would present difficulties with pattern alignment if it was desired to change the patterns with time. Considering this information, it was thought that the development of a dynamic patterning strategy using light as a stimulus to create chemically-patterned cell-adhesive regions had the potential to address some of the above-noted patterning challenges. Light can potentially be used to create a wide range of different spatial patterns at different time points, and alignment can readily be accomplished using a microscope connected to a light source.

One way to introduce light as a stimulus into a cell patterning platform is to employ chemical photocaging techniques. As it was our goal to photocage a cell adhesive peptide

which could be inactivated upon caging and activated again to become cell adhesive upon light exposure, Chapter 4, published as a book chapter, was written to review caging groups and the caging of various biomolecules in the literature to date. It also examined the application of caging groups in materials for biological applications, such as the development of biomaterials which can undergo light-stimulated changes to physical and chemical properties, and applications in the development of biological devices, such as those for controlled drug release. Our review was novel in that the majority of previous literature reviews on the topic of photocaging focused on the chemistry of the caging groups, caging specific molecules, or applications in biochemistry, whereas our review had a focus on applications in biomaterials and biological devices.

9.2 Gel Development

Chapters 5-8 dealt with the experimental development and analysis of our cell patterning platform using a hyaluronic acid (HA) hydrogel base incorporating photocaged cell adhesive peptides towards the formation of dynamic cell patterns whereby control was achieved over the spatial localization of multiple cell types and cells over time according to our hypothesis. The development of our patterning strategy first began with the design of the various system components. The first was the base HA hydrogel. A chemically crosslinked hydrogel, as opposed to formation via physical forces, was desired for stability. ADH was chosen for the crosslinker due to its availability, relatively low cost, ease of reaction, and use of ADH-crosslinked HA gels in recent neural regeneration experiments.[1-4] The cross-linking reaction is outlined in further detail in Figure 9.1.

The first step in the HA crosslinking reaction employed involved EDC hydrochloride, which can react with a carboxyl group on HA to form an amine-reactive *O*-acylisourea intermediate. EDC itself is water soluble allowing the reaction to take place in aqueous solution, so that toxic solvents do not have to be washed from the final product. However, EDC loses its reactivity over time in water and requires a slightly acidic environment to be effective.[1] In the desired reaction pathway, the terminal -NH_2 group of the ADH crosslinker reacts with the *O*-acylisourea intermediate to bind the ADH to the HA carboxyl group. In order to crosslink the HA polymer, the free end of the same ADH

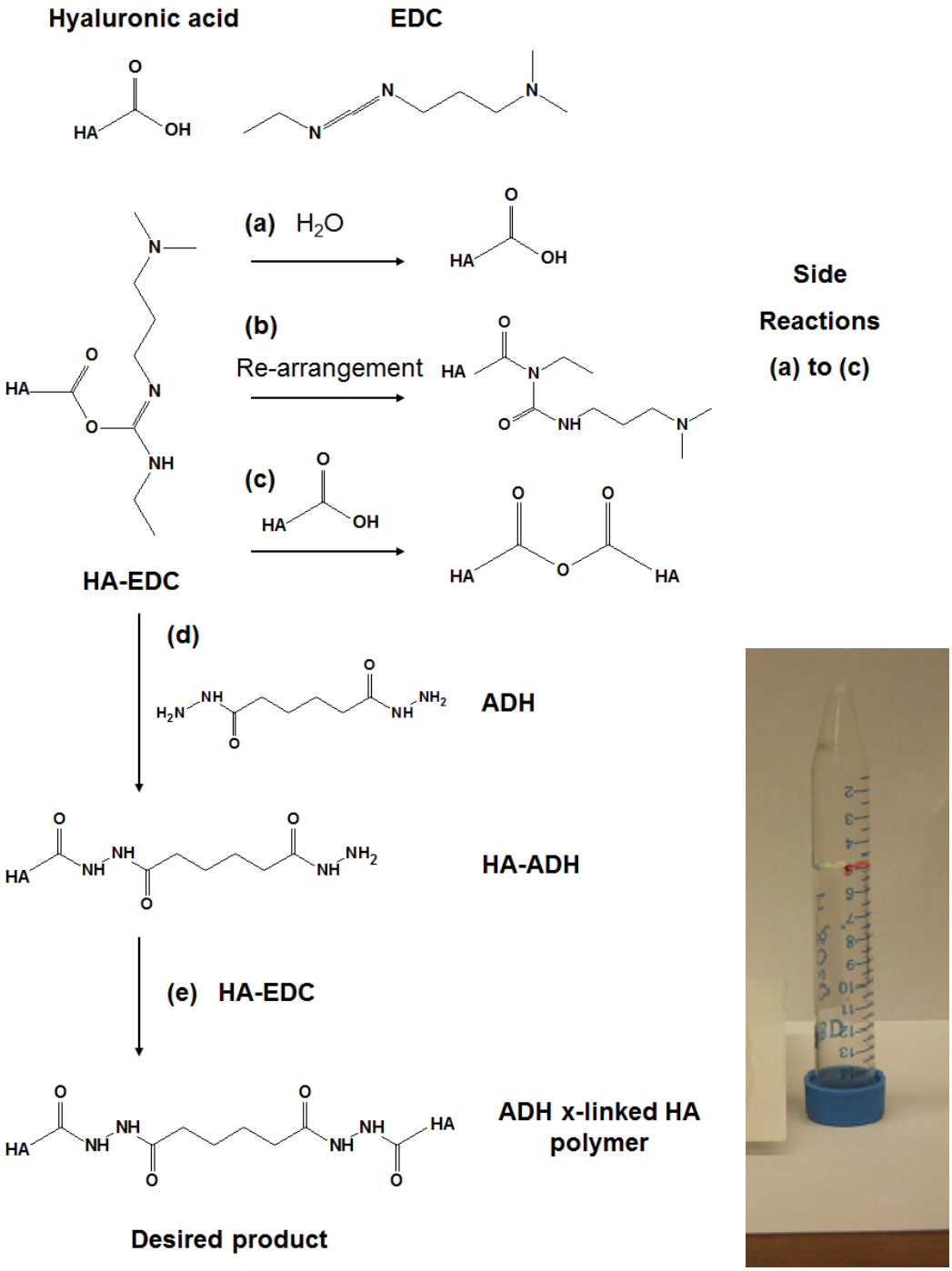

Figure 9.1: The reaction of HA with EDC to form an ADH-modified HA polymer which can react with another HA polymer chain to form an ADH-crosslinked HA polymer chain which is the desired product. Undesired side reactions are illustrated producing **(a)** regenerated HA**, (b)** a stable N-acylurea product resulting from the re-arrangement of the O-acylurea formed from EDC binding to HA, or **(c)** weakly crosslinked HA via a carboxylic ester bond, but which can also react with ADH towards the formation of the desired product. Image of the final, clear inverted hydrogel in a centrifuge tube (right).

molecule must react with an EDC-activated carboxyl group on another HA chain. Several side reactions are possible as illustrated in Figure 9.1.[2]

Parameters for the gelation reaction were initially modeled after the work of Vercruysse et al. who conducted extensive studies of hydrazide-crosslinked HA.[3] However, since the HA used in this work was derived from a different source, a variety of gelation parameters were investigated for hydrogel formation. Gelation was determined by an inversion test; if the material could maintain its shape in an inverted position after the crosslinking reaction, it was deemed to have gelled. The parameters varied and held constant will be briefly discussed. The concentration of HA was not varied, but kept near the solubility limit since we desired a high concentration of HA in the final gels for pattern resolution. The molar ratio of carboxyl groups in HA to ADH crosslinker (COOH:ADH) was varied and gels were found to form from 1:0.25 to 1:1.5 COOH:ADH. The EDC:ADH molar ratio was also varied from 1:1 to 3:1, with the 1:1 EDC:ADH ratio producing stable gels and further increases in EDC produced gels that tended to shatter. When varying pH, visibly weaker gels were formed when pH was increased above 3.5. Furthermore, NHS was added to the reaction at a ratio of 1:1 NHS:EDC. NHS can react with the unstable o-acylisourea ester produced by EDC to create a more stable intermediate for further reaction with an amine group.[1] The reactions with NHS also produced gels, but at the lower COOH:ADH ratios, the final reaction material remained pourable, while in comparison to gels with no NHS, the material was a solid gel. For the above reasons, the parameters in Table 9.1 were chosen. Final gels were clear, colorless (as seen in Figure 9.1), and showed no visible degradation after one month at 37°C in sterile 1XPBS buffer.

Table 9.1: Conditions to form solid HA gels via EDC activation and ADH crosslinking

Parameter	Current work	Vecruysse et al. [3]
Concentration of HA in water (mg/mL)	4	8
Aqueous solution pH	3.5	3.5
COOH:ADH	1:0.25 to 1:1.5	1:1.5
EDC:ADH	1:1	1:1
NHS (mM)	0	NI

NI = not investigated

In order to verify the crosslinking reaction was occurring as expected, ^{13}C NMR was used to confirm the incorporation of ADH into the final hydrogel after extensive washing (Figure 9.2). The spectrum of lyophilized ADH-crosslinked gel was obtained in addition to the spectrum of the HA sodium powder used in gel preparation (purchased from Sigma Aldrich). A difference spectra was obtained from the subtraction of the ADH-crosslinked HA spectrum from the pure HA spectrum in order to highlight the additional carbon peaks found in the ADH-crosslinked gel. Peak assignments were determined from comparison with the work of Pouyani et al, who pioneered studies in ADH-modified and hydrazido-modified HA.[4] The new peaks seen in the ADH-crosslinked HA gel corresponded to the α-carbon of the ADH molecule (35 ppm vs 34 ppm measured by Pouyani et al.[4]) and the carboxyl group of the ADH molecule (170 ppm vs 170ppm measured by Pouyani et al.[4]). The difference spectra also showed the β-carbon of the ADH molecule (26 ppm vs 25 ppm by Pouyani et al.[4]). This provided evidence that ADH was incorporated into the hydrogel as expected.

It was desired to produce a base hydrogel that was cell non-adhesive to prevent background binding of cells to the final patterning platform. Cells have receptors on their surface capable of specific binding to HA including the receptors CD44 and RHAMM.[5] However, at the same time, HA is known for its anti-adhesive properties in its pure state, which can be attributed to its high degree of hydrophilicity.[6] Therefore, it was necessary to determine the cellular adhesivity of the ADH-crosslinked HA, and this was outlined in Chapter 5 (5.3.2, Figure 5.4). It was found that a single layer of the freshly gelled HA material was insufficient for repelling cells. It hypothesized that this might be due to too low a density of HA in the gel, so new gels were developed by drying the initially deposited gel layer in order to concentrate the HA in the gel. Motokawa et al. noted that when their HA-ADH hydrogels were dried for a day, they obtained longer release times for a drug, erythropoietin encapsulated within the hydrogel and suggested the reason may be due to additional crosslinking via hydrogen bonds formed during the drying process.[7] The dried and rehydrated gels were visible less swollen than the original freshly gelled HA hydrogels. This could be due to hydrogen bonding between HA chains themselves and with incorporated ADH molecules as the gel dried. In addition, gels were layered to create three layers of dehydrated gel bound atop one another to form the final HA hydrogel product.

(a) ADH bound to HA

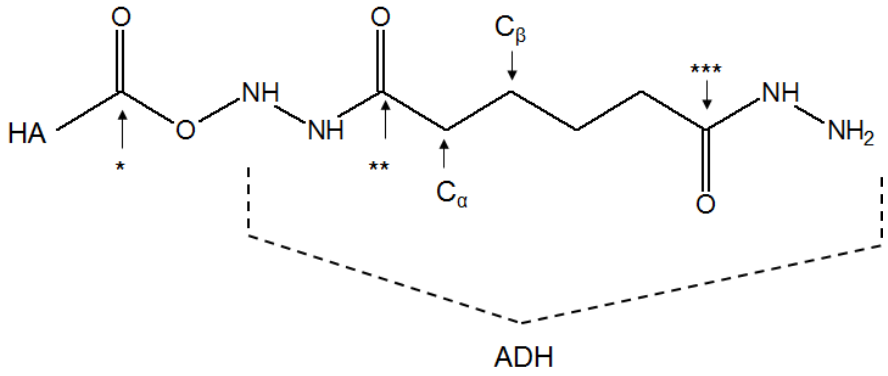

(b) ADH crosslinking HA

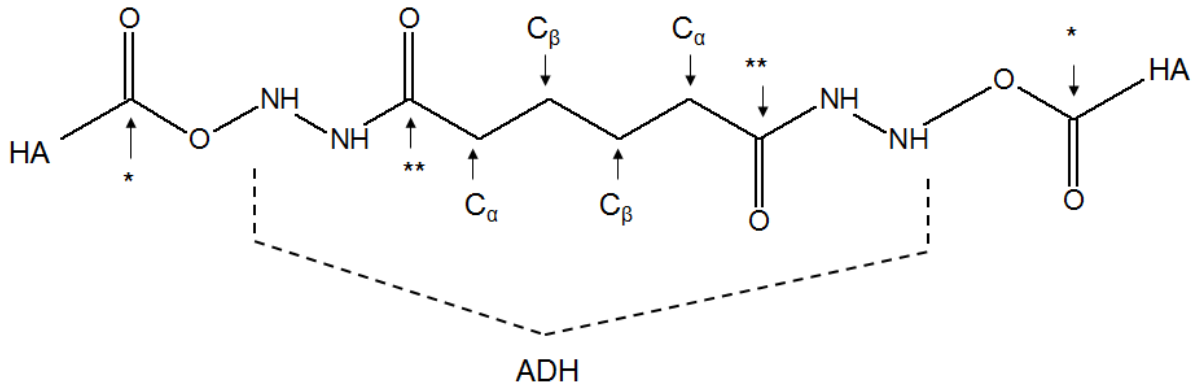

(c)

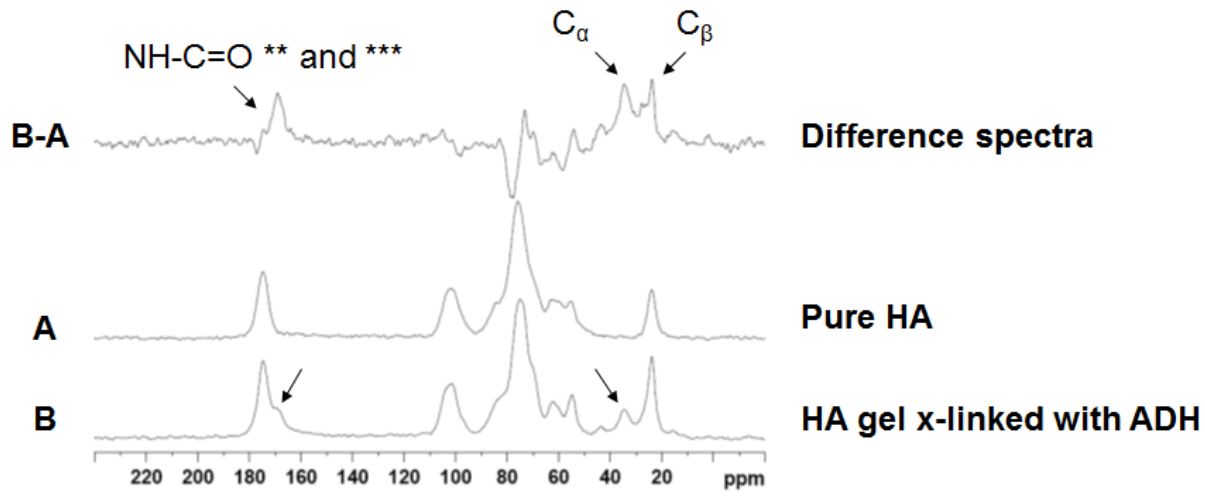

Figure 9.2: (a) Structure of ADH bound on only one side by HA via an HA carboxyl group and **(b)** the structure of HA crosslinked by ADH. **(c)** Solid state ^{13}C NMR spectra for pure HA and ADH-crosslinked HA with arrows indicating new peaks. A difference spectrum was obtained by subtracting the pure HA spectra from the ADH-crosslinked spectra. Peak identifications obtained from Pouyani et al.[4]

As noted in Chapter 5, cells no longer bound to this final hydrogel product, and so this gel design was incorporated into our cell patterning strategy.

The next research goal with respect to the gel was to establish that peptides could be bound to the hydrogel base material. Figure 9.3 outlines the reaction scheme using EDC/NHS chemistry to covalently bind peptides to the HA hydrogel. Peptides were bound via carboxyl groups remaining on HA after crosslinking. In Chapter 5, FITC-BSA was used as a model peptide/protein with dye to enable visualization after binding, and provided evidence that peptides or proteins could be covalently bound to the hydrogel base as follows. FITC-BSA presented in solution to control gels without EDC/NHS activation washed away after 22 hours such that the gel surfaces showed no fluorescence. Conversely, gels activated with EDC/NHS and then exposed to FITC-BSA strongly fluoresced even after washing for the same 22 hour period.

The peptide sequence RGDS was selected to create adhesive regions on the HA peptide and was synthesized in the protein lab of Dr. Basak at the OHRI as described in Chapter 5. Binding RGDS to the non-adhesive hydrogel was found to promote cell adhesion as hypothesized. To better determine the gel parameters for further study, RGDS peptide was bound to HA gels with varying amounts of crosslinker, and the same quantity of 3T3 fibroblast cells ($1X10^4$ cells/cm^2) were allowed to adhere for 12 hours following the culture procedures found in Chapter 5 before being removed and counted. Results are seen in Figure 9.4. The gels with less crosslinker – having 0.25 and 0.5 mol ADH per mol of COOH in HA – bound significantly less cells than the gels with more crosslinker. This was unexpected since no difference was found in the quantity of peptide that these gels could bind in Chapter 8. One explanation could be that gels with less crosslinker are expected to be weaker in terms of compressive strength and ridgitity, and such substrate (material) mechanical properties are known to impact cell behaviors such as adhesion and migration.[8-10] Furthermore, it was observed qualitatively that the gels with less crosslinker had fewer micro-cracks at the surface. The increased “roughness” or micro-topography of the more highly crosslinked hydrogels may have aided in cell adhesion since cells are known to respond to differences in material topography.[11]

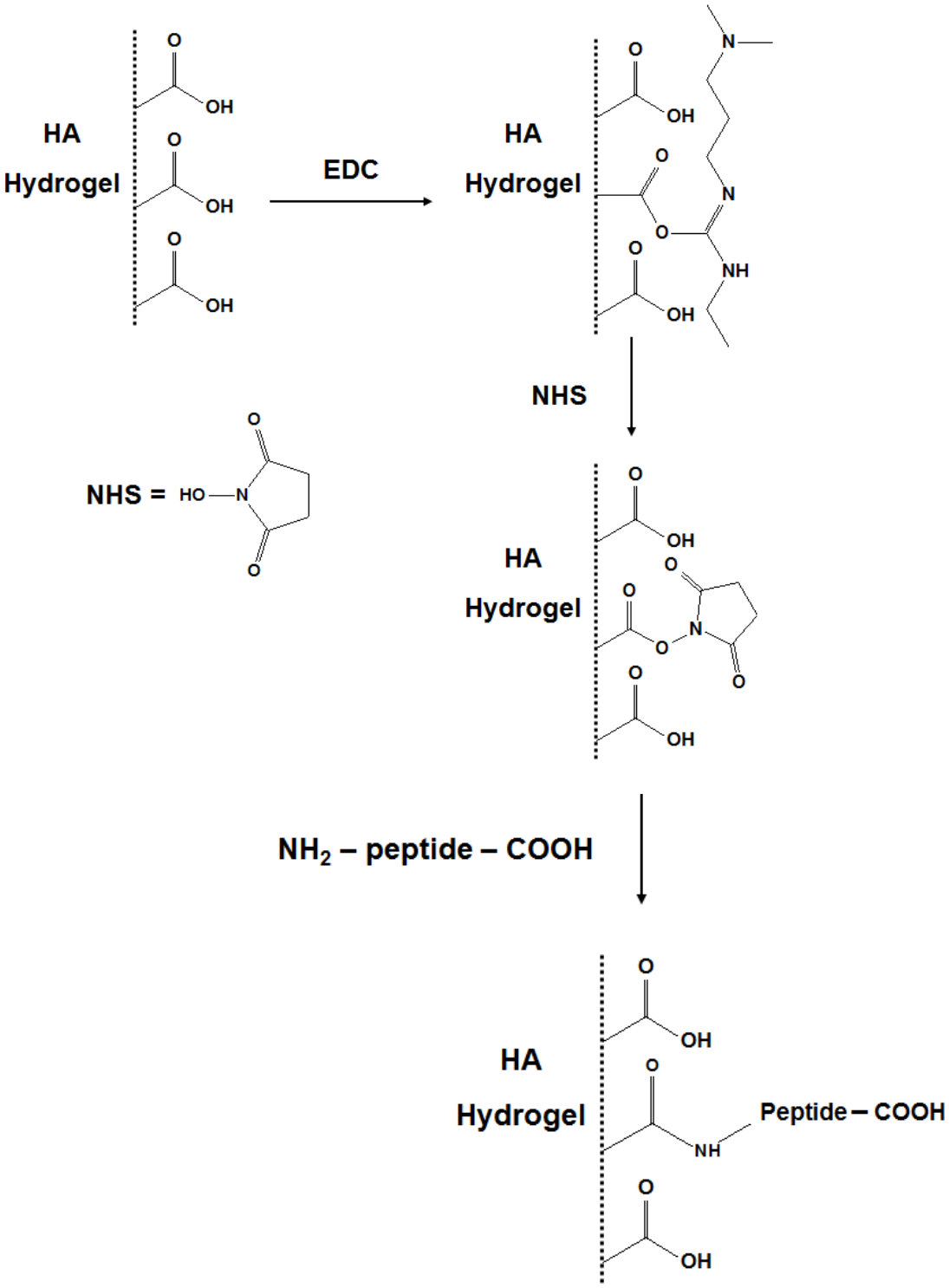

Figure 9.3: The reaction of HA gel with EDC and NHS to form a peptide-bound hydrogel.

It was ultimately decided to proceed making the gel containing 1:0.75 mol COOH to mol ADH crosslinker as the base material for the patterning platform. From preliminary results in Figure 9.4, it can be seen that increasing the amount of crosslinker beyond this molar ratio does not result in a significant increase in cell adhesion. Keeping the amount of crosslinker as low as possible will theoretically leave more COOH groups available after crosslinking. This increases chance of having free COOH groups for adherent cells to recognize the natural HA polymer, and benefit from its bioactive properties.

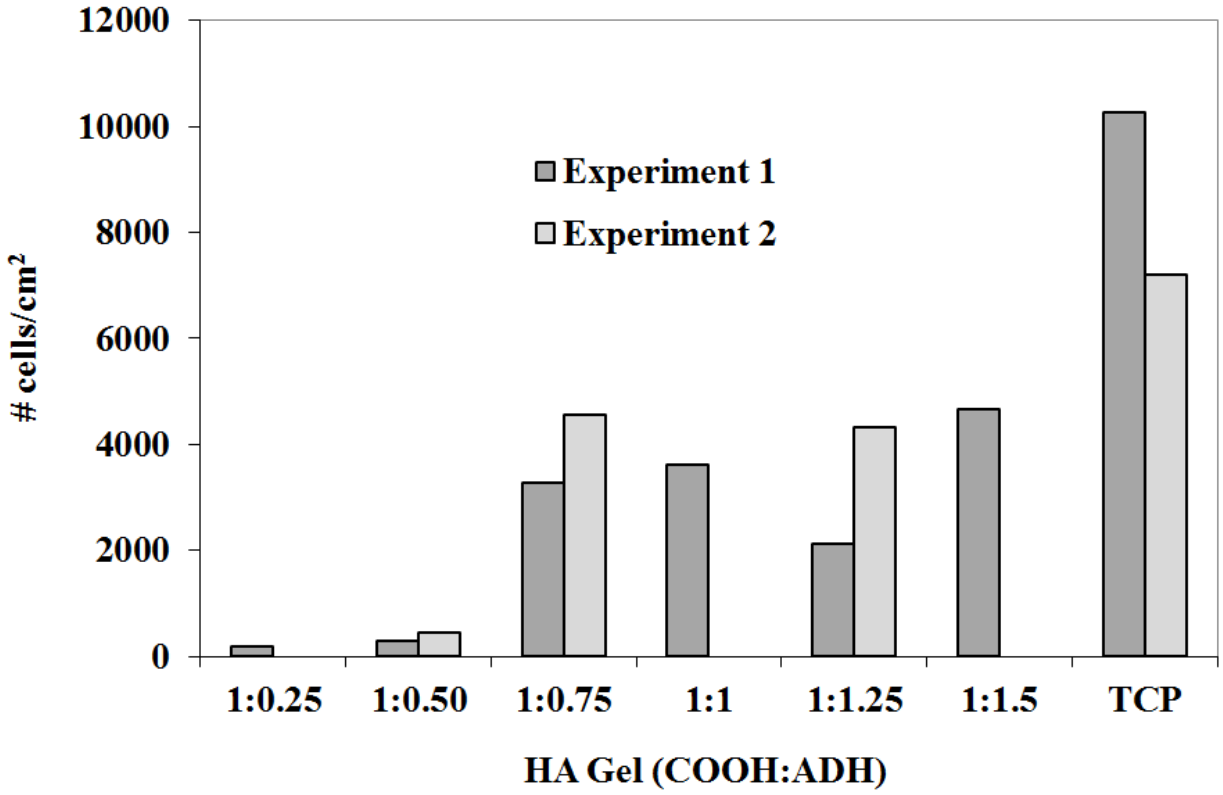

Figure 9.4: The number of cells bound per cm^2 of HA-RGDS gel surface for gels with varying moles of ADH crosslinker used in the gelation reaction per mol of HA carboxyl group.

Another base gel modification that was investigated was the production of gels without surface cracks (seen in Chapter 5, Figure 5.4(c)). Cracks interfered with visualization of the cells by phase-contrast microscopy, and they created a non-homogenous surface at the micro-scale. Several methods were attempted; gelation time was increased from approximately 5 minutes to 30, and rehydration time for the gels was slowed by placing them in a 100% humidified environment. However, cracking still occurred during rehydration of the gels after drying. Literature on the prevention of polyacrylamide gel cracking when drying gels for biochemical analysis recommended soaking the gels in 2% DMSO with 10% acetic acid in water overnight prior to drying,[12] and this method was found to be successful for the HA gels (Figure 9.5). Unfortunately, very few cells adhered to these gels compared to those with micro-cracks, so these gels were not used in further studies. One potential explanation is that the micro cracks provided a topography that assists in cell adherence to the hydrogel. It has been noted in the literature that in some instances where materials have a naturally high energy for binding that increasing surface roughness can increase cell adhesion.[13]

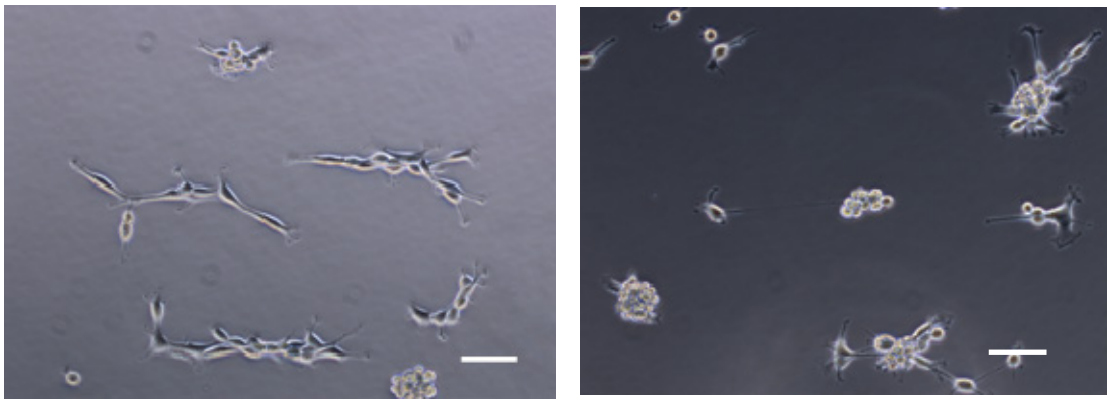

Figure 9.5: Dried and rehydrated patterned HA gels formed without cracks by soaking the gels in 2% DMSO with 10% acetic acid in water overnight prior to drying. Gels were seeded NIH 3T3 fibroblasts. Scale bars = 100 μm.

9.3 Peptide Experiments

After developing the cell non-adhesive hydrogel base capable of binding peptides, synthesis of the caged RGDS peptide began under the supervision of Dr. Basak at the OHRI. The first step was to decide to which function the 2-NB caging group should be added within the Arg-Gly-Asp peptide sequence. The various options were shown in Chapter 6, Figure 6.5. The goal was to covalently bind the 2-NB cage in a critical location such that its presence significantly interrupted binding between cellular integrin receptors and the RGDS sequence. A combination of literature reviews and modeling work were carried out to investigate such locations.

Previous works found that N-substituted peptide analogues are greatly restricted in their conformational freedom, which supports caging at the amide nitrogen of the peptide backbone.[14] In further support, Dechantsreiter et al. suggested that close contact between the polar amide groups adjacent to Gly and the integrin receptor is essential for integrin mediated cell attachment.[15] In support of caging the peptide backbone at the Gly residue, it has been noted that the Gly residue lies directly on the integrin surface and makes several hydrophobic interactions with the integrin receptor critical for RGD binding.[16] Substituting Gly for Ala, with the only structural difference between the two being a methyl group, destroys binding activity to the $\alpha_v\beta_3$ integrin.[17] Support in the literature also existed for caging the side chain Asp residue which participates extensively in integrin binding. The Asp carboxylate forms a large network of polar interactions with the integrin and one oxygen from the group co-ordinates with a divalent cation in the binding pocket, while the other oxygen H-bonds with the $\alpha_V\beta_3$ integrin amino acids, Tyr^{122} and $Asn.^{215}$.[16] Changing even the Asp to Glu, which has only an extra methyl group, is known to abolish cell adhesion to the RGD sequence.[17] Evidence also existed supporting the caging of the Arg side chain whose guanidinium group is known to make strong contacts with the integrin receptor. A bidentate salt bridge binds it to the integrin residue Asp^{218} while an additional salt bridge forms to Asp^{150}.[16]

A review of the literature was also conducted to find protocols for caging these different amino acids. A 2-NB derivative was placed on the Arg residue on the side chain

guanidinium group in a synthesis by Wood et al.,[18] and a 2-NB derivative was placed on the side chain carboxyl group of the Asp residue by others.[19,20] Other possible caging locations include the peptide backbone amide nitrogen atoms. Tatsu et al. caged peptide backbones by synthesizing a Gly residue with 2-NB bound to its amine group.[14] Other have caged the peptide backbone,[21] but to the best of our knowledge no one has synthesized a peptide with a caging group on the amino group of an Asp, which would be necessary to synthesize RGDS caged on the backbone between Gly and Asp.

Studies were conducted using the software, Autodock where the binding between a cell integrin receptor and a RGDS molecule caged at different functions was modeled. We proposed the use of this novel technique in Chapter 6 to aid in the selection of caging group placement within peptides prior to synthesis, which has been historically difficult.[22,23] The software provided a predicted binding conformation and calculated a theoretical free energy of binding for each caged RGDS ligand in addition to non-caged RGDS to compare and rank integrin binding affinities. These studies provided theoretical insight into how the caging group impacted RGDS-integrin binding when bound to different functions on the RGDS peptide as discussed in Chapter 6, Section 6.3.4. The software predicted that binding the caging group on the side chain of the Arg residue would have little impact on RGDS-integrin binding, and so caging at this location was not explored experimentally. It furthermore predicted that binding the caging group on the peptide backbone between Arg and Gly, and between Gly and Asp, and on the Asp side chain carboxyl would produce an increase in the free energy of binding to integrin to different degrees as compared to non-caged RGDS.

Since there existed no literature protocols for the caging of the amino group on Asp (in order to cage the peptide backbone between Gly and Asp), or convenient starting materials for such a synthesis, it was decided to proceed with synthesizing two caged RGDS peptides; one caged on the Asp side chain carboxyl (RG[D]S) and one caged on the amide nitrogen of the peptide backbone between Arg and Gly (R[-]GDS). Furthermore, during the course of this thesis, two communication papers were produced whereby the authors caged an Asp residue in an RGD peptide derivative[24] and a Gly residue to cage the peptide backbone nitrogen atom between Arg and Gly in another RGD peptide derivative.[25] We then published the first full-length paper using caged R[-]GDS to form cell patterns (Chapter 5).[26]

We ultimately decided to compare the synthesis of RGDS peptide caged in the two aforementioned locations both due to our modeling and literature review results combined with interest in the literature in caging at these two particular functions. We contrasted other properties of the final caged peptides relevant to their application in controlling cell adhesion (Chapter 6).[27] Such a comparison had not been made in the literature previously, and was timely considering this new interest by other groups as well as ours in caging this important peptide sequence for light-activation.

The first step in the chemical synthesis was the addition of the 2-NB caging group to the selected amino acids. The Gly residue was caged first via its amino group. Later, the side chain carboxyl group on the Asp residue was also caged. Liquid phase synthesis of the caged Gly was outlined in Chapter 5, Section 5.2,3.[26] An improved method was introduced in Chapter 6, Section 6.2.2, which also outlined the liquid phase synthesis of caged Asp in Section 6.2.1.[27] Figure 9.6 shows the structure of the Gly and Asp amino acids, both caged and not, as well as the structure of the RGDS peptide.

The next synthesis step was the incorporation of these caged amino acids into the RGDS tetrapeptide. Each amino acid, caged and not, has an amino group on one end and a carboxyl group on the other separated by a carbon atom termed the alpha carbon, to which is bound the amino acid's "side chain" which can be comprised of a variety of functions, or hydrogen as in the case of Gly as seen in Figure 9.6. Peptide synthesis first involves coupling two amino acids together. This is accomplished by activating the terminal carboxyl group of one amino acid allowing for a nucleophilic attack by the amino group of a second amino acid to form an amide, or peptide, bond. A common group of activators which were used in this work are carbodiimides, whose chemistry was discussed in Section 9.2 with EDC as an example.[28] For peptide synthesis, DIC, another carbodiimide was used. During peptide bond formation all of the other functional groups - including those on the side chains and the amino group of the first amino acid and carboxyl of the second – must be protected or blocked in a reversible manner to prevent side-reactions. To add subsequent amino acids to the peptide chain, deprotection must occur to create a free amine and carboxyl group for bond formation without deprotecting the other functions. At the end of peptide synthesis, all

of the side chains must be deprotected to obtain the final product. Common protecting groups used in this work include Boc, which is cleavable with acid, Fmoc, which is cleavable under basic conditions, and t-butyl esters, t-butyl ethers, methyl esters, and Pbf, which are all acid sensitive.

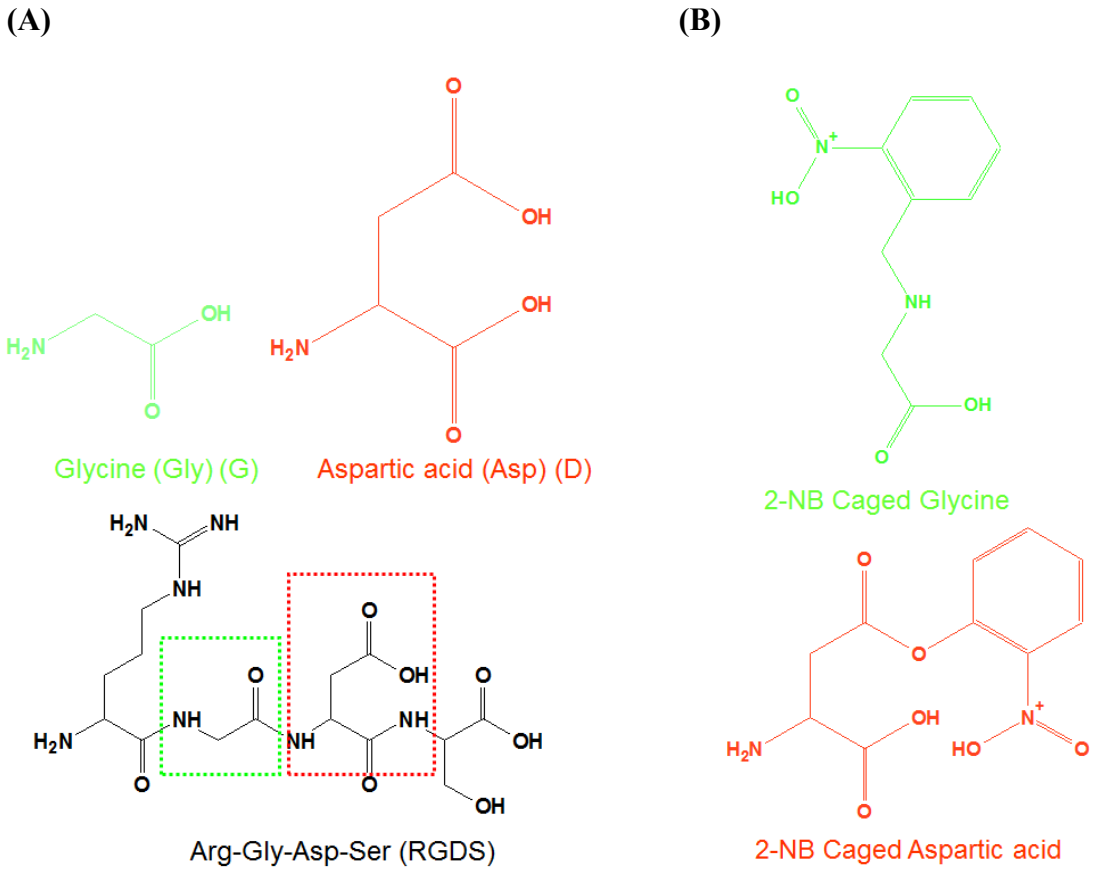

Figure 9.6: (A) Structure of amino acids Glycine and Aspartic acid and the tetrapeptide RGDS incorporating these two amino acids in the boxed locations. **(B)** Structure of 2-nitrobenzyl caged Glycine and Aspartic acid.

To accomplish such synthesis steps, two general methods for the synthesis of peptides exist including "liquid (or solution) phase peptide synthesis" (LPPS) pioneered by Du Vigneaud in 1953,[29] or "solid-phase peptide synthesis" (SPPS) pioneered by Merifield in 1963.[30] Using these methods, peptides have been synthesized for commercial development with lengths generally up to tens of amino acids long, including Zadaxin for Hepatitis C treatment containing 28 amino acids, and Preos for the treatment of osteoporosis with 84 amino acids. Both methods were explored in this work. In LPPS, the peptide synthesis steps

are carried out in organic solutions so reaction products can be isolated and purified at every step. However, LPPS is generally more labor intensive and time consuming as compared to SPPS, especially as peptides become longer. SPPS involves a solid support on which the synthesis takes place; amino acids are added to a growing peptide chain tethered to this solid support. Because the growing peptide is bound to the solid matrix throughout synthesis, peptide purification cannot be performed until the synthesis is over, which can result in a complex mixture of products closely related in structure. Preparative HPLC is used for purification post-synthesis. The major benefit of SPPS is the commercial availability of automated SPPS synthesizers that allow for a relatively rapid synthesis. Other challenges faced by SPPS include variability in solid-phase resin quality - even batch to batch from the same manufacturer - and the tendency of peptides to aggregate during the synthesis complicating deprotection and purification.[31] In industry, it is common to synthesize peptides via SPPS for laboratory investigations and small scale clinical trials due to the ease and speed of production, and then convert to a LPPS approach for the generation of larger quantities for increased purity and economic reasons.

LPPS steps incorporating the caged Gly into the tetrapeptide to form R[-]GDS were outlined in Chapter 5, Section 5.2.3.[26] The caged Asp was successfully incorporated into the tetrapeptide to form RG[D]S via SPPS. We were unable to successfully synthesize R[-]GDS via SPPS, and had to rely on LPPS. The details of these syntheses were outlined in Chapter 6.[27] Note that different protecting groups were used depending on the final peptide synthesis route. Synthesis products were analyzed by mass spectrometry and ^{1}H NMR. LPPS allowed for the production of gram scale quantities of purified caged tetrapeptide. Although LPPS synthesis took weeks to complete, the synthesis could be followed via thin layer chromatography (TLC) and purified at every step to remove byproducts. Furthermore, intermediates could be analyzed and characterized at every step. Standard SPPS techniques had to be modified in order to accommodate the incorporation of the caged amino acids. Although SPPS took only several days, a complex mixture of products was obtained that required HPLC purification. Furthermore, analysis could only be conducted on the final crude product after synthesis complicating troubleshooting attempts and meaning protocols could only be modified after synthesis. Finally, reaction yields were significantly lower with

SPPS compared to LPPS. However, once a final protocol was developed for SPPS production, ease of production and time savings were significant.

After synthesis, ^{1}H NMR experiments were conducted on the final caged products both pre- and post-irradiation to determine whether the uncaging reaction was occurring as expected according to the scheme presented in Figure 9.7. The resulting caged R[-]GDS spectrum showed two distinct sets of proton signals for the caging group prior to photolysis, indicating the existence of two different conformations of bound 2-NB to RGDS. This can be explained by the semi-rigid nature of the peptide backbone to which the cage is bound, resulting in two possible binding positions. After photolysis, there is only one conformation which would be expected for a freely rotatable caging group released into solution. For both caged R[-]GDS and RG[D]S, the disappearance of the benzylic proton peak was observed after photolysis, and a new aldehyde peak was observed which is consistent with the expected uncaging reaction scheme in Figure 9.7.

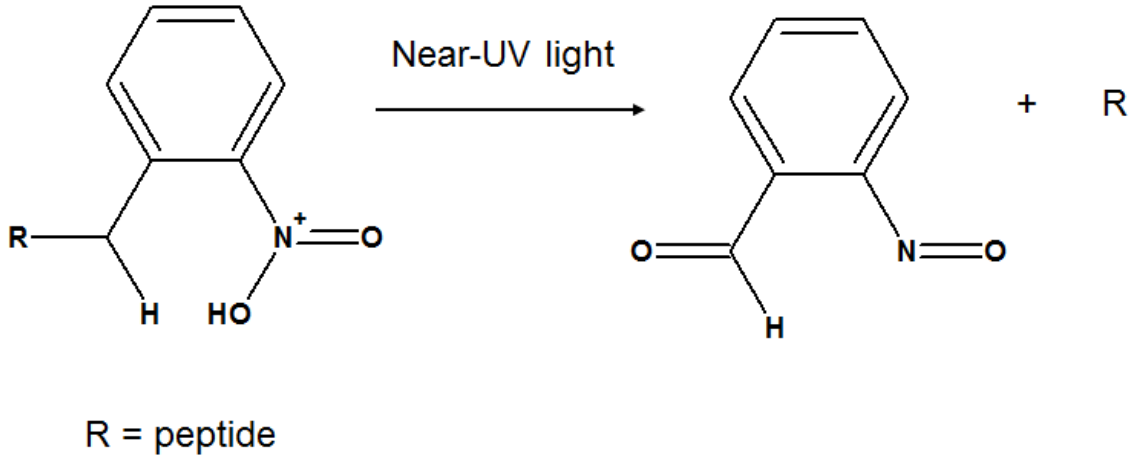

Figure 9.7: The expected photolysis/uncaging reaction for a 2-NB bound peptide.

After conducting and comparing the possible synthesis routes for the R[-]GDS and RG[D]S caged peptides, the two were further compared based on several criteria including rate of photolysis, stability to hydrolysis, and the difference in binding affinity to the $\alpha_V\beta_3$ integrin receptor between the caged and uncaged peptides.[27] The photolysis of both caged peptides could be described as pseudo first order, with RG[D]s having a photolysis rate constant approximately 3 fold higher than that of R[-]GDS. Free RG[D]S in aqueous

solution was further found to be more stable than R[-]GDS. A competitive binding ELISA assay was used to compare the binding affinity of RGDS, the caged peptides, and the uncaged peptides. A description of this assay is presented in Figure 9.8 for clarity. Although both caged peptides R[-]GDS and RG[D]S showed significantly decreased binding to integrin receptor as compared to RGDS, the difference in binding affinity to integrin between caged and uncaged peptide was the greatest for R[-]GDS. Therefore, although the RG[D]S peptide demonstrated desirable characteristics such as its ability to be synthesized via automated SPPS, increased stability to hydrolysis, and a lower energy input requirement for photolysis, the most important characteristic required for the establishment of a cell patterning strategy is the difference in binding affinity between caged and uncaged forms. R[-]GDS peptide had a significant advantage over RG[D]S in this regard, and was used for the establishment of the cell patterning strategy in this work.

9.4 Controlling Hydrogel Cell Adhesion

Once the R[-]GDS peptide was synthesized, a series of cell culture experiments were conducted to examine its ability to control cell adhesion to HA hydrogels. Throughout this work, 3T3 fibroblasts were used as model animal cells. Fibroblast cells are found in connective tissue where they synthesize ECM materials. This particular cell line was established in 1962 by G. Todaro and H. Green, originally derived from mouse tissue, and is capable of growing indefinitely. They were ideal as model cells for experimentation due to their ability to be grown relatively easily in large numbers in the laboratory, and for their adhesive properties. They require surface adhesion to survive, and so they were used to test animal cell adhesion to our patterned materials.

For the cell adhesion experiments, a number of hydrogel samples were developed with either no bound peptide, bound RGDS, R[-]GDS, or uncaged R[-]GDS. As hypothesized, cells failed to bind to the hydrogel with no peptide bound as well as to the hydrogel bound with caged R[-]GDS. However, cells did bind when RGDS was bound to the hydrogel and when the hydrogel was bound with R[-]GDS uncaged by exposure to near-UV light prior to cell seeding. Results were shown in Chapter 5, Section 5.3.4

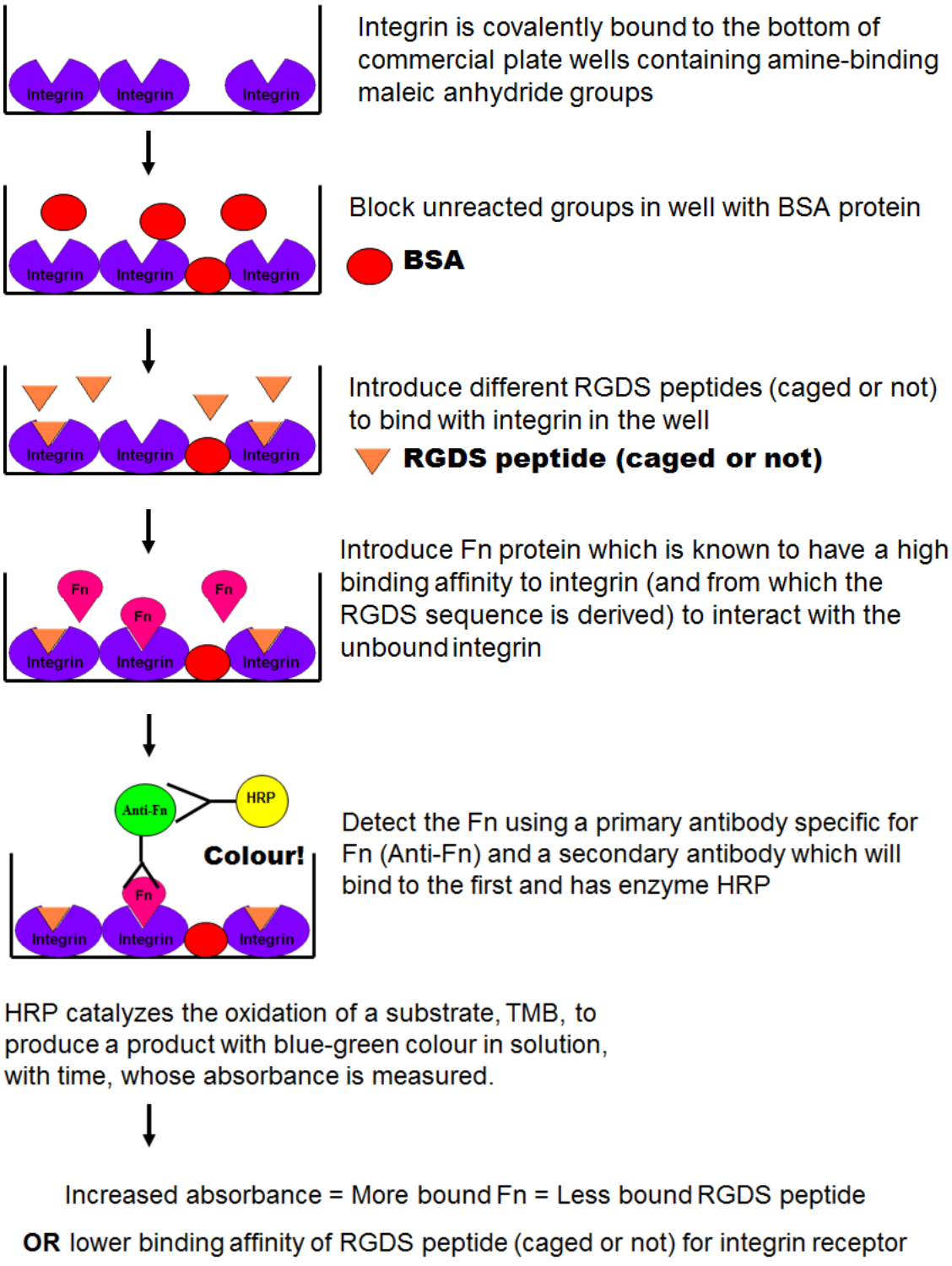

Figure 9.8: Schematic of Competitive Binding ELISA for experimental comparison of integrin binding affinity of different RGDS peptides, caged and uncaged, and controls including RGDS, RGES, R[-]GDS, and RG[D]S. Note that in each well a single peptide type was analyzed.

Two separate tests were conducted to determine whether cell adhesion to the experimental surfaces was due to specific interactions with the RGDS peptide as hypothesized, and not as a result of surface chemistry changes from the uncaging process or artifacts from near-UV light exposure. In Chapter 7 (Section 7.3), cells were pre-incubated with RGDS prior to seeding on the experimental hydrogel surfaces which were bound to uncaged R[-]GDS. It was hypothesized that if cells were binding to uncaged RGDS on the surface, pre-incubation with free RGDS peptide would result in cell integrin receptors becoming saturated with soluble RGDS peptide rendering these receptors unable to interact with the gel surface. Under these conditions cells were indeed unable to bind to the hydrogel. The second test was illustrated in Chapter 8 (Section 8.3.1, Figure 8.2). A new caged peptide, R[-]GES, was synthesized and bound to HA hydrogels along with RGES peptide. RGES is structurally very similar to RGDS except for one extra methyl group. While cells successfully attached to HA gels with bound RGDS or uncaged R[-]GDS, cells failed to adhere to gels with the bound control peptides, RGES or uncaged R[-]GES. This second piece of evidence further supported the hypothesis that cells are binding to the hydrogels due to bio-specific interactions with RGDS peptides.

9.5 Patterning Experiments with a Single Cell Type

Chemical patterns of adhesive uncaged R[-]GDS peptide surrounded by cell non-adhesive caged R[-]GDS peptides were created on HA hydrogels by shining near-UV light through patterned photomasks on the R[-]GDS-bound gels. In Chapters 5 to 7, single cell type patterns can be seen of either line or circle shapes with pattern resolutions in the range of 100 μm, and with patterns lasting for increasing amounts of time in culture. The lined pattern of fibroblasts on the hydrogel in Figure 9.9 lasted at least eight days in culture. At 8 days post-seeding, cells were beginning to reach confluence and peel off as seen with cells grown on an uncaged R[-]GDS hydrogel in Figure 9.10 at eight days post seeding. However, it was observed that some cells would re-attach and begin to re-grow on the gel. This result is significant as pattern longevity was significantly increased compared to studies where others explored light-controlled cell adhesion with caged peptides.[24,25]

Images of cell patterns consisting of 100 μm lines separated by 100 μm can be seen in Figure 9.11. Such patterns could be created consistently, and this resolution is consistent with other hydrogel patterning strategies (reviewed in Chapter 2, section 2.5). Furthermore, this scale is consistent with the length scale of most natural supracellular tissue structures making it relevant for tissue engineering applications.[32,33] The highest resolution pattern attempted consisted of 25 μm circles separated by 35 μm spaces. The results can be seen in Figure 9.12. The results show that compared to a material which is not patterned and completely adhesive, after three days cells on the patterned material remain mostly separated from one another with typically only one to two cells on each island, which indicate that the pattern influenced cell geometry. However, cells failed to adhere to many of the patterned islands and a number of the cell-occupied islands are larger than the 25 μm circular pattern.

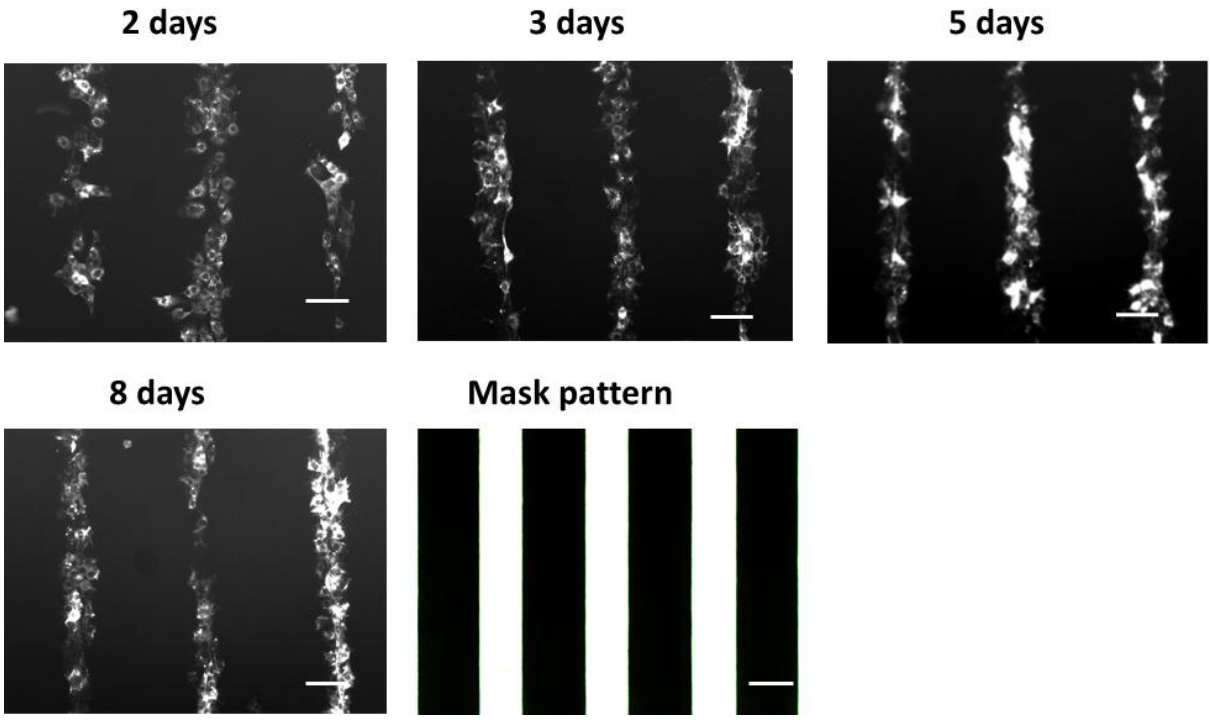

Figure 9.9: Fluorescence micrographs of 3T3 fibroblasts dyed with CellTracker™ Red and grown on the HA hydrogels bound with R[-]GDS and patterned using the photomask shown for the indicated number of days post seeding. Scale bars = 100 μm.

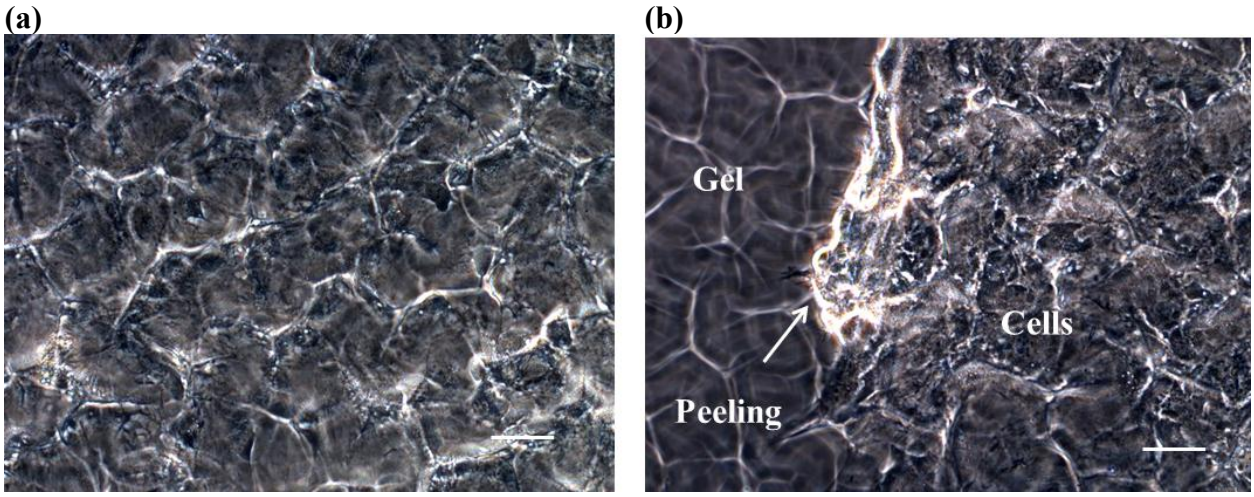

Figure 9.10: Phase contrast micrographs of 3T3 fibroblasts **(a)** bound to a HA hydrogel with uncaged R[-]GDS peptide at 8 days post seeding and **(b)** peeling from the gel at 8 days post seeding. Scale bars = 100 μm.

(a) 1 day post seeding

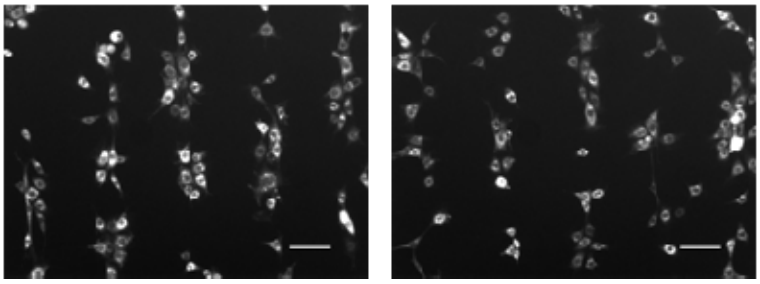

(b) 3 days post seeding

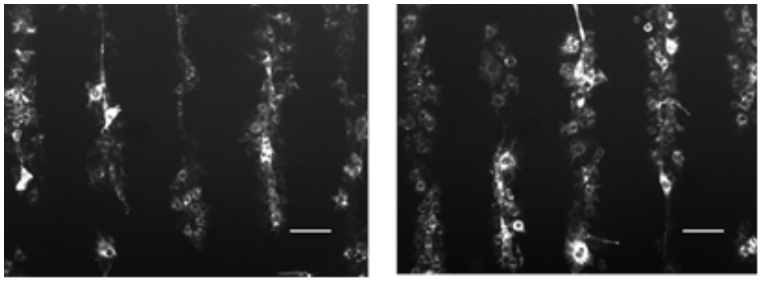

Figure 9.11: Fluorescence micrographs of 3T3 fibroblasts dyed with CellTracker™ Red on HA hydrogels bound with R[-]GDS and patterned using a photomask with 100 μm lines separated by 100 μm spaces at the indicated number of days post seeding. Scale bars = 100 μm.

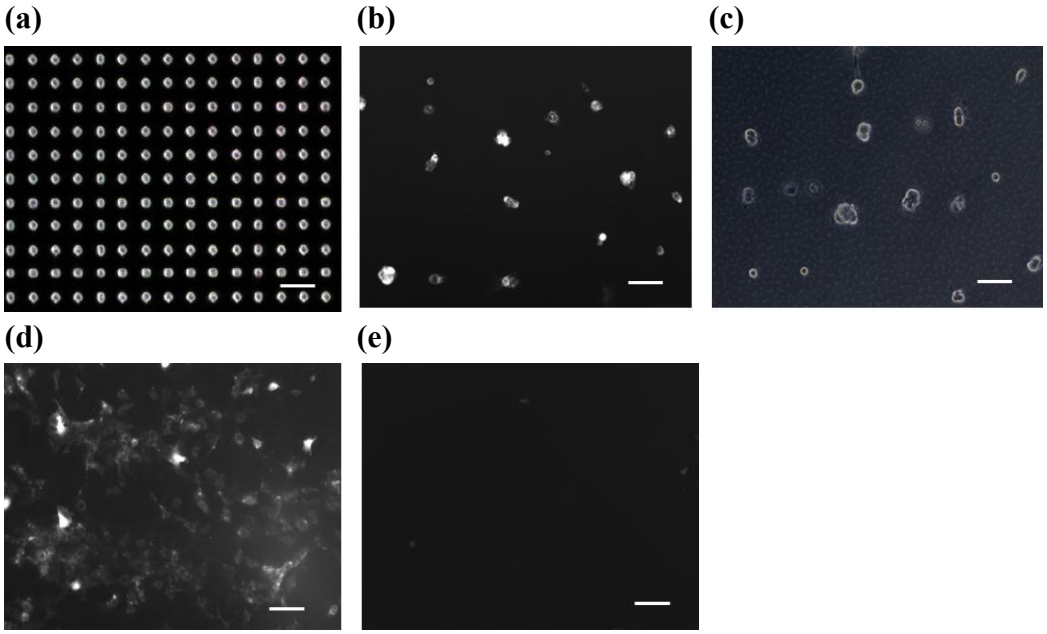

Figure 9.12: (a) Photomask used to pattern 3T3 fibroblasts **(b)** dyed with CellTracker™ Red in a fluorescent micrograph and **(c)** in a phase contrast image on HA R[-]GDS hydrogels at 3 days post seeding. **(d)** Non-patterned HA-R[-]GDS where entire gel surface was exposed to UV light and **(e)** HA-R[-]GDS gel not exposed to light at all for comparison. Scale bars = 100 μm.

9.6 Co-culture Patterning Studies

Co-culture patterns were created and shown in Chapter 7 (Figure 7.5) and Chapter 8 (Figure 8.3) featuring either 100 μm lines or circles, respectively, filled with an initial population of 3T3 fibroblasts surrounded by a subsequently seeded population of HUVECs. In this technique, the background cell-non-adhesive areas surrounding the initial cell pattern were later switched to become cell-adhesive via exposure of the whole patterning platform to near-UV light at 365 nm allowing for the seeding of the second cell type. Other techniques have been developed in the literature capable of generating similar co-culture patterns; they were termed "switchable surfaces" and discussed in Chapter 3, Section 3.3.1. Several limitations exist with these techniques; the spatial pattern of the second cell population is limited and further, after the seeding of the second cell population, there is no potential for seeding a third or creating additional adhesive patterns because the entire surface is filled with cells. Furthermore, by rendering the entire surface cell adhesive, there is no longer any chemical pattern holding the two cell populations to their initial patterned geometry; cells

became free to migrate with time and this was seen experimentally. Note, however, that in some cases this free migration may be desirable to, for example, monitor cell responses to different microenvironments with different pattern geometries or to pattern cells and then allow them the freedom to self-assemble.

With all of the patterning techniques involving "switchable surfaces," the initial cell population is exposed to mild conditions to switch the background non-adhesive surface to become cell-adhesive. Previous mild stimuli explored in the literature included serum manipulations whereby the first cells were seeded in serum-free media and the addition of serum destroyed the non-adhesive coating rendering it adhesive.[34] Others included changes in temperature,[35] and exposure to charged polymeric materials for electrostatic adsorption of adhesive materials onto a cell non-adhesive background.[36] Our technique proposed exposure of initially seeded cells to light at 365 nm.[37] All of these stimuli can be expected to impact cell behavior and may impact viability. It is likely that different cell types will be more sensitive to some of these stimuli than others. Therefore, the nature and goal of the experiments to be performed with a co-culture cell platform combined with cell types used would determine which stimulus or patterning platform would be most useful. As such, we undertook to better understand the impact of 365 nm light at different doses to our model cells, 3T3 fibroblasts.

Initial experiments investigated the impact of 365 nm light doses on initial cell survivability and growth. These experiments were outlined in Chapter 7, Section 7.3. Cell counts and live/dead staining with trypan blue were conducted at one hour post near-UV exposure and after three days post exposure upon removal of the cells. For exposure times up to and including 15 minutes, there was no significant decrease in the number of live cells at one hour post exposure, and at all exposure times cells grew over several days to reach confluence in tissue culture plates. In Chapter 8, the impact of near-UV exposure was further explored. Live/dead staining was conducted within the test plates using calcein AM to stain the cytoplasm of live cells green and ethidium homodimer to stain the nuclei of dead cells red at six hours post exposure and at one day post exposure. There was no significant decrease in the number of live cells six hour post exposure for near-UV exposure times 12

minutes and under showing high initial survivability similar to previous results in Chapter 7. But for an exposure time of 30 min, a significant decrease was seen. Furthermore, this time, cell metabolism was monitored via an MTT assay which showed significant decreases in cell metabolism for all near-UV exposure times compared to non-exposed controls. In addition, at one day post exposure live/dead staining showed a significant decrease in the number of live cells for UV exposure times of 12 min and 30 min. Cells exposed for 12 min were likely able to re-grow over two days; this explains the previous results in Chapter 7. Results therefore showed that by using the aforementioned co-culture method, whereby initially seeded cells are exposed to the UV lamp at 365 nm light (~7 mW/cm^2) for 12 min as required for uncaging, it is expected that cell metabolism will be impacted and some cells will die, but that remaining cells have the capacity for proliferation to replace dead cells.

9.7 Dynamic Cell Patterning

Due to the inherent limitations with the co-culture patterning strategy discussed above in addition to the potential for cell damage with near-UV light exposure, it was desired to develop the patterning methodology further so that initial cell populations on the patterned gels were not exposed to near-UV light once seeded and so that cell co-culture patterns could be created with less limited geometries. In Chapter 8, a new method of light exposure was introduced using a fluorescence microscope with a 365 nm near-UV filter. The field diaphragm could be adjusted to change exposure size, and thus cell pattern size. In Chapter 8, a 3T3 cell pattern was created using this technique (Figure 8.5). The cell patterning platform was subsequently used to pattern two different cell populations, each with circular geometries held apart from one another (Figure 8.6). This ability to do so on a hydrogel material containing an underlying chemical pattern of adhesivity has been rare in the literature to date (see literature reviews in Chapters 1-2). The technique was further applied to alter the geometry of a single cell population pattern with time. In Chapter 8, Figure 8.7 cell growth and migration was controlled via this dynamic patterning methodology. This dynamic patterning allows for serial manipulations of the hydrogel to add additional cell adhesive regions at selected time points to control cell growth and migration. This ability, too, has been rare to achieve on a chemically patterned hydrogel to date (see literature reviews in Chapters 1-2).

Over the past decade, several strategies for hydrogel cell patterning have emerged as reviewed in Chapter 2, section 2.4 including physical patterning. While chemical cell patterns benefit from having underlying material chemistries generating cell-adhesive and non-adhesive regions to hold cells in place, there do exist different physical patterns within body tissues, and in the future it may be interesting to combine techniques. For example, a layer of HA could be coated onto a physically patterned surface, and then an appropriate microscope could be used to create different adhesive and non-adhesive regions within the structure.

A variety of other promising techniques for hydrogel patterning using chemical methods have been developed by others without the use of light as stimuli. While they offer a variety of advantages for different applications, they cannot combine the spatial and temporal control offered by light. For example, Vermesh et al. were able to achieve close to a single-cell resolution and co-culture patterns by patterning cells on glass and then transferring them onto a hydrogel.[38] Such a technique offers excellent resolution, but does not allow for temporal control, or dynamic changes to the pattern. Furthermore, Tekin et al. were able to use temperature as a stimulus with micromoulding techniques to create patterns with a variety of shapes and even form co-cultures in limited geometries, but their method was not suited for dynamic changes.[39]

Several methods by others have also been developed implementing light as a stimulus for spatial control over cells. One method employs PEG acrylates using light as a stimulus for polymerization to form the PEG hydrogel. Biomolecules are subsequently added via light activation of remaining acrylate groups.[32,40,41] In another method pioneered by Shoichet's group (as reviewed in Chapter 4), caging groups are used to block functions such as sulfhydryl groups, which can be used to bind a biomolecule after light exposure.[42,43] Such research is very promising as it allows for the addition of virtually any biomolecule to the polymer, which can allow for increased flexibility in biomaterial synthesis.

Our strategy is limited to the use of RGDS to create cell adhesive regions. On the other hand, our methodology may be better suited for co-culture and dynamic patterns. In

our strategy, upon light exposure, the 2-NB group is released and adhesive regions are created directly. For the required sequential exposure steps in the other strategies, acrylate groups must be stimulated in the presence of potentially toxic photo-initiators and/or a biomolecule must be added in solution surrounding initially seeded cells and allowed to bind. All of the molecules in this multi-step reaction have the potential to impact already-seeded cells. Furthermore, extensive washing steps must be used to wash away the often "sticky" unbound biomolecules, which can create stress on cells that populate the biomaterial.

In summary, as can be seen in the literature, there is a significant and growing interest in patterning hydrogels which are an ideal substrate for mimicking natural tissue physicochemical properties for both cell biology research and tissue engineering. While there are several varieties of exciting hydrogel patterning strategies being developed, each has distinct benefits for different applications. Our patterning strategy developed within this thesis has distinct advantages compared to existing technology for dynamic patterning applications, including the manipulation of cell patterns with time and patterned co-culture formation.

9.8 Conclusion

In support of our initial hypothesis, we were able to create a cell-patterned hyaluronic acid hydrogel using photocaged cell-adhesive peptides. The base hydrogel, consisting of HA polymer crosslinked with ADH, was found to be non-adhesive to model animal cells. Adhesive regions were created via the synthesis and covalent binding of RGDS peptides to the hydrogel. These RGDS peptides were rendered light-responsive, and non-adhesive, via the binding of a 2-NB caging group. This 2-NB group was bound to two different functions within the peptide: to the peptide backbone amide nitrogen between Arg and Gly (termed R[-]GDS) and to the Asp side chain carboxyl group (termed (RG[D]S). The two photocaged peptides were modeled, compared, and contrasted. Ultimately, R[-]GDS was selected for incorporation into gels for cell patterning. Uncaging via 365 nm light either with a UV lamp plus patterned photomask, or a focused fluorescence microscope with a UV light source, rendered the HA gel bound with caged R[-]GDS peptides adhesive in the regions of light

exposure. This strategy allowed for patterning of NIH 3T3 fibroblasts, the model animal cells. This hydrogel patterning strategy further allowed for the formation of patterns containing multiple cell populations, or patterned co-cultures. This novel technique also demonstrated the ability to form dynamic patterns that could be changed with time.

9.9 References

1. Hermanson GT. *Bioconjugate Techniques*. Rockford, Illinois: Academic Press; 1996.

2. Prestwich GD, Marecak DM, Marecek JF, vercruysse KP, Ziebell MR. Controlled chemical modification of hyaluronic acid: synthesis, applications, and biodegradation of hydrazide derivatives. *Journal of Controlled Release.* 1998;53:93-103.

3. Vercruysse KP, Marecak DM, Marecek JF, Prestwich GD. Synthesis and in Vitro Degradation of New Polyvalent Hydrazide Cross-Linked Hydrogels of Hyaluronic Acid. *Bioconjugate Chemistry.* 1997;8(5):686-694.

4. Pouyani T, Harbison GS, Prestwich GD. Novel Hydrogels of Hyaluronic Acid: Synthesis, Surface Morphology, and Solid-State NMR. *Journal of the American Chemical Society.* 1994;116(17):7515-7522.

5. Lapčík J, L., Lapčík L, De Smedt S, Demeester J, Chabreček P. Hyaluronan: Preparation, Structure, Properties, and Applications *Chemical Reviews.* 1998;98(8):2663-2684.

6. Necas J, L. Bartosikova L, Brauner P, Kolar J. Hyaluronic acid (hyaluronan): a review. *Veterinarni Medicina.* 2008;53(8):397–411.

7. Motokawa K, Hahn SK, Nakamura T, Miyamoto H, Shimoboji T. Selectively crosslinked hyaluronic acid hydrogels for sustained release formulation of erythropoietin. *Journal of biomedical Materials Research.* 2006;78A(3):459-465.

8. Pelham Jr. RJ, Wang Y-L. Cell locomotion and focal adhesions are regulated by substrate flexibility. *Proceedings of the National Academy of Sciences.* 1997;94(25):13661-13665.

9. Lo C-M, Wang H-B, Dembo M, Wang Y-l. Cell Movement Is Guided by the Rigidity of the Substrate. *Biophysical Journal.* 2000;79:144–152.

10. Seidlits SK, Khaing ZZ, Petersen RR, et al. The effects of hyaluronic acid hydrogels with tunable mechanical properties on neural progenitor cell differentiation. *Biomaterials.* 2010;31(14):3930-3940.

11. Kim D-H, Han K, Gupta K, Kwon KW, Suh K-Y, Levchenko A. Mechanosensitivity of fibroblast cell shape and movement to anisotropic substratum topography gradients. *Biomaterials.* 2009;30(29):5433-5444.

12. Walker JM. *The Protein Protocols Handbook*. Totowa, New Jersey: Humana Press Inc.; 1996.

13. Decuzzi P, Ferrari M. Modulating cellular adhesion through nanotopography. *Biomaterials.*31(1):173-179.

14. Tatsu Y, Nishigaki T, Darszon A, Yumoto N. A caged sperm-activating peptide that has a photocleavable protecting group on the backbone amide. *FEBS Lett.* 2002;525(1-3):20-24.

15. Dechantsreiter MA, Planker E, Matha B, et al. N-Methylated Cyclic RGD Peptides as Highly Active and Selective αvβ3 integrin antagonists. *Journal of Medicinal Chemistry.* 1999;42(16):3033-3040.

16. Xiong J-P, Stehle T, Zhang R, et al. Crystal Structure of the Extracellular Segment of Integrin αVβ3 in Complex with an Arg-Gly-Asp Ligand. *Science.* 2002;296(5565):151-155.

17. Cherny RC, Honan MA, Thiagarajan P. Site-directed mutagenesis of the arginine-glycine-aspartic acid in vitronectin abolishes cell adhesion. *Journal of Biological Chemistry* 1993;268(13):9725-9729.

18. Wood JS, Koszelak M, Liu J, Lawrence DS. A Caged Protein Kinase Inhibitor. *Journal of the American Chemical Society.* 1998;120(28):7145-7146.

19. Bourgault S, Létourneau M, Fournier A. Development of photolabile caged analogs of endothelin-1. *Peptides.* 2007;28(5):1074-1082.

20. Petersen S, Alonso JM, Specht A, Duodu P, Goeldner M, del Campo A. Phototriggering of Cell Adhesion by Caged Cyclic RGD Peptides. *Angew. Chem., Int. Ed.* 2008;47(17):3192-3195.

21. Nandy SK, Agnes RS, Lawrence DS. Photochemically-Activated Probes of Protein–Protein Interactions. *Organic Letters.* 2007;9(12):2249-2252.

22. Shigeri Y, Tatsu Y, Yumoto N. Synthesis and application of caged peptides and proteins. *Pharmacol. Ther.* 2001;91(2):85-92.

23. Ellis-Davies GCR. Caged compounds: photorelease technology for control of cellular chemistry and physiology. *Nat Meth.* 2007;4(8):619-628.

24. Petersen S, Alonso JM, Specht A, Duodu P, Goeldner M, del Campo A. Phototriggering of Cell Adhesion by Caged Cyclic RGD Peptides. *Angewandte Chemie International Edition.* 2008;47(17):3192-3195.

25. Ohmuro-Matsuyama Y, Tatsu Y. Photocontrolled Cell Adhesion on a Surface Functionalized with a Caged Arginine-Glycine-Aspartate Peptide. *Angewandte Chemie International Edition.* 2008;47(39):7527-7529.

26. Goubko C, Majumdar S, Basak A, Cao X. Hydrogel cell patterning incorporating photocaged RGDS peptides. *Biomedical Microdevices.* 2010;12(3):555-568.

27. Goubko CA, Basak A, Majumdar S, Jarrell H, Huan Khieu N, Cao X. Comparative analysis of photocaged RGDS peptides for cell patterning. *Journal of Biomedical Materials Research - Part A* 2013;101 A (3):787-796.

28. Montalbetti CAGN, Falque V. Amide bond formation and peptide coupling. *Tetrahedron.* 2005;61(46):10827-10852.

29. du Vigneaud V, Ressler C, Swan CJM, Roberts CW, Katsoyannis PG, Gordon S. The synthesis of an octapeptide amide with the hormonal activity of oxytocin. *Journal of the American Chemical Society.* 1953;75(19):4879-4880.

30. Merrifield RB. Solid Phase Peptide Synthesis. I. The Synthesis of a Tetrapeptide. *Journal of the American Chemical Society.* 1963;85(14):2149-2154.

31. Verlander M. Industrial Applications of Solid-Phase Peptide Synthesis - A Status Report. *International Journal of Peptide Research and Therapeutics.* 2007;13(1-2):75-82.

32. Liu VA, Bhatia SN. Three-dimensional photopatterning of hydrogels containing living cells. *Biomed. Microdevices.* 2002;4(4):257-266.

33. Bhatia SN, Chen CS. Tissue Engineering at the Micro-Scale. *Biomedical Microdevices.* 1999;2(2):131-144.
34. Bhatia SN, Yarmush ML, Toner M. Controlling cell interactions by micropatterning in co-cultures: Hepatocytes and 3T3 fibroblasts. *Journal of Biomedical Materials Research* 1997;34(2):189 - 199.
35. Yamato M, Kwon OH, Hirose M, Kikuchi A, Okano T. Novel patterned cell coculture utilizing thermally responsive grafted polymer surfaces *Journal of Biomedical Materials Research.* 2001;55(1):137-140.
36. Yang IH, Co CC, Ho C-C. Spatially controlled co-culture of neurons and glial cells. *Journal of Biomedical Materials Research - Part A.* 2005;75A(4):976-984.
37. Goubko CA, Majumdar S, Basak A, Cao X. Novel cell patterning platform employing photocaged RGDS peptides on a hydrogel. In: AIChE, ed. *AIChE Annual Meeting*. Nashville, TN: AIChE; 2009.
38. Vermesh U, Vermesh O, Wang J, et al. High-Density, Multiplexed Patterning of Cells at Single-Cell Resolution for Tissue Engineering and Other Applications. *Angew. Chem., Int. Ed.* 2011;50(32):7378-7380.
39. Tekin H, Tsinman T, Sanchez JG, et al. Responsive Micromolds for Sequential Patterning of Hydrogel Microstructures. *J. Am. Chem. Soc.* 2011;133(33):12944-12947.
40. Hahn MS, Taite LJ, Moon JJ, Rowland MC, Ruffino KA, West JL. Photolithographic patterning of polyethylene glycol hydrogels. *Biomaterials.* 2006;27(12):2519-2524.
41. Moon JJ, Hahn MS, Kim I, Nsiah BA, West JL. Micropatterning of poly(ethylene glycol) diacrylate hydrogels with biomolecules to regulate and guide endothelial morphogenesis. *Tissue Engineering - Part A.* 2009;15(3):579-585
42. Luo Y, Shoichet MS. A photolabile hydrogel for guided three dimensional cell growth and migration. *Nature Materials.* 2004;3:249-253.
43. Musoke-Zawedde P, Shoichet MS. Anisotropic three-dimensional peptide channels guide neurite outgrowth within a biodegradable hydrogel matrix *Biomedical Materials.* 2006;1(3):162-169

CHAPTER 10:
FUTURE DIRECTIONS

10.1 Introduction to Preliminary Results and Future Directions

With the hydrogel chemical patterning platform, several paths for future study are envisioned. First of all, the HA hydrogel could now be coated into the interior of the polymeric conduits developed by Dr. Cao's laboratory group for SCI treatment. The HA coating can be patterned with lanes to guide cells through the device as described in Figure 1.1a of the introduction chapter. Furthermore, 2D cell biology studies could be conducted on the cell patterning device to determine optimal gel properties and patterns for treatment, which can then be incorporated into the tissue engineering device. Furthermore, the works published as part of this thesis relied on the use of 3T3 fibroblast cells as model animal cells to test the components and functionality of our patterning platform. In the context of developing a patterned device for SCI treatment, it would be of interest to be able to pattern neural stem/progenitor cells (NSPCs). To this end, background information on NSPCs was collected and some preliminary experiments were conducted using these cells. This work as well as recommendations for future study along this path will be outlined in the following Section 10.2.

In the introduction to this thesis, 3D hydrogels with patterned adhesive channels were also discussed. Another branch of future work could involve the translation of the patterning strategy developed in this thesis from 2D hydrogel surface patterning to patterning 3D volumes of hydrogel. A change in the light source for uncaging to a 2-photon laser source, which has the ability to focus on a volume within a material with 3-D specificity, would assist in this translation to 3D. Background information, preliminary results, and some recommendations for future study involving this technology can be found in Section 10.3. To accommodate 3D patterning, the HA hydrogel chemistry used in this thesis would have to be altered, and ideas for this future research are discussed in Section 10.4 along with potential methods for analyzing 3D gel patterns. Please note that the work shown in this chapter is in the very preliminary stages and should not be used to draw conclusions, but is instead meant to inspire ideas for future research paths based on the hydrogel patterning strategy developed in this thesis.

10.2 Preliminary Neural Stem Cell Work

10.2.1 Introduction to Neural Stem/Progenitor Cells (NSPCs)

Twenty years ago, it was widely believed that the central nervous system (CNS), including the human brain and spinal cord, was incapable of self-regeneration. We now know that there exist stem cells in the adult CNS, termed neural stem cells (NSCs), which actively proliferate throughout one's lifetime to generate new neurons with the ability to functionally integrate into the existing neural circuitry.[1,2] This development offers new hope for the treatment of neurodegenerative diseases and CNS trauma like spinal cord injuries (SCIs).

Stem cells, including NSCs, can be defined as cells which demonstrate the following characteristics: (1) the ability to proliferate in order to make copies of themselves over multiple generations, (2) possess the ability to become, or differentiate, into the major cell types present in the tissue from which they are derived, and (3) possess the ability to regenerate the tissue from which they were isolated.[3] NSCs have the ability to generate new neurons (process of neurogenesis), astrocytes, and oligodendrocytes, and to proliferate to generate more NSCs. Neurons serve as the functional units of the nervous system and perform the bulk of the information processing in the body. The other cells present in the nervous system are referred to as glial cells. Glial cells are thought to be supporting cells for neurons, and they include astrocytes and oligodendrocytes. Astrocytes are the most numerous glia in the brain, and are found to fill the space between neurons. They appear to regulate the chemical composition of the extracellular space surrounding neuronal cells. Oligodendrocytes, on the other hand, surround neuronal axons with layers of insulating membrane to enhance signal transduction.[4]

In the CNS, NSCs are found to mainly reside in two regions of the brain. First, is the subgranular zone (SGZ) of the hippocampal dentate gyrus (DG) which produces new neurons locally in the hippocampus. The hippocampus is a region of the brain known to be involved in memory and spatial learning. The second region is in the subependymal layer of the lateral ventricle, also referred to as the sub-ventricular zone (SVZ).[1] In the SVZ, neurons are generated continuously and have been found to migrate into the olfactory bulb, which is

involved in the perception of odors, where they mature into interneurons. This neurogenesis provides the brain with a level of plasticity. Existing neural circuits are altered by the addition of new cells and the subsequent structural remodeling. Studies have also noted that most brain injuries cause an increase in proliferation of NSCs in the SGZ and the SVZ, and can lead to new neurons migrating to the site of injury. Thus, these cells may be used as an endogenous repair mechanism.[2] Therefore, it is of great interest to implement these cells in the future within the tissue engineering devices our lab group is designing to aid in the repair of SCI.

10.2.2 Potential Applications of our Patterning Platform to NSC Research

First of all, our hydrogel base comprised of HA may have the potential to mimic the natural environment of NSCs (i.e. the areas where they are found in the human body) as follows. HA is highly expressed during CNS development when NSCs are especially active, and even in adulthood the structural organization of the ECM in this tissue is based heavily on HA.[5] HA hydrogels have been shown to exhibit mechanical properties similar to that of brain tissue.[6] Furthermore, NSPCs have been seeded into 3D hydrogels incorporating HA where they survived and matured *in vivo*; implanted materials comprised of HA have also been shown in preliminary studies to minimize glial scar formation after injury, and to promote vascularization and cell migration into damaged tissue.[7]

Patterning of a cell type on a material allows for increased control over the cell microenvironment, and the microenvironment has been shown to be critical in determining NSC behavior and function. For example, adult NSCs from the SVZ have been shown to give rise to new hippocampal neurons when placed in the hippocampus. Alternatively, NSCs from the SVZ that are removed from their niche to areas that are normally non-neurogenic (do not generate new neurons), fail to give rise to new neurons. Conversely, stem cells from normally non-neurogenic regions, when transplanted into the neurogenic SVZ have been found to generate neurons.[1] Therefore, it would seem that stem cells and NSCs can be manipulated to generate new neurons in the correct microenvironment, and so new techniques to gain better control over the design of this environment, such as cell patterning, are critical.

In the body, NSCs do not exist in a randomly distributed fashion. Instead, they exist within specific geometric patterns; in the SVZ region of the brain, cells are organized in a distinct, highly organized "pinwheel" structure[8] so their geometry may be very important for function. Preliminary studies involving the patterning of NSCs suggested that patterning density and shape can influence differentiation.[9] Varying cell patterns has been shown to impact differentiation of other stem cells; for example, stem cells cultured on smaller adhesive islands preferentially differentiated into adipocytes (fat cells), while those on larger sized islands were found to favor an osteogenic (bone cells) fate.[10] Therefore, NSCs could be patterned in different geometries using our platform *in vitro* to investigate its impact on cell adhesion, migration, growth, and differentiation into different cell types. Knowledge generated from such works can be translated into improved tissue engineering device designs employing cell patterning *in vivo*.

Furthermore, our hydrogel patterning strategy has been shown to support patterned co-cultures, whereby the spatial localization of multiple cell types on the hydrogel surface can be controlled. Studies have shown that NSC behavior, including differentiation, is highly influenced by neighboring cells. For example, in the body, NSCs make direct contact with endothelial cells; Tavazoie et al. found that most regenerative NSC proliferation occurs at these sites of direct contact with vasculature.[11,12] Recent work has begun to look at systems co-culturing endothelial cells and NSCs.[13,14] Meng et al. showed that grafts containing both cell types were able to improve NSC survival and differentiation as compared to NSCs alone when used to treat SCI.[15] Astrocytes are another major cell type identified as a component of the NSC niche,[16] and co-culture of adult NSCs with astrocytes have been shown to promote differentiation towards a neuronal cell type.[2] Lim and Alvarez-Buylla found that SVZ NSCs, when cultured on a monolayer of astrocyte cells, demonstrated significant neurogenesis and that direct cell-cell contacts played an important role in encouraging differentiation to neurons.[17] Song et al. showed that adult astrocytes from the hippocampus were capable of directing NSCs towards a neuronal fate.[18] Therefore, co-culture patterning could be used to present these cell types to each other in geometries found *in vivo*. Also, different spatial geometries could be investigated to optimize NSC survival and

differentiation in the presence of different cell types. Results from such work could also potentially be translated into improved tissue engineering device designs for regeneration.

Our platform can also be dynamic and change with time. Theoretically, patterns could be slowly altered with time to add additional adhesive regions to guide where NSPCs adhere and migrate and to control the directional growth of neurites to produce deliberate and ordered neural networks *in vitro* for investigation, and eventually for *in vivo* tissue engineering applications.

The versatility of our patterning platform holds many potential applications for NSPCs. However, prior to realizing these goals, it was necessary to conduct preliminary experiments to determine whether NSPCs could adhere and survive on HA gels bound with RGDS peptides and whether they could be patterned. Early experiments to these ends are described in this section.

10.2.3 Materials and Methods

Please refer to Chapter 8 for the materials and methods necessary to synthesize HA hydrogels, RGDS peptides, caged R[-]GDS peptides, to bind peptides to the hydrogel, to pattern with a fluorescence microscope, and for live/dead staining and imaging techniques. NSPCs of the brain and spinal cord, from the SVZ and ependymal zone of the central canal, respectively, in 2-3 month old female Sprague Dawley rats were harvested and cultured in the laboratory of Dr. Eve Tsai. The NSPCs discussed herein were harvested and donated by Dr. Tsai's lab group.

10.2.4 Preliminary Results and Discussion

A preliminary study was conducted to investigate the cytocompatability of our hydrogel patterning platform with NSPCs. NSPCs were harvested from the spinal cord and the brain of rats and were cultured on the surface of both pure HA hydrogel and the gel bound to RGDS. After one week, the cells were stained with a live/dead kit whereby live cells were stained green with Calcein AM and dead or dying cells stained red from Ethidium homodimer. From Figure 10.1 and 10.2, the populations of stained green cells indicate that

the base of our patterning platform - HA hydrogel bound with RGDS peptide - is capable of supporting live NSPCs from both the spinal cord and brain for at least one week in culture.

Preliminary visual observations noted that fewer cells tended to bind to the pure HA hydrogels, and those that did bind tended to remain round in shape (Figures 10.1A, 10.2A) compared to the gels with bound RGDS (Figures 10.1B, 10.2B). In the literature, hydrogels made of pure HA were found to have low adhesivity to NSPCs.[19] Studies also showed that RGDS peptides could stimulate NSC adhesion when bound to otherwise non-adhesive surfaces.[20] Interestingly, linear RGDS at low densities was found to promote neurogenesis in mesenchymal stem cells.[21] Therefore, RGDS density may impact differentiation patterns and this should be investigated in the future.

Figures 10.1 B and C contain numerous spinal-cord derived cells bound to the HA-RGDS hydrogels. In Figure 10.1 B, many of the cells have extended neurites, and in Figure 10.1 C, some of the cells appear to have extended neurites over 100 μm in length. The extension of neurites is promising, as this is needed to establish contact with other neural cells to form functioning neural networks. Figures 10.2 B-D show a number of brain-derived cells bound to HA-RGDS gels with some extending neurites. From preliminary visual observations, spinal-cord derived cells seemed to exhibit different morphologies compared to those from the brain; they appeared to produce more cells with numerous neurites. It is too early to draw conclusions, but in future studies it should be kept in mind that there may be differences in behavior between the two cells types placed in similar microenvironments which could also be studied in the future.

Interestingly, the hydrogel in Figure 10.2 C, typical of the hydrogels produced, has lined microcracks at the edge of the hydrogel where it connected with the walls of the TCP. In this region, the NSPCs appeared to produce neurites aligned with such microcracks. Recent literature has also noted that NSCs can produce neurites aligned with microgrooves or channels in polymeric materials.[22] This preliminary work suggests that combining physical patterning with our chemical patterning in the future may assist in guiding neurite growth.

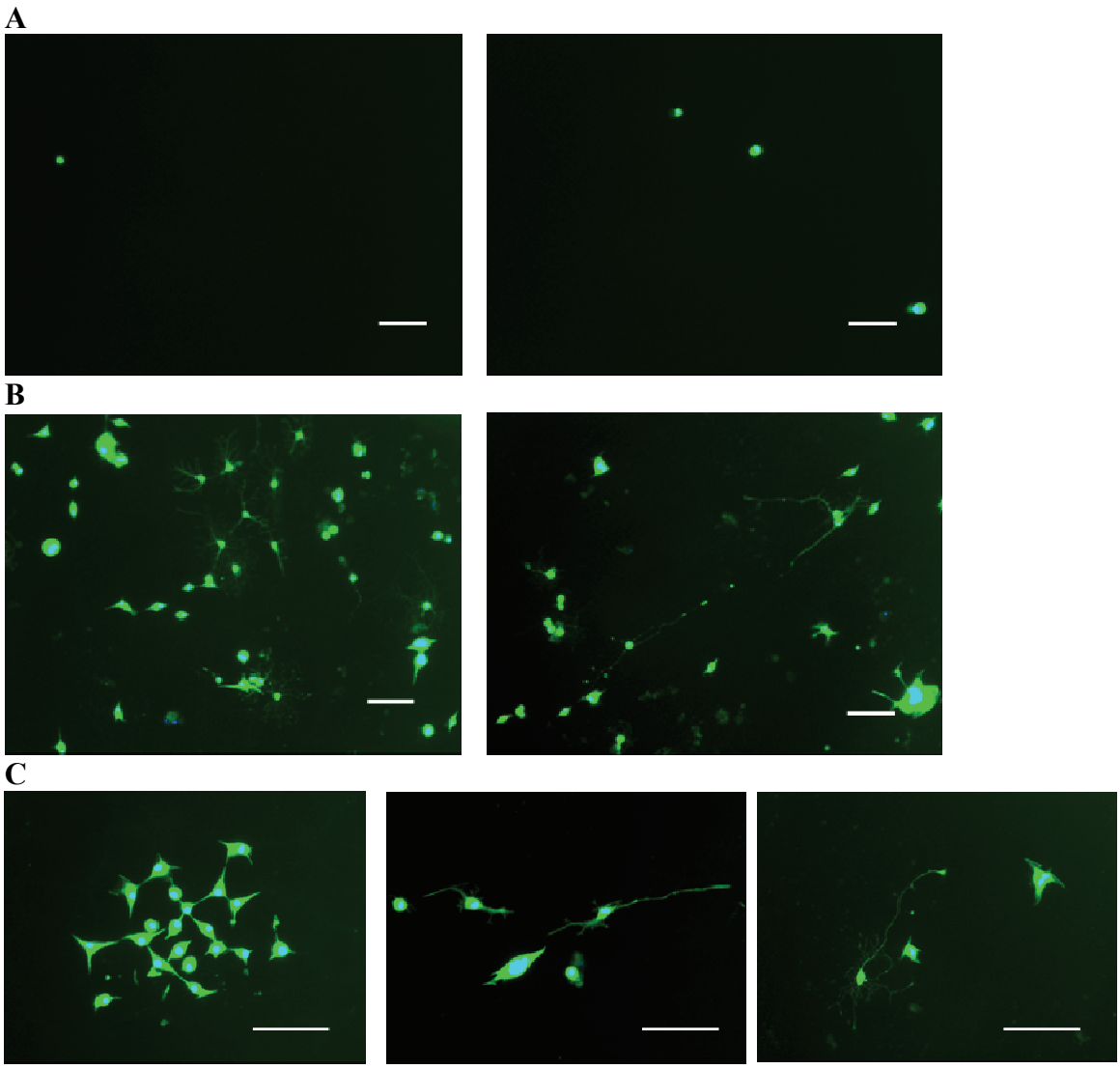

Figure 10.1: Fluorescence images of spinal cord-derived NSPCs stained with a live/dead kit (Calcein AM/Ethidium homodimer) after seven days of culture on the following gels: **(A)** HA **(B)** HA-RGDS and **(C)** HA-RGDS (higher magnification) Scale bars = 100 μm.

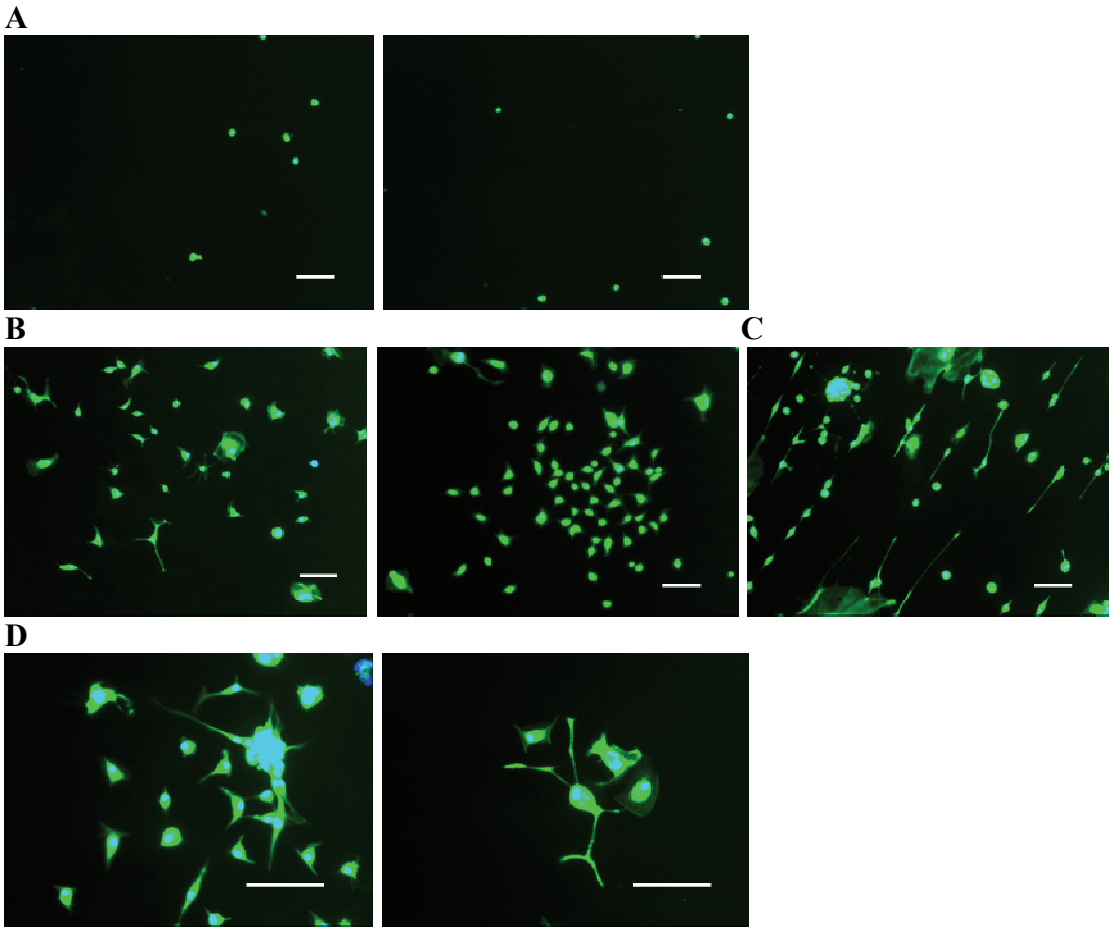

Figure 10.2: Fluorescence images of brain-derived NSPCs stained with a live/dead kit (Calcein AM/Ethidium homodimer) after seven days of culture on the following surfaces: **(A)** HA **(B)** HA-RGDS **(C)** HA-RGDS at the edge of the gel where it meets the edge of the TCP well and **(D)** HA-RGDS (higher magnification). Scale bars = 100 μm.

Preliminary patterning attempts were made with the NSPCs. A fluorescence microscope was used to irradiate HA-R[-]GDS gels to produce patterned circular islands of uncaged RGDS. Initially, few cells were harvested and upon seeding on the hydrogel, almost none (fewer than 10-20 in 3.8 cm^2 area) could be found under the microscope. In the previous study, non-adhered NSCs were washed away within 24 hours post seeding, but in the patterning study they were not. After five days, patterns could be seen of adhesive cells (Figure 10.3) and some larger, floating cell clusters could be seen which were not initially present. This could possibly indicate that some cell growth occurred above the hydrogel and some of the cells produced adhered to the patterned regions, but this would need to be

verified experimentally. NSCs are known to proliferate as spherical aggregates termed "neurospheres" on non-adhesive surfaces, and form adhered monolayers on adhesive surfaces.[20] Hydrogels made of pure HA have been found to promote cell aggregation into clusters.[19]

Figure 10.4 is a phase contrast image, and shows a circular pattern present at 12 days post seeding. Note cells appear well-spread and dense within a confined region outside of which few cells appear to be bound. In Figure 10.3C, a fluorescence micrograph image of 3T3 fibroblasts was taken with the microscope diaphragm in the same position as was used to create the circular patterns seen in this study. So, the size of the circular NSPC patterns created on the hydrogels should be of similar size to the circular region in which the fibroblasts were viewed in Figure 10.3C. To compare, a white dashed line was drawn around this region and placed over the NSPC patterns with the same scale. It can be seen that the NSPC cells generally adhere within the confines of the circle, demonstrating that the pattern sizes appear to correlate with that expected to be generated from the fluorescence microscope exposure.

These preliminary patterns need to be repeated with different time frames and different pattern geometries in order to draw conclusions. However, it will prove to be very exciting if our material can be developed to exhibit the dual properties of off-pattern cell growth in non-adhesive areas combined with adhesive region cell-binding. The ability to direct adhesion/differentiation and encourage growth simultaneously on the same material could offer the opportunity for interesting future work towards tissue regeneration.

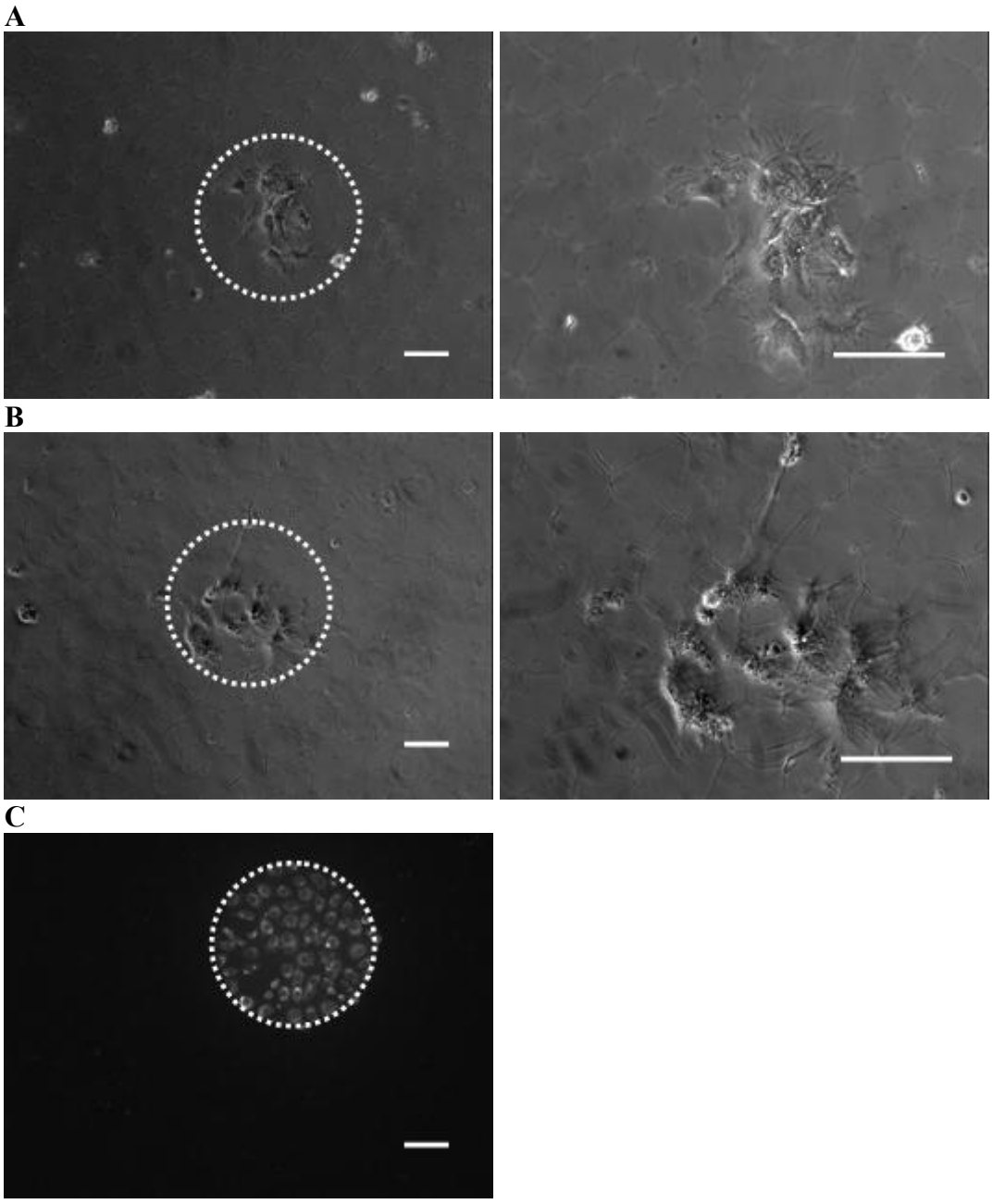

Figure 10.3: Phase contrast micrographs **(A)** and **(B)** show separate circular patterns of neural progenitor cells at 5 days post seeding, each showing two different magnifications of the same pattern created on HA-R[-]GDS hydrogels. **(C)** Image of 3T3 fibroblasts viewed through the opening size of the microscope field diaphragm used to create the circular patterns shown here. Scale bars = 100µm.

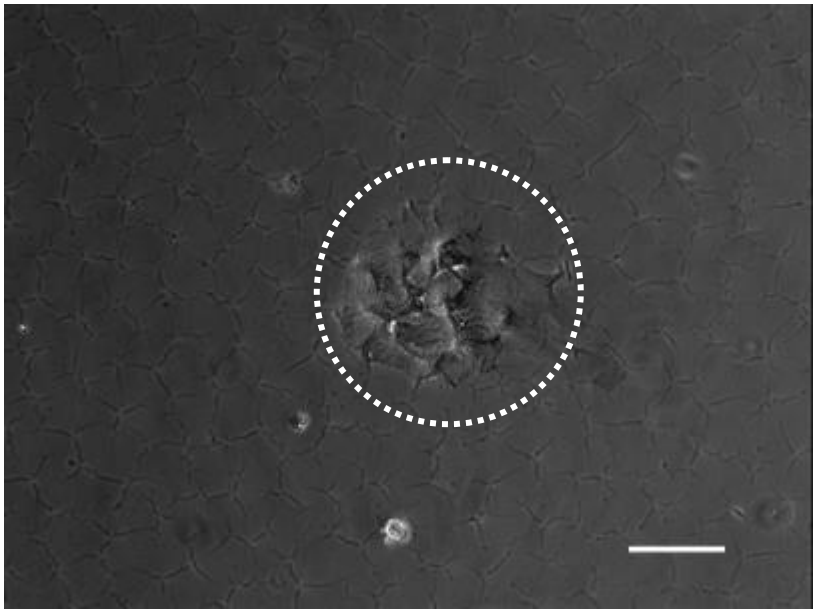

Figure 10.4: Phase contrast micrograph of a NSPC circular patterns at 12 days post seeding on a HA-R[-]GDS patterned hydrogel. Scale bars = 100μm.

10.2.5 Recommended Future Directions

Some preliminary studies were carried out examining the adhesion and viability of NSPCs on our HA-RGDS hydrogels, and it is suggested that these preliminary studies be repeated and expanded to culture brain and spinal cord derived NSPCs on the following gel samples: HA, HA-RGDS, HA-caged R[-]GDS, and HA-uncaged R[-]GDS. Adherent cells could be counted, viability established, and differentiation markers explored to determine the number of cells remaining NSPCs, or differentiating into neurons, oligodendrocytes, or astrocytes with time. Furthermore, patterning could be attempted on different geometries to further demonstrate that the cells can be patterned effectively. Then, as previously discussed, future studies can be designed to evaluate how different patterning platform features – such as different pattern geometries, the presence of another cell type in a patterned co-culture, among others – influence NSPC behaviour and differentiation. Information generated from 2-D culture studies with these cells can later be incorporated into the design of tissue engineering devices, such as for the promotion of tissue regeneration post-SCI, which has been the general focus of this research group.

One exciting potential co-culture application is the patterning of NSPCs on patterned gels atop another cell type, like glial cells. In the early CNS, during development, neurons migrate along radial glial cells which appear to guide them. Therefore, Mattotti et al. created physical micropatterns of lined grooves to direct glial growth and differentiation into radial glial-like cells and then observed that neurons could be guided along such patterned cells, moving approximately five times longer distances at speeds almost three times as fast as controls.[23] Such a strategy using our patterning platform to pattern glial cells in order to guide NSPCs or other neural cells in a device for SCI could result in an interesting study for the future.

10.3 Preliminary 2-Photon Laser Work

10.3.1 Background on 2-Photon Lasers for Uncaging

The experiments conducted throughout this thesis relied on 365 nm light from either a UV lamp or fluorescence microscope light source with near-UV filter. These light sources resulted in single-photon excitation of 2-NB caging groups bound to RGDS peptides whereby a single photon had the energy necessary to excite the caging group, and ultimately generate a free RGDS peptide. Although most photosensitive molecules in biological experiments are activated with single photon sources, there are some drawbacks to their use when compared to the multi-photon excitation that can be employed using two-photon laser technology.[24]

In order for the uncaging reaction to occur using a two-photon laser, the caged sample must simultaneously absorb two quanta of near-infrared light (700-1100 nm) instead of one photon of near-UV light using conventional single-photon processes. Since infrared light is of much lower energy than UV light, two-photon processes have the potential to cause less damage to sensitive biological and biochemical materials. The second major advantage to the use of two-photon lasers for photoactivation is their ability to focus on a volume of material with a high degree of 3-D spatial selectivity. The probability of two photons being simultaneously absorbed by a caged molecule - as required for uncaging with a two-photon laser - is proportional to the square of the light intensity. It is due to this

relationship that two-photon excitation is often referred to as a non-linear process. This property results in the probability being extremely low that excitation of a caged species would occur outside the focal point of the laser in use, since only at this point are the necessary intensities reached. This results in the excellent spatial selectivity of two-photon processes, and in most experiments a spatial resolution of less than 1 μm^3 can be reached. In a single photon process, any scattered light or unintentional light exposure can result in uncaging reactions occurring outside of the desired area since each photon can result in a reaction. Therefore, using a two-photon laser, a wide variety of cell patterns can theoretically be created. Furthermore, since many animal cell sizes are on the order of tens of microns and the two-photon laser has a resolution of at least 1 μm^3, patterning can theoretically reach the single cell level.

Another potential advantage to the use of a two-photon laser is that the IR light used is not significantly absorbed by biological materials. The absorption coefficient of water for IR light in the range of the wavelengths typically used is very low.[24] This property helps to achieve minimum out-of-focus absorption, which allows for an increased depth penetration of excitation light through such biological materials.[24-26] In fact, the light used for two-photon excitation in fluorescence microscopy applications has been found to penetrate up to 1 mm in tissue, at which point the depth of penetration is limited by light scattering.[27] All of these advantages promote the use of a two-photon laser in future patterning studies.

There is one notable disadvantage to the use of two-photon lasers: high intensities of light are sometimes required for certain photoreactions in order to achieve a reasonable probability of two photons being simultaneously absorbed. It has been found that the 2-NB family of caging groups shows relatively small cross sections for two-photon uncaging. Two-photon cross sections (unit = GM) are proportional to the ability of the caging group to absorb the two-photon light, and the quantum yield, which is related to the number of caging groups that react upon absorbing the appropriate light. If the two-photon cross section is low for a given molecule, more laser power must be used in order for uncaging to occur.[24] It has been found that above 10 mW of power, which is sometimes required, damage to biological systems due to multiphoton absorption is likely to occur; it is often cited that 2-nitrobenzyl

derivatives typically demonstrate low quantum yields - well under 0.1 GM - which is a recommended lower limit for biological applications.[28] In addition, researchers have sometimes found a significant time delay for the release of the caging group after excitation.[27] However, for our application, this may not be of concern, since our caged peptides are covalently bound to the hydrogel, and so are held in place and unable to diffuse. These often cited drawbacks to the use of 2-NB groups for 2-photon laser uncaging have resulted in other groups designing photoactive hydrogels with other, newer, caging groups such as those based on coumarin.[29,30] However, two-photon laser excitation has been utilized in the uncaging of 2-NB groups in the literature.[31,32] One of the earliest studies to utilize two-photon excitation to remove a caging group from a molecule was carried out in 1990 by Denk et al. This group successfully used two-photon excitation to trigger the release of ATP, a cell's energy source, from a 2-NB based caging group, DMNPE.[33] It was desired to evaluate whether our HA hydrogel patterning platform based on 2-NB photocaged RGDS could be switched from cell non-adhesive to adhesive using two-photon laser technology.

10.3.2 Materials and Methods

HA-R[-]GDS hydrogels were synthesized as described earlier,[34] with the exception that they were cast on microscope cover slips instead of in the wells of tissue culture plates. Cover slips were pre-cleaned with 2N NaOH, and then pre-coated with poly-D-lysine, which is positively charged and can therefore interact electro-statically with the negatively charged HA hydrogel to bind it to the cover-slip surface. Hydrogel precursor solution was pipetted on top of the cover slips, and allowed to gel. All other gel sample preparation procedures and cell culture procedures were carried out as in Chapter 5. Two-photon laser irradiation of samples was carried out by the laboratory group of Dr. Anis at the University of Ottawa, SITE.

10.3.3 Preliminary Results and Discussion

Our previous work had demonstrated that non-derivatized HA hydrogels crosslinked with ADH and containing no bound peptide failed to adhere cells. HA hydrogels bound to caged R[-]GDS hydrogels were similarly non-adhesive to fibroblasts.[34] As a control, non-derivatized gels were produced, and 3T3 fibroblast cells were seeded and allowed to adhere to the gels for 24 hours. Another set of control non-derivatized gels were exposed to two-

photon laser radiation prior to cell seeding. Since no peptide was bound to these gels, it was expected that the gels would remain cell non-adhesive post-irradiation, and they did so as seen in Figure 10.5A and B. The few cells that can be seen on these gels in the micrograph are clumped and/or rounded in shape. These control gels provided evidence that the laser itself is not capable of switching the HA gel material from non-adhesive to adhesive through some artifact when the photoactive peptide is not present.

Figure 10.5C shows HA hydrogels bound to R[-]GDS peptide exposed to two-photon laser radiation prior to fibroblast seeding. It was hoped that the laser would uncage the peptide to produce adhesive RGDS and thus render the hydrogels adhesive. In Figure 10.5C, numerous cells adhered and spread onto these irradiated hydrogels providing evidence that two-photon laser exposure can be used to switch the HA-R[-]GDS hydrogels to a cell-adhesive state. Furthermore, a visual inspection of the hydrogel macroscopically and via light plus phase-contrast microscopy did not reveal any physical damage to the HA gel.

These preliminary results were promising considering that existing literature warns of the inefficiency and/or ineffectiveness of using 2-photon irradiation to uncage 2-NB groups. It should be noted that some other studies in the literature support our findings, and have also used two-photon laser exposure to stimulate chemical changes in hydrogels employing 2-NB cages. For example, Peng et al. designed a dextran hydrogel incorporating 2-NB and PEG which could release protein or degrade upon two-photon excitation.[35] Wong et al. created a photodegradable hydrogel consisting of PEG and a 2-NB ether moiety to create a biocompatible photoresist. The gel was shown to be easily degraded via two-photon laser exposure.[36] Furthermore, 2-NB groups have been introduced into peptides in the past and released via two-photon irradiation. In such a work, Shigenaga et al. irradiated peptide samples resulting in uncaging which further served to stimulate peptide bond cleavage. The two photon cross-section at 740 nm was estimated to be 0.23 GM for this compound, which is well above the 0.1 GM stated in previous literature as the recommended lower limit for biological applications.[37] These studies suggest it is possible that the chemical environment surrounding the 2-NB group can influence the ease of two-photon laser uncaging, which could explain some of the mixed results achieved in the literature.

(A) Control HA hydrogel not exposed to laser

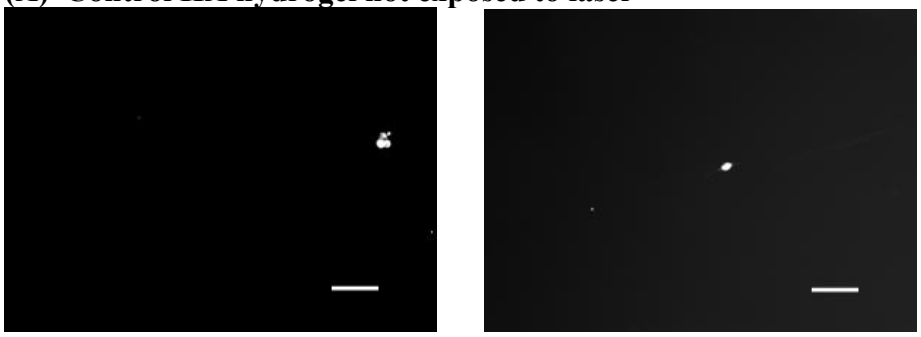

(B) Hydrogel (with no bound R[G]DS) exposed to two-photon uncaging process

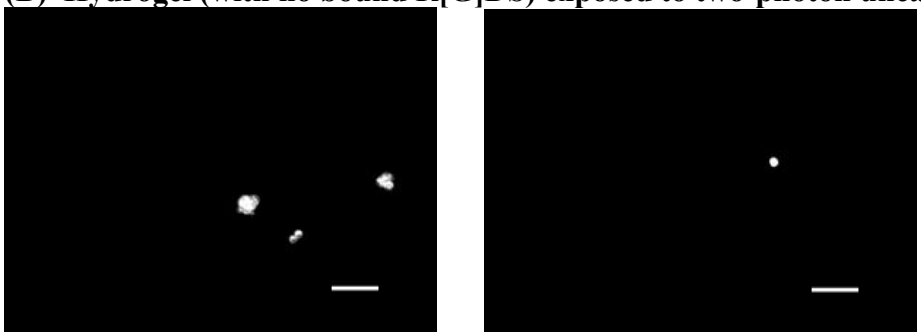

(C) HA hydrogel exposed to two-photon uncaging process

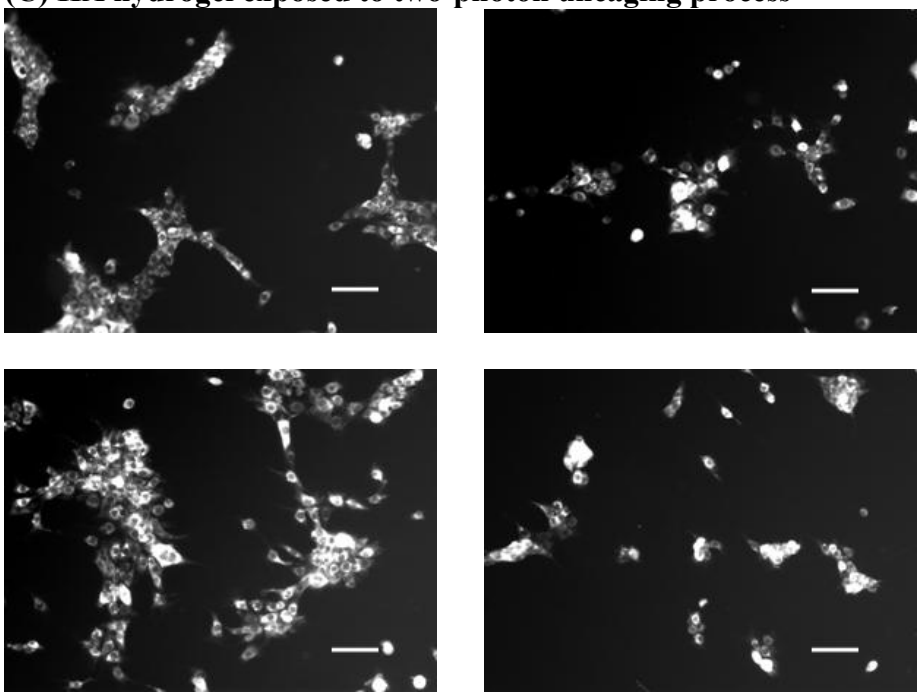

Figure 10.5: Fluorescence micrographs of Cell Tracker Red™ dyed 3T3 fibroblasts 24 hours post seeding on HA hydrogels without peptide and **(A)** no laser exposure (control) and **(B)** exposed to two-photon laser radiation. **(C)** HA-R[-]GDS hydrogels exposed to two-photon laser radiation. Scale bars = 100μm.

Several other studies even suggest that the 2-NB group can be uncaged using cytocompatible laser radiation. A two-photon laser was used successfully to free IP3 (involved in cellular Ca^{2+} regulation) caged with a 2-NB derivative in live cells, such as HELA cells.[38,39] Zhao et al. uncaged ligands for vanilloid receptors, found on neuronal cells, which were caged with a 2-NB derivative. Two-photon excitation was shown to readily release the ligands at light intensities cytocompatible with the neurons.[40] Furthermore, Neveu et al. caged retinoic acid, involved in organ formation, with a 2-NB derivative and demonstrated its release upon 2-photon excitation within a live zebrafish embryo using intensities that were non-detrimental to the biological environment.[41]

With the previous works in mind, and our preliminary results, there is some promising evidence to support the use of two-photon laser radiation for uncaging 2-NB from RGDS peptides for patterning, without damaging the HA hydrogels. Furthermore, it would be ideal for dynamic and co-culture patterning applications if cells previously seeded within the material, and outside the laser focal point, would remain safe if exposed to the laser path. In their work, Wong et al., demonstrated a way to increase the 2-photon sensitivity of 2-NB, which makes it safer to use in a cellular environment, and decreases the chances of harming delicate biomolecules and materials. They conjugated a coumarin fluorophore directly to their 2-NB ether caging group which enhanced the gel's two-photon sensitivity and had the added benefit of allowing for visualization of the areas of the gel containing the caging group.[36] If cell viability issues arose in the future, this might be a promising method to improve the patterned biomaterial production process.

10.3.4 Future Directions

Preliminary results encourage further experimentation using a two photon laser as the source of uncaging for cell patterning. In the future, it will be necessary to repeat these uncaging experiments; hydrogels should be exposed to different laser powers to determine the lowest power required for uncaging. The laser should be finely controlled to form a line or circular pattern on the hydrogel, and verify that cells can repeatedly form this pattern upon seeding.

Once this is accomplished, the laser could be used to attempt to refine the resolution of the current patterning technique. With the laser, one could potentially program a large variety of geometric exposure patterns on the hydrogel, where we were limited to the use of several printed masks, or the shape of the microscope diaphragm in this thesis work.

One of the exciting possibilities from this work is the future formation of 3-D patterns. This would allow for the development of 3D hydrogels containing 3-D adhesive channels with any number of geometries. Therefore, the implementation of the two-photon laser for uncaging can allow the translation of our cell patterning platform to a 3-D device to mimic *in vivo* conditions, with promising future applications in tissue engineering.

10.4. Hydrogels for 3D Patterning

10.4.1. Hydrogel Chemistry

Prior to creating 3D patterns within HA hydrogels, it is desirable to seed cells evenly throughout the hydrogel volume. This can be accomplished by seeding cells in a HA pre-polymer solution and mixing prior to gelation. It would be beneficial to modify the HA hydrogel chemistry used in this work for this application, since gelation occurred at an acidic pH. A literature search was performed to find an appropriate HA gel chemistry close to that of the current work, and the following option was proposed as per the scheme in Figure 10.6. In the proposed scheme, ADH (in 4X excess) is bound to HA using EDC but without crosslinking, as was described by Pouyani et al.[42] Crosslinking of HA-ADH occurs with BS^3 to form a stable hydrogel, as was also described by Prestwich's group.[43] The two terminal N-hydroxysulfosuccinimide groups of BS^3 are primary amine-reactive and have been found to react readily with the hydrazide groups of ADH,[44] and not expected, at neutral pH, to significantly react with bound RGDS or caged RGDS which contains no primary amines. The activity of the peptide should therefore be protected during crosslinking. Furthermore, since BS^3 can be crosslinked at neutral pH, it would be feasible to seed cells prior to gelation.

(A)

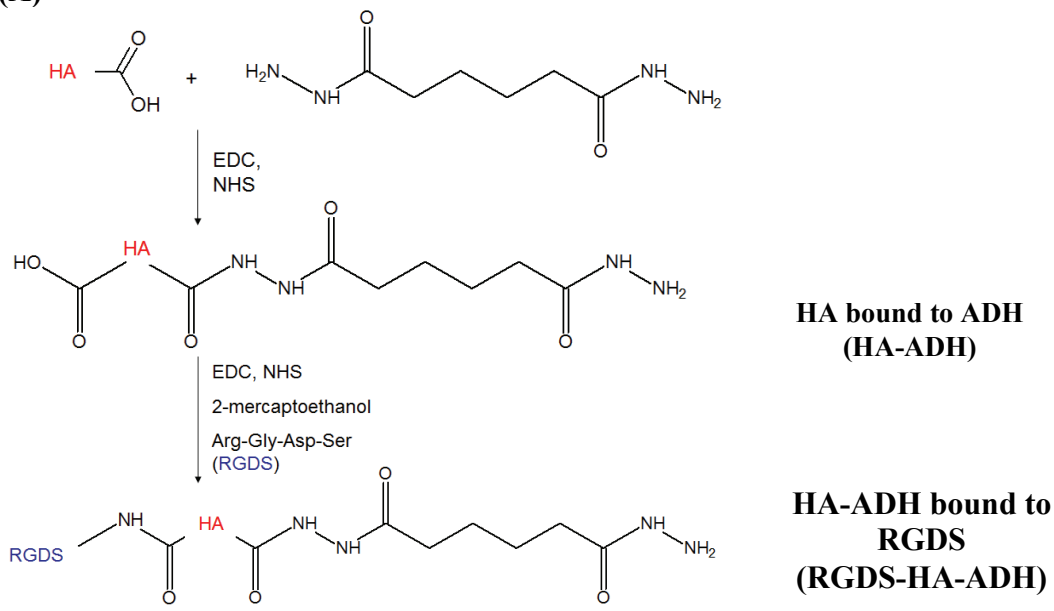

(B) Bissulfosuccinimidyl suberate (BS^3) crosslinker

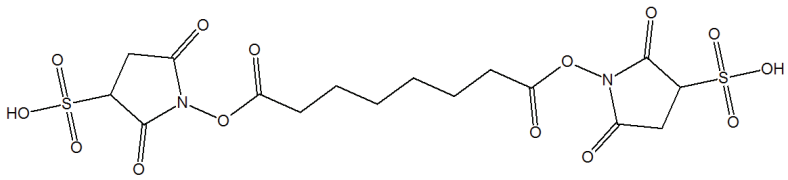

Figure 10.6: (A) HA contains numerous carboxyl groups which react with ADH hydrazide groups in the presence of EDC. EDC and NHS can then activate remaining carboxyl groups for the covalent binding of RGDS. Note that 2-mercaptoethanol serves to inactivate any remaining EDC to prevent a reaction with the subsequently added RGDS. **(B)** The HA polymer bound to RGDS and ADH can be crosslinked with BS^3 – structure seen here.

One benefit to this proposed scheme is existing literature supporting the biocompatibility of the final crosslinked polymer. Cui et al. found HA-ADH hydrogels with bound RGDS to be biocompatible when implanted into the brains of rats.[45] Furthermore, Motokawa et al. found HA-ADH gels crosslinked with BS^3 to last without full degradation in rats for at least 3 months with no observed adverse effects.[44]

A preliminary study was conducted following the reaction steps to produce a crosslinked HA-ADH-BS^3 hydrogel both without peptide and with RGDS bound. Both

procedures produced a hydrogel material such that the material did not flow upon inversion. Gels were sterilized with 70% v/v ethanol in water for at least one hour. 3T3 fibroblasts were then cultured on the gel surfaces (as per the procedures described in Chapter 5) as seen in Figure 10.7. Cells were observed over a period of 1.5 weeks. During this time, cells formed large clumps, and failed to significantly adhere to the hydrogel without bound peptide (Figure 10.7 A). On the other hand, numerous cells adhered to the RGDS-bound hydrogel (Figure 10.7 B), and projections could be seen extending from the cells. This preliminary qualitative study demonstrated that gels could be formed via the chemistry outlined in Figure 10.6, which included an RGDS incorporation step, and that cells will adhere to the final RGDS bound crosslinked HA gel. However, cells remained rounded, and failed to penetrate into the gel volume from the surface which supported the need for cell seeding prior to polymerization. Further studies are needed to verify RGDS incorporation and quantitate the differences in cell binding between the RGDS-HA gel and the non-peptide bound gels. This study serves merely to provide an option for 3D gel chemistry for future work.

10.4.2 Analytical Methods for Peptide Patterning

As the patterning becomes more complex geometrically, or it is desired to move to a higher resolution or into three dimensions, it becomes necessary to develop a method to visualize the underlying peptide pattern of caged and uncaged RGDS. This is challenging since both peptides possess many of the same functional groups.

Initially, attempts were made to find an antibody to bind to free RGDS to aid in visualization. A search of the literature revealed that the antibody MAB 1926 is known to bind to the RGD region in fibronectin.[46,47] Hydrogels bound to RGDS were exposed to solutions of this antibody up to 0.01 mg/mL in 1XPBS, which was 6-7 X more concentrated than recommended in the literature for detection,[46] followed by incubation with a fluorescent secondary antibody. Gels were incubated with each antibody for 2 hours at 37ºC followed by rinsing 3X with 1XPBS. However, the antibody was unable to bind to the shorter RGDS sequence bound to our HA hydrogels as seen by the absence of any fluorescent signal after the antibody binding steps. This was likely due to the short length of the RGDS peptide;

antibodies usually bind to longer peptide sequences with the ability to take on a unique 3D shape that the antibody recognizes.[48]

(A) Native HA gel (no bound peptide)

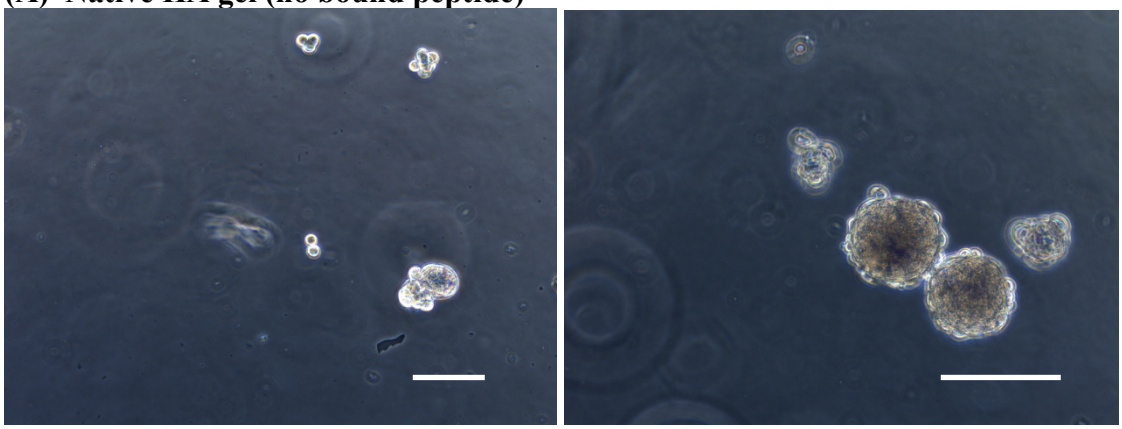

(B) HA gel with bound RGDS

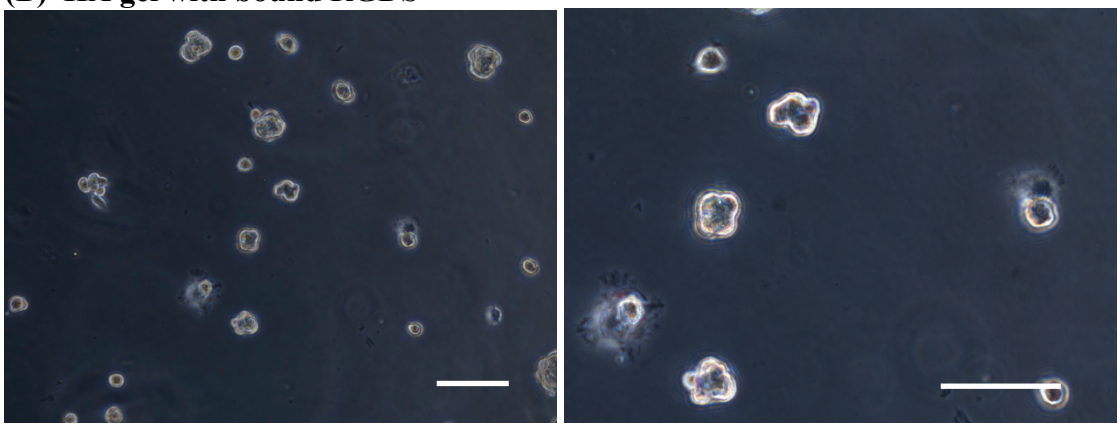

Figure 10.7: Phase contrast images of 3T3 fibroblasts bound to HA-ADH gels crosslinked with BS^3 with either no peptide or bound RGDS peptide 1.5 weeks post seeding with scale bars = 100 μm.

Shimizu et al. developed an antibody with the ability to bind specifically to 2-NB groups.[49] The binding of such an antibody also serves to physically enlarge the caging group, which would theoretically further inhibit binding of integrin receptors to caged RGDS molecules. However, Shimizu et al. also found that this antibody was unable to bind to peptides caged on the backbone amide nitrogen atom. Thus, it is unlikely to work with our caged R[-]GDS, but may bind to RGDS caged in other locations. Furthermore, the antibody is not commercially available.

Another possibility is to bind a fluorescent molecule to the 2-NB caging group for visualization. Removal of the caging group in patterned regions would expose free non-fluorescent RGDS so patterned regions would appear dark, while unpatterned regions would fluoresce. Such chemistry was employed by Wong et al.[36] One disadvantage to this method is that binding a fluorescent group to the 2-NB cage could alter the energy required for uncaging or the solubility of the caged peptide. This possibility would have to be studied.

Another possible method for pattern visualization is to purchase a commercial 2-NB caging group bound to a fluorescing molecule, such that fluorescence is suppressed in the caged state. Such caged fluorescent molecules could be pre-mixed with caged R[-]GDS and bound to the HA hydrogel. In this way, irradiation would produce free RGDS for cell adhesion, as well as free fluorescing molecules which would illuminate the previously irradiated areas which also correspond to the cell-adhesive patterned regions. Prior to trying this approach, it would have to be verified that cells do not bind to the caged fluorescent molecules. Furthermore, the two caged species may require different energies of irradiation. However, this method is much simpler than the others described. It also illuminates the patterned cell-adhesive regions instead of the background non-adhesive regions, which would make it easier to view adhesive patterns.

10.4.3 Recommended Future Directions

In summary, the cell patterning methodology developed in this thesis work lends itself well to a number of future research opportunities. Studies can be continued with the goal of incorporating cell-patterned HA hydrogels into a device for SCI treatment under development by Dr. Cao's laboratory group. For this application, further research can be conducted into the behavior of NSPCs on the patterned hydrogels and final device, and the impact of various hydrogel and patterning parameters on cell behavior, such as differentiation. Two photon laser technology could further be used to improve patterning resolution, and can also be used to expand our patterning strategy into 3D – a possible second future research goal. A hydrogel synthesis protocol was suggested herein for 3D patterning. This method can be further tested by seeding cells in 3D throughout the gel volume, conducting tests for cell viability and cellular metabolism over time, and

quantitating the amount of bound peptide in 3D while optimizing it for cell patterning. One of the analytical methods previously discussed should be explored to distinguish between the locations of RGDS molecules versus uncaged R[-]GDS in order to visualize cell adhesive patterns in 3D. Therefore, new material research into the development a 3D hydrogel cell patterning platform and further research into a tissue engineering application in the form of a SCI treatment device make for exciting future opportunities based off of the current work presented in this thesis.

10.5 References

1. Kokovay E, Shen Q, Temple S. The Incredible Elastic Brain: How Neural Stem Cells Expand Our Minds. *Neuron.* 2008;60(3):420-429.

2. Ming G-l, Song H. Adult neurogenesis in the mammalian central nervous system. *Annual Review of Neuroscience.* 2005;28(1):223-250.

3. Sohail A. The culture of neural stem cells. *Journal of Cellular Biochemistry.* 2009;106(1):1-6.

4. Bear MF, Connors BW, Paradiso MA. *Neuroscience : exploring the brain*. 3rd ed. Philadelphia, PA: Lippincott Williams & Wilkins; 2007.

5. Rauch U. Extracellular matrix components associated with remodeling processes in brain. *Cellular and Molecular Life Sciences* 2004;61(16):pp. 2031-2045

6. Seidlits SK, Schmidt CE, Shear JB. High-Resolution Patterning of Hydrogels in Three Dimensions using Direct-Write Photofabrication for Cell Guidance. *Adv. Funct. Mater.* 2009;19(22):3543-3551.

7. Preston M, Sherman LS. Neural Stem Cell Niches: Critical Roles for the Hyaluronan-Based Extracellular Matrix in Neural Stem Cell Proliferation and Differentiation. *Front Biosci (Schol Ed)*. 2011;3:1165–1179.

8. Mirzadeh Z, Merkle FT, Soriano-Navarro M, Garcia-Verdugo JM, Alvarez-Buylla A. Neural Stem Cells Confer Unique Pinwheel Architecture to the Ventricular Surface in Neurogenic Regions of the Adult Brain *Cell Stem Cell.* 2008;3(3):265-278

9. Ruiz A, Buzanska L, Gilliland D, et al. Micro-stamped surfaces for the patterned growth of neural stem cells. *Biomaterials.* 2008;29(36):4766-4774.

10. McBeath R, Pirone DM, Nelson CM, Bhadriraju K, Chen CS. Cell shape, cytoskeletal tension, and RhoA regulate stem cell lineage commitment. *Developmental Cell.* 2004;6(4):483-495.

11. Tavazoie M, Van der Veken L, Silva-Vargas V, et al. A Specialized Vascular Niche for Adult Neural Stem Cells. *Cell Stem Cell.* 2008;3(3):279-288.

12. Whalley K. Stem cells: At home with neural stem cells. *Nat Rev Neurosci.* 2008;9(11):801-801.

13. Milner R. A novel three-dimensional system to study interactions between endothelial cells and neural cells of the developing central nervous system *BMC Neuroscience.* 2007;8(3).

14. Lai B, Mao XO, Greenberg DA, Jin K. Endothelium-Induced Proliferation and Electrophysiological Differentiation of Human Embryonic Stem Cell-Derived Neuronal Precursors. *Stem Cells and Development.* 2008;17(3):565-572.

15. Meng X-t, Li C, Dong Z-y, et al. Co-transplantation of bFGF-expressing amniotic epithelial cells and neural stem cells promotes functional recovery in spinal cord-injured rats. *Cell Biology International.* 2008;32(12):1546-1558.

16. Walker MR, Patel KK, Stappenbeck TS. The stem cell niche. *Journal of Pathology.* 2009;217(2):169-180.

17. Lim DA, Alvarez-Buylla A. Interaction between astrocytes and adult subventricular zone precursors stimulates neurogenesis *Proceedings of the National Academy of Sciences of the United States of America* 1999;9(13):7526-7531.

18. Song H, Stevens CF, Gage FH. Astroglia induce neurogenesis from adult neural stem cells. *Nature.* 2002;417(6884):39-44.

19. Pan L, Ren Y, Cui F, Xu Q. Viability and differentiation of neural precursors on hyaluronic acid hydrogel scaffold. *Journal of Neuroscience Research.* 2009;87(14):3207-3220.

20. Fischer SE, Liu X, Mao H-Q, Harden JL. Controlling cell adhesion to surfaces via associating bioactive triblock proteins. *Biomaterials.* 2007;28(22):3325-3337.

21. Kilian KA, Mrksich M. Directing Stem Cell Fate by Controlling the Affinity and Density of Ligand–Receptor Interactions at the Biomaterials Interface. *Angewandte Chemie International Edition.* 2012;51(20):4891-4895.

22. Béduer A, Vieu C, Arnauduc F, Sol J-C, Loubinoux I, Vaysse L. Engineering of adult human neural stem cells differentiation through surface micropatterning. *Biomaterials.* 2012;33(2):504-514.

23. Martino S, D'Angelo F, Armentano I, Kenny JM, Orlacchio A. Stem cell-biomaterial interactions for regenerative medicine. *Biotechnology Advances.* 2012;30(1):338-351.

24. Goeldner M, Givens R. *Dynamic studies in biology : phototriggers, photoswitches and caged biomolecules*. Weinheim: Wiley-VCH; 2005.

25. Callaway EM, Yuste R. Stimulating neurons with light. *Current Opinion in Neurobiology.* 2002;12(5):587-592.

26. Khurana M, Collins HA, Karotki A, Anderson HL, Cramb DT, Wilson BC. Quantitative In Vitro Demonstration of Two-Photon Photodynamic Therapy Using Photofrin® and Visudyne® *Photochemistry & Photobiology.* 2007;83(6):1441-1448.

27. Svoboda K, Yasuda R. Principles of Two-Photon Excitation Microscopy and Its Applications to Neuroscience. *Neuron.* 2006;50:823–839.

28. Furuta T, Wang SSH, Dantzker JL, et al. Brominated 7-hydroxycoumarin-4-ylmethyls: Photolabile protecting groups with biologically useful cross-sections for two photon photolysis. *Proceedings of the National Academy of Sciences.* 1999;96(4):1193-1200.

29. Wylie RG, Shoichet MS. Two-photon micropatterning of amines within an agarose hydrogel. *Journal of Materials Chemistry.* 2008;18(23):2716-2721.

30. Aizawa Y, Wylie R, Shoichet M. Endothelial Cell Guidance in 3D Patterned Scaffolds. *Advanced Materials.* 2010;22(43):4831–4835.

31. Aujard I, Benbrahim C, Gouget M, et al. O-nitrobenzyl photolabile protecting groups with red-shifted absorption: Syntheses and Uncaging Cross-Sections for One- and Two-Photon Excitation. *Chemistry - A European Journal.* 2006;12(26):6865-6879.

32. Diaspro A, Federici F, Viappiani C, et al. Two-Photon Photolysis of 2-Nitrobenzaldehyde Monitored by Fluorescent-Labeled Nanocapsules. *Journal of Physical Chemistry B.* 2003;107(40):11008-11012.

33. Denk W, Strickler JH, Webb WW. Two-Photon Laser Scanning Fluorescence Microscopy. *Science.* 1990;248(4951):73-76.

34. Goubko C, Majumdar S, Basak A, Cao X. Hydrogel cell patterning incorporating photocaged RGDS peptides. *Biomedical Microdevices.* 2010;12(3):555-568.

35. Peng K, Tomatsu I, van den Broek B, et al. Dextran based photodegradable hydrogels formed via a Michael addition. *Soft Matter.* 2011;7(10):4881-4887.

36. Wong DY, Griffin DR, Reed J, Kasko AM. Photodegradable Hydrogels to Generate Positive and Negative Features over Multiple Length Scales. *Macromolecules.* 2010;43(6):2824-2831.

37. Shigenaga A, Yamamoto J, Sumikawa Y, Furuta T, Otaka A. Development and photo-responsive peptide bond cleavage reaction of two-photon near-infrared excitation-responsive peptide. *Tetrahedron Letters.* 2010;51(21):2868-2871.

38. Kantevari S, Hoang CJ, Ogrodnik J, Egger M, Niggli E, Ellis-Davies GCR. Synthesis and Two-photon Photolysis of 6-(ortho-Nitroveratryl)-Caged IP3 in Living Cells. *ChemBioChem.* 2006;7(1):174-180.

39. Dakin K, Li W-H. Cell membrane permeable esters of d-myo-inositol 1,4,5-trisphosphate. *Cell Calcium.* 2007;42(3):291-301.

40. Zhao J, Gover TD, Muralidharan S, Auston DA, Weinreich D, Kao JPY. Caged Vanilloid Ligands for Activation of TRPV1 Receptors by 1- and 2-Photon Excitation *Biochemistry.* 2006;45(15):4915-4926.

41. Neveu P, Aujard I, Benbrahim C, et al. A Caged Retinoic Acid for One- and Two-Photon Excitation in Zebrafish Embryos. *Angewandte Chemie International Edition.* 2008;47(20):3744-3746.

42. Pouyani T, Harbison GS, Prestwich GD. Novel Hydrogels of Hyaluronic Acid: Synthesis, Surface Morphology, and Solid-State NMR. *Journal of the American Chemical Society.* 1994;116(17):7515-7522.

43. Pouyani T, Prestwich GD. Functionalized Derivatives of Hyaluronic Acid Oligosaccharides: Drug Carriers and Novel Biomaterials. *Bioconjugate Chemistry.* 1994;5(4):339-347.

44. Motokawa K, Hahn SK, Nakamura T, Miyamoto H, Shimoboji T. Selectively crosslinked hyaluronic acid hydrogels for sustained release formulation of erythropoietin. *Journal of biomedical Materials Research.* 2006;78A(3):459-465.

45. Cui F, Tian W, Hou S, Xu Q, Lee IS. Hyaluronic acid hydrogel immobilized with RGD peptides for brain tissue engineering. *Journal of Materials Science: Materials in Medicine.* 2006;17(12):1393-1401.

46. Tzoneva R, Faucheux N, Groth T. Wettability of substrata controls cell-substrate and cell-cell adhesions. *Biochimica et Biophysica Acta (BBA) - General Subjects.* 2007;1770(11):1538-1547.

47. Nagai T, Yamakawa N, Aota S, et al. Monoclonal antibody characterization of two distant sites required for function of the central cell-binding domain of fibronectin in

cell adhesion, cell migration, and matrix assembly. *J. Cell Biol.* 1991;114(6):1295-1305.

48. Gershoni JM, Roitburd-Berman A, Siman-Tov DD, Freund NT, Weiss Y. Epitope mapping: The first step in developing epitope-based vaccines. *BioDrugs.* 2007;21(3):145-156.

49. Shimizu M, Yumoto N, Tatsu Y. Preparation of caged compounds using an antibody against the photocleavable protecting group. *Analytical Biochemistry.* 2006;348(2):318-320.